Iowa State University

Digital Repository

2010

Modified sheet pile abutments for low volume road bridges

Ryan Richard Evans
Iowa State University

Follow this and additional works at: https://lib.dr.iastate.edu/etd

Part of the Civil and Environmental Engineering Commons

Recommended Citation

Modified sheet pile abutments for low volume road bridges

by

Ryan Richard Evans

A thesis submitted to the graduate faculty

in partial fulfillment of the requirements for the degree of

MASTER OF SCIENCE

Major: Civil Engineering (Structural Engineering)

Program of Study Committee:
David J. White, Major Professor
F. Wayne Klaiber
Terry J. Wipf
Loren W. Zachary

Iowa State University

Ames, Iowa

2010

TABLE OF CONTENTS

LIST OF FIGURES

LIST OF TABLES

ACKNOWLEDGMENTS

EXECUTIVE SUMMARY

Iowa Highway Research Board Project TR-568 was initiated in January 2007 to investigate the use of steel sheet piling as an alternative foundation component for Low Volume Road (LVR) bridges. A total of 14 different sites were initially investigated in several counties as potential candidates for the construction of demonstration projects utilizing steel sheet pile abutments. Based on site conditions, three sites were selected for demonstration projects; these are located in Black Hawk, Boone, and Tama Counties. Each of the demonstration projects utilizes a different experimental abutment system.

Steel sheet piling, typically used for retaining structures in the United States, has been used as bearing piles in Europe for the past 50 years and is a potential alternative for use as the primary component in LVR bridge substructures. To investigate the viability of axially-loaded sheet pile abutments, a demonstration project was constructed in Black Hawk County, Iowa. The project involved construction of a 40 ft, single-span bridge utilizing axially-loaded steel sheet piling as the primary foundation component. The site chosen for the project consisted of primarily silty clays underlain by shallow bedrock into which the sheet piling was driven. An instrumentation system (consisting of strain gages, deflection transducers, earth pressure cells, and piezometers) was installed on the bridge for obtaining live load test data as well as long term performance data.

Live load testing of the bridge structure was performed on November 3, 2008 by placing two loaded trucks (approximately 24 ton each) at various locations on the bridge and recording data. Maximum axial stresses occurring in the piles were approximately 0.5 ksi and were comparable to estimates made by analysis for a design lane-load distribution width of 10 ft. Flexural stresses, in general, were significantly less than those estimated by analysis and maximum values were approximately 0.2 ksi. Earth pressures recorded during live load testing (with maxima of approximately 100 psf) were also significantly lower than earth pressures estimated by analysis. These results suggest the method of analysis for lateral earth pressures applied to the sheet pile wall was conservative. Long-term monitoring of the bridge from November 2008 through February 2009 was also performed; the datalogging system was damaged by flooding in March 2009 and subsequent long-term monitoring was terminated. Variations in earth pressure over time were observed with the largest variations in earth pressure occurring behind the abutment cap. The earth pressures experienced cycles that varied in magnitude from 50 psf to 1500 psf, suggesting long-term loading due to freeze/thaw cycles of the soil and the thermal deformation of the superstructure elements may be the critical factors in the design of sheet pile abutment and backfill retaining systems rather than vehicular live loads.

The demonstration projects in Boone and Tama Counties were designed using a geosynthetically reinforced soil backfill with a steel sheet pile backfill retention abutment system. Each of the bridge superstructures is supported by spread footings bearing on the reinforced soil mass abutment systems. The bridge superstructure in Boone County is a 100 ft long, three span J30C-87 continuous concrete slab bridge while the superstructure for Tama County utilizes two 89 ft railroad flatcars bolted together. Structural monitoring systems (including strain gages, earth pressure cells, and piezometers) were developed for load testing and long-term monitoring of these projects as well. Construction of the project in Boone County was completed in fall 2009 and live load testing was subsequently performed on November 13, 2009. Maximum flexural stresses experienced in the sheet pile elements were 0.08 ksi and were significantly lower than estimated by analysis. Vertical and horizontal earth pressures in the backfill (with maxima of 410 psf and 50 psf, respectively) were also lower than expected, suggesting a conservative design approach. Construction of the project in Tama County was completed in August 2010 with subsequent load testing performed in October 2010.

This thesis presents a summary of the existing research on steel sheet piling, documentation of the design and construction of the demonstration bridges in Black Hawk County and Boone County, as well as an analysis of the design procedures used through information collected during live load testing of the Black Hawk County and Boone County projects. Information on the design and site investigation of the Tama County project is presented in this thesis as well. Preliminary results indicate that steel sheet piling is an effective alternative for LVR substructures. Results and analysis of live load testing for the Tama County project will be presented in the final report for project TR-568.

CHAPTER 1. INTRODUCTION

The state of Iowa has approximately 22,936 bridges on low volume roads (LVR). Based on the National Bridge Inventory data, 22% of the LVR bridges in Iowa are structurally deficient while 5% of them are functionally obsolete (Federal Highway Administration, 2008). The substructure components (abutment and foundation elements) are known to be contributing factors for some of these poor ratings. Steel sheet piling was identified as a possible long-term option for LVR bridge substructures, but due to lack of experience in Iowa needed investigation with regard to vertical and lateral load resistance, construction methods, design methodology, and load test performance. Project TR-568 was initiated in January 2007 to investigate use of sheet pile abutments.

Objective and Scope

The primary objectives of this research were:

- Investigate a design approach for sheet pile bridge abutments for short span, LVR bridges including calculation of lateral stresses from retained soil and bearing support for the superstructure.

- Formulate an instrumentation and monitoring plan to evaluate performance of sheet pile abutment systems including evaluation of lateral structural forces and bending stresses in the sheet pile sections.

- Produce a report and technology transfer materials that provide an understanding of the associated costs and construction effort as well as recommendations for use and potential limitations of sheet pile bridge abutment systems.

The resulting key tasks from this research were:

- Select three sites for sheet pile abutment system demonstration projects and perform detailed site investigations.

- Design alternative abutment systems for demonstration projects utilizing steel sheet piling as a primary foundation component. (continued)

- Document construction activities of demonstration projects and install instrumentation for structural monitoring and performance evaluation of sheet pile abutment system.

- Perform live load testing of each demonstration project upon completion of construction.

- Produce final report including analysis of live load test data and recommendations for future sheet pile abutment systems.

A total of 14 different project sites were investigated in several different counties as potential sites for demonstration projects. Three sites located in Black Hawk, Boone, and Tama Counties were selected based on site conditions for demonstration projects. As of August 2010, three bridges have been constructed in the respective counties, each utilizing different alternative sheet pile abutments. Each bridge project was instrumented and data have been collected and analyzed from load tests. Data collection of long-term performance is still ongoing.

Since axially loaded sheet piling is relatively new in the United States, a specific design procedure does not currently exist. Because of this, the design approach taken by Iowa State University (ISU) is a hybrid between sheet pile retaining walls and driven piles. For determining the lateral forces experienced by the abutment (and thus the bending stresses) the structure is analyzed as a retaining wall. Bending stresses induced by axial load in the piling, however, must be considered. For determining the bearing capacity of the pile elements, the structure is analyzed as driven piling according to the American Association of State, Highway, and Transportation Officials (AASHTO, 1998) load and resistance factor design (LRFD) bridge design specifications.

In addition to the three counties selected for the demonstration projects, several other Iowa counties have expressed their willingness to participate in these projects and are very interested in the results of the investigation. This thesis presents case histories for each of the demonstration projects constructed. Information regarding site investigation, design, construction, load testing, data analysis, an overall analysis of the applicability of the design methods used, as well as conclusions and recommendations for additional research are included in this report.

CHAPTER 2.   BACKGROUND

Introduction

With the current state of bridge substructures throughout the United States, particularly the secondary road system, there exists a need for bridge repairs and replacements. Many Iowa counties, however, need alternative solutions that are relatively low cost with adequate long-term performance. Many of the deficient bridges exist on vital roadways that cannot afford to be out of service for long periods of time.

Steel sheet pile bridge abutment systems were identified as one possible alternative for bridge replacements because they allow for rapid construction and can serve the dual purpose of retaining backfill soils and as foundation bearing elements to support the abutment.   Previously in the United States, steel sheet piling has been used for mainly retaining structures and temporary installations. In a few states, such as Alaska and New York, steel sheet pile abutment systems have been constructed.

The purpose of this review is to summarize information pertaining to the application, design, availability, and methods for construction and monitoring of steel sheet pile bridge abutment systems.

Application of Steel Sheet Piling Bridge Abutment Systems

For use as the primary bearing foundation component, steel sheet piling has several potential advantages. A sheet pile abutment system can retain abutment fill while simultaneously providing a foundation for the bridge abutment whereas driven H-piles require a separate retaining structure. Sheet pile bridge abutment systems also do not require earth embankments in front of the upper portion of the piles (McShane, 1991). In areas where materials such as concrete are not available locally, steel sheet pile bridge abutment systems provide an alternative material. When used for bridges over rivers or streams, sheet pile abutment systems can protect against scour. Along with the potential for accelerated construction, sheet pile bridge abutment systems facilitate installation and maintenance by county engineers and their construction crews (Carle and Whitaker, 1989).

When considering steel sheet piling for use as a bridge abutment system there are two main alternatives for design: (1) axially loaded sheet piling, or (2) backfill retaining structures. The backfill retaining structures allow the bridge superstructure to be supported by a shallow foundation

on stabilized backfill soil. The application of these two alternatives is discussed in the following sections.

Axially Loaded Sheet Pile Foundation Elements

Most research and design for steel sheet piling to date has been focused on sheet piles as backfill retaining structures. This means that primarily lateral forces control the design approach. A case study on the application of sheet pile structures acting as bridge abutment systems (by computer analysis) has shown this method to be practical for design (Chung et al., 2004). In this study, the structure analyzed was a 68.9 ft single span bridge with 26.9 ft long sheet pile lengths (12.1 ft embedment depth, fully backfilled) in a cohesionless soil with a 35 degree angle of internal friction; standard penetration test (SPT) N-values ranged from 30 to 40.

The results of the analysis revealed that steel sheet piles can be designed for the combined axial and lateral loading of a bridge abutment. The influence of bridge span length and abutment height was also investigated. When increasing span length from 32.8 ft to 78.7 ft (with a constant abutment height of 14.8 ft), an increase in the stress ratio (of axial and bending stresses) in the piling did occur; the required embedment depth did not change at the maximum span length investigated. When increasing the abutment height, anchor forces and embedment depth both increased gradually.

A second order (or P-Delta) analysis was also performed to investigate the combined loading effects on the structure. It was found that, since the maximum deflection was only 0.15 in., stresses induced by the eccentricity of the axial load can be considered negligible (Chung, 2004).

Consideration should be given to construction of the sheet pile abutment systems integral with the superstructure. Though settlement and thermal changes will induce stresses into the superstructure, it is possible that the elimination of bearings and joints will result in overall cost savings for short span bridges (McShane, 1991).

One example of sheet piling used in bridge abutments is the Small Creek Bridge in Seward, Alaska. This replacement bridge consists of an 80 ft single-span that bears directly on Z-pile sections that are driven to bedrock. For this project, the connection between the piling and superstructure was made by bolting two channels to the Z-piling and welding on a 1 in. thick steel plate. Prestressed concrete girders were then set on elastomeric bearing pads (see Figure 2-1). To properly seat the sheet piling

in the bedrock, fitted cast steel tips were attached to the toe of the piles. To provide resistance for the wingwalls, tie rods anchored to concrete deadman were attached with a wale system composed of back-to-back channels bolted on the backfill side of the wall (Carle and Whitaker, 1989).
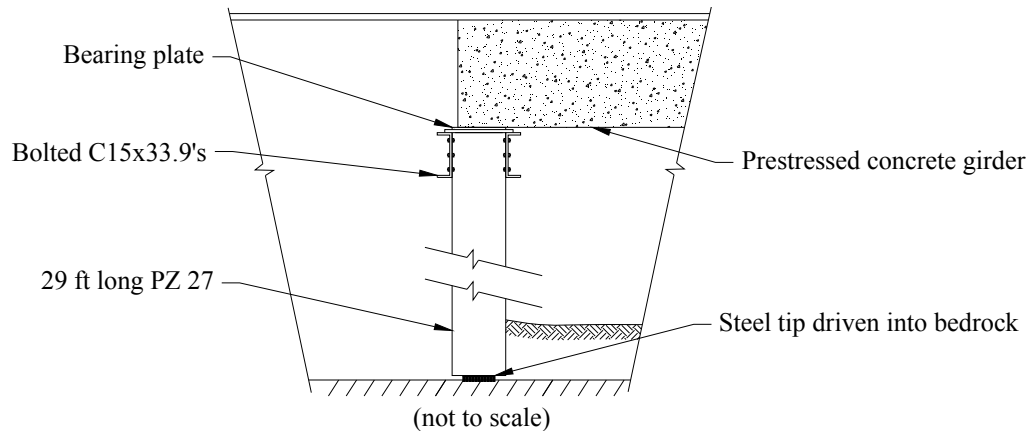
Figure 2-1. Small Creek Bridge, Seward, Alaska (reproduced from Carle and Whitaker, 1989).

Located in New York, the Taghkanic Creek Bridge (a 42 ft single-span) is an example of an axially loaded sheet pile abutment utilizing a reinforced concrete cap bearing on a steel plate (see Figure 2-2). Z-profile sheet piling was driven in granular soil to a specified tip elevation (approximately 22 ft below grade) for developing the required bearing capacity through skin friction and tip resistance. The wingwalls, which are capped with steel channels, are driven to the same depth as the abutment walls (Carle and Whitaker, 1989).
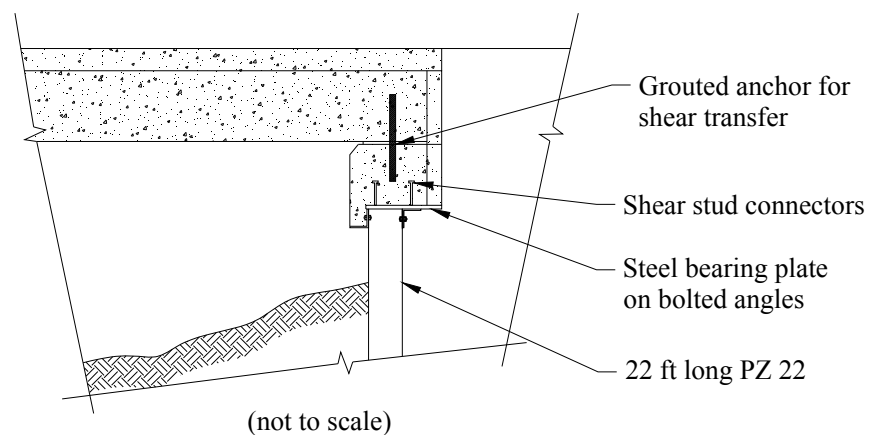
Figure 2-2. Taghkanic Creek Bridge, New York (reproduced from Carle and Whitaker, 1989).

For the Banks Road Bridge in New York, a 65 ft single-span structure, 16 sheet piles were used for each abutment although only 10 were required for support (the remaining piles were used to provide backfill retention and were not driven to full depth). The bridge utilizes a unique method of eliminating the requirement for a reinforced concrete pile cap. For the interface between the substructure and superstructure, the sheet piling is capped with a steel channel on which a steel distribution beam is placed; the steel bridge girders are bolted to the distribution beam as shown in Figure 2-3. The abutment and wingwalls are tied back with anchors by a steel W-shape wale system (Carle and Whitaker, 1989).
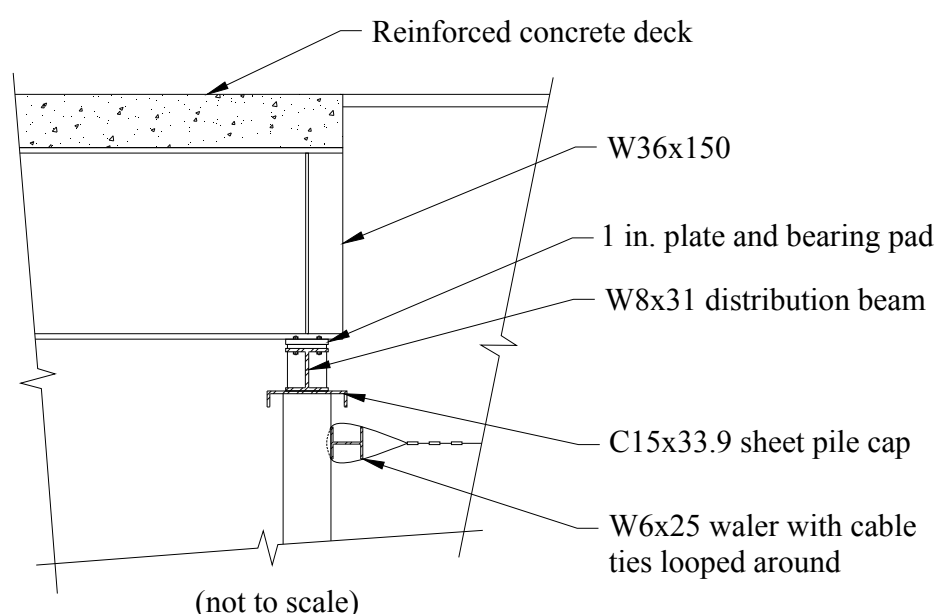
Figure 2-3. Banks Road Bridge, New York (reproduced from Carle and Whitaker, 1989).

Four miles south of Buffalo Center in Winnebago County, Iowa, an 89 ft replacement bridge was constructed on 390th street over Little Buffalo Creek. This bridge was designed and constructed as part of a joint project between Iowa State University and Winnebago County (Massa, 2007).

The project consisted of a three-span bridge (66 ft main span with 11.5 ft end spans) that used railroad flatcars for the superstructure. Although the primary purpose of this project was to investigate the use of railroad flatcars for the bridge superstructures, steel sheet pile abutments were installed and instrumented for preliminary investigation. The two piers consisted of steel-capped H-piles driven to a specified depth.

For the design of the abutments approximate soil properties were determined using SPT blow count values from soil borings obtained from the county. Lateral earth pressures were calculated using "at-rest" conditions (conservatively assumed due to the lateral restraint provided by the bridge structure) with a factor of safety of approximately 1.5. The bearing capacity of the sheet piling, consisting of pile tip resistance and skin friction, was determined using AASHTO (1998). For the pile tip resistance, the cross-sectional area of a sheet pile section was used. For the computation of skin friction, twice the width of a section multiplied by its depth was used to estimate the surface area. To determine the axial load resisted by each pile, superstructure loads at each bearing point were initially assumed to distribute between two sheet pile sections. Due to the uncertainty of this assumption, a factor of safety of 3.75 was applied to axial capacity.

The bridge structure was supported by the sheet pile abutments using stiffened angles bolted to the pile wall (see Figure 2-4). The flexibility of the sheet piling and the soil behind it was assumed to provide adequate allotment for thermal expansion and contraction (approximately 0.5 in. assuming a 100° F temperature change); therefore, no expansion joints were used.

The selected sheet pile sections were approximately 0.21 in. thick (PZ piles). Although the sections were sufficiently designed to resist axial and flexural loads, damage occurred to the pile sections during driving operations due to local buckling of the portion of the piling within the jaws of the vibratory driver. This resulted in driving to less than design depths. After driving was completed, the abutments were backfilled using material on site. The use of granular backfill material was recommended to allow sufficient drainage and reduce lateral earth pressures on the sheet pile abutment system (Massa, 2007).

To evaluate design assumptions, the abutments were instrumented and tested using loaded trucks. Results from the bridge load test are only applicable for observing general trends due to the limited amount of data collected. Distinction between flexural and axial pile stresses are unable to be made due to the use of strain transducers only on exposed faces of the sheet pile sections.

Although an in-depth analysis of results is beyond the scope of this report, general deflections and strains (instrumentation located in approximately the same areas on the pile shown in Figure 2-4a) are presented in Figure 2-5. It can be seen that the greatest loads in the pile occur as the truck is approaching the east abutment. The strains are positive at this point, meaning the exterior face is in

tension, while the deflection of the pile is away from the backfill soil. The probable cause for this situation is, as the soil is pushing the sheet pile abutment out, the relatively rigid superstructure is restraining the top of the pile. The effect of superstructure restraint is significant and thus must be included in theoretical analysis and design of sheet pile abutment systems.

a.) View of abutment and pier

b.) Stiffened angles bolted to piling supporting superstructure

Figure 2-4. Overview of sheet pile bridge abutment in Winnebago County, Iowa.

Time, T, sec
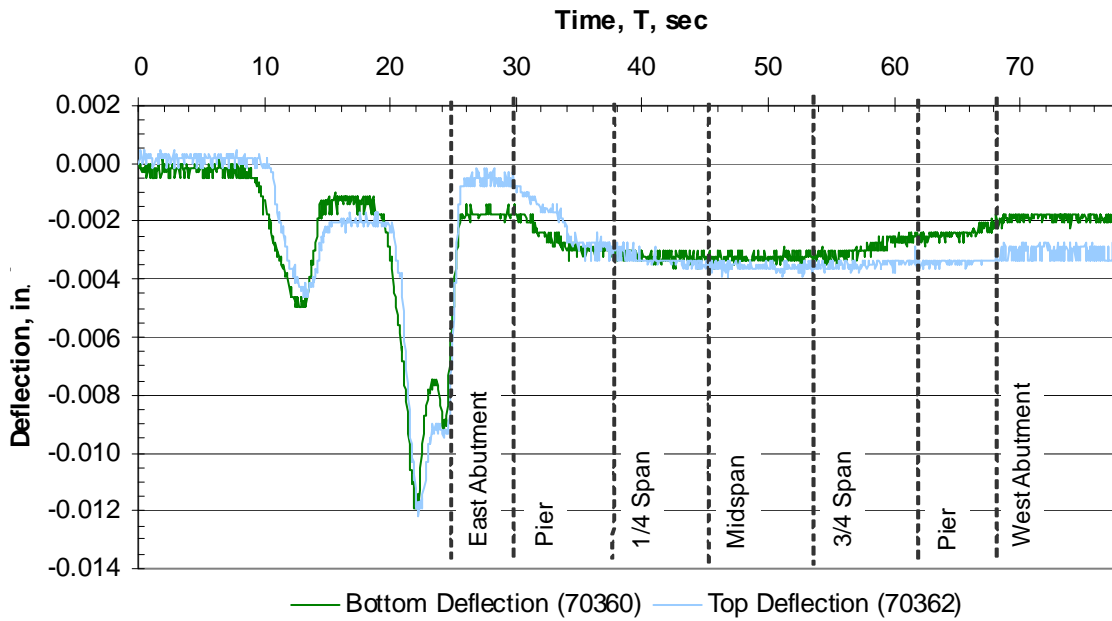
a.) Deflection of sheet pile element

Time, T, sec
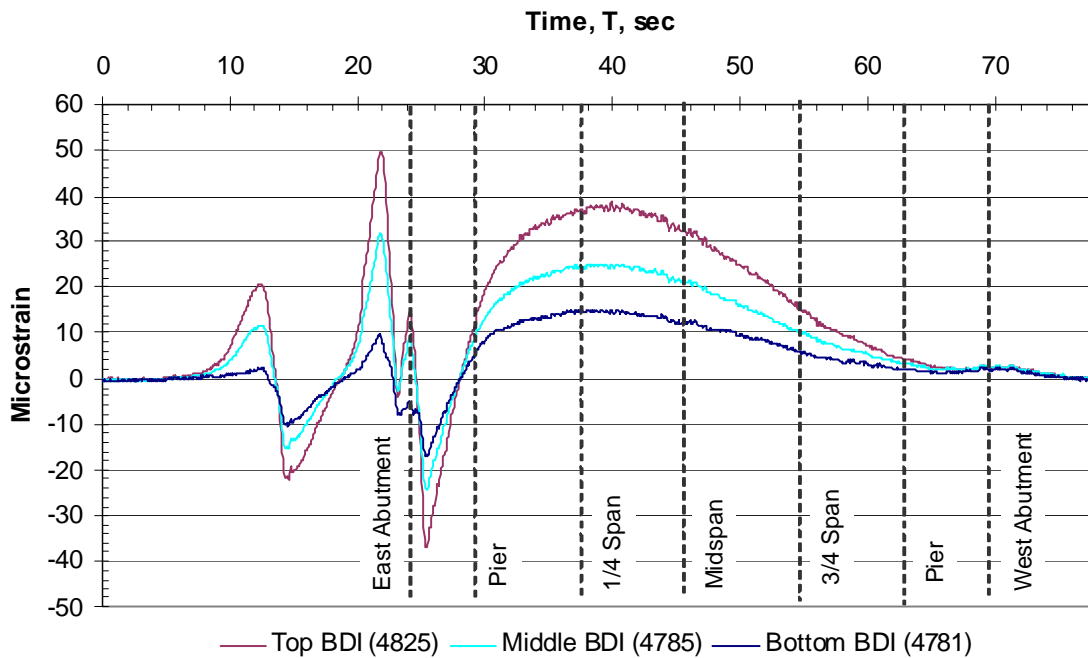
b.) Strains in sheet pile element

Figure 2-5. Measurements on single sheet pile in the east abutment of the Winnebago County, Iowa bridge during live load testing.

Cellular Sheet Pile Abutment Systems

Open Cell® Systems

Open Cell® sheet pile systems offer another alternative for sheet pile bridge abutment and backfill retaining systems. Instead of deriving bearing support by axially loading the sheet pile, Open Cell® technology uses a cellular structure (acting as a membrane) to support the soil inside, allowing the use of a shallow foundation for supporting the bridge superstructure.

The Open Cell® geometry is a partial cellular structure that is open with a method of anchorage attached to the free ends of the cell (Braun, Nottingham, & Thieman, 2002). This is advantageous because the structure does not require strict driving tolerances to ensure closure of the cell as well as providing access for earthwork and compaction equipment.

The forces in the soil (due to superstructure loads and soil weight) place an outward pressure on the cell structure. This outward pressure develops a hoop stress in the cell, placing each individual sheet pile along the wall in tension. For the structure to hold the soil, the tensile forces developed in the wall must be restrained by anchoring the walls of the cell. This can be accomplished by either driving an H-Pile anchor into the soil or extending the tail wall a length sufficient to develop skin friction capable of resisting the tensile forces throughout the wall. According to Braun (2002), the interlocks on flat sheet piling provide sufficient strength to resist tensile forces as well as increasing the developed soil-sheet pile frictional resistance to almost double that calculated by classical techniques. When designing an Open Cell® sheet pile structure, special considerations must be made for scour, settlement, weak soils, seismic, and ice floe forces depending on site conditions (Braun, 2002).

Unlike anchored and cantilevered wall systems, Open Cell® structures do not depend on embedment depth for stability (Gilman, Nottingham, & Pierce, 2001). The resistance to loads is developed entirely by the wall anchorage system. In the presence of weak soils, compensation is accomplished by increasing the tail wall length or providing an H-pile anchor at the end. By lengthening the wall, the unit load on the soil can be reduced to acceptable limits. If the system is designed for a river crossing, scour action from water flow can remove soil from beneath the sheet pile wall. To prevent scour, proper embedment into the soil must be made according to expected water flow at the site. If the system is exposed to very active water flow conditions, a mechanism to resist scour (such as

revetment) should be installed at the tail wall to prevent a loss of wall anchorage (Braun, 2002). Methods to account for scour effects in design are provided by Davis and Richardson (2001).

Although Open Cell® technology is a relatively new concept for bridge abutment design several projects have already been completed and are currently in use. Since the early 1980's, over 40 open cell abutment bridges have been constructed in Northern Alaska where there is exposure to scour, ice floes, seismic activity, temperature fluctuations, and heavy vehicles (Braun, 2002).

In Hunter Creek, Alaska, a cellular abutment bridge was used as a temporary replacement for a bridge "wiped out" in a flood. The bridge was evaluated by the Alaska Department of Transportation and was determined to be sufficient for the permanent structure. Construction of the replacement bridge required 17 days to complete (Braun, 2002).

In Anchorage, Alaska, the C Street Bridge was constructed over a salmon stream crossing where there were soft clay soils. A cellular bridge abutment was selected as it was able to be built with a minimal environmental impact on the stream (Braun, 2002).

In New Iberia, Louisiana, the Open Cell® sheet pile concept was used for the design of a wharf. Although it is not a bridge abutment, the use of Open Cell® technology in a wharf structure presents system benefits that are applicable to bridges. Initially, the wharf structure was to consist of a tied-back bulkhead with a series of piles driven to support loads in the range of 6,000 tons. However, the use of an Open Cell® structure with straight-web sheet piling was found to be a more economical solution. Due to the high capacity for lateral loads, the Open Cell® structure was able to support the design loads without the use of piles for support (Gilman, 2001).

A project in Venice, Illinois, involved a wharf structure that was to be constructed on layers of loose sands and silts about 60 ft above bedrock. To account for the significant settlements expected, sheet piling and supporting soils were placed above desired elevations before densification of the surrounding soils. Vibratory compaction was used to compact the soils in the area; some locations had soil settlements close to 3 ft. After this process, new soils properties were verified and final grades were set (Gilman, 2001).

Closed-Cellular Systems

A highway bridge in Russell, Massachusetts spans a total of approximately 415 ft and uses 4 closed-cell sheet pile structures (two abutments and two piers) for its foundation (see Figure 2-6). Each cell is 21.5 ft in diameter and uses PS 28 sheet pile sections. The bridge superstructure bears directly on the granular fill material in each cell through a reinforced concrete spread footing (Carle and Whitaker, 1989).

According to Braun (2002), construction costs of cellular walls can be almost 50% lower than other conventional abutment types. Since there are no tie rods and wale systems, cellular sheet pile structures are potentially less expensive and avoid components that are difficult to inspect or replace.

a.) Profile view

b.) Plan view
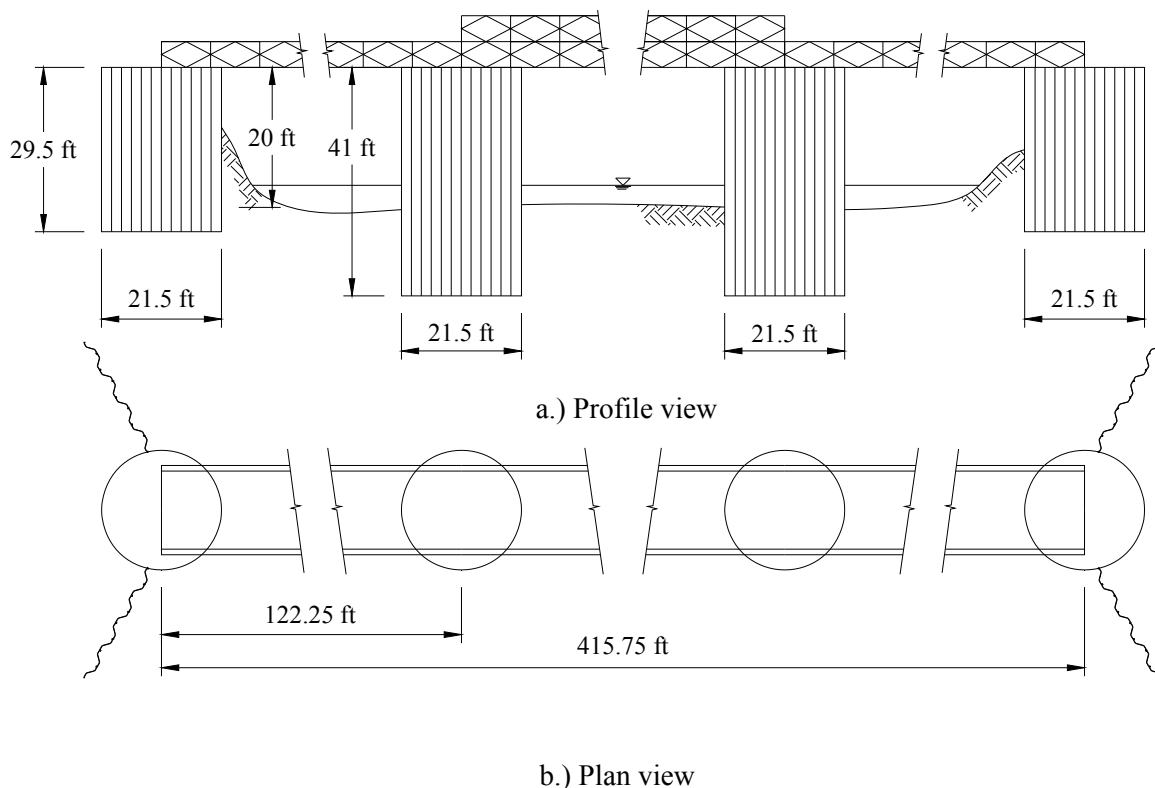
Figure 2-6. Highway bridge substructure in Russell, Massachusetts (reproduced from Carle and Whitaker, 1989)

Geosynthetically Reinforced Soil Abutment Systems

Another alternative to axially-loaded sheet piling is the use of a geosynthetically reinforced soil (GRS) abutment foundation in conjunction with a traditional sheet pile retaining wall. This type of system utilizes a spread footing that bears on a GRS backfill, retained by sheet piling, which significantly reduces lateral earth pressures generated from bridge surcharge loads. Although concrete facing blocks and panels are most commonly used with GRS systems, the use of sheet piling would potentially increase scour protection and wall loading capacity over traditional facing.

Application of Shallow Foundation GRS Abutment Systems

For bridge substructures, shallow footings on soil have traditionally been avoided by designers due to movement tolerances, uncertainty in methods of settlement calculation, uncertainty in subsurface conditions, and other factors that are not typically concerns for driven piling. Consequently, bridge structures with shallow footings have been constructed in very few states. A team of researchers at Ohio University, in an attempt to promote the use of shallow footings in bridges, conducted a study of five bridge structures to present case histories of successful shallow footing use. In general, it was found that highway bridge structures have been successfully supported by shallow foundations given that the soil is free of unsuitable materials and other unfavorable conditions. It is recommended that, when designing shallow footings, the average of several methods of settlement prediction is used (Engle et al., 1999).

GRS systems can be utilized with spread footings to further reduce settlements and provide higher bearing capacities. GRS systems have typically been used in transportation systems for supporting backfill and vehicular loads in roadway structures. The application as a bridge foundation, however, is relatively new (Abu-Hejleh et al., 2001c). In the following paragraphs, several projects in which GRS systems (or similar systems) have been utilized are presented.

Full-Scale Test of GRS Abutment and Piers

At the Havana Maintenance Yard in Denver, Colorado a full-scale test of a GRS bridge abutment and two bridge piers was performed. The GRS systems consisted of several layers of woven polypropylene geotextile placed between levels of concrete blocks used for facing. Concrete pads were used to distribute loads from the steel girders to the GRS foundation systems (see Figure 2-7).
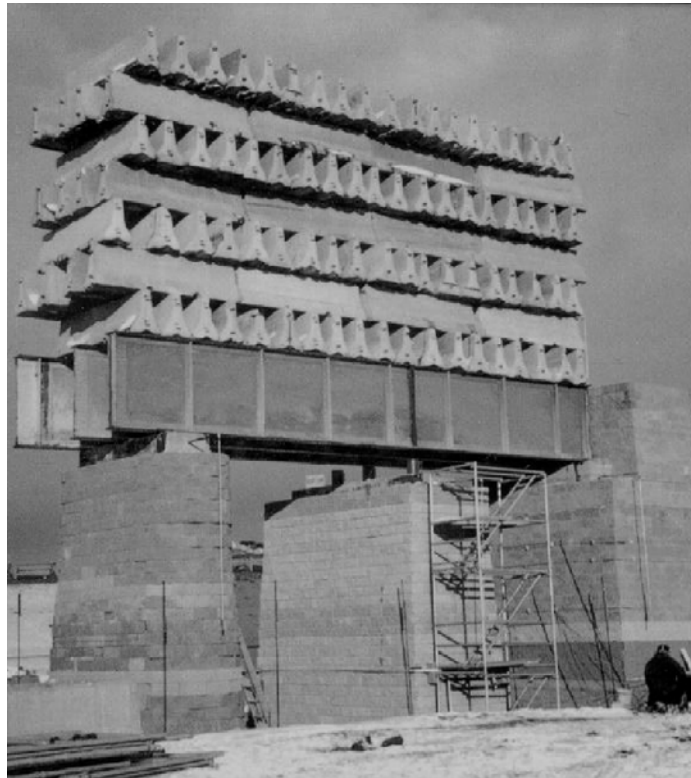
Figure 2-7. Full-scale GRS bridge abutment and two bridge piers (Abu-Hejleh et al., 2001b).

Although the performance of these structures was good during load testing, a failure of one of the bridge piers occurred approximately 5 months after construction. A forensic study of the pier was performed after removal of the surcharge loads and showed that poor compaction, not the geotextile material, was responsible for the failure (Abu-Hejleh et al., 2001b). As a result of this study, the following recommendations resulted for future projects:

- GRS piers should not be used in the case of excessive loads and may not be economical for typical highway projects when compared to concrete piers. GRS systems are however beneficial when concrete is unavailable or if it is undesirable to wait for curing to open the structure for service. It should be noted that the GRS *abutment* performed well over the course of a year and only the pier experienced failure.

- High-strength geosynthetic materials should be used in a relatively close spacing (6 in. to 12 in.), in conjunction with well-compacted granular backfill, to maximize strength of the GRS system. (continued)

- Light equipment should be used during compaction. Compaction requirements must be enforced and controlled during construction as poor compaction will result in higher lateral earth pressures induced on facing elements.

- Geosynthetic material should be wrapped behind the retaining wall face (instead of simply being placed in layers between facing blocks) to decrease load transfer to walls as well as erosion susceptibility. The GRS system should also be as free-draining as possible.

- Spread footings should be designed to effectively distribute surcharge loads over the entire surface area.

Ramp Connecting I-25 to I-70

Another project in Denver, Colorado (constructed in 1996) utilized a mechanically stabilized earth (MSE) wall that consisted of a welded wire fabric reinforced soil mass (versus the use of geotextile material) that was independent of its concrete panel facing unit. The facing panels were designed to be flexible enough to allow for movements of the soil mass to mobilize the resistance of the welded wire fabric (instead of transferring loads to the facing units).

Although different than a GRS system, this system is of interest as it shows the potential for creating a reinforced soil mass that is completely independent of its facing wall. A field inspection was conducted after 4.5 years of service and concluded the system was still in good condition (Abu-Hejleh et al., 2001a).

Founders/Meadows Bridge

The Founders/Meadows Bridge, a two-span structure approximately 225 ft long, was considered the first major bridge to be supported with a GRS foundation system (Abu-Hejleh et al., 2001c). The design of the bridge (completed in 1996) specified the use of a 12.5 ft by 2 ft reinforced concrete slab, bearing on a GRS backfill, for both of the bridge abutments. Each abutment contains several layers of UX6 geogrid spaced at approximately 16 in. for the bearing surface below the concrete footing. Layers of UX3 and UX 2 geogrid (also spaced at 16 in.) are utilized for the areas below the approach slab and roadway in the backfill. Each layer of geogrid is placed between layers of concrete blocks

(providing some degree of anchorage for the facing wall). One of the abutments, with an approximately 20 ft high facing wall consisting of concrete blocks, is shown in Figure 2-8. Embedment lengths of the geogrid layers vary from 26.25 ft (from the face of the wall) at the base layer to 52.7 ft for the upper portion of the abutment. Excavation for the base layer was continued until shallow bedrock was reached. Well-compacted Colorado DOT Class 1 crushed stone backfill was used in the abutment, with a size limit of 0.75 in. within the 1 ft region behind the facing wall. A cross-section of the abutments is shown in Figure 2-9.

As part of a research study, instrumentation was used to monitor wall movements, foundation settlement, vertical and lateral earth pressures, as well as geogrid tensile strains during construction and service of the GRS abutment systems. Except during construction (where geogrid tensile loads and lateral earth pressures on the wall were twice those expected), the Founders/Meadows Bridge abutment systems experienced loads and deflections significantly lower than those expected. Post-construction geogrid reinforcement loads (due to traffic live loads) were found to be approximately 50% of the load expected. This project and three other GRS abutment systems were all found to have negligible creep deformations under long-term loads and showed acceptable deformations under service loads up to approximately 4000 psf. In all cases, lateral earth pressures experienced on facing walls were low after construction was complete.

Due to the performance of the Founders/Meadows Bridge, the researchers suggest that GRS abutment systems be considered as a standard alternative to deep foundation bridge abutments for future projects. GRS abutment systems are also recommended for consideration with any project requiring a fill retaining structure (Abu-Hejleh et al., 2001c). To maximize strength and durability, it is recommended that a closer spacing of geogrid be used (around 6 in. to 12 in. on center), a wrap-around procedure used when placing the geogrid, a well-compacted granular backfill (having a friction angle of 40 degrees) used, and construction performed during warm, dry seasons.

A study performed 5 years after the Founders/Meadows Bridge was opened for service concluded that, after accounting for long-term effects and fluctuations in measured earth pressures, the wall for a GRS abutment system similar to the Founders/Meadows Bridge (in terms of loading and wall height) can be designed for a uniform lateral earth pressure of approximately 730 psf (Abu-Hejleh et al., 2006).

Figure 2-8. GRS abutment system for Founders/Meadows Bridge in Denver, Colorado (Abu-Hejleh et al., 2001c).
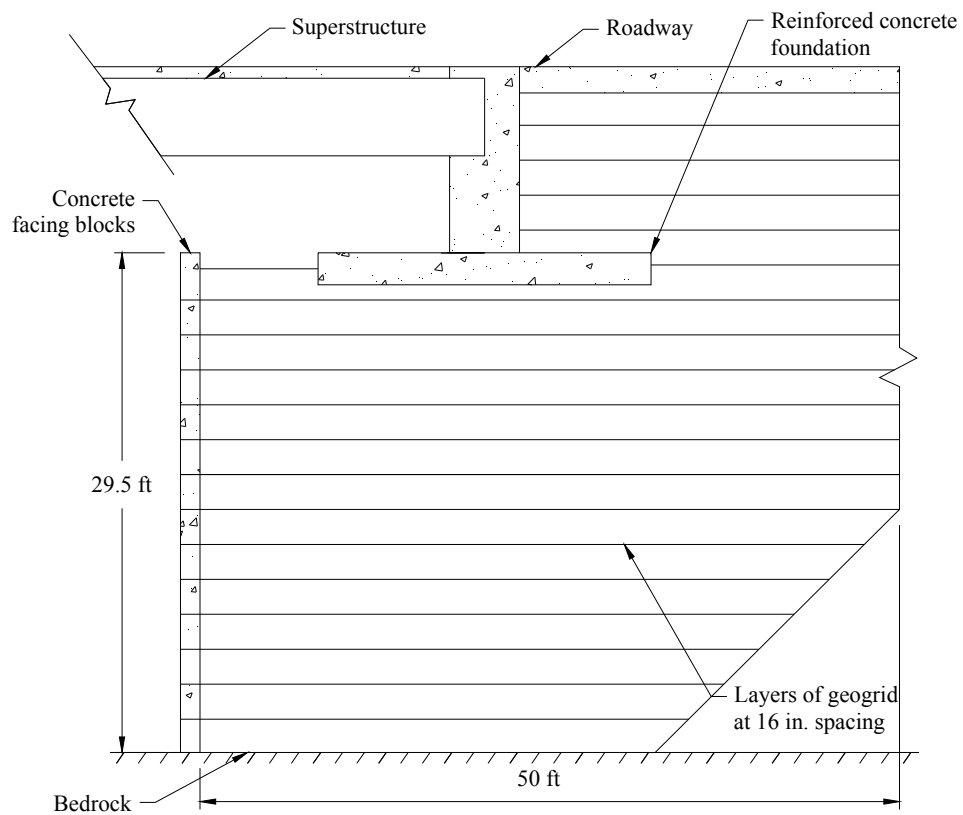
Figure 2-9. Cross-section of Founders/Meadows Bridge abutment (reproduced from Abu-Hejleh et al., 2001c).

Summary

Through a review of existing literature and construction projects, it is apparent that steel sheet piling are increasingly being considered as alternatives for the primary foundation elements in bridge abutments. Two main types of sheet pile abutments, axially loaded and cellular, provide alternatives for sites with varying subsurface conditions; the use of a GRS sheet pile abutment systems is a new alternative to be investigated. At project sites with strong soils or shallow bedrock, axially loaded sheet pile abutments can simultaneously provide high bearing capacities and a soil retention structure. In areas were soils are weak and driving to bedrock is not feasible, cellular abutments may provide an economical alternative to axially loaded piles; the use of GRS with cellular abutments (or similar systems) can provide further strength and durability.

CHAPTER 3. MATERIALS

Three commonly rolled Z-shaped sections are the PZ 22, PZ 27, PZ 35, and PZ 40. In sheet piling nomenclature, "P" denotes that it is steel sheet piling, "Z" denotes that it is a Z-shaped profile, and the remainder denotes the weight per sq ft of wall (Askar, 1988). Straight-web and Z-profile sheet piling as well as high-modulus (combi-wall) systems are readily available in the United States in various steel grades ranging in yield strengths from 39 ksi to 65 ksi.

Straight Web (PS) Sheet Piling

The PS pile provides minimal flexural strength as it is not designed for use in bending. PS piling is the section that is used for construction of cellular sheet pile structures. These sections have high-strength interlocks designed to withstand the tensile forces developed in the wall. A typical PS section is shown in Figure 3-1 with section dimensions and properties provided in Table 3-1.
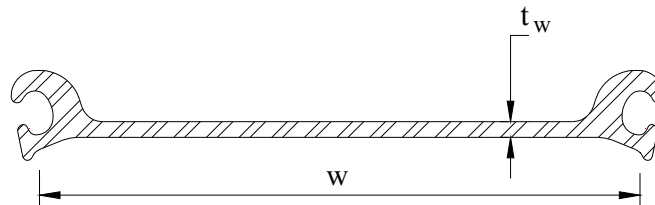
Figure 3-1. PS sheet pile section.

Table 3-1. Section dimensions and properties for commonly rolled PS sections.

Section	Width (w) in.	Web (t_w) in.	Max. Interlock Strength k/in	Min. Cell Dia. ft	Cross Sectional Area in^2/ft	Weight Pile lb/ft	Weight Wall lb/ft^2	Elastic Section Modulus in^3/sheet	Moment of Inertia in^4/sheet	Coating Area Single Pile ft^2/ft	Coating Area Wall Surface ft^2/ft^2
PS 27.5	19.69	0.4	24	30	8.09	45.1	27.5	3.3	5.3	3.65	1.11
PZ 31	19.69	0.5	24	30	9.12	50.9	31.0	3.3	5.3	3.65	1.11

Z-Profile (PZ and PZC) Sheet Piling

Z-profile steel sheet piling provides a section which is designed primarily for resisting flexural loads. They have a higher section modulus and moment of inertia per lb of steel compared to PS sections. A PZ-profile sheet pile section is shown in Figure 3-2a with section dimensions and properties provided

in Table 3-2. PZC sections are the most recent generation of sheet piling and have a higher ratio of section modulus to weight than traditional PZ sections. As a comparison, a PZC 17 section has a weight of approximately 80% of a PZ 27 section with both having the same flexural strength. While PZ sections are named for weight per sq ft of wall, PZC sections are listed by section modulus (a PZC 13 has a section modulus of 1300 cm^3/m). A PZC section is shown in Figure 3-2b with section dimensions and properties provided in Table 3-3.
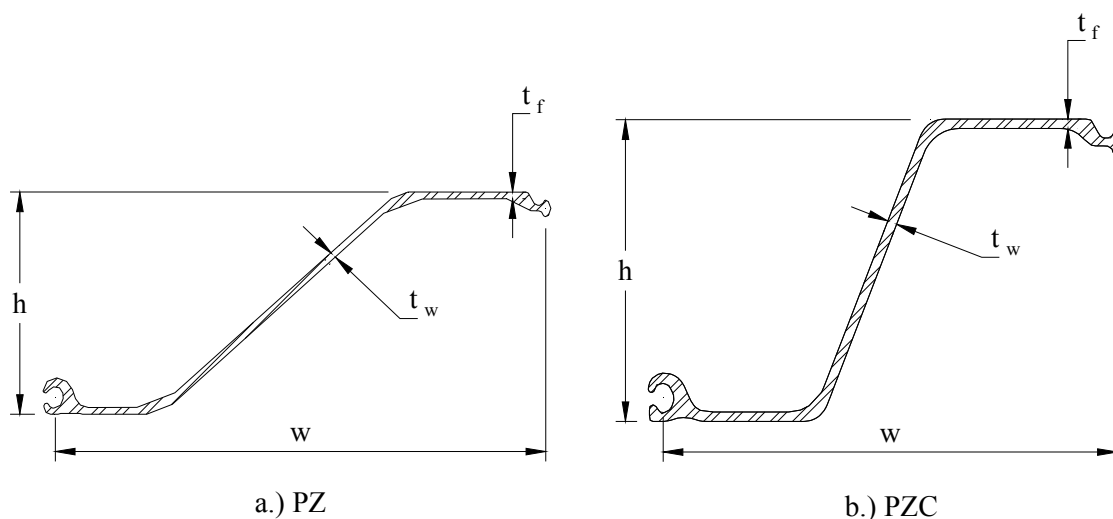
Figure 3-2. Z-profile sheet pile sections.

Table 3-2. Section properties for commonly rolled PZ sections.

Section	Width	Height	Thickness		Cross Sect. Area	Weight		Section Modulus		Mom. of Inertia	Coating Area	
			Flange	Wall		Pile	Wall	Elastic	Plastic		Pile	Wall Surface
	(w)	(h)	(t_f)	(t_w)								
	in.	in.	in.	in.	in^2/ft	lb/ft	lb/ft^2	in^3/ft	in^3/ft	in^4/ft	ft^2/ft	ft^2/ft^2
PZ 22	22.0	9.0	0.375	0.375	6.47	40.3	22.0	18.1	21.79	84.38	4.48	1.22
PZ 27	18.0	12.0	0.375	0.375	7.94	40.5	27.0	30.2	36.49	184.20	4.48	1.49
PZ 35	22.6	14.9	0.600	0.500	10.29	66.0	35.0	48.5	57.17	361.22	5.37	1.42
PZ 40	19.7	16.1	0.600	0.500	11.77	65.6	40.0	60.7	71.92	490.85	5.37	1.64

Table 3-3. Section properties for commonly rolled PZC sections.

Section	Width	Height	Thickness		Weight	Section Modulus	Moment of Inertia
			Flange	Wall	Wall	Elastic	
	(w)	(h)	(t_f)	(t_w)			
	in.	in.	in.	in.	lb/ft^2	in^3/ft	in^4/ft
PZC 13	27.88	12.56	0.375	0.375	21.7	24.2	152.0
PZC 18	25.00	15.25	0.375	0.375	24.2	33.5	255.5
PZC 26	27.88	17.70	0.600	0.525	31.8	48.4	428.1
PZC 36	24.80	19.93	0.655	0.600	39.6	67.0	667.4

High Modulus Sections

Large lateral pressures caused by surcharge loading may induce significant bending stresses in the sheet piling. The use of standard sheet pile sections would require large sections which may make the use of a sheet pile abutment uneconomical. In such cases, Dondelinger and Sommerfield (1986) recommend the use of combination walls. These walls combine light sheet pile sections with elements that are more efficient for flexural resistance (such as wide flange sections). An example of a system using a specialized high-modulus section is shown in Figure 3-3. The disadvantage to these systems is the special fabrication required. Although many steel manufacturers provide specialized wide-flange sections (HZ), adapters are readily available to allow the use of standard W and HP shapes in combination walls (see Figure 3-4).
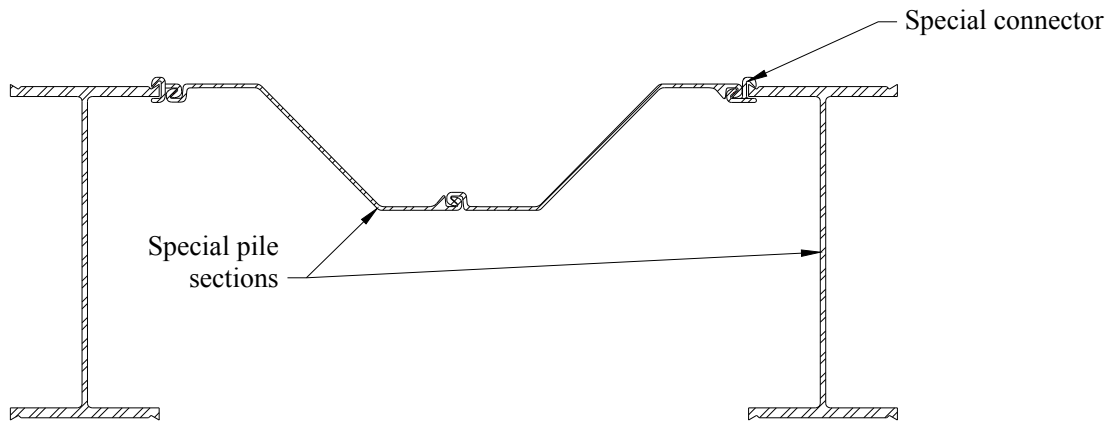
Figure 3-3. Combination wall using specialized high-modulus shapes.
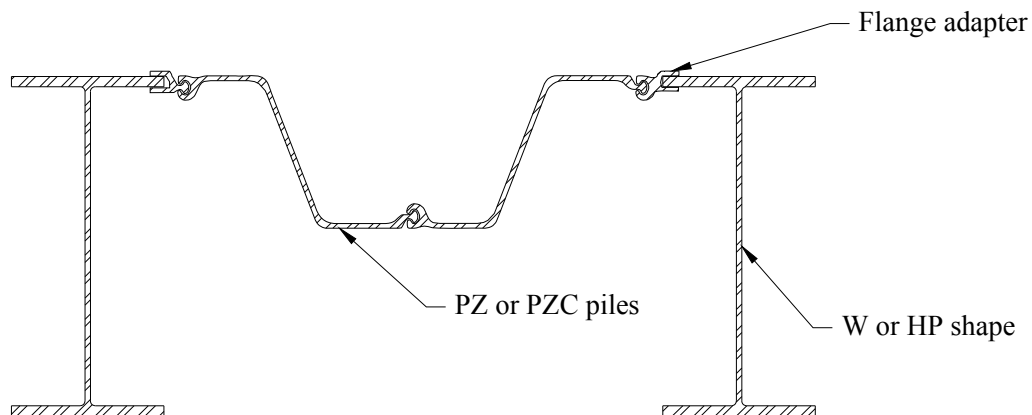
Figure 3-4. Combination wall system using standard shapes with flange adapters.

Vinyl Sheet Piling

Although steel is the primary material used in sheet pile construction, other materials are available which may provide benefits over steel. One alternative is vinyl sheet piling, made from polyvinyl chloride (PVC). In general, vinyl sheet piles are approximately half the cost of steel as well as being about 20% of the weight; these benefits have resulted in the successful construction of several retaining structures utilizing the material (Dutta and Vaidya, 2003).

Although vinyl is lighter and cheaper, steel is the superior material when it comes to structural properties. The average modulus of elasticity of the PVC piles is 300 ksi; vinyl sheet piles will deflect approximately 100 times more than similar steel piles under the same loads.

An analysis of the long-term applications of vinyl sheet piling was completed by Dutta and Vaidya (2003). Accelerated aging tests, including testing of ultraviolet radiation exposure and impact resistance degradation, were performed on the piles. Through these tests, severe discoloration from ultraviolet radiation and impact resistance degradation was observed. The primary concern, however, is the visco-elastic properties of the material. Over time the modulus of elasticity will undergo degradation under a static load, causing the piling to creep and show excessive deformation without any failure occurring. Creep is an issue which must be accounted for in the selection of piling; creep modulus information should be available from PVC sheet pile manufacturers (Dutta and Vaidya, 2003). Other concerns that are more prominent for PVC sheet piling than steel are vandalism and fire damage; extra effort must be made to remove combustible materials from the abutment areas.

Geogrid for GRS Systems

One type of material used for the construction of GRS system is geogrid and is available in uniaxial, biaxial, and triaxial designs; biaxial geogrid was utilized for project TR-568. Uniaxial geogrid provides soil reinforcement in one direction while biaxial provides strength in both the longitudinal cross-machine direction (XMD) and the transverse machine direction (MD). Triaxial geogrid is constructed to have no weak axis and thus provides strength in all directions. A geogrid material with strength in at least two directions is desirable for sheet pile bridge abutment systems to provide reinforcement transversely for the wingwalls.

Biaxial geogrid is stronger in the XMD due to the nature of its fabrication. As can be seen in Figure 3-5, the XMD consists of continuous fibers throughout the length of the material; the MD is not continuous and does not provided the same strength.
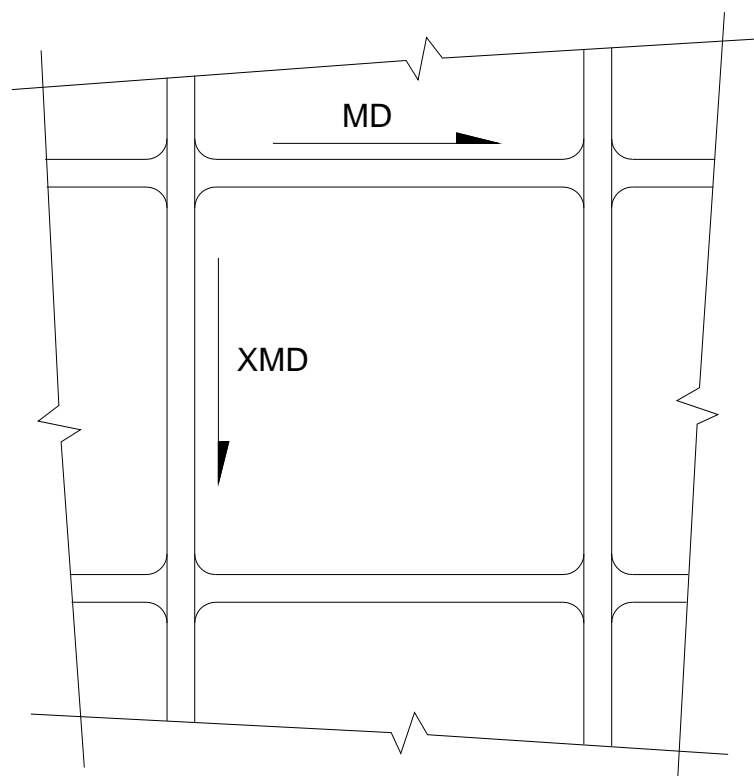
Figure 3-5. Diagram of geogrid material depicting MD and XMD.

Tensar$^{®}$ International Corporation provides several types of biaxial geogrid; select product specifications are provided in Table 3-4. The damage resistance of the material is considered to be the percentage of strength retained after installation damage (based on testing performed with gravel).

Table 3-4. Geogrid specifications.

Geogrid Type	Tensile strength @ 5% strain		Ultimate tensile strength		Damage Resistance
	MD	XMD	MD	XMD	
	(lb/ft)	(lb/ft)	(lb/ft)	(lb/ft)	%
BX1100	580	920	850	1300	90
BX1200	810	1340	1310	1970	90
BX1500	1200	1370	1850	2050	90

CHAPTER 4. EXPERIMENTAL APPROACH

This section outlines the general approach to the site investigation, design, construction, and load testing of the bridges included the project. Results and analysis for each bridge replacement project are presented in Chapter 5.

Geotechnical Site Investigation and Lab Analysis

The geotechnical investigation for each project provided soil parameters for the design of the sheet pile abutment foundation elements and backfill retention systems. The geotechnical investigation included the following:

- Site Reconnaissance
- Cone Penetrometer Testing
- Soil Borings
- Laboratory Testing

Field Investigation

The field investigation included a site reconnaissance to document site characteristics pertinent to the geotechnical investigation and development of a soil exploration program. The information collected during each field investigation was documented by a member of the ISU Research Team.

Site Reconnaissance

The site reconnaissance consisted of a visual review and documentation of site conditions pertinent to the geotechnical study at the time of the field exploration. Research team members walked the project sites and documented observations that were of significance to the geotechnical investigation. Such observations include topography, vegetation, trees, drainage, other structures present, and surface soil conditions.

Cone Penetrometer Testing

At selected sites, electronic piezo-cone penetrometer test (CPT) soundings were advanced to depths of interest or practical refusal. The CPT soundings were completed by Geotechnical Services, Inc. (GSI) located in Des Moines, Iowa.

The CPT soundings were advanced using a 20-ton capacity truck-mounted rig. The hydraulically advanced probe was a Hogentogler Type 2, 10-ton subtraction cone. The electronic cone has a 60° tip angle, tip area of 10 cm^2, net area ratio of 0.8, and a friction sleeve area of 150 cm^2. The cone was advanced at a rate of approximately 1 in/sec. The data collection system recorded data at 5 cm intervals. The CPT testing was performed in accordance with ASTM D5778 (2007).

The soil behavior types, based on the Simplified Soil Classification Chart for Electric Friction Cone (Robertson, 1989), were determined from each CPT sounding and are a general indication of the soils encountered at each site. Behavior types are displayed as values (from 1 through 12) with 3 representing clay, 6 representing sandy to clayey silt, 9 representing sand, and 10 and above representing stiff sand or other harder materials.

Soil Borings

Soil borings were drilled and sampled using the truck-mounted drilling rig shown in Figure 4-1. The soil boring logs, which are the source of the field and laboratory data collected, provide details of the conditions encountered at each boring location.

a.) Drilling rig   b.) Auger

Figure 4-1. Drilling rig used for collection of soil borings.

Soil borings were advanced by rotating a continuous-flight earth auger (4 in. diameter) with the drilling rig, removing the auger from the boring, and cleaning the cuttings from the auger before sampling or reinserting the auger into the bore hole. This technique allowed for the observation of soil cuttings and description of soil conditions encountered and also allowed for the detection of free groundwater within the borings.

The soil sampling program included the collection of undisturbed and disturbed soil samples. Relatively undisturbed samples were obtained by pushing a Shelby tube sampler (3 in. diameter) a distance of 2 ft into the soil in general accordance with ASTM D1587 (2008). Depths at which these undisturbed samples were obtained are indicated in the "Sample" column of the boring logs presented in the Appendices.

After the Shelby tube was removed from the boring, the sample was visually classified based on the exposed soil in the bottom of the tube. Relative strength estimates of the sample were obtained by penetrometer readings. These penetrometer readings (in units of tsf) are given in the "Field Data" column of the boring logs. The Shelby tube was capped and sealed in the field for transportation to the ISU soils laboratory.

Disturbed soil samples were also collected by the auger method in accordance with ASTM D1452 (2009). The spiral-type (solid-stem) auger consisted of a flat thin metal strip in a spiral configuration of uniform pitch capable of attaching a shaft or extension at the opposite end. Depths at which these auger samples were obtained are indicated by the letters "AG" in the "Samples" column of the boring logs presented in the Appendices. The soil content from the auger was visually classified, labeled, and placed in a sealed container to prevent moisture loss during transportation to the ISU soils laboratory. Upon completion of the field investigation phase of this study, the boreholes were filled with soil cuttings from the exploration.

Laboratory Testing

As previously noted, the soil samples were delivered to the ISU soils laboratory for testing. The principal investigator reviewed the soil boring logs developed in the field and assigned laboratory testing on select samples to provide the data necessary for the anticipated designs. It should be noted

that laboratory testing varied for each site and the specific tests performed are outlined in the corresponding section for each project.

Consolidated-undrained (CU) tests were performed in general accordance with ASTM D6528 (2007) to determine engineering properties of the soils encountered in the soil borings. The shear strength of selected undisturbed soil samples was determined by means of unconfined compression tests performed in general accordance with ASTM D2166 (2006).

Moisture content tests were performed on select boring samples to determine the classification and shrink/swell potential of the soils encountered. These tests were performed in general accordance with ASTM D2216 (2005). The undrained shear strength of the selected undisturbed soil samples was determined by means of unconsolidated undrained (UU) triaxial compression tests performed in general accordance with ASTM D2850 (2007).

Liquid limit (LL) and plastic limit (PL) determinations were performed to assist in classification by the Unified Soil Classification System (USCS). These tests were performed in general accordance with ASTM D4318 (2005). The plasticity index (PI) was calculated as LL - PL for each Atterberg limit determination. Selected soil samples were tested to determine the particle gradation to aid in classification and to further understand the engineering characteristics; these tests were performed in general accordance with ASTM D421 and ASTM D422.

Consolidation tests were also performed to provide parameters for consolidation settlement estimation according to ASTM D2435 (2004).

Site Conditions

In geotechnical investigations of this nature (local topography and surface conditions), geologic setting and site-specific soil and groundwater conditions are important. Site conditions for each project are summarized in the corresponding sections.

Analysis and Design Methods

After completing a geotechnical site investigation, selection of the wall type is the first step in design. Two common types are cantilever and anchored walls. The American Society of Civil Engineers (ASCE, 1996) recommends the use of anchored walls whenever lateral displacements are a consideration (which is the case in a laterally and axially loaded member such as an abutment). Another consideration is the type of steel sheet pile section to be used. Common sections are straight-web, arched, or Z-shaped profiles. The use of a Z-shaped profile is recommended whenever bending is likely to be the controlling factor in design.

Bearing Capacity

The bearing capacity of steel sheet piling is assumed to be derived from end-bearing and skin friction resistance (Chung, 2004). For the purposes of calculating ultimate bearing capacity, steel sheet pile retaining wall abutments can be considered as driven piling. In Equations (1) through (3), the American Association of State Highway and Transportation Officials (AASHTO, 1998) defines the ultimate strength of driven piles:

$$Q_r = \phi_{qp}Q_p + \phi_{qs}Q_s \tag{1}$$

$$Q_p = q_pA_p \tag{2}$$

$$Q_s = q_sA_s \tag{3}$$

where:

Q_r = bearing resistance of a single pile

Q_p = bearing resistance due to pile tip

Q_s = bearing resistance due to skin friction

q_p = unit pile tip resistance

q_s = unit pile shaft resistance

A_p = cross-sectional area of pile tip

A_s = surface area of pile shaft

ϕ_{qp} = resistance factor for pile tip resistance

ϕ_{qs} = resistance factor for pile shaft resistance

Pile Tip Resistance

The unit pile tip resistance, in saturated clay, is defined by Equation (4) (AASHTO, Section 10.7.3.3.3-1, 1998):

$$q_p = 9S_u \tag{4}$$

where:

S_u = undrained shear strength of clay (tsf)

According to the Steel Construction Institute (SCI, 1998) the development of a soil plug during driving is negligible for sheet piling making the area of the pile tip, A_p, equivalent to the cross-sectional area of the sheet pile; when H-piles are used, the presence of soil plugging may be considered.

Pile Shaft Resistance

There are three methods outlined by AASHTO (1998) Section 10.7.3.3.2 that can be used for estimating pile shaft resistance: the α-method, β-method, and λ-method. The α-method relates the adhesion between the pile and the surrounding clay to the undrained shear strength of the clay by an adhesion factor; this method is considered to provide reasonable results for displacement and non-displacement piles in clay. The β-method relates skin friction to the vertical effective stress and is recommended for use with piles in normally consolidated or lightly overconsolidated clays; the method tends to overestimate skin friction for heavily overconsolidated soils (AASHTO, Section C10.7.3.3.2, 1998). The λ-method, which relates unit skin friction to passive earth pressure based on vertical effective stress, will be the only method outlined within this review.

Unit skin friction may be determined using Equation (5):

$$q_s = \lambda(\sigma'_v + 2S_u) \tag{5}$$

where:

$(\sigma'_v + 2S_u)$ = passive lateral earth pressure (tsf)
λ = surface depth coefficient (AASHTO, Figure 10.7.3.3.2c-1, 1998)

For steel sheet piling, the SCI (1998) states that the coated area of the pile shaft for friction resistance, A_s, can be conservatively taken as 80% of the surface area of the pile.

Because the abutment will be acting as a retaining structure during loading, consideration must be given to the soil behavior when estimating pile capacity. According to the SCI (1998), "soil on the active or retained side of the wall moves down relative to the wall to mobilize friction in the beneficial direction…" On the passive side of the wall, mobilization of friction is obtained by upward soil displacement. The significance of this difference is that, as the abutment undergoes axial loading, the piling will displace downward and reduce the shaft friction that is mobilized on the active (retained) side of the abutment. To account for this effect, it may be conservatively assumed that pile shaft resistance is only developed where the pile is in contact with the passive soil zone. If sheet pile depths are greater than those required for stability, it can be assumed that the remaining length of pile will develop friction resistance on both faces of the pile (SCI, 1998).

Earth Pressure Loads

The amount of vertical earth pressure transferred laterally to a retaining wall is dependent on the flexibility of the wall. AASHTO (1998) Section C3.11.1 states that a wall that can move away from the retained soil mass shall be designed between the active and at-rest conditions depending on the magnitude of tolerable movement of the wall; approximate top wall movements, Δ, relative to wall height, H, required to develop minimum active and maximum passive earth pressure conditions are provided in Table 4-1. Determination of lateral loads may be accomplished using any of the applicable earth pressure theories: Rankine, Coulomb, and Log-Spiral. The Coulomb or Log-Spiral theories are considered more accurate because they account for friction between the retaining wall and soil. In the active pressure case, both Coulomb and Log-Spiral theories produce similar results. For the passive case, however, Coulomb theory must be used with an appropriate factor of safety since it predicts unrealistically high soil pressures compared to Log-Spiral theory (United States Steel, 1974). The ASCE (1996) recommends Coulomb theory to be used for the design of sheet pile walls. Coulomb theory determines lateral effective earth pressure as proportional to vertical effective pressure (due to soil weight, pore water pressure, and any surface loading) by an earth pressure coefficient, K, as shown in Equation (6):

$$K = \frac{\sigma'_h}{\sigma'_v} \tag{6}$$

For the active (minimum) limit-state, the pressure is given by Equation (7):

$$p_a = \gamma z K_a - 2c\sqrt{K_a} \tag{7}$$

and the passive (maximum) limit-state is given by Equation (8):

$$p_p = \gamma z K_p - 2c\sqrt{K_p} \tag{8}$$

Where K_a and K_p (active and passive pressure coefficients) are given in Equations (9) and (10):

$$K_a = \frac{\cos^2(\phi-\theta)}{\cos^2\theta\cos(\theta+\delta)\left[1+\sqrt{\frac{\sin(\phi+\delta)\sin(\phi-\beta)}{\cos(\delta+\phi)\cos(\beta-\phi)}}\right]^2} \tag{9}$$

$$K_p = \frac{\cos^2(\phi-\theta)}{\cos^2\theta\cos(\theta+\delta)\left[1-\sqrt{\frac{\sin(\phi+\delta)\sin(\phi-\beta)}{\cos(\delta+\phi)\cos(\beta-\phi)}}\right]^2} \tag{10}$$

where:

σ'_h = lateral effective earth pressure

σ'_v = vertical effective earth pressure

γ = unit weight of homogeneous soil

ϕ = angle of internal soil friction

c = cohesive strength of the soil

δ = angle of wall friction

θ = angle between the wall and the failure plane

z = depth below the ground surface

β = slope of the soil surface

Equations for earth pressure coefficient calculations are also provided by AASHTO (1998) Section 3.11.5. For active lateral earth pressure, the method is the same as presented in Equation (9). The passive lateral earth pressure coefficient for a soil is determined using AASHTO (1998) Figure 3.11.5.4-1 and was developed using log-spiral theory which is more accurate than Equation (10).

Table 4-1. Approximate values of relative movement required to reach minimum active and maximum passive earth pressure conditions (AASHTO, Table C3.11.1-1, 1998).

Type of Backfill	Values of Δ/H	
	Active	Passive
Dense sand	0.001	0.01
Medium-dense sand	0.002	0.02
Loose sand	0.004	0.04
Compacted silt	0.002	0.02
Compacted lean clay	0.010	0.05
Compacted fat clay	0.010	0.05

Surcharge loads also have an impact on the lateral earth pressure. The various types of surcharge loads are uniform, strip, line, ramp, triangular, area, and point loads. While a uniform surcharge load will increase the vertical pressure an amount equal to the magnitude of the load, the other types of surcharge loads increase lateral pressure by multi-variable functions. These functions are provided in AASHTO (1998) Section 3.11.6 and are presented below. For a uniformly loaded strip (parallel to the wall) applying pressure, p (ksf), as shown in Figure 4-2a, the lateral pressure, Δp_H (ksf), is given by Equation (11):

$$\Delta p_H = \frac{2p}{\pi}(\alpha - \sin\alpha\cos(\alpha + 2\delta)) \tag{11}$$

For a point load, P (kip), as shown in Figure 4-2b, the lateral pressure is given by Equation (12):

$$\Delta p_H = \frac{P}{\pi R^2}\left[\frac{3ZX^2}{R^3} - \frac{R(1-2v)}{R+Z}\right] \tag{12}$$

For an infinitely long line load, Q (k/ft), parallel to the wall (same dimensions as Figure 4-2b), the lateral pressure is given by Equation (13):

$$\Delta p_H = \frac{4Q}{\pi}\frac{X^2Z}{R^4} \tag{13}$$

For a finite line load, Q (k/ft), perpendicular to the wall, as shown in Figure 4-2c, the lateral pressure is given by Equation (14):

$$\Delta p_H = \frac{Q}{\pi Z}\left(\frac{1}{A^3} - \frac{1-2v}{A+\frac{Z}{X_2}} - \frac{1}{B^3} + \frac{1-2v}{B+\frac{Z}{X_1}}\right) \tag{14}$$

in which:

$$A = \sqrt{1 + \left(\frac{z}{x_2}\right)^2} \text{ and } B = \sqrt{1 + \left(\frac{z}{x_1}\right)^2}$$

where:

a = angle shown in Figure 4-2a (rad)

d = angle shown in Figure 4-2a (rad)

v = Poisson's ratio for the retained soil

R = radial distance from point of load application to elevation of point on wall (ft)

x = horizontal distance from wall to point of load application (ft)

Z = vertical distance from point of load application to elevation of point on wall (ft)

x_1 = distance from wall to start of line load (ft)

x_2 = length of live load (ft)
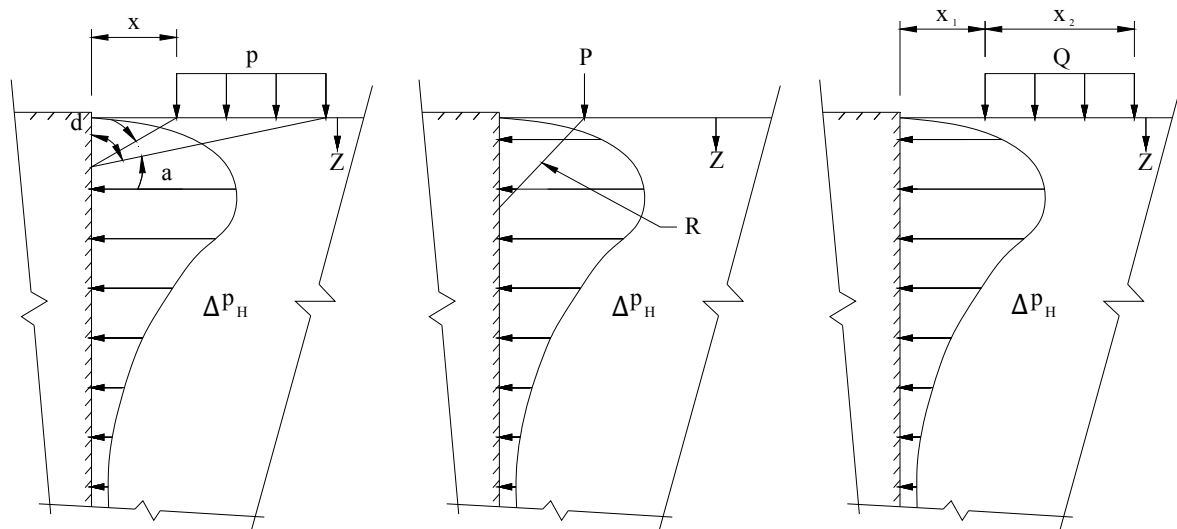
a.) Uniformly loaded strip   b.) Point load   c.) Finite line load perpendicular to wall

Figure 4-2. Diagram of surcharge load effects on wall (reproduced from AASHTO, 1998).

For live load surcharge, Δp_{ll} (ksf), on the retained backfill (due to vehicles approaching the superstructure), AASHTO (1998) Section 3.11.6.4 recommends the use of the Equation (15):

$$\Delta p_{ll} = k * \gamma_s * h_{eq} \tag{15}$$

where:

  k = coefficient of lateral earth pressure

  γ_s = weight of backfill material (kcf)

  h_{eq} = equivalent height of soil for the design truck determined from Table 4-2 (ft)

Table 4-2. Equivalent soil height for vehicular loading (reproduced from AASHTO, 1998).

Wall height (ft)	h_{eq} (ft)
≤ 5.0	5.5
10.0	4.0
20.0	2.5
≥ 30.0	2.0

AASHTO (1998) also recommends that abutments be made free-draining whenever possible. If not, the effect of hydrostatic water pressure must be added to earth pressure. If heavy compaction equipment is used within the vicinity of the wall, the effect of additional earth pressures shall be taken into account. Duncan et al., (1991) provide a method for estimating compaction induced lateral earth pressures based on several factors. For soils compacted by rollers the compaction induced lateral earth pressure, $\Delta\sigma_H$, based on roller load (equivalent line load, $q = \frac{Static+Dynamic\ Load}{Roller\ Width}$) is presented in Table 4-3. For soils compacted by vibratory plates the compaction induced lateral earth pressure, $\Delta\sigma_H$, based on plate load (compaction pressure, $q = \frac{Static+Dynamic\ Load}{Plate\ Area}$) is presented in Table 4-4. To account for other compaction conditions, the reader is referred to Duncan et al., (1991) for various adjustment factors.

Table 4-3. Total induced lateral earth pressure for compaction of 120 pcf backfill by roller in 6 in. lifts a distance of 6 in. from the wall (8 ft total depth of compacted material).

$\varphi' = 25°$		$\varphi' = 30°$	
q (lb/in)	$\Delta\sigma_H$ (psf)	q (lb/in)	$\Delta\sigma_H$ (psf)
200	325	200	400
400	470	400	580
600	624	600	768
800	780	800	960

Table 4-4. Total induced lateral earth pressure for compaction of 120 pcf backfill by vibratory plate in 4 in. lifts next to wall (8 ft total depth of compacted material).

$\varphi' = 25°$		$\varphi' = 30°$	
q (psi)	$\Delta\sigma_H$ (psf)	q (psi)	$\Delta\sigma_H$ (psf)
4	250	4	260
8	310	8	340
12	380	12	410
16	430	16	460

Failure Mechanisms

When analyzed as a retaining structure, the ASCE (1996) presents several failure modes for a steel sheet pile system that must be considered in design: deep-seated failure, rotational failure due to inadequate pile penetration, overstressing of the sheet pile, and anchorage component failure (see Figure 4-3). In the case of piles under combined axial and lateral loads, second-order bending effects reduce the lateral load capacity of the wall; an investigation of the load capacity of piles subjected to combined loading was performed by Greimann (1987).

Deep-seated failure occurs when the entire soil mass containing the retaining wall system rotates along a single failure surface. This type of failure is a soil failure only, independent of the structural capacities of the wall and any anchorage system. Another form of rotational failure occurs when the retaining wall rotates due to the exerted soil pressures. This type of failure can be prevented by either adequate wall penetration into the soil or by implementing an anchorage system.

Other failures that can occur in the retaining wall system are sheet pile overstressing, passive anchorage failure, tie rod failure, and wale system failure. Overstressing of the pile due to both lateral and axial loads will result in the development of a plastic hinge leading to a failure. A passive anchorage failure occurs when the anchor moves laterally within the soil due to the force exerted on it. The tie rod may fail if it does not have the required tensile capacity, and the waler system (the method of connecting the anchor to the sheet pile wall) may have a bearing failure if loads are not adequately distributed.
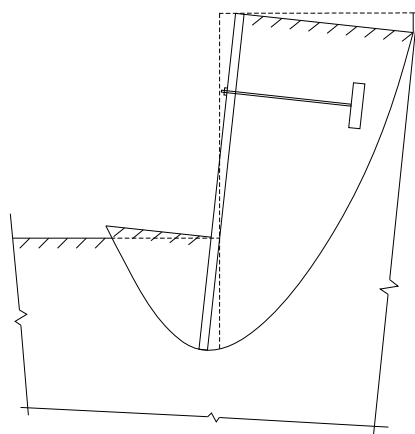
a.) Deep-seated failure
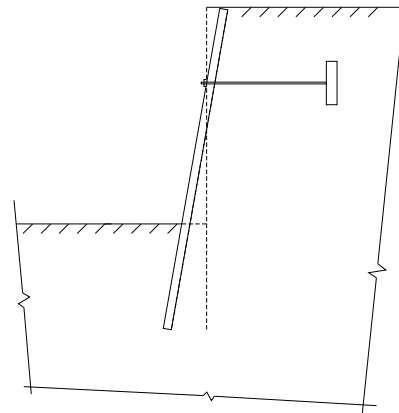
b.) Rotational failure
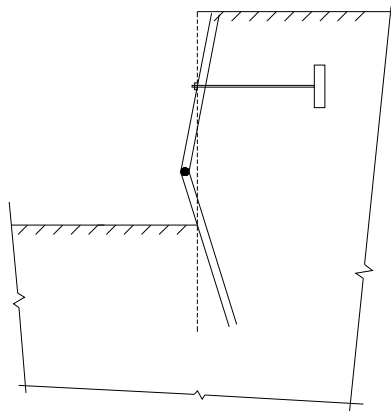
c.) Flexural failure of sheet piling
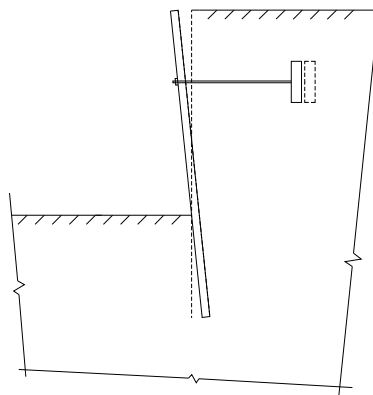
d.) Passive resistance failure of deadman
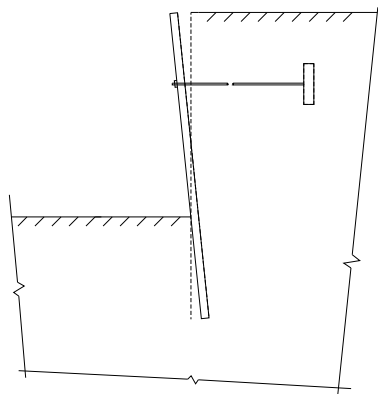
e.) Tensile rupture of tie rod
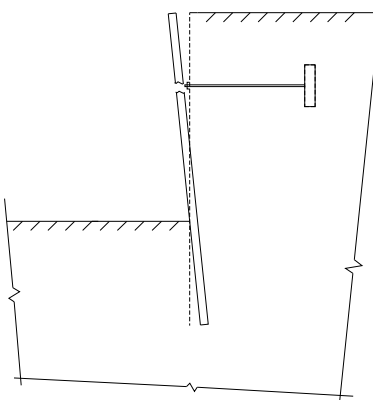
f.) Failure of waler system component

Figure 4-3. Failure modes for sheet pile retaining wall (reproduced from ASCE, 1996).

Design Methods and Assumptions

The ASCE (1996) presents design methods for both cantilever and anchored walls. For analysis of lateral loads in anchored walls, the free earth support method is recommended for its simplicity and economy in design (Chung, 2004). The free earth method tends to overestimate maximum moments however by using Rowe's moment reduction curves (ASCE, 1996) one can compensate for this overestimation.

The free earth method uses a few key assumptions to simplify analysis. The first assumption is that the anchor acts a simple support that the entire sheet pile wall rotates about (as a rigid body). Also, although rotation would tend to cause passive soil pressures above the anchor, the entire wall is assumed to be subject to the net active pressure distribution. Using the free earth method, the embedment depth is first determined by moment equilibrium about the anchor point; the anchor force is then determined using lateral force equilibrium. Since anchor position will affect both anchor force and wall embedment depth, multiple anchor positions must be investigated to determine the most economic location. Methods for anchor system design are outlined in the ASCE (1996).

For structural design of the sheet piling, support conditions must be assumed for a particular wall type. The cantilever wall is assumed to be fixed at the bottom of the wall, while the anchored wall is composed of simple supports at the bottom of the wall and the anchor location (ASCE, 1996).

Structural Design

Methods by Allowable Stress

Once design moments and shears are determined, a section must be selected that satisfies design criteria. For steel sheet pile walls under usual load conditions, the allowable combined bending and axial load stresses, f_b, and shear stresses, f_v, are determined in Equations (16) and (17):

$$f_b = 0.5f_y \tag{16}$$

$$f_v = 0.33f_y \tag{17}$$

where f_y is the yield stress of the steel. For unusual and extreme loadings, the allowable stresses may be increased by 33% and 75%, respectively (ASCE, 1996).

Due to effects of corrosion, abrasion, and other such problems on structural integrity, certain requirements must be met. For anchored walls, the minimum required section modulus is given by Equation (18):

$$S_{min} = [M_{des} + T_{av}(y_m + e_a)]/f_b \tag{18}$$

where:

M_{des} = design bending moment

T_{av} = axial component of anchor force (if any)

y_m = deflection at elevation of maximum moment

e_a = eccentricity due to anchor connection

The minimum required shear area is given by Equation (19):

$$A_{v,min} = V_{max}/f_v \tag{19}$$

where:

$A_{v,\ min}$ = minimum shear are per ft of wall

V_{max} = maximum shear per ft of wall

f_v = allowable shear stress of material

When combined loading is present (other than the axial load due to the anchor force), the minimum required section modulus is given by Equation (20):

$$S_{min} = [M_{max} + T_{av}(y_m + e_a) + P(y_m - y_p + e_p)]/f_b \tag{20}$$

where:

P = additional axial load

y_p = deflection at the point of application of P

e_p = eccentricity of the point of application of P

The ASCE (1996) recommends that $[T_{av}(y_m + e_a) + P(y_m - y_p + e_p)] < M_{max}/10$ unless it can be shown that buckling is of no concern.

Due to the conservative assumptions made in anchor wall design, the ASCE (1996) recommends the use of Rowe's moment reduction factor. The reduced design moment is given by Equation (21):

$$M_{des} = (R_m)(M_{max}) \tag{21}$$

where R_m is a factor obtained from ASCE (1996) Figure 6-4.

Other moment reductions are available for both granular and cohesive foundation soils. The ASCE (1996) also provides required cross section properties for cantilever walls and design methods for tie rod and wale systems.

Methods by LRFD

For sections under combined axial compression and flexure, AASHTO (1998) requires that, if $\frac{P_u}{P_r} < 0.2$, Equation (22) must be satisfied:

$$\frac{P_u}{2.0P_r} + \left(\frac{M_{ux}}{M_{rx}} + \frac{M_{uy}}{M_{ry}}\right) \le 1.0 \tag{22}$$

If $\frac{P_u}{P_r} \ge 0.2$, then Equation (23) must be satisfied:

$$\frac{P_u}{P_r} + \frac{8}{9}\left(\frac{M_{ux}}{M_{rx}} + \frac{M_{uy}}{M_{ry}}\right) \le 1.0 \tag{23}$$

where:

P_u = axial compressive load

M_{ux} = flexural moment about the x-axis

M_{uy} = flexural moment about the y-axis

P_r = compressive resistance (AASHTO, Section 6.9.2.1, 1998)

M_{rx} = flexural resistance about the x-axis (AASHTO, Section 6.10.4 and 6.12, 1998)

M_{ry} = flexural resistance about the y-axis (AASHTO, Section 6.10, 6.11 and 6.12, 1998)

It should be noted that all loads used in the equations are the maximum loads, including second-order effects, calculated using appropriate load factors and combinations provided in AASHTO (1998) Section 3.4.

AASHTO (1998) Section 6.9.3 requires that all primary compressions members must satisfy the slenderness limitations imposed by Equation (24):

$$\frac{K\ell}{r} \leq 120 \tag{24}$$

where:

K = effective length factor (AASHTO, Section 4.6.2.5, 1998)
ℓ = unbraced length of the member
r = minimum radius of gyration of the member

Requirements for shear resistance are provided in Sections 6.10, 6.11, and 6.12 (AASHTO, 1998). It is recommended that the designs of all elements of the bridge structure are performed according to the AASHTO (1998) LRFD bridge design specification.

Other Steel Sheet Pile Design Considerations

In the design of sheet pile walls, significant cost savings can be achieved using plastic design methods. Previously, steel sheet pile wall design has used the elastic section modulus for member selection. Plastic design allows for the development of a fully plastic section within the wall, creating a plastic hinge. The use of plastic design methods for sheet piling material selection may result in savings of up to 35% (Kort, 2002).

Though it is common practice in other areas of the steel industry, plastic design has not yet become a standard in the design of sheet piling. Elastic design, which is most commonly used, requires that the extreme fibers of a selected section must be less than or equal to the yield stress of the material under design loads. This design method, however, is conservative due to the ductile properties of steel.

In plastic design theory, once the outermost fibers begin to yield, additional load will not cause catastrophic failure. Instead, the fibers furthest from the neutral axis begin yielding, progressing until

the entire section has yielded; this is the plastic limit-state. Any additional loading beyond the plastic limit-state will induce rotation about this section known as a "plastic hinge."

Plastic design is considered an acceptable method because, although significant deformation will occur, design loads will only be reached in instances of extreme loading. According to Kort (2002), designing the section to fully develop the plastic limit alone will save approximately 15% to 20% in material costs. By allowing for rotation about the plastic hinge (and thus formation of multiple plastic hinge locations), additional cost savings up to 20% may be achieved.

Design of GRS systems

The use of a GRS system significantly increases the bearing capacity of the backfill soil. Each layer of geogrid in the backfill soil is analogous to steel reinforcement in concrete. When a vertical compressive load is placed on a soil, both vertical and horizontal deformations occur. The amount of horizontal deformation that occurs under a given vertical deformation is defined as Poisson's Ratio and is approximately 50% for typical soils. The presence of geogrid material reinforces the soil by developing internal strain energy (in tension) as the soil undergoes horizontal deformation. Essentially, for a soil that undergoes a given deformation, δ, under a vertical load, P_1, the presence of geogrid (or other similar types of soil reinforcement) would require a greater vertical load, P_2, to induce the same amount of soil deformation (see Figure 4-4); the bearing capacity of the soil has increased ($P_2 > P_1$).

a.) Unreinforced   b.) Geogrid reinforced
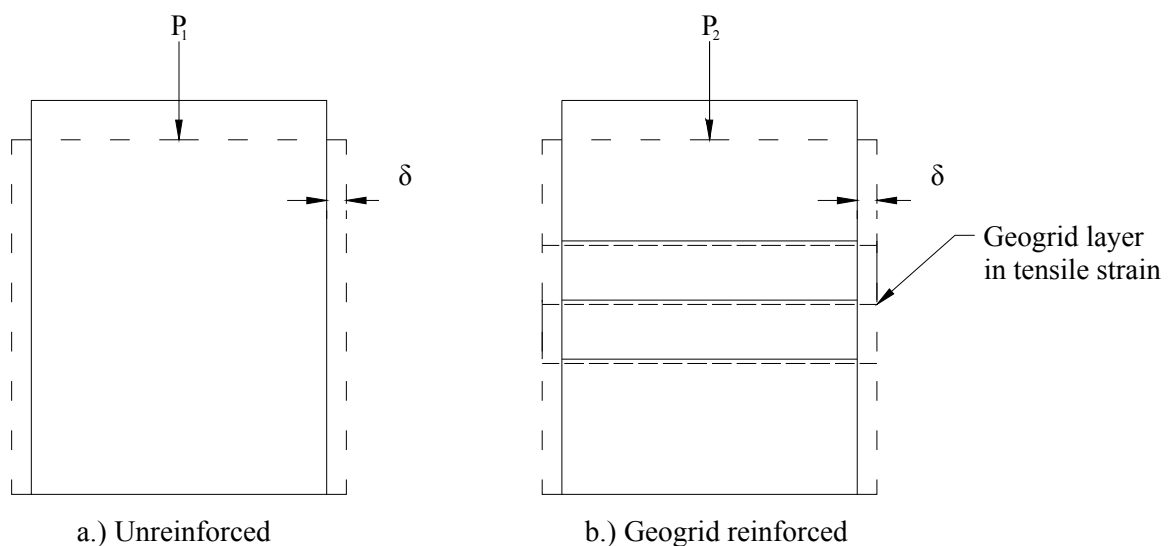
Figure 4-4. Deformation of soil mass under applied vertical load.

<u>Internal Strength of Geogrid Reinforcement</u>

Each layer of geogrid must be designed to resist the total lateral earth pressure at the corresponding location in the GRS system. To resist the maximum lateral earth pressure, σ_{max}, for a certain vertical spacing, S_v, the ultimate strength of the geogrid, T_{ult}, must satisfy Equation (25):

$$T_{ult} \geq \sigma_{max} * S_v \tag{25}$$

If Equation (25) is not satisfied, an alternative to selecting stronger material would be to reduce the vertical spacing of geogrid layers.

<u>External Stability of Reinforcement</u>

To develop the full strength of the geogrid material, sufficient embedment must be provided or another means of mechanically developing the strength (such as wrapping each layer into the layer above as shown in Figure B2 of Appendix B). To provide sufficient embedment length, the geogrid layer must extend beyond the active zone of the backfill (shown in Figure B14 for the Boone County project) soil a minimum length that develops the ultimate strength of the material through friction against the surrounding soil.

<u>Other Design Considerations</u>

The factor of safety of the GRS mass must also be satisfied for sliding, overturning, slumping failure, and bearing capacity on the material at the base of the excavation.

Design Summary and Recommendations

A detailed site investigation should be performed for all bridge designs considering the use of a steel sheet pile bridge abutment and backfill retaining system to determine the type (axially loaded or GRS system) best suited for site conditions present; the designer may refer to the selection flowchart presented in Figure 4-5 for guidance in determining the sheet pile bridge abutment system best suited for the project site conditions. A summary of the design of each type of sheet pile bridge abutment and backfill retaining system is presented in this section.
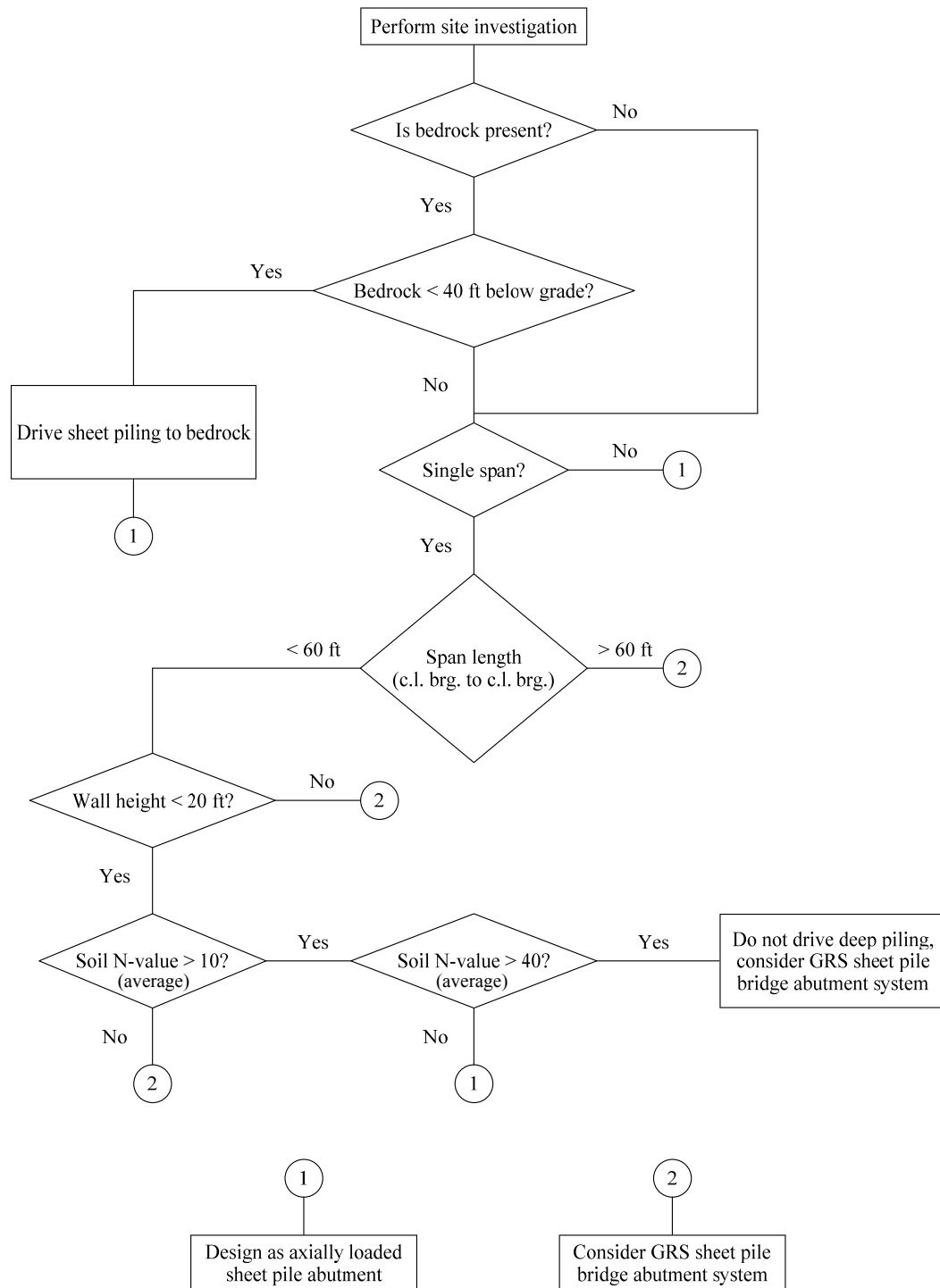
Figure 4-5. Flowchart for preliminary selection of sheet pile bridge abutment system.

Design Summary for Axially Loaded Sheet Pile Bridge Abutment and Backfill Retaining Systems

1. Determine design loads on the sheet pile wall. For estimating lateral earth pressure, refer to AASHTO (1998) Section 3.11.5. Consideration must be given to the flexibility of the wall, which is dependent on wall height and lateral restraint, when determining earth pressure (at-rest or active); if short piles are restrained against lateral movement at the top of the wall (i.e., bridge superstructure), at-rest earth pressure conditions should be assumed. Effects of surcharge loads on the backfill may be approximated using AASHTO (1998) Section 3.11.6; the equations in this section are conservative for a flexible wall. For design according to HL-93 loading, AASHTO (1998) Section 3.11.6.2 provides an equivalent surcharge pressure to account for vehicular live load on the backfill soil. For all types of loading in the projects included in this thesis, a load distribution of 10 ft width per design lane was used for live loads; this was determined to be a conservative assumption from the test data analysis presented later in this report.

2. Select location of the anchorage system. Various positions may be investigated to determine the optimum location for minimizing the embedment depth and required anchor force. In general, a distance below the top of the sheet pile wall of approximately 25% to 33% of total wall height is the most efficient. Consideration should be given to the exclusion of an anchor system for significant cost reduction; the need for temporary bracing of a cantilevered sheet pile wall during construction must be investigated.

3. Determine preliminary depth of piling. If bedrock is within 40 ft of grade, piling should be driven into bedrock; an assumed embedment depth of 5 ft is recommended for specifying pile length. If driving to bedrock is not feasible, the minimum required embedment depth may be determined by analyzing the wall as a beam with a single pinned support at the location of the tie rods; the length of beam required for equilibrium of lateral forces on the wall provides the minimum embedment depth. For an axially loaded abutment, pile length will typically be controlled by the required depth for development of axial capacity through soil friction. As mentioned previously in this chapter, it should be conservatively assumed that pile shaft resistance is only developed where the pile is in contact with the passive soil zone (the opposite side of the retained backfill). If sheet pile depths are greater than those required for stability, it can be assumed that the remaining length of pile will develop friction (continued)

resistance on both faces of the pile. If the bridge is over a stream, design pile depth must include the effects of scour; depending on local conditions, scour during flooding may be significant (10 ft or more) and can be estimated using methods presented by Davis and Richardson (2001).

4. Design sheet pile and superstructure interface. Reinforced concrete caps, steel channels with plates, or the precast abutment caps developed by Black Hawk County are some alternatives.

5. Select a sheet pile section for the wall. PZC sections are recommended for piles with significant lateral loading.

6. Design anchor system elements. How far the deadman is positioned behind the sheet pile wall is determined by the minimum distance required so the active soil zone behind the sheet pile wall and the passive soil zone of the deadman do not intersect; refer to Figure B14 of Appendix B. Waler design may be performed by assuming the waler is a continuous beam with simple supports at all tie rod locations; if the bridge is skewed, significant detailing of the connection between tie rods, waler, and sheet pile wall is required due to translational forces developed (see Figure B1).

7. Perform design checks. Determine if the resistance of the sheet pile section selected is adequate for combined loading. Check local buckling of web and flange elements as well as combined loading of the structure, including second-order bending moments. At a minimum, all failure modes presented in Figure 4-3 must be investigated for the system. A check of the effects on the sheet pile wall due to thermal expansion of the bridge superstructure must be performed, as well as effects of frost heave in the backfill soil (if applicable). If overtopping of the bridge deck during a 100-year flood will occur, the potential for unseating of the bridge (considering force of water flow and buoyant weight of superstructure) should be investigated.

Design Summary for GRS Sheet Pile Bridge Abutment and Backfill Retaining Systems

1. Determine design loads on the sheet pile wall. For estimating lateral earth pressure, refer to AASHTO (1998) Section 3.11.5. Consideration must be given to the flexibility (continued)

of the wall, which is dependent on wall height and lateral restraint, when determining earth pressure (at-rest or active); if short piles are restrained against lateral movement at the top of the wall (i.e., bridge superstructure), at-rest earth pressure conditions should be assumed. Effects of surcharge loads on the backfill may be approximated using AASHTO (1998) Section 3.11.6; the equations in this section are conservative for a flexible wall. For design according to HL-93 loading, AASHTO (1998) Section 3.11.6.2 provides an equivalent surcharge pressure to account for vehicular live load on the backfill soil. For all types of loading in the projects presented in this thesis, a load distribution of 10 ft width per design lane was used for live loads; this was determined to be a conservative assumption from the test data analysis presented later in this report.

2. Select location of the anchorage system. Various positions may be investigated to determine the optimum location for minimizing the embedment depth and required anchor force. In general, a distance below the top of the sheet pile wall of approximately 25% to 33% of total wall height is the most efficient. Consideration should be given to the exclusion of an anchor system for significant cost reduction; the need for temporary bracing of a cantilevered sheet pile wall during construction must be investigated.

3. Determine preliminary depth of piling. The minimum required embedment depth may be determined by analyzing the wall as a beam with a single pinned support at the location of the tie rods; the length of beam required for equilibrium of lateral forces on the wall provides the minimum embedment depth. All regions of the sheet pile wall within the GRS zone may be considered to have no lateral forces applied to the wall. If the bridge is over a stream, design pile depth must include the effects of scour; depending on local conditions, scour during flooding may be significant (10 ft or more) and can be estimated using methods presented by Davis and Richardson (2001).

4. Select a sheet pile section for the wall. PZC sections are recommended for piles with significant lateral loading.

5. Design geogrid reinforcement. Select a geogrid type and spacing adequate to resist maximum lateral earth pressures experienced within the backfill. It is recommended to use biaxial or triaxial geogrid to minimize loading on wingwalls. (continued)

6. Design spread footing for transfer of superstructure loads to GRS backfill.

7. Design anchor system elements. How far the deadman is positioned behind the sheet pile wall is determined by the minimum distance required so the active soil zone behind the sheet pile wall and the passive soil zone of the deadman do not intersect; refer to Figure B14 of Appendix B. Waler design may be performed by assuming the waler is a continuous beam with simple supports at all tie rod locations; if the bridge is skewed, significant detailing of the connection between tie rods, waler, and sheet pile wall is required due to translational forces developed (see Figure B1).

8. Perform design checks. Determine if the resistance of the sheet pile section selected is adequate for combined loading. At a minimum, all failure modes presented in Figure 4-3 must be investigated for the system. A check of the effects of frost heave in the backfill soil (if applicable) should be performed. If overtopping of the bridge deck during a 100-year flood will occur, the potential for unseating of the bridge (considering force of water flow and buoyant weight of superstructure) should be investigated.

Other Design Recommendations

Design of the sheet pile and superstructure interface should be considered when using either axially loaded, cellular, or GRS abutment systems; the shallow footings required for cellular or GRS abutment systems may be significantly simpler to design and construct.

When designing sheet pile elements, combined loading effects must be considered due to the nature of the loading. Design methods for typical steel piling may be used in conjunction with special consideration for the development of soil friction as described in this section. Use of the AASHTO (1998) LRFD bridge design specifications is recommended for the design of all elements of the bridge structures (including equations for determination of lateral loads). Compaction-induced earth pressures must be accounted for utilizing the methods presented in this section. When selecting steel sheet pile shapes, the plastic section modulus should be utilized for selection; PZC piling is preferred over PZ piling due to a greater strength to weight ratio. Epoxy coating of all steel elements exposed to soil is recommended where feasible.

Monitoring Methods and Instrumentation Selection

Three main types of monitoring equipment that are applicable for steel sheet pile bridge abutments are piezometers, earth pressure cells, and strain gages. Other equipment such as extensometers, tiltmeters, and inclinometers may also provide valuable information about the behavior of the project site. For long-term recording of instrumentation readouts, the use of a datalogger is necessary (as well as other components to allow communication with computer software). Select components are explained in the following paragraphs.

Two common types of transducers (methods for converting physical measurements into electrical signals) used in geotechnical instrumentation are vibrating wires and semiconductors. The theory behind vibrating wire technology is that the resonant frequency of a wire is dependent on the tension it is subjected to. The wire is "plucked" using an electromagnetic coil and the frequency of the vibration is then recorded. The measured frequency of vibration is proportional to the desired information (earth pressure, strain, etc). Semiconductor transducers utilize a material that changes resistance under strain. Vibrating wire systems are more stable over time while semiconductor systems have significantly higher sampling rates useful for dynamic measurements.

Piezometers

The piezometer can be used to measure groundwater table elevation for long-term monitoring of the project. By placing multiple piezometers on both the stream side and backfilled side of a retaining wall, water height can be measured to determine the development of pore water pressure behind the abutment. The ASCE recommends that piezometers be installed prior to driving piling and backfilling for simplicity, although steps must be taken to prevent damage to them as a result of the driving (ASCE, 1996).

Earth Pressure Cells

Earth pressure cells can measure the total contact soil pressure at any location. A cell essentially consists of two steel plates separated by a fluid. As pressure on the plates change, a transducer converts the fluid pressure into an electrical signal. The cells can be attached directly to the sheet pile wall and measure the soil pressure due to backfill and surcharge loads. It is recommended that earth

pressure cells be installed in a pocket of fine-grained sand (Geokon, 2006). When used in conjunction with a piezometer, effective soil stress can be determined at a desired point.

Strain Gages

Strain gages will measure the strain at a given point on the sheet pile wall. Since strain is proportional to stress, the gages will indirectly provide stresses, loads, and bending-moments at the desired locations. At a minimum, two gages must be used (on opposite sides of the neutral axis of bending) to distinguish between axial and flexural strains in the section.

Previous field tests have shown that strain gages installed prior to construction are capable of surviving driving operations. Further protection may be provided by welded steel angle sections over the gages; care must be taken to avoid welding near strain gage locations (ASCE, 1996).

Extensometers

Borehole extensometers allow for measurement of the deformations of the soil mass retained by a retaining wall. When placed behind a sheet pile bridge abutment, extensometers measure the deformations of the soil at various points within the borehole by using up to 6 rods with anchors. These measurements can assist in the recognition of developing failure planes within the soil (Geokon, 2006).

Tiltmeters

The tiltmeter is capable of measuring the tilt of structures. In a vibrating wire tiltmeter, a strain gage measures the deflection of a pendulous mass inside the tiltmeter as the center of gravity shifts due to rotation of the structure it is attached to. The instrument can be attached via brackets to either a vertical or horizontal face of the structure being monitored (Geokon, 2006).

Inclinometers

Inclinometers can be used to measure the deflected shape of a structure or the movement of a soil mass. An inclinometer is essentially an accelerometer probe that is run through a tube installed on a structure or in a soil to detect changes in deflected shape. Because of damage during driving,

inclinometers attached to sheet piles are limited to the length of the sheet pile. If information of soil movements below the pile is required, a second inclinometer installed deep into the soil (deep enough to be considered non-moving) can be used (ASCE, 1996).

Data Collection System

A system is needed to read the electrical output from the instrumentation. A datalogger system is capable of storing information for short-term or long-term applications (depending on the type of datalogger used). In a vibrating wire system, the datalogger sends an electrical signal (one instrument at a time) to excite vibration of the wire and measure its resonant frequency; the frequency is then converted to a data value (i.e. strain or pressure) and is stored for subsequent data collection. An interface with a computer (with the appropriate software) is necessary for programming of the datalogger as well as collection of data.

Construction Methods

For construction of sheet pile walls, the most common methods are driving, jetting, and trenching. With steel sheet piles, it is recommended that driving be used. Various types of driving and vibratory hammers (which can be faster and minimize damage to the piles) are available. Several driving hammers are described below. When impact hammers are used, a protective cap should be placed to prevent damage to the pile. Templates or guides are also used to help ensure proper placement of the sheet pile during driving. A common vertical tolerance is plus or minus 1.5 in. from design elevation, while sheet piling should not be more than 0.125 in/ft of wall out of plumb (either in-plane or perpendicular to the wall) after driving (ASCE, 1996). With axially loaded abutments, these tolerances would likely be further reduced.

When sheet piling is used as a bridge abutment, standard practice has been to use a vibratory pile driving hammer unless difficult driving is encountered (where impact hammer driving would be necessary). For a typical cellular sheet pile bridge abutment, previous projects have shown that installation can be completed in less than one week with a crew of four people. After the piling has been installed, standard earthwork equipment can be employed for soil movement and compaction (Braun, 2002).

Driving Equipment

<u>Diesel Hammers</u>

The diesel impact hammer is a system that compresses and ignites a combination of air and diesel fuel. As the piston falls, compressing the air inside the chamber, diesel fuel is sprayed on the impact block. When the piston strikes the impact block the fuel-air combination ignites and simultaneously thrusts the piston upward and drives the pile into the ground. As the piston falls back down, the compression cycle is restarted.

Single Acting Drop Hammers

Drop hammers consist weights (up to 11 tons) dropped from variable drop heights to drive the piles into the ground. To minimize noise and pile head damage, heavy weights with short drop heights are recommended (NASSPA, 2005). The three main drop hammer types are cable operated, steam, and hydraulic; the difference being the means of lifting the weight.

Double Acting Hammers

These hammers are similar to other impact hammers, with the exception that they employ means of adding additional energy to the hammer. This is accomplished by using hydraulics or compressed air/steam to add energy as the piston is falling.

<u>Vibratory Pile Drivers</u>

The principal of a vibratory pile driver is the use of eccentric oscillating weights that disturbs the soil around the pile, decreasing soil resistance. By doing this, piles are able to be driven with little extra applied loads such as pile self weight and the weight of the driver. According to the NASSPA (2005), the best soils for use with vibratory drivers are water-saturated non-cohesive soils as well as mixed and cohesive soils with high water contents. If difficult soil strata are encountered, impact drivers may be used to finish the driving operations after vibratory drivers have been used to set piles.

Driving Methods

The North American Steel Sheet Piling Association (NASSPA, 2005) outlines two methods of pile driving: set-and-drive and panel driving.

In the set and drive method, each sheet pile element is driven to its full depth until another is placed as shown in Figure 4-6a. This method, however, is only applicable for use in loose soils with relatively short piling, as the free-leading interlock is constantly susceptible to deviation. For more difficult driving situations, panel driving is recommended (NASSPA, 2005).

a.) Set-and-drive   b.) Panel driving

c.) Staggered driving
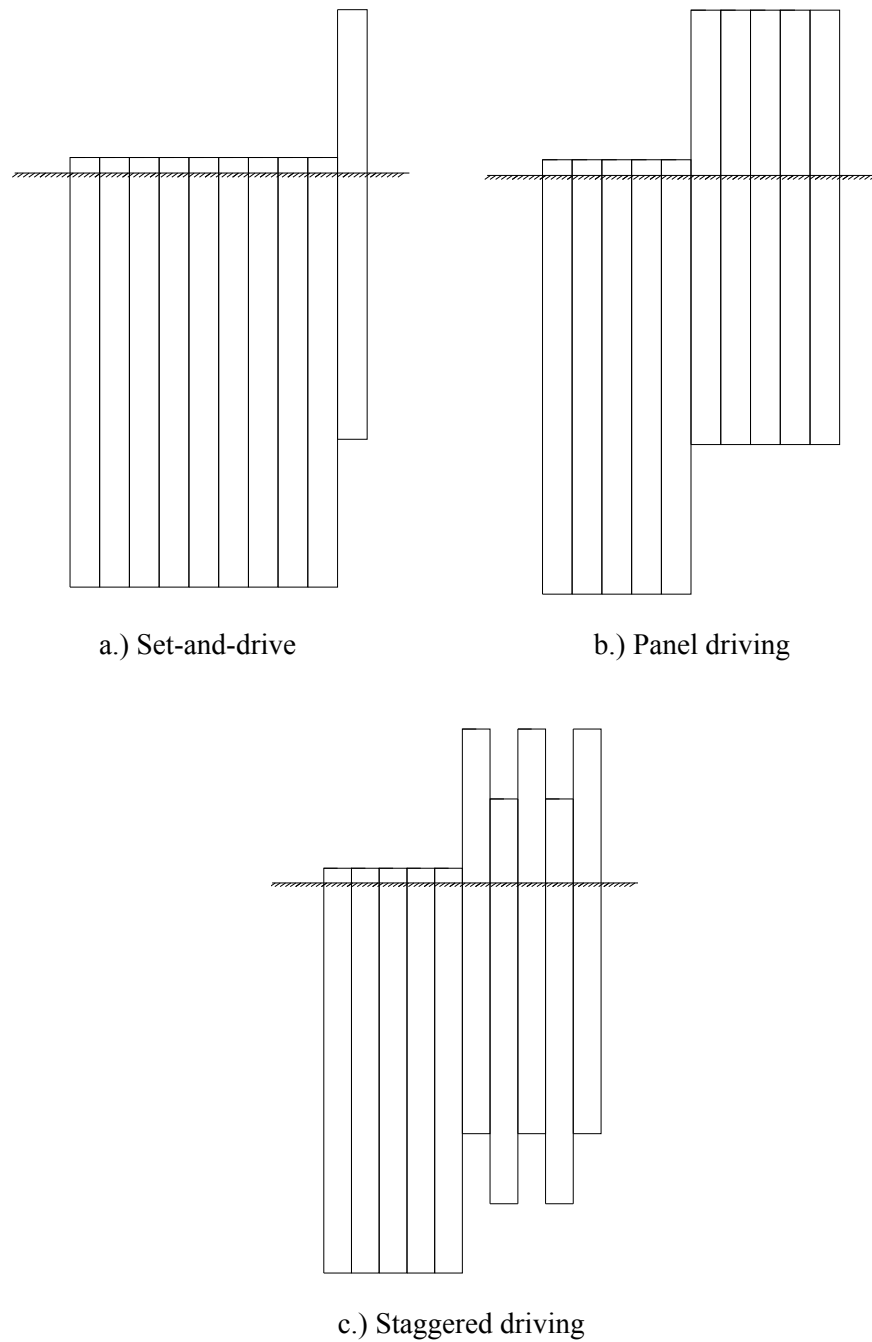
Figure 4-6. Sheet pile driving methods (NASSPA, 2005).

Panel driving is a technique that minimizes installation difficulties. The piles are driven in groups (or panels) as shown in Figure 4-6b. The first two piles are set on the guide (pitched), aligned, and made plumb. The rest of the group is then pitched, with driving beginning from the last pair in the panel. After the first panel is driven to a minimum depth, the second panel is pitched and driven in a manner like the first panel. After the second panel has reached the minimum depth, the first panel can be driven to the design depth and the third panel should be pitched. This process continues until all piles have been driven to design elevations. If significantly difficult driving conditions are encountered, staggered driving of piles (see Figure 4-6c) is recommended as it minimizes the potential for development of friction between interlocks that is developed when adjacent piles deviate due to soil behavior or obstacles encountered during driving (NASSPA, 2005).

Bridge Live Load Testing and Monitoring

Live Load Testing

The instrumentation and monitoring systems were used in conjunction with load tests to investigate the behavior of the structure under loading. The live load test involved driving trucks of a known weight and axle spacing over the bridge and taking readings when the trucks were at specified locations. Data recorded were reduced and compared to results expected by theoretical analysis to determine the performance of the sheet pile abutment and backfill retaining systems and the viability of the design methods utilized.

Long-Term Monitoring

For long-term monitoring of bridge behavior, the permanent instrumentation system was used. Readings were taken at various daily intervals described in the corresponding section for each project. The data recorded for each project were reduced and analyzed to determine the performance of the sheet pile abutment and backfill retaining system over long time periods.

CHAPTER 5. RESULTS AND DISCUSSION

Black Hawk County

Project Details

The first demonstration project was constructed in Black Hawk County (BHC), Iowa. The site that was selected was a low volume road bridge crossing Spring Creek (a tributary of the Cedar River) on Bryan Road near La Porte City; the location of the bridge is shown in Figure 5-1.

This project was undertaken to investigate the feasibility of using sheet piling as the primary abutment foundation element and backfill retaining system. Construction of the new bridge was initiated on August 13, 2008 and completed on October 20, 2008. A load test of the bridge foundation system and superstructure was subsequently performed and data were collected by Iowa State University (ISU). This thesis presents information on the design of the new sheet pile abutment bridge system, its construction, the instrumentation installed, load testing, as well as data analyses and conclusions. The following sections give an overview of the previous structure and the new sheet pile abutment bridge system.
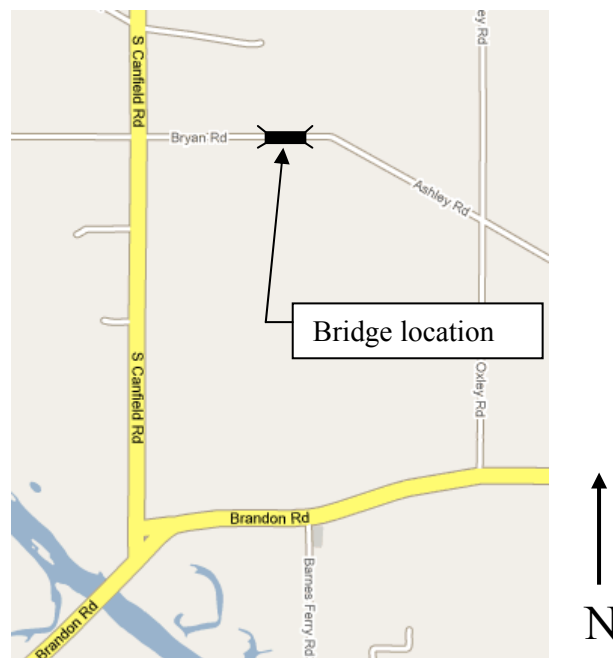
Figure 5-1. Location of demonstration project outside of La Porte City in BHC, Iowa.

<u>Previous Bridge Structure</u>

The bridge that was replaced was a 20 ft wide, 40 ft single span originally constructed in 1942. The structure was a pony truss bridge supported on a timber pile foundation and was constructed approximately 10 ft above stream level. The substructure was previously retrofitted with steel piles on each abutment. These retrofit piles were reportedly driven into the existing bedrock to provide reinforcement for the timber abutments. One of these piles can be seen in Figure 5-2.

Retrofit pile

Figure 5-2. Previous bridge structure at demonstration project site in BHC, Iowa with retrofit pile.

<u>New Sheet Pile Abutment Bridge System Overview</u>

The new bridge system (a 31 ft wide, two-lane 39 ft single-span beam-in-slab bridge) was a joint design effort between BHC and ISU. The design of the superstructure was performed by the BHC Engineer's Office and utilized precast elements previously developed. The substructure, which was primarily designed by ISU, utilized steel sheet piling as the primary abutment foundation element and backfill retaining system.

Superstructure

Custom precast beam-in-slab units (40.75 ft long) were used for the bridge superstructure. Each unit contained two W14x61steel beams (for additional details on the BHC precast elements, refer to Appendix A). There were a total of 6 units required for the bridge, each unit spanning the entire

length. Between each unit there was a closure joint that was cast in the field after the units were placed. A cross-section of two joined deck units (exterior and interior) is presented in Figure 5-3. The design width of the bridge was 31.8 ft. Figure 5-4a and Figure 5-4b illustrate a cross-section and side view, respectively, of the bridge deck and abutment elements; a full set of bridge plans are provided in Figure A1 through Figure A5 of Appendix A.
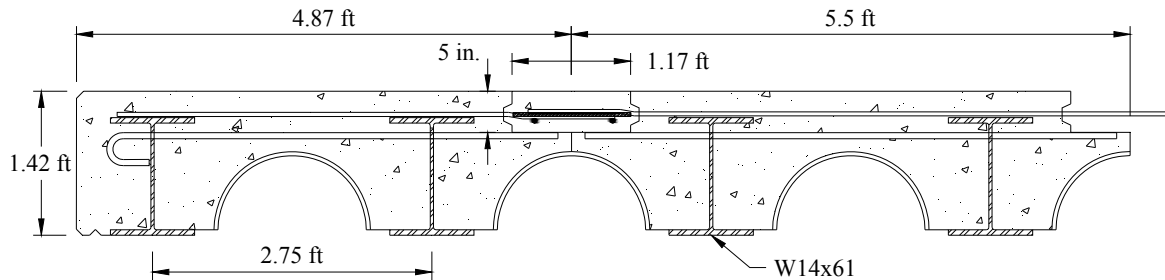
Figure 5-3. Cross-section of precast deck units for demonstration project in BHC, Iowa.

a.) Cross-section

b.) Side view
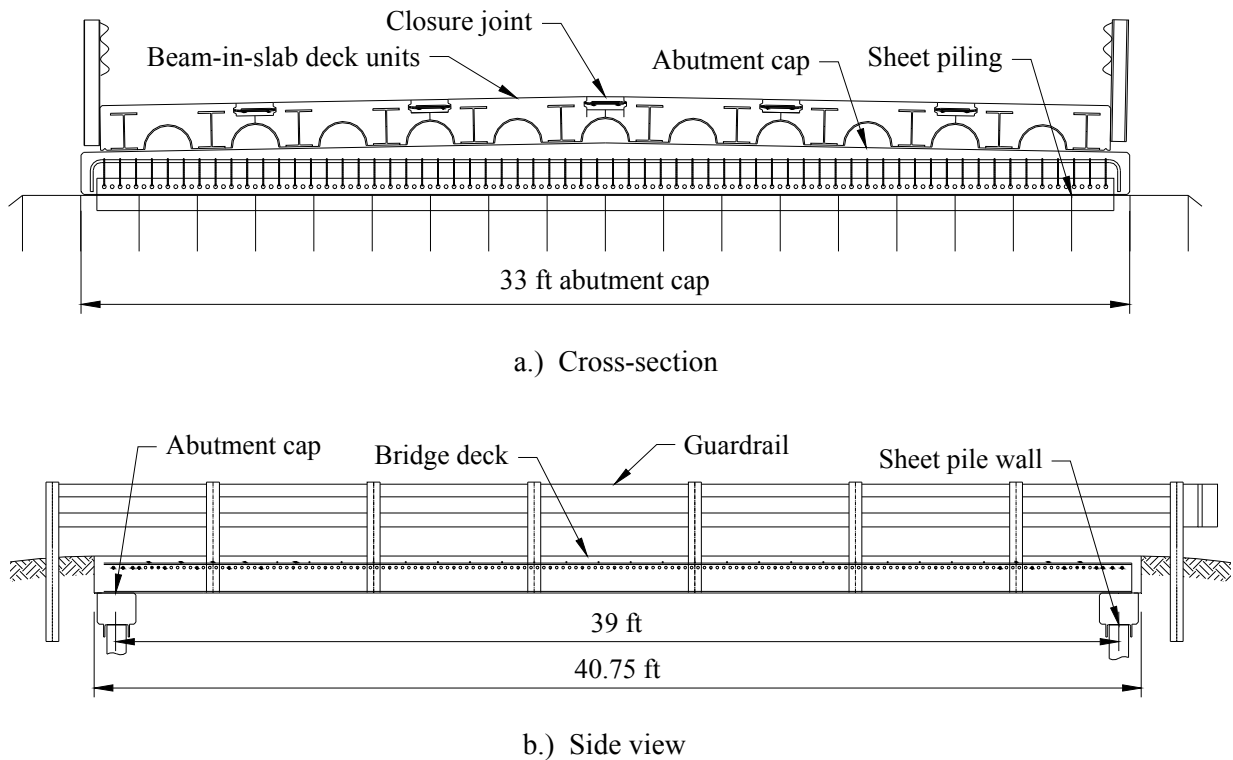
Figure 5-4. Replacement bridge deck and abutment elements for demonstration project in BHC, Iowa.

Substructure

Steel sheet piling was used for the abutment foundation elements of the new bridge. Each abutment consisted of a precast abutment cap bearing on sheet pile sections driven into shallow bedrock. The sheet piles selected were PZ 22 sections (purchased from Skyline Steel, Inc.). Dimensions of a PZ 22 are shown in Figure 3-2. A total of 64 sheet pile sections were needed for completion of both abutments. The main wall of the abutment required 20 sheet pile elements with each of the wingwalls consisting of 6 elements (each 15 ft long). The main wall was anchored with two 1 in. diameter tie rods that were attached to a 14 ft by 4 ft by 2 ft cast-in-place reinforced concrete deadman placed approximately 20 ft back from the main wall. The wingwalls were tied together using a 46 ft long 1 in. diameter tie rod (non-epoxy coated). A plan view of the abutment design is shown in Figure 5-5.

The abutment cap was a precast element designed and fabricated by BHC that consisted of a W12x65 steel beam cast in reinforced concrete. The web of the steel beam cast in the abutment cap beared directly on top of the driven sheet piling with no connection between them. The bridge deck units were placed on the abutment cap using bearing pads between the deck unit beams and the concrete abutment cap. A cross-section of the beam-in-slab bridge, abutment cap, and sheet pile wall is presented in Figure 5-6.
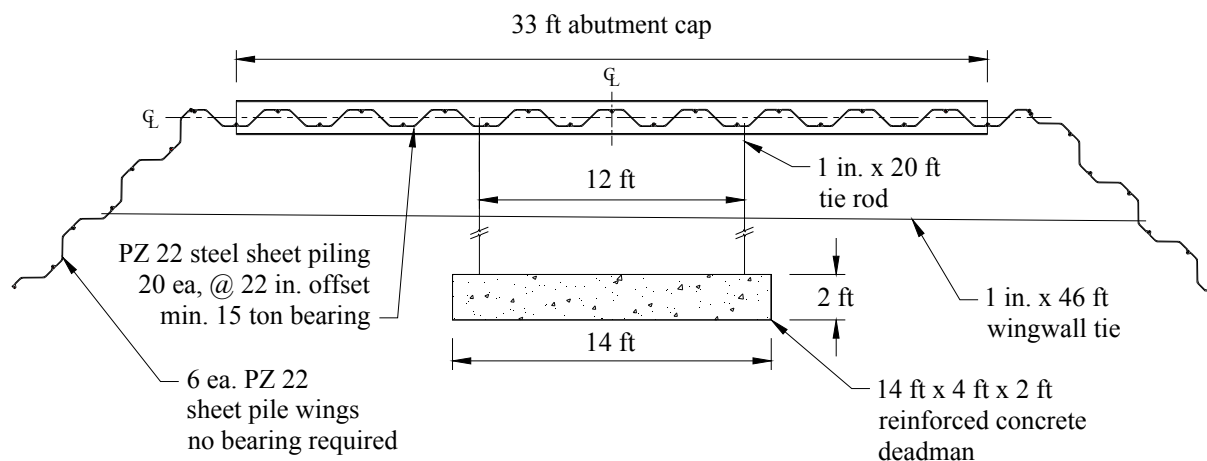
Figure 5-5. Plan view of sheet pile abutment and backfill retaining system for demonstration project in BHC, Iowa.
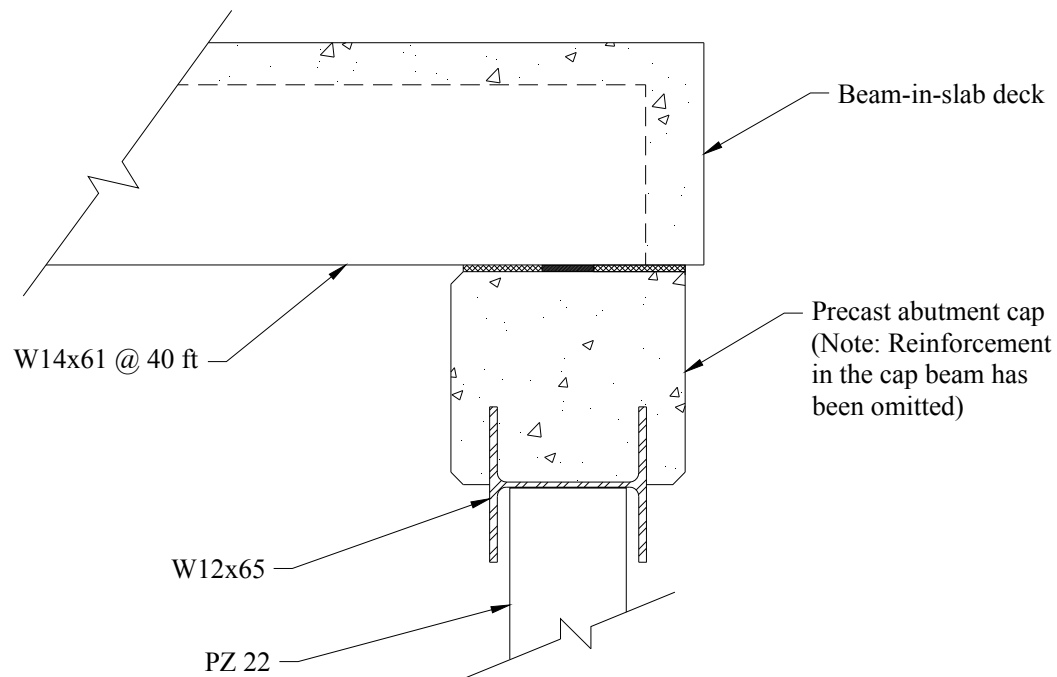
Figure 5-6. Precast abutment cap and contact between bridge deck, abutment cap, and sheet piling foundation in BHC, Iowa demonstration project.

Site Investigation

Field Investigation

Cone Penetrometer Testing

CPT soundings were performed east and west of the bridge abutments on August 14, 2007. The test locations are shown in Figure 5-7. CPT 1 and CPT 2 were advanced to depths of 15.9 ft and 17.4 ft below existing grades, respectively. Logs of the soundings, showing cone tip stress and sleeve friction, are presented in Figure 5-8a and Figure 5-8b, respectively. The soundings were advanced to practical refusal based on the equipment and the operator's experience. After being withdrawn from the CPT 2 sounding hole, the cone tip was found to be covered with light gray weathered limestone.

Soil behavior types determined from CPT 1 and CPT 2 are illustrated in Figure 5-9a and Figure 5-9b, respectively. As can be seen these figures, the majority of material present is clay with sandy seams occurring near stream level (from depths of 6 ft to 8 ft); the spike in resistance at the bottom of each CPT being a strong indicator of bedrock. Soil shear strengths and SPT resistance estimates from

correlations presented by Lunne, Powell, and Robertson (1997) are shown in Figure 5-10a and Figure 5-10b.
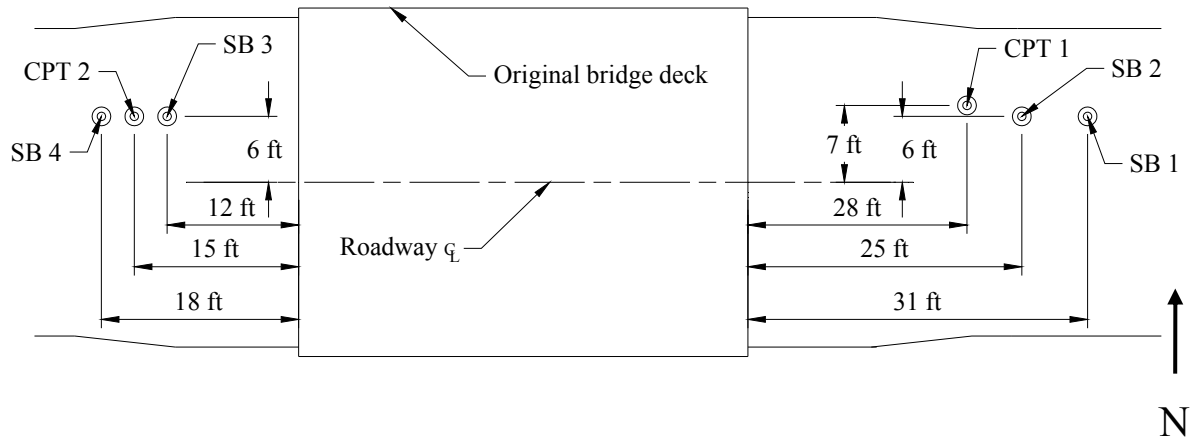
Figure 5-7. Plan view of CPT and soil boring locations in BHC, Iowa demonstration project.

a.) CPT 1

b.) CPT 2
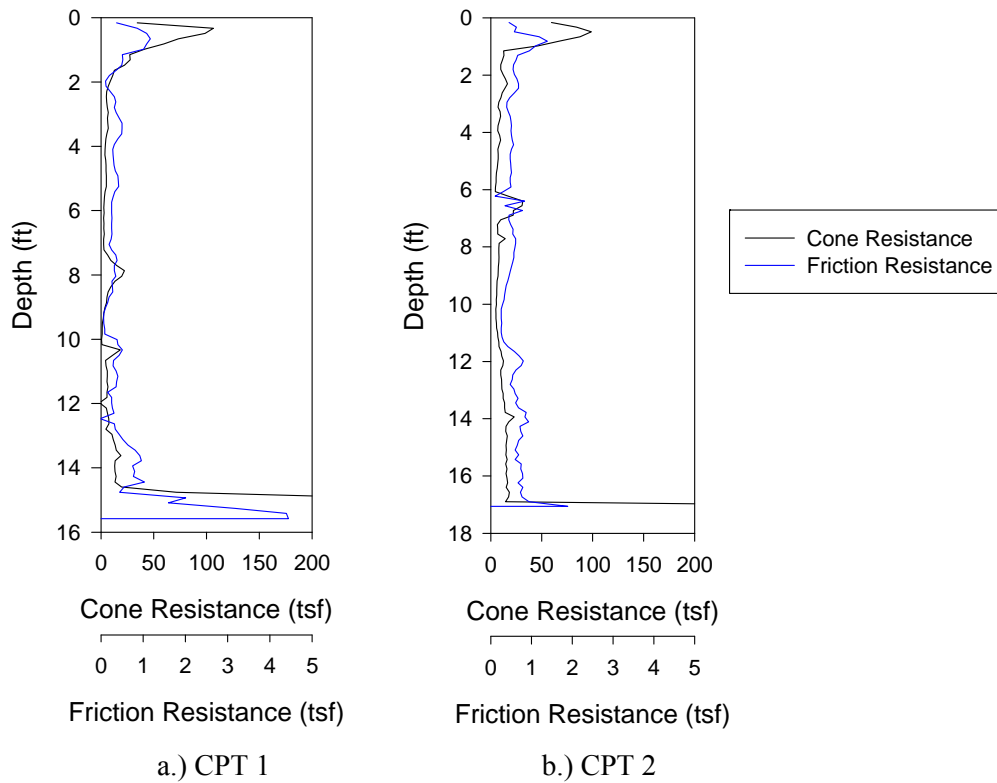
Figure 5-8. Results of CPT's showing cone tip and friction resistance.
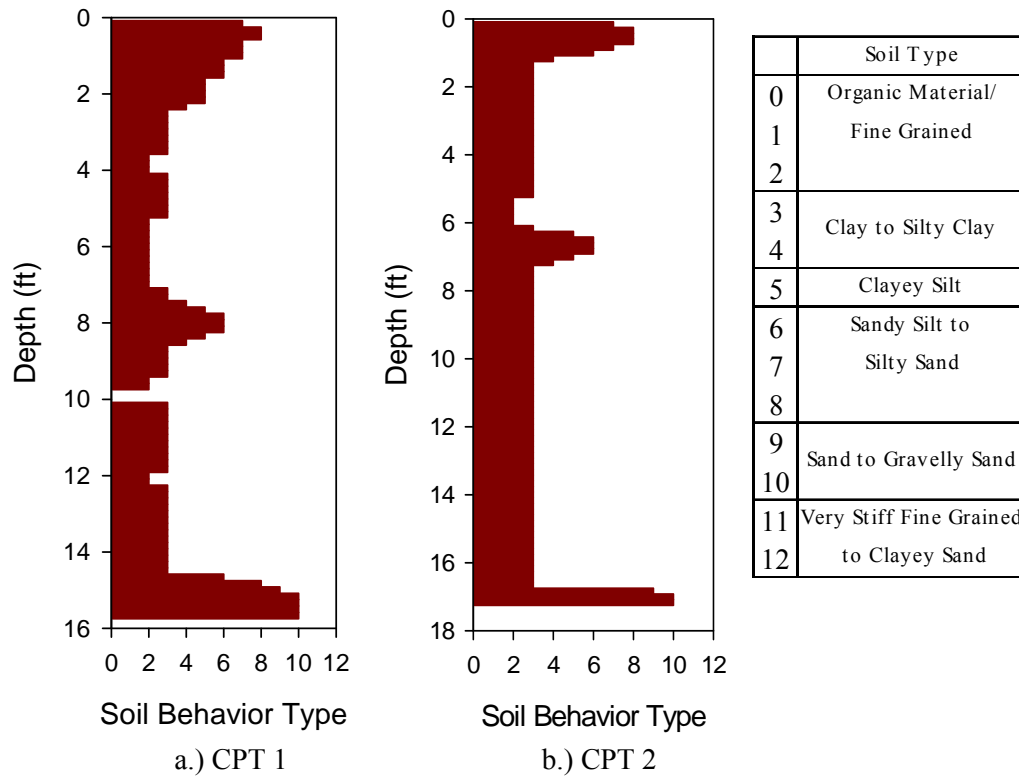
Figure 5-9. Soil behavior types determined from CPT's.
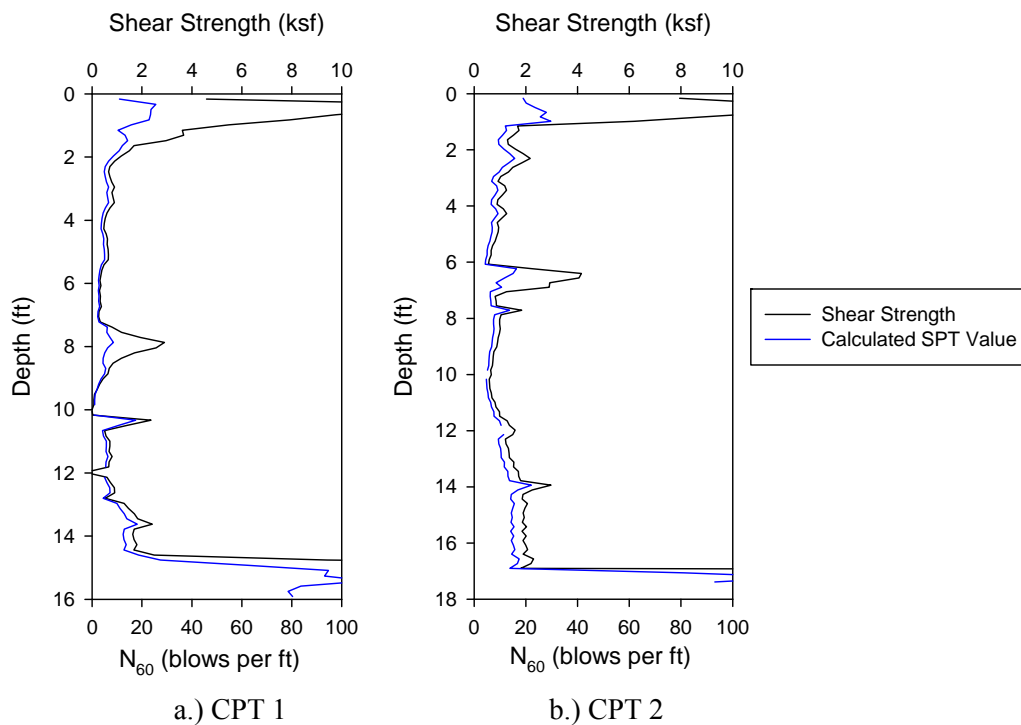
Figure 5-10. Shear strength and SPT correlations for CPT's.

Soil Borings

The soil borings were performed by members of the ISU research team on September 7, 2007. The location of each boring is shown in Figure 5-7, while boring logs are provided in Figure A8 through Figure A11.

Laboratory Testing

Averaged results of the CU triaxial tests performed for each boring (along with soil boring depths) are presented in Table 5-1 Results of the moisture content and UU triaxial tests performed on select soil samples are presented in Table 5-2. The results of the Atterberg tests and the percentage of soil passing the No. 200 sieve (percent fines) for select samples are presented in Table 5-3. USCS classifications determined are shown in the boring logs.

Table 5-1. Results from CU lab analysis of soil borings.

Boring Location	Boring Depth (ft)	Cohesion, c' (psf)	Friction Angle, φ' (degrees)
SB 1	10.3	50	35
SB 2	16.8	0	36
SB 3	16.0	125	27
SB 4	15.8	50	28

Table 5-2. Moisture content and UU test results on select soil samples.

Boring Location	Depth Range (in.)	Moisture (%)	Undrained Shear Strength (psf)	Dry Density (pcf)	Void Ratio
SB 1	20 - 30	15.3	1408	112.2	0.475
SB 2	107 - 118	23.1	1017	131.1	0.262
SB 2	180 - 202	18.5	1452	135.4	0.222
SB 3	30 - 50	18.1	1829	133.9	0.236
SB 3	114 - 123	20.6	1079	133.9	0.235
SB 3	123 - 130	16.8	1045	132.4	0.250
SB 4	168 - 176	16.8	506	136.6	0.211
SB 4	176 - 184	14.5	2688	144.3	0.146
SB 4	184 - 192	14.3	2424	143.4	0.154

Table 5-3. Atterberg test and gradation results for select boring ranges.

Boring Location	Depth Range (in.)	LL (%)	PL (%)	PI (%)	Passing No. 200 (%)
SB 1	12 - 40	33	20	13	48
SB 1	42 - 94	39	27	12	62
SB 2	96 - 199	23	15	8	-*
SB 3	23 - 50	30	19	11	51
SB 3	119 - 180	31	17	14	-
SB 4	144 - 168	30	15	15	-
SB 4	168 - 192	29	16	13	-

* No data available

<u>Site Conditions</u>

Geologic Setting

The project site is located on the "Iowan Surface", a distinct geomorphic region limited to the northeastern portion of Iowa. According to GSI (see Figure A7 for CPT report), transected surficial drainage imparts the topography consisting of gently rolling hills with long slopes and gentle relief. Prominent isolated elliptical hills, termed "pahas", tend to be concentrated along the region's southern border and karst features, including sinkholes, are common to the northern portion of the Iowan Surface due to the thin overburden deposits underlain by limestone bedrock formations. Overburden deposits within the stream valleys generally consist of colluvium (slopewash) overlying alluvium of varying thickness which is underlain by the glacial till soils over bedrock. The colluvial deposits are derived from parent soil materials on hillsides while the underlying alluvium may consist of cohesive clayey silt and silty clay soils and/or deposits. This project is located on a creek upland of the Cedar River floodplain which may have deposited alluvium consisting of interbedded sand and clay soils.

Soil Conditions

Soil borings SB 1 and SB 4 encountered fill materials consisting of very stiff, tan and light gray sandy clay (USCS symbol CL), and medium dense, red and tan clayey sand (SC) and silty sand (SM) from the ground surface to depths of 2 ft and 4 ft. Underlying the fill materials and present from the ground surface at the remaining three boring locations were relatively lean, stiff to hard, tan and light gray silty clay (CL) and sandy clay (CL) soils that extended to depths ranging from 8 ft to 10 ft. Stiff, light gray and tan, high-plasticity clay (CH) was encountered in boring SB 4 from 10 ft to 17 ft. Loose to very dense, tan and light gray silty sand (SM) with clay seams was then encountered below a

depth of 12 ft to bedrock in SB 1 and SB 2. Soil borings SB 3 and SB 4 encountered dark gray and orange silty clays from a depth of approximately 11 ft to bedrock.

Groundwater Observations

During the soil boring advancement and sampling operations, observations for free groundwater were made. Information regarding water level observations is recorded in the "groundwater" column on the soil boring logs. Groundwater was encountered at depths below existing grade of approximately 10 ft in borings SB 1 and SB 2 and at 12 ft in borings SB 3 and SB 4. Where free water was encountered, the depth of this observation is noted in the stratigraphy column of the soil boring logs. From the CPT soundings, the observed drop in tip stress and sleeve friction near depths of 10 ft likely coincides with the ground water surface.

Design

The bridge design was completed as a joint effort between ISU and the BHC Engineer's Office. The county engineer designed the superstructure while ISU was responsible for the design of the sheet pile abutment foundation and backfill retaining system. The design of the substructure elements was performed using the AASHTO LRFD Bridge Design Specification (1998).

Loading

According to the BHC Engineer's Office, the precast superstructure elements were designed for HS20 loading and a permit truck with five 10 ton axles spaced at 4.17 ft on center. Substructure elements were designed to resist HL-93 loading; the substructure was determined to be sufficient for the permit truck loading when analyzed with no lane load, using a 33% increase in axle loads for impact, and no live load factor. The 39 ft bridge was loaded with the design truck and lane load as per AASHTO (1998) Section 3.6.1.2 to determine live loads that needed to be resisted by the foundation and backfill retaining system. The design loads were determined using the critical load factors and load combinations in AASHTO (1998) Section 3.4.

Foundation and Backfill Retaining Wall Design

Due to the nature of the loading, the sheet pile sections were analyzed as beam-columns. The combination of piling being driven into bedrock and restraint provided by wingwalls was assumed to

prevent translation at the base of the wall (but not rotation). Once in place, the bridge superstructure was assumed to provide restraint against translation at the top of the wall and thus the design element was assumed to be simply-supported at both ends of the section.

Loads from the retained soil self-weight and surcharge on the backfill were applied laterally to the element. For determining the amount of vertical earth pressure transferred laterally to the wall, at-rest (K_o) conditions were assumed due to the effect of the bridge structure in resisting lateral displacement at the top of the wall. Soil parameters and the assumed design profile are shown in Figure 5-11a. The loading and support conditions assumed are shown in Figure 5-11b. The concentrated force, P, represents the dead and live loads applied from the superstructure.

a.) Design profile   b.) Loading diagram
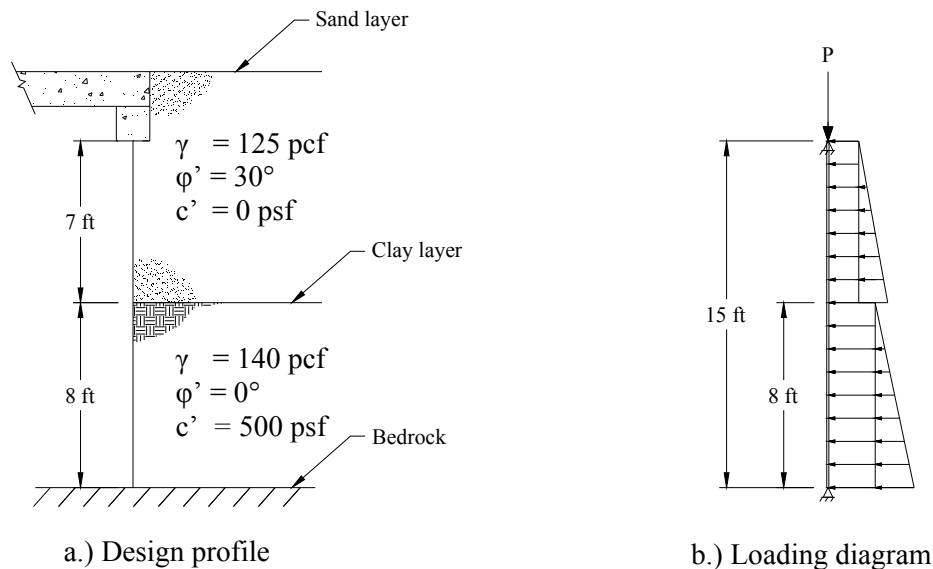
Figure 5-11. Design profile and loading and support diagram for the BHC, Iowa demonstration project.

Conservative assumptions were made for the behavior of the clay layer. The stream-side materials were assumed to provide no lateral resistance to the wall due to the mobilization requirements for passive lateral earth pressure to develop and the potential for removal of material from scouring effects. Another assumption was that, due to the effects of creep over time, the coefficient of lateral earth pressure (K_o) of the clay layer was assumed to be unity (full transfer of vertical stresses laterally to the wall).

The coefficient of at-rest lateral earth pressure was determined according to AASHTO (1998) Section 3.11.5.2 for the sand layer. Vehicular live loads on the backfill were accounted for in design by using

the equivalent surcharge loading outlined in AASHTO (1998) Section 3.11.6.2. Design axial loads in the piling were determined by assuming superstructure dead loads were distributed evenly amongst all piles and live loads were distributed over a 10 ft wide lane.

The pile section chosen for the wall was the PZ 22. The section was checked for combined loading and second-order effects of an element undergoing flexure and compression as per AASHTO (1998) Section 6.9.2.2. The pile section was also checked for the limit states of flange and web local buckling. Flexural strength was determined using the elastic section modulus and assuming lateral-torsional buckling was prevented through continuous bracing of the compression flange by adjacent sheet pile members.

The final design of the abutment foundation and backfill retaining system required a total of 64 (32 per abutment) 15 ft long PZ 22 piles (Grade 50 steel). The abutment caps were to be set directly on the top of the sheet pile wall after it was finished to grade.

As stated previously, the superstructure was assumed to provide adequate lateral restraint once in place. During backfilling of the abutments, however, this was not the case. Because of this lack of lateral restraint, a reinforced concrete deadman anchor system was installed on each abutment. The system was designed by the county engineer and consists of a reinforced concrete deadman (approximately 14 ft x 4ft x 2 ft) with two 1 in. diameter tie rods connected to a waler channel on the exterior face of the abutment walls. The connection between the deadman and sheet pile abutment system is shown in Figure 5-12; the tie rod (with hooked reinforcement welded on one end) was cast into the concrete deadman. Design calculations are provided in Appendix A.
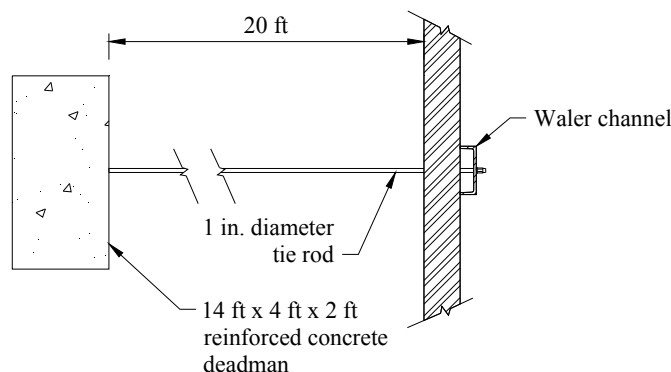
Figure 5-12. Deadman to sheet pile abutment and backfill retaining system connection.

Construction

BHC used its own forces for construction of the entire project. The bridge crew primarily consisted of three construction workers. According to the BHC engineer, average labor costs amount to approximately $1000 each day the bridge crew was on site.

The overall time required for construction of the replacement bridge was approximately 10 weeks. Several delays occurred due to equipment breakdowns (due to inexperience with specific pile types), pile splicing, and weather. A chronology of major construction events is shown in Table 5-4. Details of each significant event are also given in this section of the report.

Table 5-4. Chronology of significant construction events for demonstration project in BHC, Iowa.

Event Description	Start Date	Working Days Between Events
Demolition	08/13/08	8
Sheet Pile Driving – East Abt.	08/25/08	6
Sheet Pile Driving – West Abt.	09/02/08	11
Abutment Finishing	09/17/08	11
Deck Unit Placement	10/02/08	9
Bridge Finishing	10/15/08	3
Open for Service	10/20/08	-
Bridge Load Test	11/3/08	-

Demolition of Existing Structure

Removal of the superstructure and east abutment was the first task of the demolition and required one week for completion. The west abutment was left in place to assist in the construction of the replacement bridge. The demolition was performed with a crane equipped with a wrecking ball and an excavator. The bridge deck was crushed by dropping of a wrecking ball while the excavator was used to remove exposed reinforcement. The excavator was also used to pull down the superstructure and demolish the timber abutments.

The east abutment had one H-pile retrofit that had been driven into the bedrock. An initial attempt to pull out this pile with the excavator was unsuccessful. The excavator was used to bend the pile back and forth until it fatigued slightly below the stream level and the upper portion was removed. The west abutment (containing two retrofitted H-piles) was never fully removed since the location of the new bridge was slightly east of the existing abutment.

Sheet Pile Driving – East Abutment

For both of the abutment sheet pile walls, pile driving was completed using both vibratory and impact hammers. The piles, after being placed in a guide rack to help ensure proper wall construction, were initially driven as far as possible using an excavator equipped with a vibratory plate as shown in Figure 5-13. The piles were then driven to a minimum specified 15 ton bearing capacity using a crane equipped with a drop hammer. Bearing capacity was estimated using the Modified Engineering News Record pile-driving formula (Das, 2006). Using a 4,120 lb hammer dropped from a height of 6 ft, less than 2 in. of observed pile penetration after 5 blows of the hammer corresponded to approximately a 33 ton capacity. All piles were driven until a maximum of 2 in. penetration per 5 blows was observed. The wingwalls, which did not require bearing capacity, were driven to bedrock with the vibratory plate and then trimmed. The wingwalls were placed at a 45 degree angle to the main wall using the special connector shown in Figure 5-14.

Figure 5-13. Driving of sheet pile sections with vibratory plate equipped excavator boom.

(not to scale)
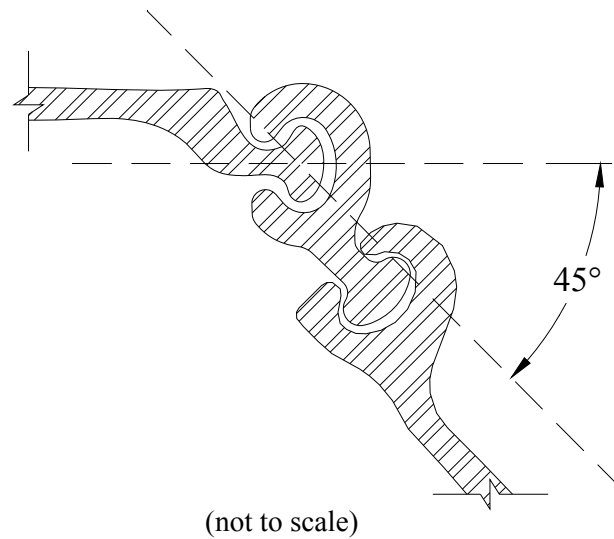
Figure 5-14. Sheet pile connector for 45 degree turn (PilePro® PZ Colt).

The guide rack was 1 in. wider than the width of the sheet pile sections used to ensure the sheet piles would fit inside the rack. As depicted in Figure 5-15a, significant rotation between adjacent sheets occurred which resulted in extending the actual width of the wall by approximately 1.5 ft. As can be seen in Figure 5-15b, the slightly rotated sections are wider by approximately 1 in. and have less distance between flanges (0.6 in. less). It was realized after construction that the guide rack should have been constructed with spacing closer to the design width of the wall. Efforts to ensure adjacent sections are flush will result in a wall with greater flexural strength by maximizing the distance of the sheet pile flanges from the neutral axis.

a.) Angle between sections
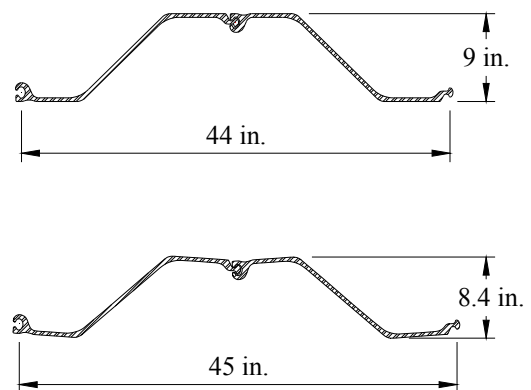
b.) Comparison of flush and rotated sections

Figure 5-15. Rotation between adjacent sheet pile sections.

CPT results showed refusal at 15 ft below grade. During impact driving, specified bearing capacity (2 in. of pile penetration per 5 hammer blows) was not reached until significantly below the assumed bedrock depth from the CPT results. This was not an issue for the east abutment since pile lengths longer than necessary were ordered.

Sheet Pile Driving – West Abutment

The west abutment required modification of the guide rack to accommodate the width of the instrumented piles due to the protective angles that were attached (see Figure 5-16a and Figure 5-16b). As with the east abutment, the width of the rack was wider than necessary thus introducing undesired rotations between the adjacent pile sections and an overall lengthening of the wall.

a.) Guide rack with angles attached   b.) Instrumented sheet pile section
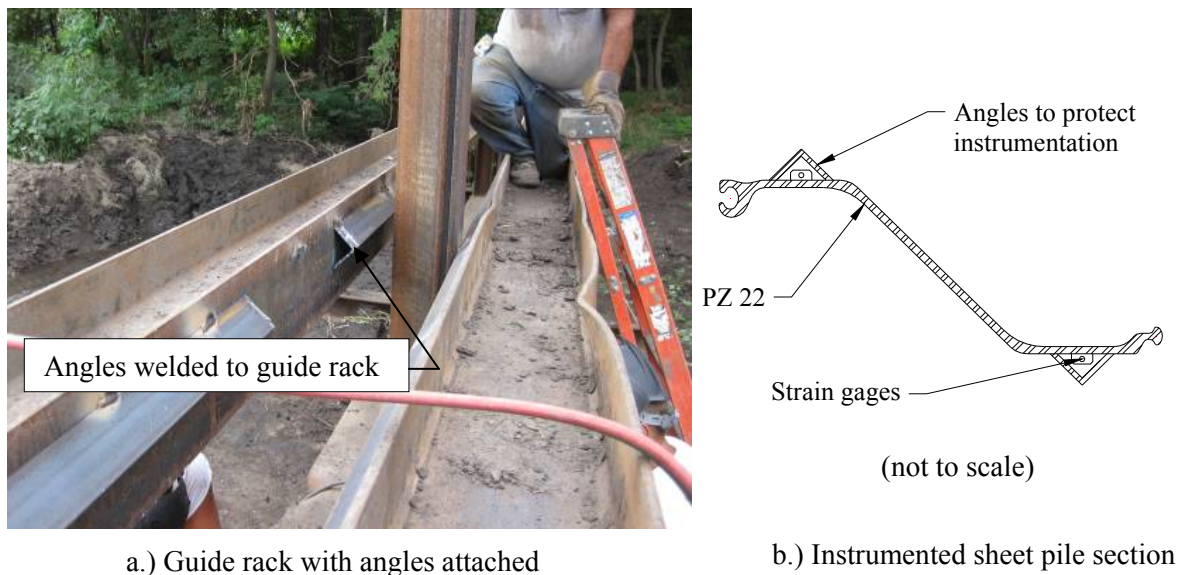
Figure 5-16. Modification of guide rack to accommodate the instrumented piles.

The plan for driving the west abutment sheet pile wall was similar to the east abutment; vibratory and impact driving was used. During the vibratory driving phase, one pile (Pile 2 in Figure 5-34) was misaligned. Since the pile couldn't be pulled back out, a field decision was made to adjust its position by forcing it laterally with the excavator boom. While being held, the pile was welded to the guide rack until the next pile section had been driven; this adjustment may have affected results (creating locked-in stresses) as Pile 2 was an instrumented pile.

CPT results for the west abutment showed refusal at approximately 17 ft below grade. During the impact driving phase, it became evident that the lengths of piling ordered were too short. The depth required for specified bearing capacity on the west side of the stream was significantly lower than that predicted by the CPT results and varied from 17.9 ft to 23.9 ft along the abutment wall. All of the sheet piles in the main wall required splicing to achieve design elevations. In some cases, piles needed to be driven more than 1 ft lower than the adjacent section; this required splices as well for the pile driving mechanism to fit in place. Required splice lengths ranged from 0.5 in. to 72 in.

Another issue encountered was fracturing of the pile driving cap. The BHC bridge crew had constructed a custom driving cap for the sheet piles by welding sections of angle iron to a steel plate (see Figure 5-17); on two occasions, the welds failed and thus the driving cap needed repair.

Figure 5-17. Custom sheet pile driving cap fabricated by BHC.

<u>Completion of Abutment</u>

After all sheet piling had been driven to the specified bearing capacity, several tasks were performed to bring the abutments to a finished state. The major tasks that needed to be performed before backfilling were placement of the subdrain, installation of the anchor system, placement of the abutment cap, and installation of the monitoring instrumentation.

Subdrain

To provide drainage of the backfill, a drain tile system was placed on the backfill side of each sheet pile wall. These systems, placed at approximately the same elevation of the stream, consisted of a flexible, perforated pipe surrounded by porous backfill. The pipes were placed along the length of each abutment wall and were wrapped around and exited at the end of the wingwalls downstream from the bridge (see Figure 5-18).

Perforated pipe to exit at downstream end of wingwall

Figure 5-18. Drain tile installation on backfill side of west abutment in BHC, Iowa.

Anchor System

The anchor system consisted of a cast-in-place concrete deadman that supported the wall through two 1 in. threaded rods (non-epoxy coated) connected to a steel channel waler. An overview of the anchor system was previously presented in Figure 5-5. The deadman was cast in a trench excavated from the existing soil as shown in Figure 5-19. After hex nuts were threaded on the main wall tie rods, another rod was placed parallel to the wall to tie the wingwalls together (see Figure 5-20).

Figure 5-19. Reinforced concrete deadman placement behind east abutment.

Figure 5-20. Installation of wingwall tie.

The construction of the deadman differed between the two abutments. For the east abutment, a continuous deadman (approximately 14 ft x 4 ft x 2 ft) was used for anchoring both tie rods. On the west abutment, however, only one tie rod was attached to the concrete deadman (approximately 6 ft x 4 ft x 2 ft) constructed. The other tie rod was welded onto a driven H-pile that was part of the demolished bridge (see Figure 5-21).

Figure 5-21. Tie rod to H-pile connection.

Abutment Cap

The abutment cap consisted of a precast element designed by BHC. The 33 ft long cap consists of a W12x65 section capped with reinforced concrete as shown previously in Figure 5-6a. Because the web of the W12x65 was to bear directly on top of the driven sheet pile wall, the wall needed to be trimmed to a precise elevation. To eliminate the process of torch-cutting and grinding, the BHC engineer subcontracted a company (Iowa Wall Sawing Service) that cut the wall using a 2 ft diameter circular saw. On the East abutment, the blade became misaligned and required torch-cutting for removal causing slight delays. The cutting operation on the west abutment was completed without error. No grinding of the sheet piling was required after the cutting operation was completed.

The abutment caps were placed on top of the sheet piling as shown in Figure 5-22. No attachment was made between the sheet pile wall and the steel surface of the abutment cap (the web of the W12x65).

Figure 5-22. Placement of abutment caps on sheet pile walls.

Instrumentation Installation

Although strain gages were attached to the sheet pile sections before driving, earth pressure cells and tie rod strain gages needed to be installed both before and during the backfilling operations. Tie rod strain gages were attached to each tie rod and protected by welding angle iron around them (see Figure 5-23). Earth pressure cells were placed at various depths along the abutment wall and required backfilling operations to be halted several times for placement. Location and information about all instrumentation used is given later. For placement of each earth pressure cell, a small trench was made in which the cell was placed approximately 2 in. from the sheet piling and surrounded by fine silica sand as shown in Figure 5-24.

Figure 5-23. Tie rod strain gage installation.

Figure 5-24. Earth pressure cell installation.

Two piezometers were installed to monitor the height of the groundwater table. The instruments were placed at the centerline of the west abutment on opposite sides of the sheet piling and were attached to a specified point on a 3 ft length of PVC pipe. A pocket of fine sand was then created around each piezometer (as shown in Figure 5-25) to prevent contact with unwanted materials. Elevations of the top of each PVC pipe were taken after the piezometer assembly was placed in its final position.

Figure 5-25. Piezometer assembly for water table monitoring.

Backfilling

Before each abutment was backfilled, a layer of rip-rap was placed against the stream side face of the sheet pile walls. The existing material within 3 ft of the stream side of the wall was first excavated to approximately 4 ft below stream level. Rip-rap was then placed in the trench to an average thickness of 5 ft. A profile of the bridge is shown in Figure 5-26; the as-built span length was approximately 8 in. shorter than the design span (potentially due to lateral movement of the abutments).

Both abutments were backfilled with 1 in. roadstone within a short zone (approximately 10 ft) behind the sheet pile wall. Outside of these zones existing material was left in place. On the east abutment, the existing material that was left consisted primarily of soil. On the west abutment, the majority of the abutment from the previous bridge was left in place; see Figure 5-27. Backfill material was primarily used to fill the void between the new sheet pile wall and the abutment from the previous bridge. The backfill material was placed in 1 ft lifts and compacted using the vibratory plate attached to the excavator boom. Laboratory analysis of a sample taken of the backfill material was performed to determine the engineering properties of the material. After performing a direct shear test (ASTM D3080, 2004), the backfill material was found to have a friction angle of approximately 45 degrees thus the design assumption of 30 degrees was significantly conservative. The direct shear test report is presented in Figure A12.
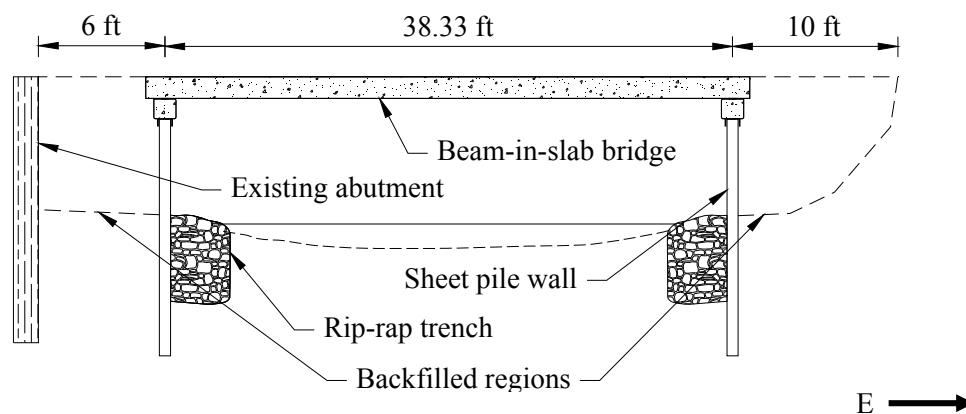
Figure 5-26. As-built profile of bridge for demonstration project in BHC, Iowa.

Placement of the Deck Units

Placement of the precast deck elements required one day to complete. As previously noted, the deck elements were designed and constructed by BHC (see Figure A3 for details on deck elements). A

total of six elements were used for the entire superstructure (each 40 ft long) to create a bridge width of 31.8 ft. Each beam-in-slab element consisted of two W14x65 beams cast within the bridge deck. Each of the beams was set on bearing pads placed on top of the abutment caps.

Figure 5-27. West abutment of previous bridge remained in place (behind wall).

Figure 5-28. Precast beam-in-slab bridge deck element.

Each element was brought to the west abutment of the bridge where it was lifted off the truck using the first crane. The element was then partially placed (as far across the span as the capacity of the first crane would allow) on a temporary roller assembly which spanned the bridge as shown in Figure 5-29. At this time a second crane (at the east end of the bridge) was attached to one end of the element to enable proper placement of the deck element (see Figure 5-30). The roller assembly allowed the deck units to slide as they were first lifted using both cranes. For placement of the final element, the roller assembly was set on the in-place deck elements instead of the abutment cap.

Roller assembly

Figure 5-29. Roller assembly used to assist in placement of deck elements.

Figure 5-30. Dual crane operation for placement of bridge superstructure.

Bridge Finishing and Summary

After all deck elements were placed, finishing of the deck required casting of the closure joints
between each element. Concrete for each joint was poured after exposed reinforcement was trimmed
and tied into position as shown in Figure 5-31. For more details on the procedure used in the
construction of the superstructure, see the final report for Iowa Highway Research Board project TR-
561 (Bigelow et al., 2009)

The remainder of construction required placement of guardrails and the grading of the roadway
approaching the bridge. The bridge was opened for service on October 20, 2008; an overview of the
bridge after completion is shown in Figure 5-32.

Figure 5-31. Finishing of bridge deck joints.

| a.) Profile view | b.) End view |

Figure 5-32. Completed bridge in BHC, Iowa.

Instrumentation and Monitoring System

The bridge was instrumented with vibrating wire instruments as well as strain and displacement transducers. The vibrating wire instruments (strain gages, earth pressure cells, and piezometers) were installed for long-term data recording. The strain and displacement transducers were installed and later removed after the live load test.

Permanent System (Vibrating Wire)

Strain gages were placed on four of the sheet pile sections and on each tie rod of the west abutment. At each location instrumented on the piles, two gages were placed on opposite sides of the pile to provide the ability to distinguish between axial and flexural stresses (strains) in the section. Strain gages were welded on the pile flanges at various locations along the pile. Sections of angle iron were then welded over the gages to provide protection during pile driving (shown previously in Figure 5-16b). Bending moments in the pile sections were calculated from the strains measured by the gages using a section modulus that included the contribution of the angle iron to the stiffness of the section. Locations of each strain gage pair are shown in Figure 5-34 (as well as a profile of the wall). Letters A through D denote backfill side of wall while E through F denotes stream side. Table 5-5 shows the distance to each gage measured from the top of the wall.

Angles welded over gages

Exposed gages
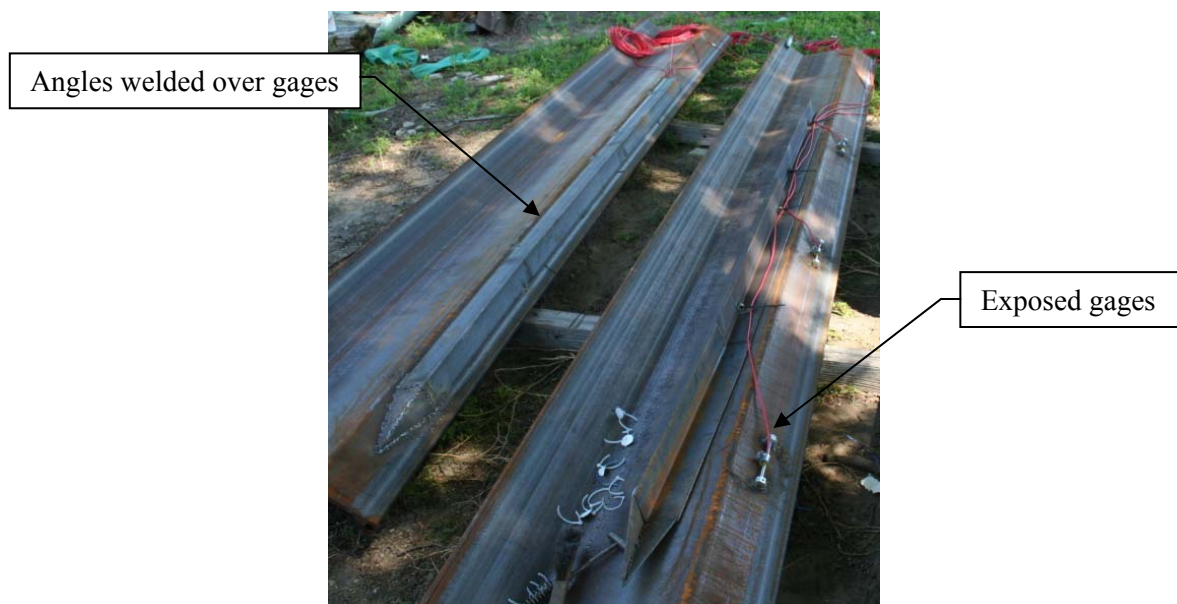
Figure 5-33. Sheet pile instrumented with vibrating wire strain gages.

A total of nine vibrating wire earth pressure cells were placed in the backfill of the west abutment to measure lateral earth pressures. Position of the cells in side and plan views are shown in Figure 5-35 and the associated dimensions given in Table 5-6; piezometer locations are also shown in the plan view. Four cells were placed at the centerline of the abutment at 1 ft, 3 ft, and 5 ft below the top of the abutment cap (TOC) with other cells placed at wingwalls and various positions in the backfill.

The vibrating wire system readings were recorded using a Geokon® datalogging system that included a Micro-10 datalogger with 3 multiplexers. This system was used for long-term monitoring of the abutment as well as short-term datalogging during the live load test.
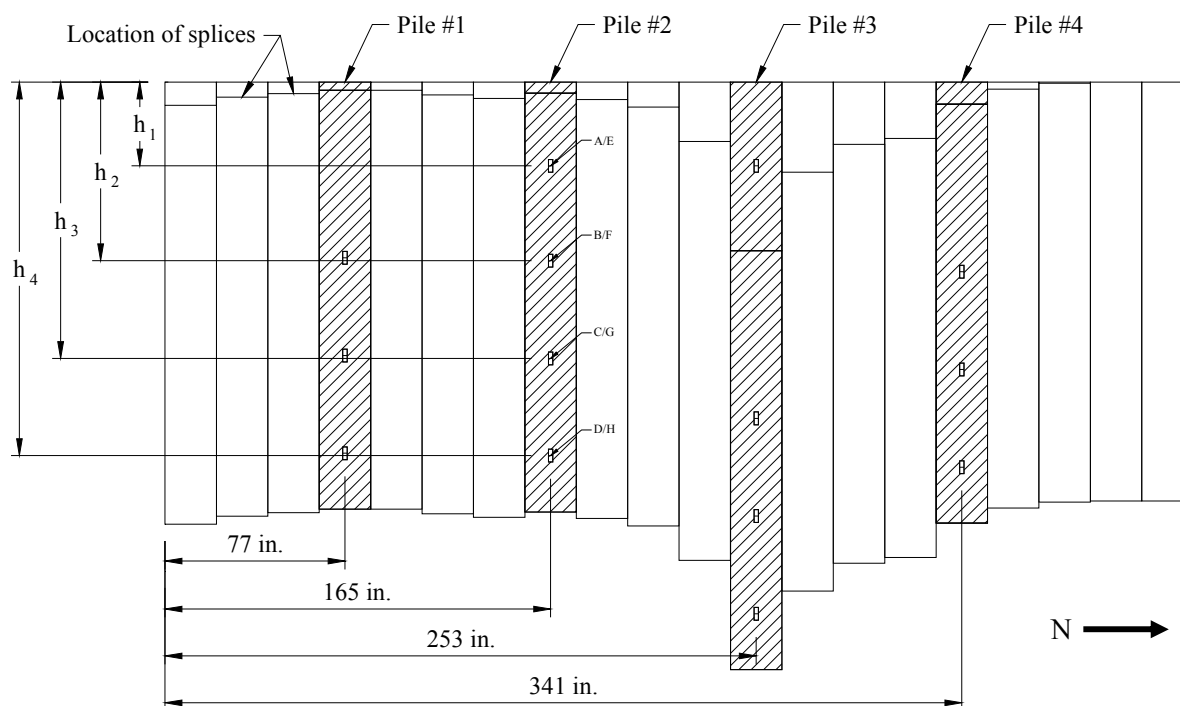
Figure 5-34. Profile of sheet pile wall showing locations of pile strain gages.

Table 5-5. Distance of strain gages from top of wall.

Dimension	Distance from top of wall (ft)			
	Sheet Pile 1	Sheet Pile 2	Sheet Pile 3	Sheet Pile 4
h_1	-	3.0	3.0	-
h_2	6.3	6.4	12.0	6.8
h_3	9.8	9.9	15.5	10.3
h_4	13.3	13.4	19.0	13.8

a.) Side view

b.) Plan view
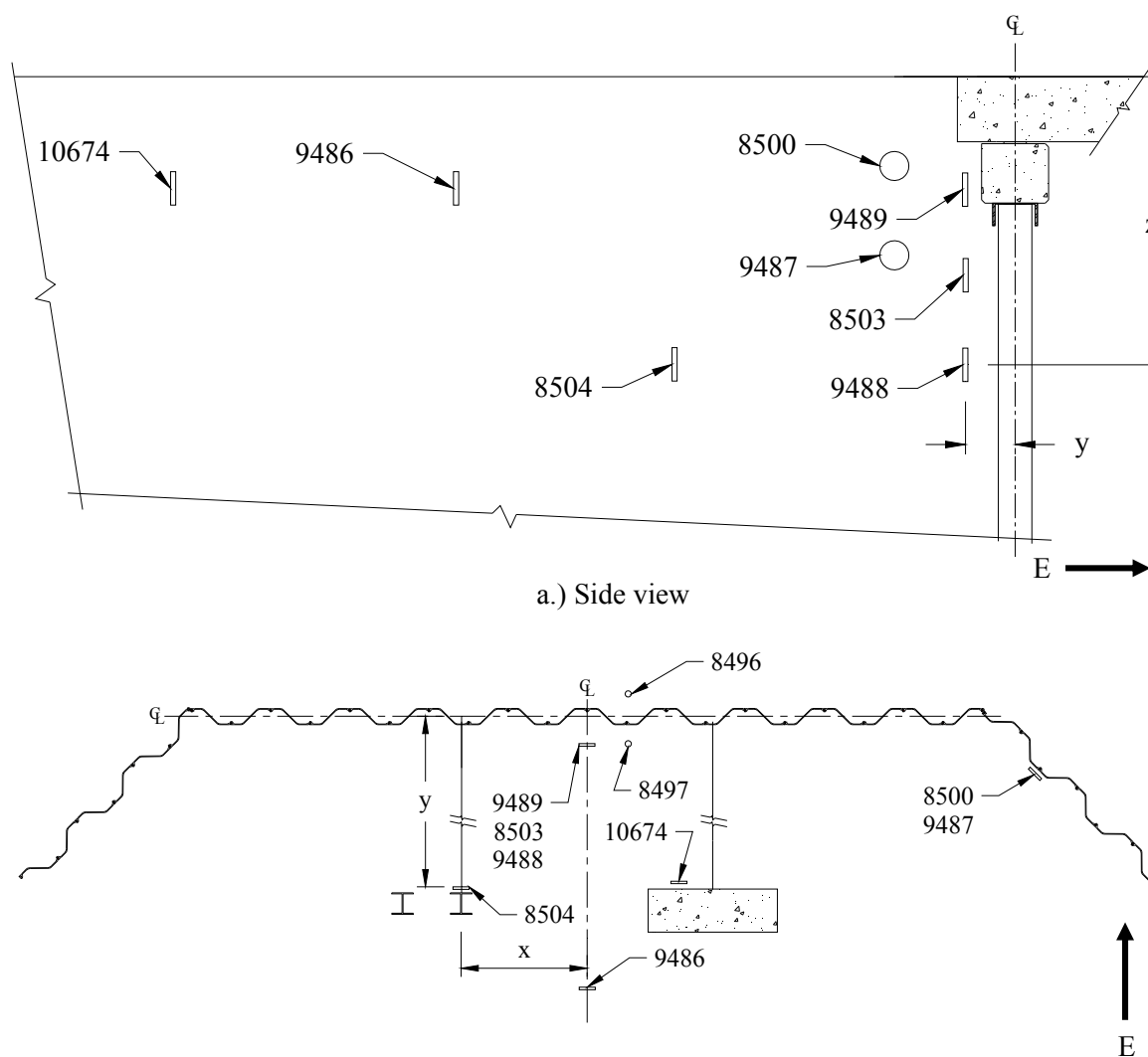
Figure 5-35. Earth pressure cell and piezometer layout in west abutment.

Table 5-6. Instrumentation locations with respect to dimensions shown in Figure 5-35.

Instrument	*x (ft)*	*y (ft)*	*z (ft)*
8496	2.0	0.5	13.8
8497	2.0	1.0	13.4
9486	0.0	12.5	2.5
9487	20.7	2.7	4.0
9488	0.0	1.0	6.5
9489	0.0	1.0	2.5
8500	20.7	2.7	2.0
8503	0.0	1.0	4.5
8504	5.8	8.0	6.5
10674	4.3	18.0	2.5

To obtain structural displacements and additional strains a second (temporary) instrumentation system was installed after construction of the bridge was completed. Deflection and strain transducers were attached to the structure and measurements were recorded with a datalogger at a rate of one set of readings per second (compared to the vibrating wire system rate of approximately one set per three minutes). Instrumentation was placed at the midspan of the bridge (measuring vertical deflections as well as strains in some of the bottom beam flanges) and on the exposed face of the west sheet pile abutment (measuring horizontal deflections of the wall and strains on the outside face of the piles). Locations of this instrumentation are shown in Figure 5-36 and Figure 5-37 with coordinates given in Table 5-7 and Table 5-8, respectively. The "BDI" and "Disp" instruments measure strains and displacements of the sheet pile wall, respectively.   An overview of the instrumentation setup is shown in Figure 5-38.
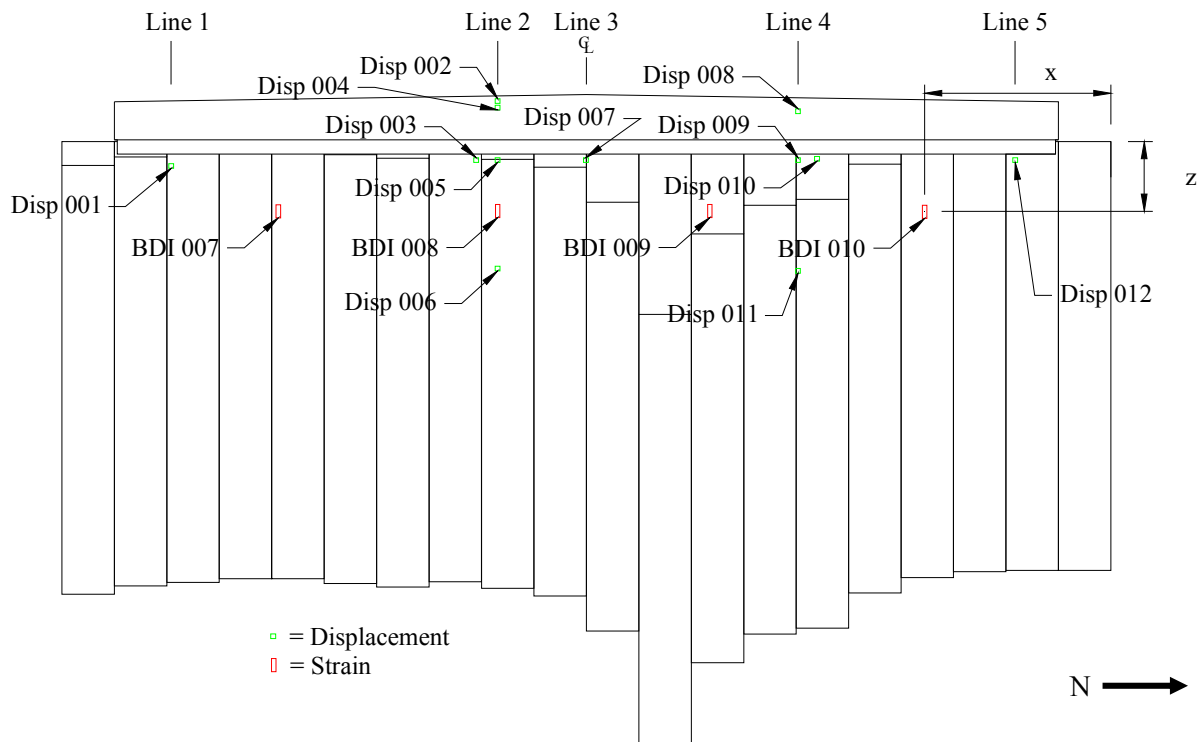
Figure 5-36. Strain (BDI) and displacement (Disp) instrumentation placed on west abutment system wall for bridge live load testing.

Three of the displacement transducers (Disp 002, Disp 003, and Disp 010) were used to measure differential movements between elements. Two transducers (Disp 003 and Disp 010) were used to measure displacement of the abutment cap relative to the sheet pile wall and another (Disp 002) was used to measure displacement of the abutment cap relative to the bridge deck. The setup for Disp 003 is shown in Figure 5-39; Disp 002 was fixed to the bottom of the deck with the string attached to the abutment cap.

Coordination between datalogging systems was achieved by using an instrument to provide a marked location in the data whenever the trucks were at the desired positions.
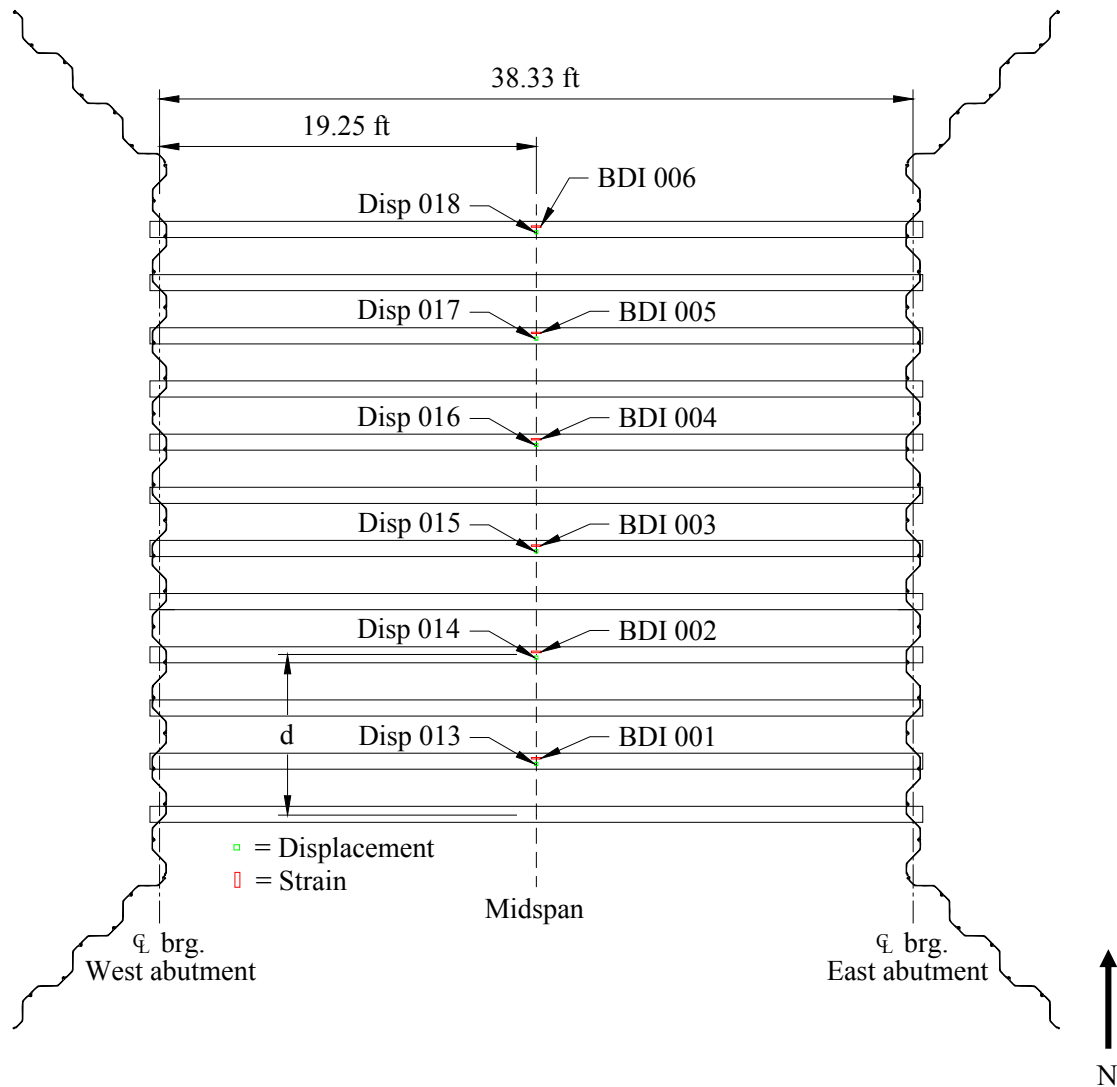
Figure 5-37. Strain (BDI) and displacement (Disp) instrumentation placed on superstructure for bridge live load testing.

a.) View of west abutment   b.) Side view of west abutment and midspan
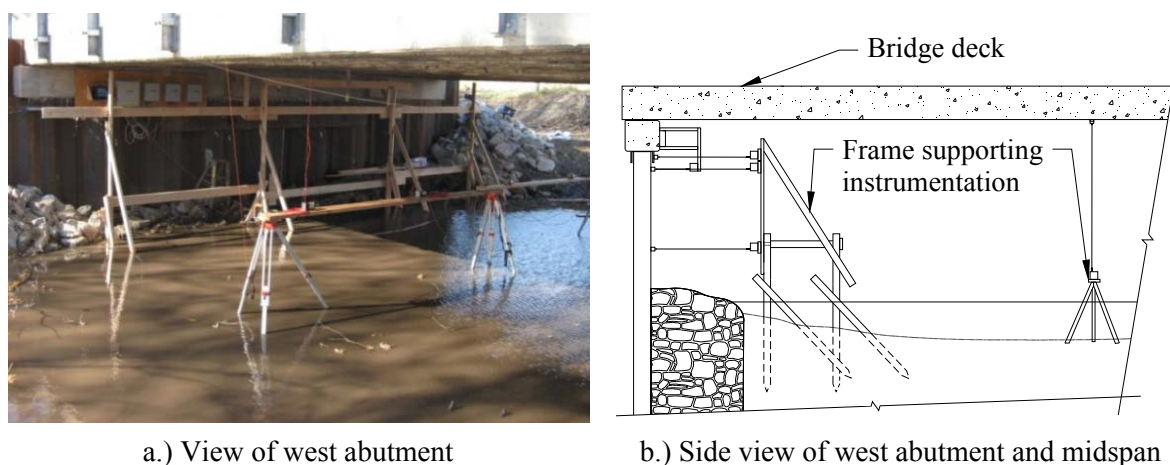
Figure 5-38. Strain and displacement instrumentation setup for live load test.

Table 5-7. Locations of live load test instrumentation attached to west abutment system wall with respect to coordinate system shown in Figure 5-36.

Instrument	x (ft)	z (ft)
Disp 001	32.8	0.9
Disp 002	21.4	-1.4
Disp 003	22.2	0.6
Disp 004	21.4	-1.2
Disp 005	21.4	0.6
Disp 006	21.4	4.4
Disp 007	18.3	0.6
Disp 008	10.9	-1.1
Disp 009	10.9	0.6
Disp 010	10.3	0.6
Disp 011	10.9	4.5
Disp 012	3.3	0.6
BDI 007	29.1	2.4
BDI 008	21.4	2.4
BDI 009	14.0	2.4
BDI 010	6.5	2.4

Table 5-8. Locations of live load test instrumentation attached to superstructure at midspan relative to center of beam on south side of bridge shown in Figure 5-37.

Instrument	d (ft)
Disp 013/ BDI 001	2.8
Disp 014/ BDI 002	8.3
Disp 015/ BDI 003	13.8
Disp 016/ BDI 004	19.3
Disp 017/ BDI 005	24.8
Disp 018/ BDI 006	30.3
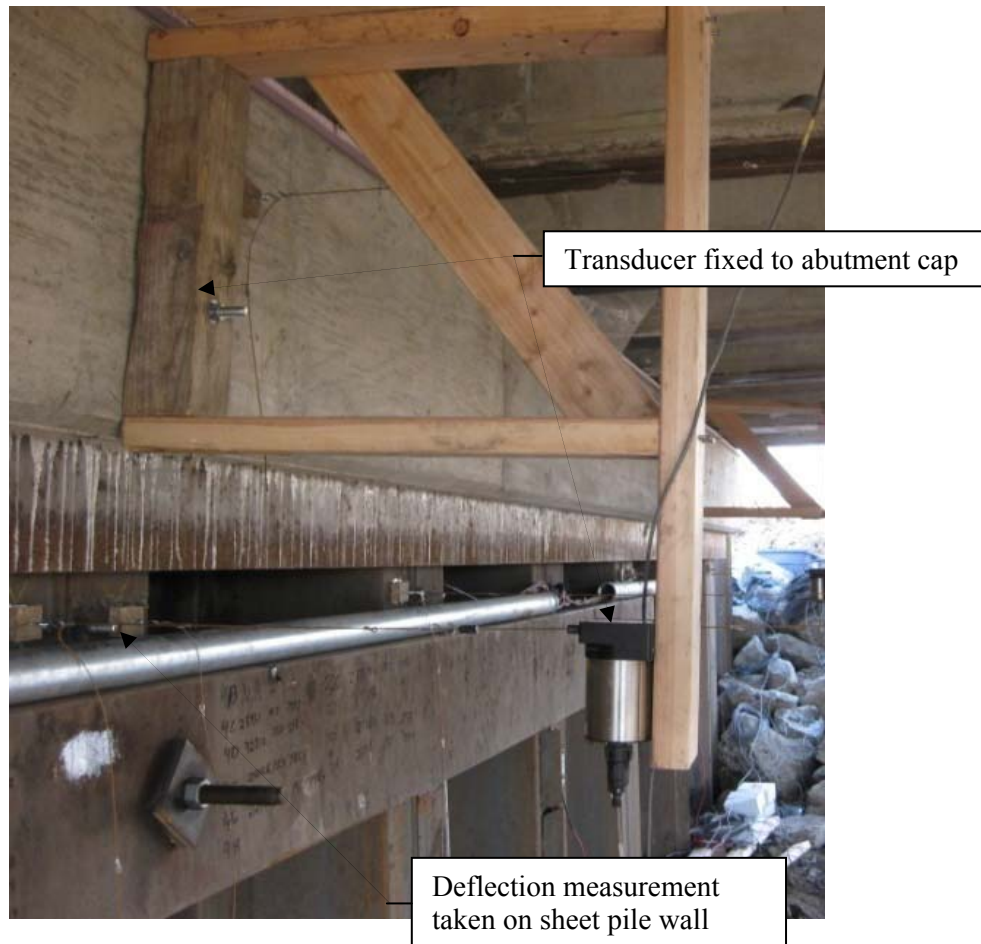
Figure 5-39. Instrumentation setup for measuring displacement of abutment cap relative to sheet pile wall (Disp 003).

Bridge Load Testing

Due to the unexpectedly high post-construction stress readings in the tie rods on the west abutment, it was decided that a test be performed on the south tie rod to verify the accuracy of the readings. The details of this test are outlined in the following section.

Tie Rod Test

The objective of the tie rod test was to unload and load the south tie rod in the west abutment to determine if the level of strain (stress) measured by the attached strain gage was accurate. In this test, the tie rod hex nut was loosened at specific intervals, and readings of tie rod strain (stress) were taken after each interval. The four steps (intervals) during the tie rod test were:

1. Loosen hex nut 0.25 of a turn

2. Tighten 0.25 of a turn (returned to starting position)

3. Loosen hex nut in 0.50 turn intervals until 2 full turns achieved

4. Loosen at full turn intervals until a total of 4 full turns achieved

Initial stress in the south tie rod, which was calculated by the increase in strain from the initial values measured after installation of the gage, was approximately 44 ksi. Steps 1 and 2 of the tie rod test revealed that the stress decreased and returned to the initial level. Results of the stress readings for Steps 3 and 4, with data taken between each test interval, are shown in Figure 5-40. Since significant relatively linear and elastic changes in strain (stress) were observed during the tie rod test, it was concluded that the stress levels initially indicated in the rods were reliable.

Stress levels in the tie rods were also monitored during the live load test of the bridge. Stresses produced in the south rod during the test involving both trucks (the highest load) are also given in Figure 5-40. Monitoring of the north tie rod in the west abutment was attempted during the bridge load test but was unsuccessful as the strain gage on this tie rod was damaged during construction. It should be noted that, since the north tie rod was attached to a relatively flexible steel H-pile (versus a reinforced concrete deadman), the stresses developed in the north tie rod would have been less than the south tie rod system (assuming each was exposed to the same levels of load).

Conclusions drawn from the tie rod test were:

- The initial tie rod gage readings were reliable and high stresses were induced in the south tie rod during the construction stages.

- After performing the live load test, no significant increase in stress (less than 0.5 ksi) occurred in the south tie rod. By theoretical analysis, the test truck was expected to induce a maximum stress of 3 ksi assuming lateral restrain was provided by the superstructure; the low levels of stress developed confirm this assumption made in design. The stresses initially induced in the tie rods (approximately 45 ksi) occurred during backfilling of the abutment before the superstructure was installed, confirming the necessity of a lateral restraint system during construction of the abutments. (continued)

- Since initial readings in the south tie rod indicated stress levels near the yield stress of the steel, it is possible the tie rods experienced yielding at some point during compaction of the abutment backfill and placement of the superstructure elements. This could also explain the span length of the bridge being approximately 8 in. shorter than designed (due to lateral displacements of abutments toward each other) although other construction factors may have had an influence as well.
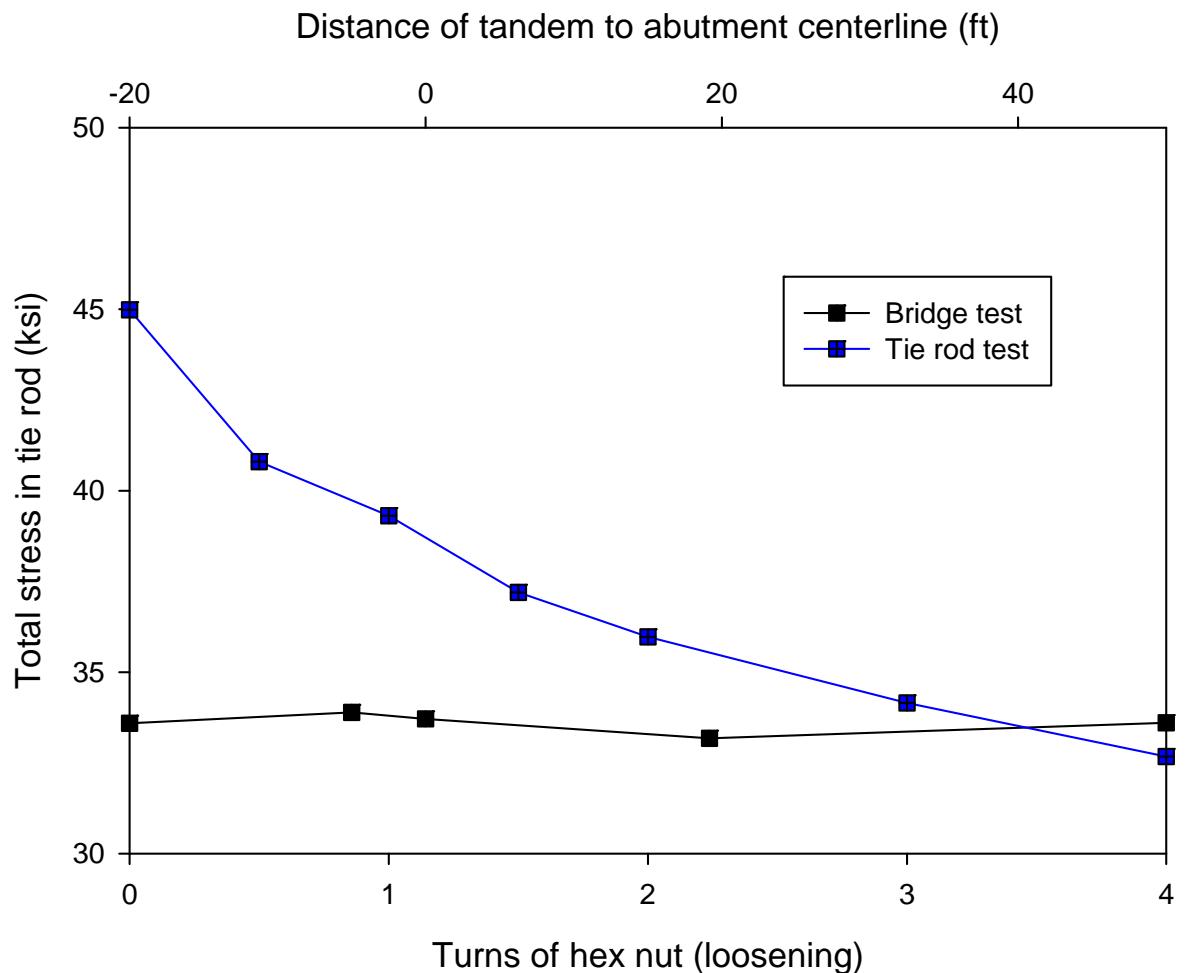
Figure 5-40. Comparison of stress level in south tie rod during live load testing and the tie rod test.

Live Load Test

Test Procedure

Test truck axle weights are given in Table 5-9; test truck dimensions are given in Table 5-10 along
with the truck diagrams shown in Figure 5-41.

Table 5-9. Test truck axle loads and total weight.

Load type	Truck 48 (lbs)	Truck 38 (lbs)
Front axle	17,460	16,980
Tandem axle	31,360	30,260
Total weight	48,820	47,240

Table 5-10. Test truck dimensions.

Dimension	Truck 48 (ft)	Truck 38 (ft)
A	5.17	4.75
B	4.50	4.25
C	14.58	14.50
D	2.33	2.42
E	6.08	6.08
F	8.00	8.00

a.) Side view   b.) Rear view
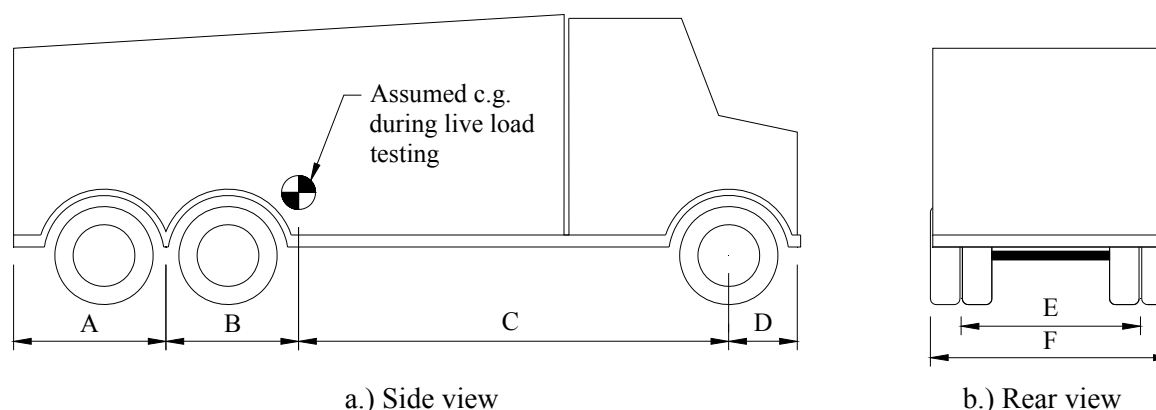
Figure 5-41. Diagram of test trucks.

The live load test consisted of the four different runs shown in Figure 5-42. Each test run involved
the truck travelling from west to east and stopping at predetermined locations along the bridge.
Figure 5-43 shows the test locations along the bridge from west to east. The test positions are labeled
by a letter (corresponding to a test run in Figure 5-42) and a location number according to position

along the bridge; Figure 5-43 presents each location number and the distance of the centerline of the tandem axle to the centerline of the west abutment.

Test Locations 6, 7 and 8 were intended for the center of gravity of the truck(s) to be positioned of the 0.25 span, midspan, and 0.75 span of the bridge; the assumed center of gravity of the truck was determined in the field as a fixed location on each truck (the mud-flap shown in Figure 5-44b). The dimension "B" in Table 5-10 gives the distance of this point relative to the centerline of the tandem axle; future calculation of the exact center of gravity of the test truck determined the dimension "B" in Table 5-10 to be 6.82 ft and 6.74 ft for Truck 48 and Truck 38, respectively; this showed field assumed values for "B" were relatively accurate. All data are displayed as centerline of the tandem axle locations for simplicity.

At each location, the trucks remained in position until all of the instrumentation was read and recorded. Due to the inherent delays involved in reading vibrating wire instruments, each test location reading required approximately three minutes to complete. Select data collected during the bridge test are presented and analyzed within this section of the report.

a.) Test Run A
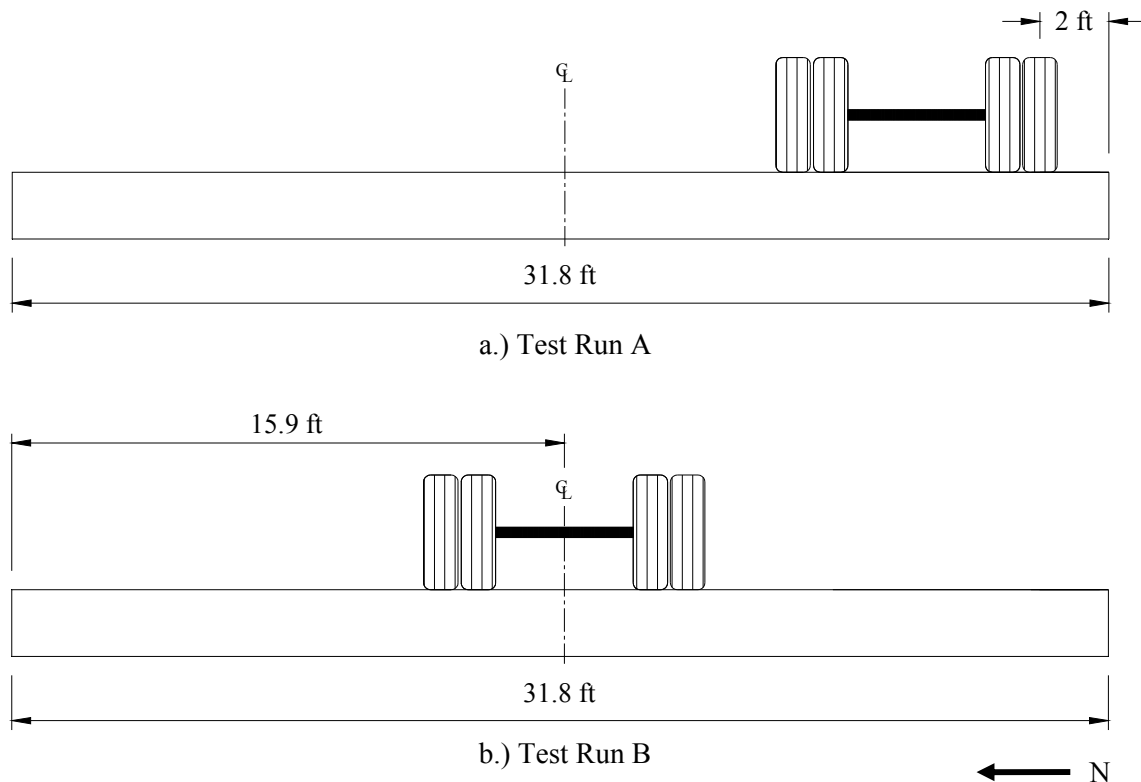
b.) Test Run B

Figure 5-42. Transverse location of truck(s) in live load tests.
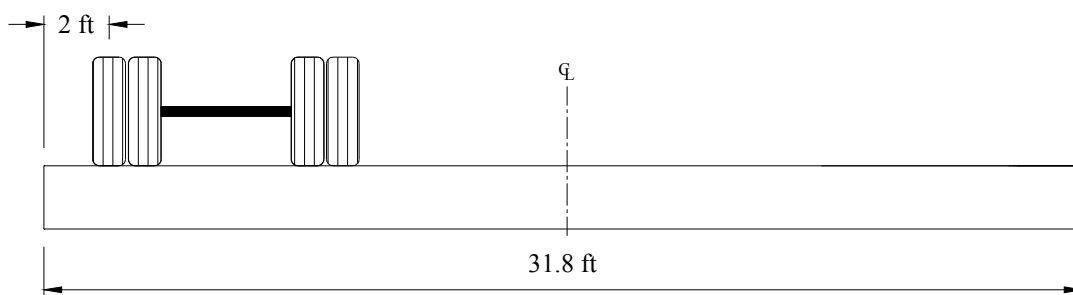
c.) Test Run C
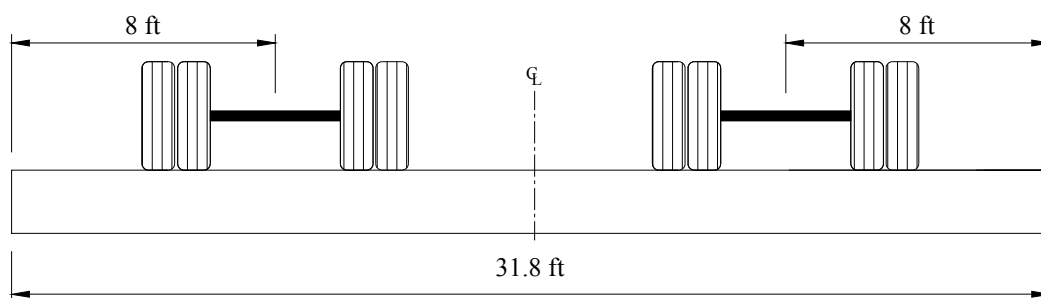
d.) Test Run D

Figure 5-42 (continued).
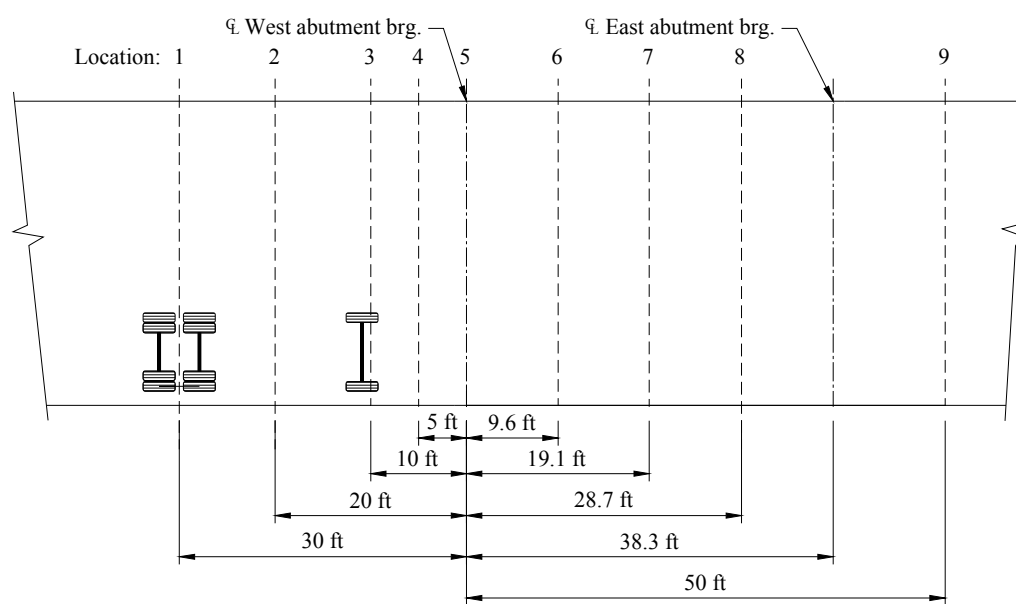
Figure 5-43. Locations of tandem axle along the bridge.

| a.) Overview of load testing | b.) Side view of Truck 48 |

Figure 5-44. Bridge live load testing of BHC, Iowa demonstration project.

Data Analysis and Discussion

It should be noted that, when designing the monitoring system, it was desired to have the ability to determine absolute values of the stress induced in the backfill soil (requiring "zero" values for earth pressure cells be recorded just after placement and before any backfilling occurred). When initially analyzing the data, it became apparent that, due to the movement of the wall (and release of stresses) which occurred during the tie rod test, the "zero" values for all the cells had changed. As a result, all data charts in this section present *relative* values of stress induced from the trucks; the "zero" values used were taken after the tie rod test (which involved removal of stress in the tie rod by loosening of the hex nut) had been performed.

The loosening of the hex nut during the tie rod test resulted in an outward movement of the sheet pile wall and subsequently affected backfill soil stresses; changes in pressure on each of the earth pressure cells resulting from the tie rod test are given in Table 5-11 (a negative value represents a reduction in pressure). A reduction in stress was seen in all cell locations except at the wingwalls which experienced little change. For the cells below TOC, special attention should be given to the magnitudes of stress released as it gives an indication of the deflected shape of the wall as the tie rod stress was released. Since the reduction in stress is greatest in the cell the greatest distance below the TOC, it can be inferred that the wall "bowed" outward. The rigidity of the superstructure resisted lateral displacement of the top of the wall at the location of the abutment cap, resulting in the deflected shape shown in Figure 5-45.

Table 5-11. Change in earth pressure cell stresses resulting from wall movements during the tie rod test (refer to Figure 5-35 for pressure cell locations).

Pressure cell		Stress released after wall movement (psf)
Number	Location	
10674	concrete deadman	- 50.1
8500	wingwall – high	+ 6.8
9487	wingwall – low	+ 1.5
9489	1 ft below TOC	- 36.8
8503	3 ft below TOC	- 83.1
9488	5 ft below TOC	- 143.0
8504	H-pile deadman	- 11.7
9486	12.5 ft back from wall	- 25.3

a.) Plan view of wingwall deformations   b.) Side view of deflected wall
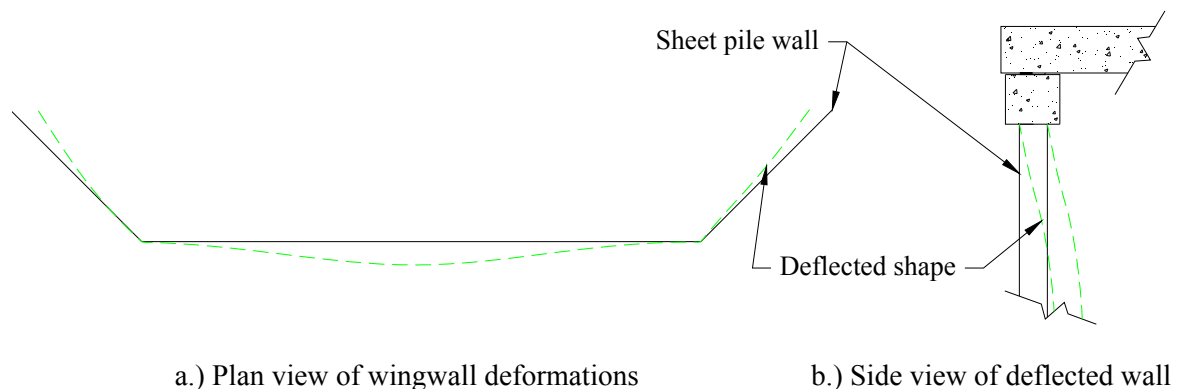
Figure 5-45. Simulated deformations of sheet pile wall under load.

Earth pressures recorded for Cell 9489 (1ft below TOC) are shown in Figure 5-46. As can be seen, the highest earth pressures were recorded during the test run (Run D) involving both trucks centered over midspan of the bridge. Although pressures would initially be expected to reach maxima when truck surcharge loads were on the abutment backfill, a potential explanation for the observed phenomenon is the deformation of the bridge superstructure (elongation of the bridge as camber is overcome as depicted in Figure 5-47) under load displacing the abutment caps toward the backfill, applying pressure on the cell which is directly behind the caps. Further evidence of this is seen when comparing Run B and Run D: although Run B shows higher stress in the cell while the tandem is on the backfill material (which is expected since the cell is located along the centerline), Run D shows greater stress when the two trucks are on the bridge (meaning greater deformation and elongation of the superstructure versus Run B which involved only one truck).

Earth pressures during live load testing for Cells 8503 (3 ft below TOC) and 9488 (5 ft below TOC) are presented in Figure 5-48 and Figure 5-49, respectively. At both locations, earth pressure variations of less than 20 psf occurred; the forces transferred to the sheet pile wall due to vehicular surcharge on the backfill are negligable.
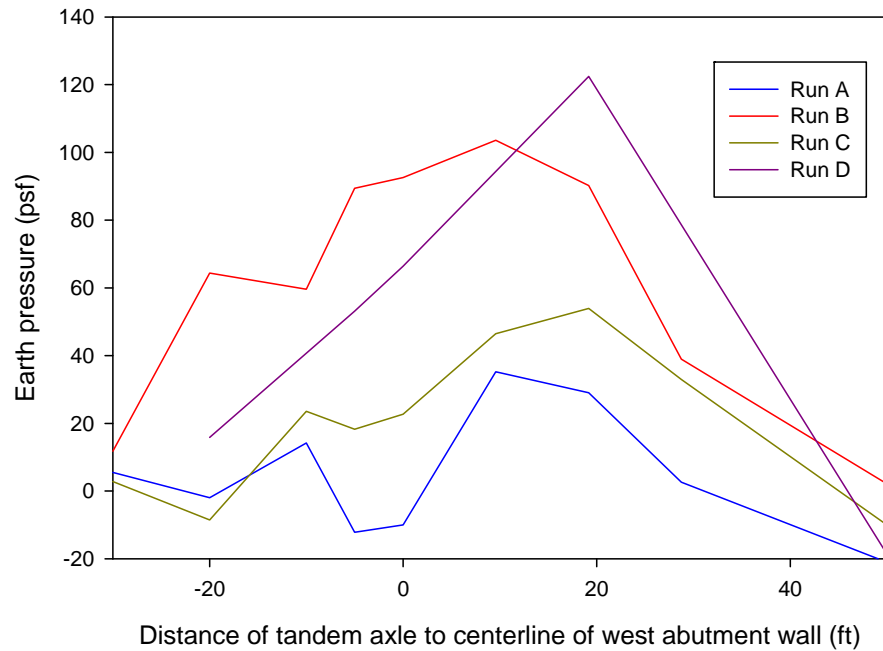
Figure 5-46. Earth pressures for Cell 9489 (1 ft below TOC) during live load testing.
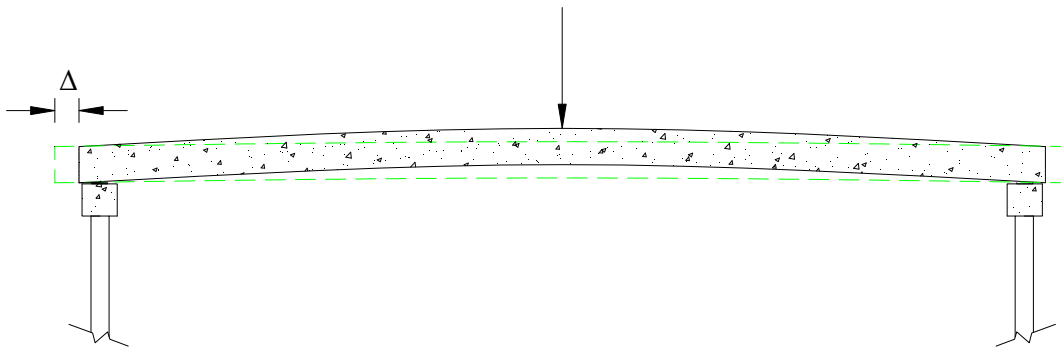
Figure 5-47. Diagram of bridge elongation under loading due to superstructure deflections.
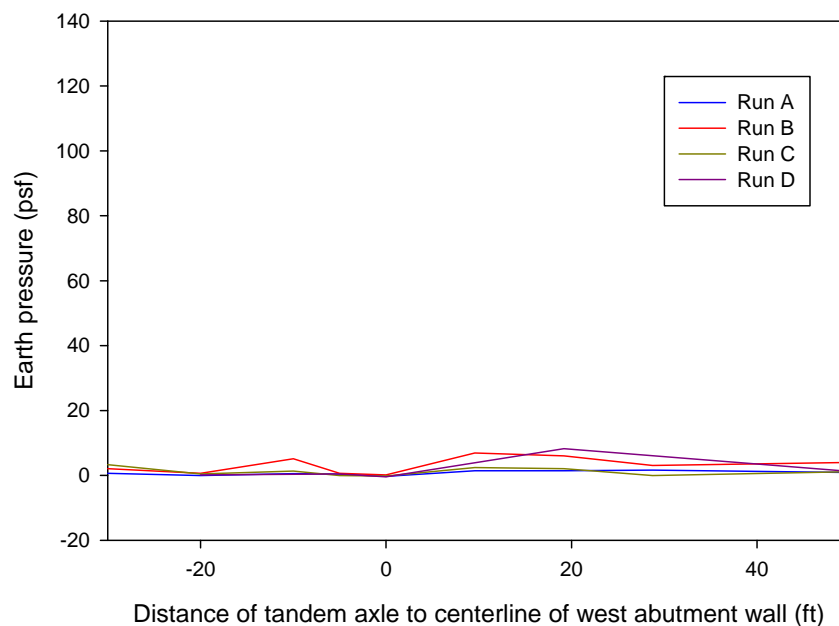
Figure 5-48. Earth pressures for Cell 8503 (3 ft below TOC) during live load testing.
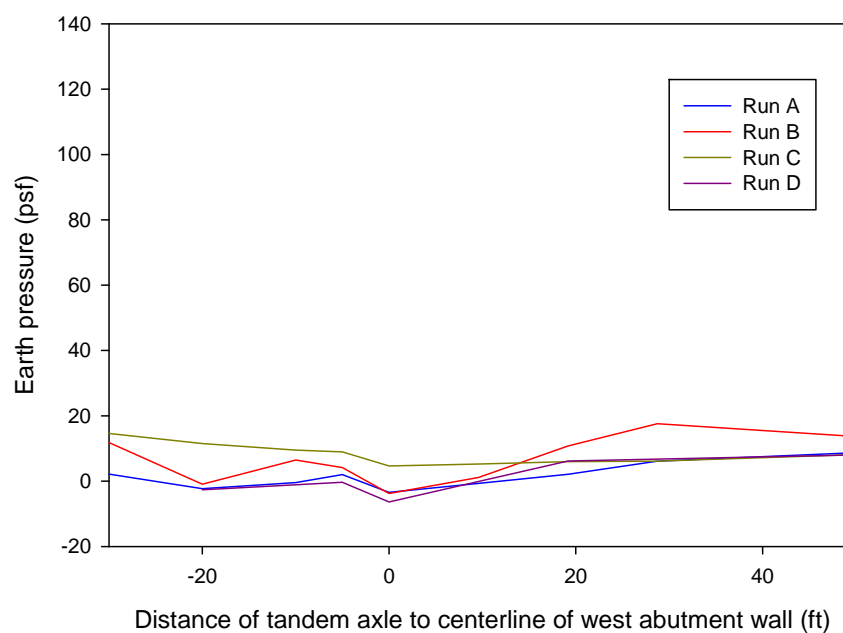
Figure 5-49. Earth pressures for Cell 9488 (5 ft below TOC) during live load testing.

The expected stresses and deflections were calculated to provide a comparison for select data obtained during the bridge test. An analysis was performed for three locations of the test trucks (Truck 48 for single-truck Runs A, B and C): Locations 3, 4, and 5 (described previously, see Figure 5-43) with results provided in Table 5-12 through Table 5-14, respectively. Total values are given as well as the values due to the live load test only. For the earth pressure cells listed, their locations are given relative to TOC. Stresses in the piles (determined from strain gages) are presented as average values for axial strains (stress) measured at multiple locations along each instrumented pile; flexural strains (stresses) are presented for the maximum value measured in each instrumented pile.

The theoretical analysis was performed to investigate the adequacy of the design methods used. This investigation was accomplished by applying the load distribution methods and other assumptions utilized in design, determining expected loads and deflections by theoretical analysis, and comparing expected results to data collected during live load testing; example analysis calculations for BHC, Iowa are provided in Appendix A.

For the theoretical analysis, truck loads were assumed to distribute over a 10 ft width of the bridge. A friction angle of 45° (determined from a direct shear test, see Figure A12) was used for the backfill material in determining lateral earth pressures. Vehicular surcharge on the backfill material was analyzed according to AASHTO (1998) Section 3.11.6.1-4 to determine the lateral loads applied to the wall. The wall was analyzed with STAAD (2008) to determine bending moments, deflections of the sheet pile wall, and tie rod forces. For determining flexural stresses in the sheet pile sections, a modified section modulus of 35.2 in^3/ft (calculated by ISU) was used to account for additional resistance provided by the angles welded to the instrumented piles (angles were continuous along the length of each pile except for negligible lengths at each end); the section modulus without the angles was 18.1 in^3/ft.

An analysis of the superstructure was also performed to estimate midspan flexural stresses and deflections. The section modulus and moment of inertia for the deck elements used were 181.4 $in.^3$ and 1741 $in.^4$, respectively, for a repeating section of a width of 2.75 ft (values obtained from BHC Engineer's Office). The section modulus and moment of inertia calculated for the repeating section are accurate for use with interior elements. An exterior element would have slightly higher values of section modulus and moment of inertia due to contribution of the guardrail in stiffness; properties of the repeating section were conservatively assumed to apply for exterior elements.

Table 5-12. Comparison of actual to estimated values of selected loads and deflections for Location 3.

Load or deflection	Estimated	
	Total	Live load only
Pile axial stress	0.80 ksi	0.21 ksi
Pile flex. stress	3.29 ksi	0.40 ksi
Earth pressure (1 ft below TOC)	139 psf	74 psf
Earth pressure (3 ft below TOC)	254 psf	119 psf
Earth pressure (5 ft below TOC)	335 psf	130 psf
Midspan flex. stress	-	1.45 ksi
Midspan deflection	-	0.13 in.
Wall deflection	0.13 in.	0.02 in.
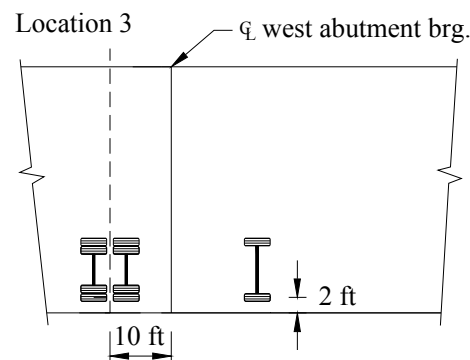
Tandem axle 10 ft west of west abutment centerline during Run A

Load or deflection	Measured (Live loads only)			
	Run A	Run B	Run C	Run D
Pile 1 axial stress (avg)	-0.05 ksi	+0.01 ksi	+0.01 ksi	
Pile 2 axial stress (avg)	-0.15 ksi	-0.17 ksi	-0.08 ksi	-
Pile 3 axial stress (avg)	-0.01 ksi	-0.04 ksi	-0.02 ksi	
Pile 4 axial stress (avg)	+0.01 ksi	-0.04 ksi	-0.07 ksi	
Pile 1 flex. stress (max)	0.06 ksi	0.03 ksi	0.05 ksi	
Pile 2 flex. stress (max)	0.23 ksi	0.21 ksi	0.06 ksi	-
Pile 3 flex. stress (max)	0.03 ksi	0.04 ksi	0.06 ksi	
Pile 4 flex. stress (max)	0.01 ksi	0.03 ksi	0.06 ksi	
Earth pressure (1 ft below TOC)	14 psf	60 psf	24 psf	
Earth pressure (3 ft below TOC)	1 psf	5 psf	1 psf	-
Earth pressure (5 ft below TOC)	0 psf	6 psf	9 psf	
Midspan flex. stress (max)	0.8 ksi	0.5 ksi	0.9 ksi	
Midspan deflection (max)	0.040 in.	0.030 in.	0.015 in.	-
Wall deflection (max)	0.002 in.	0.001 in.	0.001 in.	

Table 5-13. Comparison of actual to estimated values of selected loads and deflections for Location 4.

Load or deflection	Estimated	
	Total	Live load only
Pile axial stress	0.76 ksi	0.17 ksi
Pile flex. stress	3.40 ksi	0.53 ksi
Earth pressure (1 ft below TOC)	302 psf	237 psf
Earth pressure (3 ft below TOC)	373 psf	238 psf
Earth pressure (5 ft below TOC)	366 psf	161 psf
Midspan flex. stress	-	2.2 ksi
Midspan deflection	-	0.18 in.
Wall deflection	0.13 in.	0.02 in.
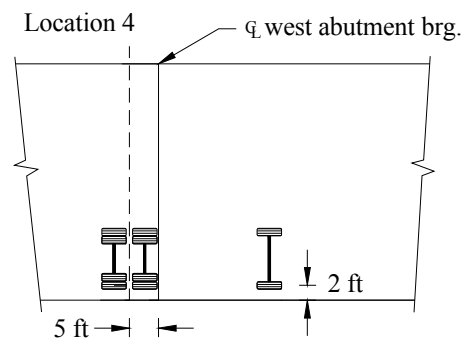
Tandem axle 5 ft west of west abutment centerline during Run A

Load or deflection	Measured (Live Loads Only)			
	Run A	Run B	Run C	Run D
Pile 1 axial stress (avg)	-0.06 ksi	+0.02 ksi	+0.01 ksi	-0.05 ksi
Pile 2 axial stress (avg)	-0.18 ksi	-0.20 ksi	-0.07 ksi	-0.27 ksi
Pile 3 axial stress (avg)	-0.03 ksi	-0.05 ksi	-0.06 ksi	-0.10 ksi
Pile 4 axial stress (avg)	+0.01 ksi	-0.05 ksi	-0.11 ksi	-0.12 ksi
Pile 1 flex. stress (max)	0.08 ksi	0.03 ksi	0.04 ksi	0.06 ksi
Pile 2 flex. stress (max)	0.24 ksi	0.19 ksi	0.07 ksi	0.30 ksi
Pile 3 flex. stress (max)	0.02 ksi	0.06 ksi	0.05 ksi	0.06 ksi
Pile 4 flex. stress (max)	0.01 ksi	0.04 ksi	0.06 ksi	0.09 ksi
Earth pressure (1 ft below TOC)	-12 psf	89 psf	18 psf	53 psf
Earth pressure (3 ft below TOC)	0 psf	1 psf	0 psf	0 psf
Earth pressure (5 ft below TOC)	2 psf	4 psf	9 psf	0 psf
Midspan flex. stress (max)	1.3 ksi	0.8 ksi	1.4 ksi	1.5 ksi
Midspan deflection (max)	0.06 in.	0.04 in.	0.02 in.	0.08 in.
Wall deflection (max)	0.004 in.	0.002 in.	0.001 in.	0.002 in.

Table 5-14. Comparison of actual to estimated values of selected loads and deflections for Location 5.

Load or deflection	Estimated	
	Total	Live load only
Pile axial stress	0.94 ksi	0.35 ksi
Pile flex. stress	3.20 ksi	0.30 ksi
Earth pressure (1 ft below TOC)	315 psf	250 psf
Earth pressure (3 ft below TOC)	215 psf	80 psf
Earth pressure (5 ft below TOC)	235 psf	30 psf
Midspan flex. stress	-	3.1 ksi
Midspan deflection	-	0.23 in.
Wall deflection	0.13 in.	0.01 in.

Location 5 — ₵ west abutment brg.

2 ft
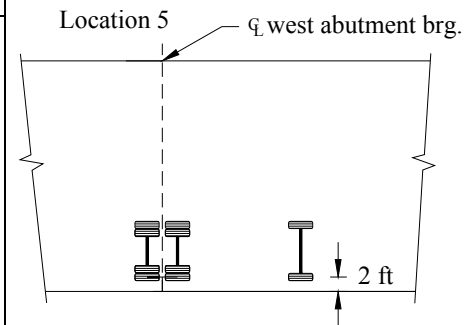
Tandem axle centered over west abutment centerline during Run A

Load or deflection	Measured (Live Loads Only)			
	Run A	Run B	Run C	Run D
Pile 1 axial stress (avg)	-0.09 ksi	+0.01 ksi	+0.02 ksi	-0.05 ksi
Pile 2 axial stress (avg)	-0.32 ksi	-0.27 ksi	-0.09 ksi	-0.43 ksi
Pile 3 axial stress (avg)	-0.04 ksi	-0.09 ksi	-0.07 ksi	-0.14 ksi
Pile 4 axial stress (avg)	+0.01 ksi	-0.08 ksi	-0.21 ksi	-0.22 ksi
Pile 1 flex. stress (max)	0.06 ksi	0.03 ksi	0.02 ksi	0.05 ksi
Pile 2 flex. stress (max)	0.40 ksi	0.29 ksi	0.07 ksi	0.50 ksi
Pile 3 flex. stress (max)	0.03 ksi	0.03 ksi	0.05 ksi	0.04 ksi
Pile 4 flex. stress (max)	0.01 ksi	0.04 ksi	0.06 ksi	0.05 ksi
Earth pressure (1 ft below TOC)	-10 psf	93 psf	23 psf	66 psf
Earth pressure (3 ft below TOC)	0 psf	0 psf	0 psf	0 psf
Earth pressure (5 ft below TOC)	-3 psf	-4 psf	5 psf	-6 psf
Midspan flex. stress (max)	2.3 ksi	1.4 ksi	2.1 ksi	2.4 ksi
Midspan deflection (max)	0.075 in.	0.050 in.	0.025 in.	0.100 in.
Wall deflection (max)	0.004 in.	0.002 in.	0.001 in.	0.002 in.

From the results previously presented in Figure 5-46, Figure 5-48, and Figure 5-49 it can be seen that earth pressures were significantly lower than estimated by theoretical analysis; conservative estimates of soil cohesion is one potential explanation for this observation. Although more pressure cells were used in the test (all measuring unexpectedly low earth pressures), the cell 1 ft below TOC showed the highest variation in stress during the live load test (a magnitude of approximately 100 psf).

In general, maximum stresses in the piles (axial and flexural) were comparable to those estimated by analysis suggesting a 10 ft wide distribution for live loads is a reasonable assumption; design of the sheet piling for axial load used an over-conservative live load distribution of 3 piles (5.5 ft). A trend noticed in the data presented in Table 5-12 through Table 5-14 is the minimal distribution of axial stress to adjacent piles through friction between the sheet pile interlocks. For example, in Table 5-14 for Run A (in which the truck would be positioned over Pile 2) instrumented Pile 2 experiences an axial compressive force of 0.32 ksi while the adjacent piles (Pile 1 and Pile 3) experience stresses below 0.10 ksi and Pile 4 experiences negligible axial load.

All horizontal wall deflections and vertical deflections of the superstructure at midspan were significantly less than estimated by analysis. Wall displacements for Line 2 and Line 4 are presented in Figure 5-50 for test Run D (both trucks); the locations of Line 2 and Line 4 were previously depicted in Figure 5-36. It should be noted that negative displacement represents an outward movement of the wall. Although magnitudes of the wall displacements are negligible (approximately 10 times lower than expected by analysis), the nature of the displacements is of interest.

As previously mentioned, two displacement transducers (Disp 003 and Disp 010) were installed to measure movement of the abutment cap relative to the sheet pile wall. In both Line 2 and Line 4, movement of the abutment cap relative to the top of the sheet pile wall occurred when the centerline of the tandem axles were 5 ft from the abutment centerline (for all test Runs) and subsequently returned to zero when the tandem axles were on the bridge; the displacement of the top of the wall was positive, suggesting that either (1) the abutment cap was being pushed outward or (2) the tie rod location is acting as a fixed point about which the wall rotates (a pinned connection) and thus the top of the wall will move inward due to lateral forces deflecting the lower portion of the wall outward ("bowing out"). The outward displacements of Disp 008 and Disp 009 suggest that case (1) is occurring as the entire wall moves outward (including the abutment cap); similar effects are seen in both Line 2 and Line 4.

Another displacement of interest is the significant *inward* movement (toward the backfill) of the abutment cap (Disp 004 and Disp 008) when the trucks are located at midspan in Run D; this can be explained by the phenomenon described earlier in which the camber of the bridge deck units is overcome and the superstructure expands laterally, pushing the abutments inward. On Line 2, a displacement transducer (Disp 002) was placed to measure movements of the abutment cap relative to the bridge deck. The significant *negative* displacement of Disp 002 when the trucks are at midspan further confirms the occurrence of this phenomenon as it suggests the bridge deck elements are expanding laterally.
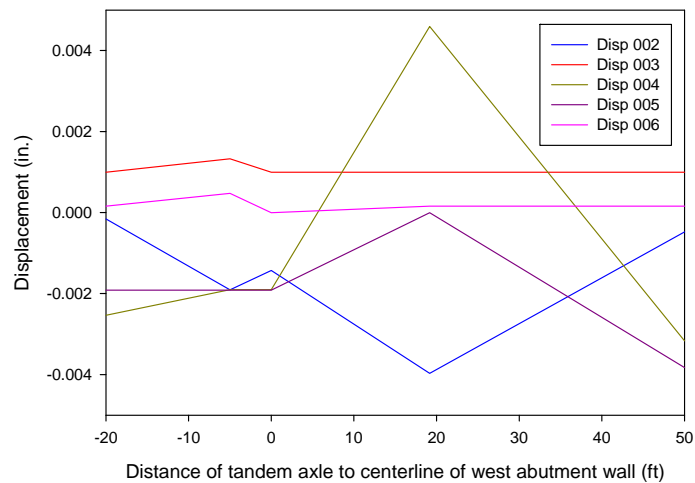
a.) Line 2 instrumentation
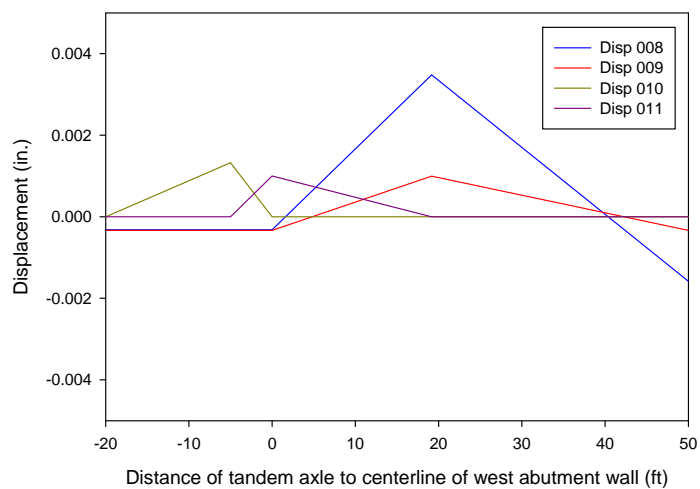
b.) Line 4 instrumentation

Figure 5-50. Wall displacements during live load test Run D (see Figure 5-36 for locations).

Long-Term Monitoring

For long-term monitoring of bridge's behavior, the permanent instrumentation system was used. Readings were taken 4 times daily (once every 6 hours) starting November 20, 2008. The system was set to record at 4:00am, 10:00am, 4:00pm, and 10:00pm to capture daily temperature fluctuations. Long-term measurement of earth pressure (as well as temperature) in the cells 1 ft and 3 ft below TOC are presented in Figure 5-51 and Figure 5-52, respectively. Although the monitoring system was destroyed in a flooding event in the spring of 2009, long-term data were collected for 80 days after November 20, 2008. For the cell 1 ft below TOC, significant variations of earth pressure with time were recorded. In the cell just below it (3 ft below TOC) the variation was less. Both cells experienced greater variations in stress during cold temperature cycles (perhaps attributable to stress development from ground freezing in the backfill behind the abutment). It should be noted that each pressure cell and piezometer was equipped with a thermistor for measuring temperatures therefore each chart will present differing temperatures corresponding to the location of the instrument. The significant variations of temperature in Cell 9489 (Figure 5-51) are most likely due to the proximity of the cell to the surface and the concrete abutments; it experienced greater daily fluctuation of temperature during the warmer part of the season.
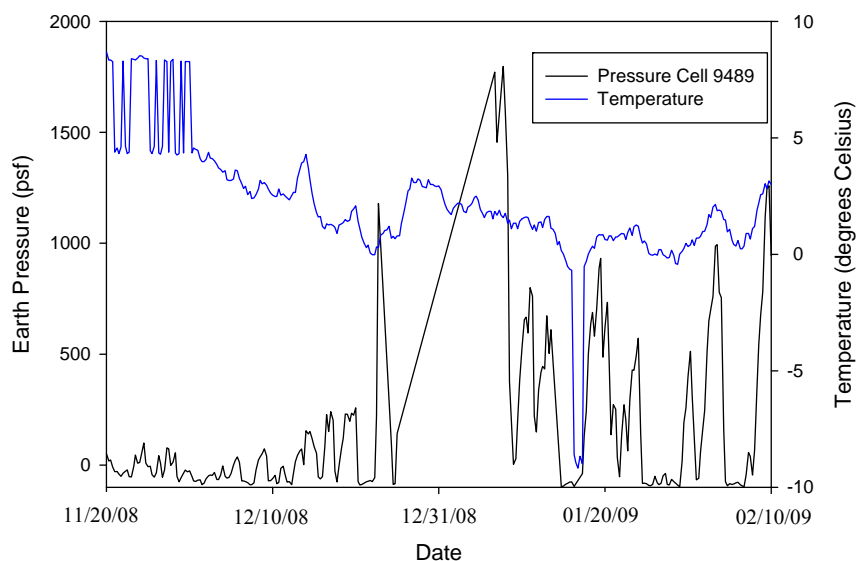
Figure 5-51. Long-term readings for Pressure Cell 9489 (located 1 ft below TOC).
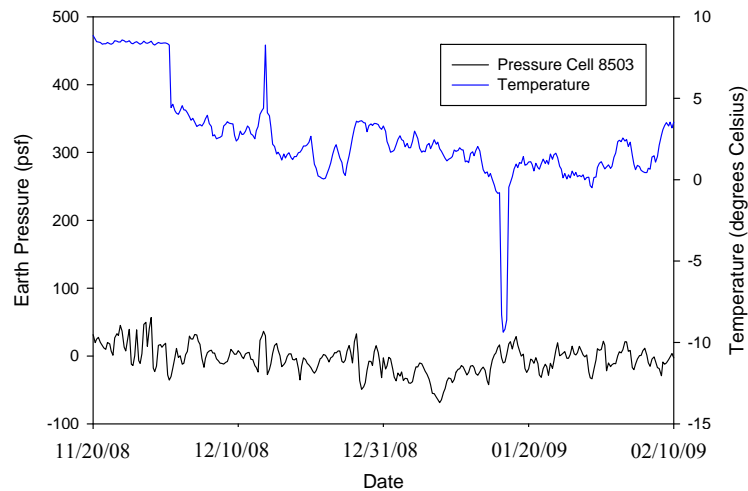
Figure 5-52. Long-term readings for Pressure Cell 8503 (located 3 ft below TOC).

Long-term groundwater table measurements, given as the distance from the bottom of the bridge deck (at the abutments) to the water level, are shown in Figure 5-53 for both sides of the abutment. Although the two piezometers measured different levels of groundwater, the offset is constant at about 3 in. to 4 in. (attributable to human error in placement of the instrument) suggesting that no significant pressure head developed behind the abutment wall.
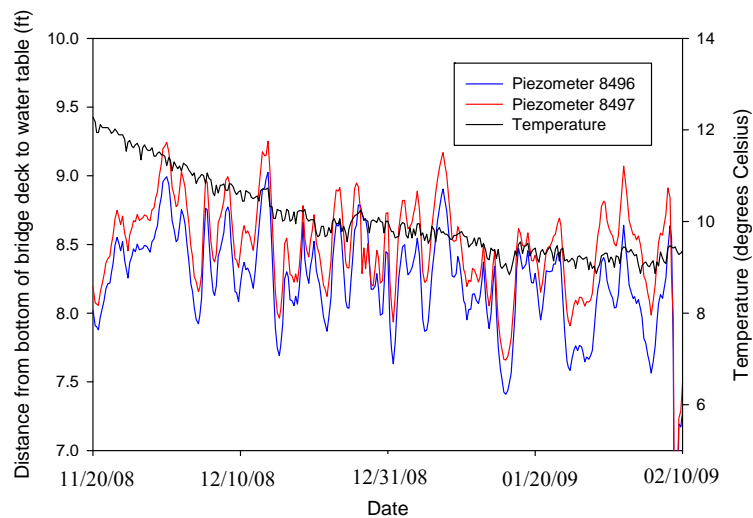
Figure 5-53. Long-term readings for Piezometer 8496 (on stream side of abutment wall) and Piezometer 8497 (on backfill side of abutment wall).

Key Findings

Analysis of the live load test data determined that maximum axial stresses occurring in the piles were approximately 0.5 ksi and were comparable to estimates made by analysis for a load distribution width of 10 ft. Flexural stresses, in general, were significantly less than those estimated by analysis and maximum values were approximately 0.2 ksi. Earth pressures recorded during live load testing (with maxima of approximately 100 psf) were also significantly lower than earth pressures estimated by analysis. These results suggest the method of analysis for lateral earth pressures applied to the sheet pile wall was conservative. Long-term monitoring data showed variations in earth pressure over time with the largest variations in earth pressure occurring behind the abutment cap. The earth pressures experienced cycles that varied in magnitude from 50 psf to 1500 psf, suggesting long-term loading due to freeze/thaw cycles of the soil and the thermal deformation of the superstructure elements may be the critical factors in the design of sheet pile abutment and backfill retaining systems rather than vehicular live loads.

Through the construction and structural monitoring of the BHC demonstration bridge, axially-loaded steel sheet piling has been shown to be a feasible alternative for bridge abutments with site conditions similar to BHC (i.e., shallow bedrock). Although the BHC project required approximately 10 weeks for construction, in the future the construction could be completed in a significantly shorter period if time is critical.

According to the BHC Engineer's Office, the total cost of this project (including labor and materials) was $151,230. The BHC Engineer's Office believes that a significant portion of the cost can be attributed to the labor and equipment time involved in developing a new method of construction for this type of bridge as well as the many associated equipment breakdowns. Future projects utilizing a similar design and construction method with comparable site conditions could be performed at a reduced cost.

Boone County

Project Details

The second demonstration project was constructed in Boone County (BC), Iowa. The site that was selected was a LVR bridge, originally constructed in 1937, crossing Eversoll Creek (a tributary of the Des Moines River) on Owl Avenue near the city of Madrid; the location of the bridge is shown in Figure 5-54.

This project was undertaken to investigate the feasibility of sheet piling combined with a GRS system for use as the primary abutment foundation element and backfill retaining system. Construction of the new bridge was initiated on June 29, 2009 and completed on November 11, 2009. This report presents information on the design of the new sheet pile abutment bridge system, its construction, and the instrumentation installed. Information on load testing and data analysis will be presented in a future report. The following sections give an overview of the previous structure and the new sheet pile abutment bridge system.
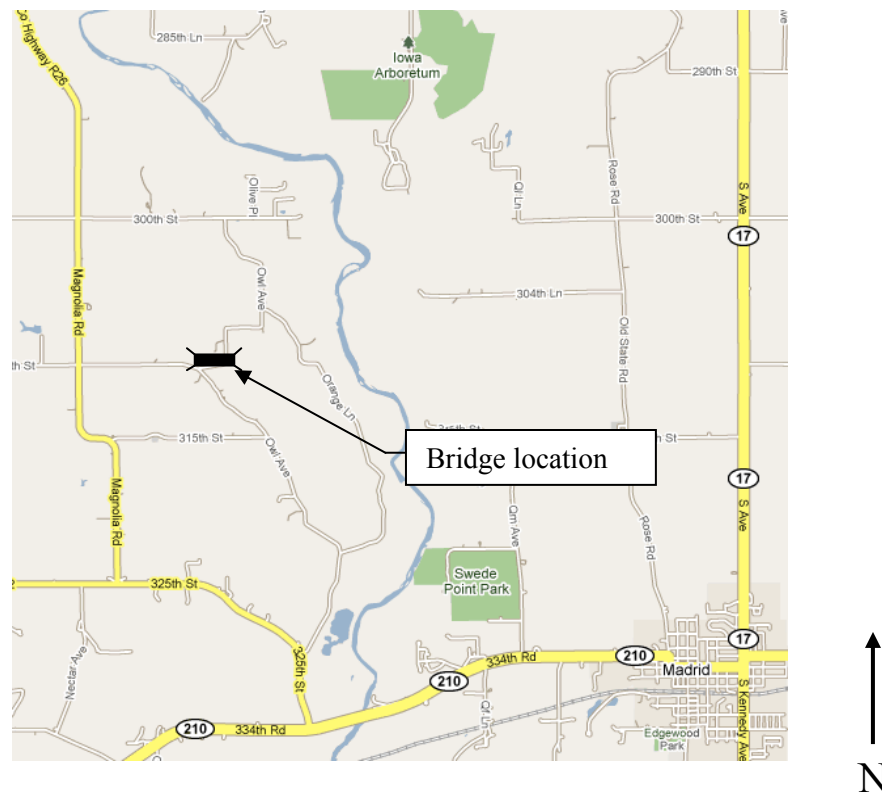
Figure 5-54. Location of bridge replacement project outside of Madrid in BC, Iowa.

<u>Previous Bridge Structure</u>

The structure that was replaced was a 19 ft wide, 95 ft long three-span bridge. The bridge had a timber deck on steel girders with timber pile abutments and piers (encased in concrete) and was approximately 17 ft above stream level (see Figure 5-55). Due to the orientation of the roadway with respect to the stream, the original structure had a 30 degree skew.

a.) Side view

b.) End view

Figure 5-55. Previous bridge replaced by BC demonstration project.

New Sheet Pile Abutment Bridge System Overview

The replacement bridge (a 30 ft wide, 100 ft long three-span continuous concrete slab with a 30 degree skew) was a joint design effort between ISU and the BC Engineer's Office. The design of the superstructure and piers was performed by the BC Engineer's Office and utilized an Iowa DOT bridge standard. The design of the bridge abutments was performed by Iowa State University and utilized steel sheet piling and a GRS system.

Superstructure and Piers

The Iowa DOT standard selected by the BC Engineer's Office was the J30C-87 county bridge standard. The specific design selected was a 33.17 ft wide continuous concrete slab structure that used an open concrete rail creating a 30.5 ft roadway. The depth of the bridge deck was 1.48 ft along the spans and 2.46 ft over the piers. Cross-sections of the bridge are shown in Figure 5-56. Each pier consisted of 8, 80 ft long HP10x42 piles made monolithic with the bridge deck. The piles were encased in reinforced concrete for a length of approximately 20 ft below the bridge deck. For more details on the design of the superstructure and piers refer to Iowa DOT county bridge standard J30C-87.

a.) Cross-section near abutments

b.) Cross-section near piers
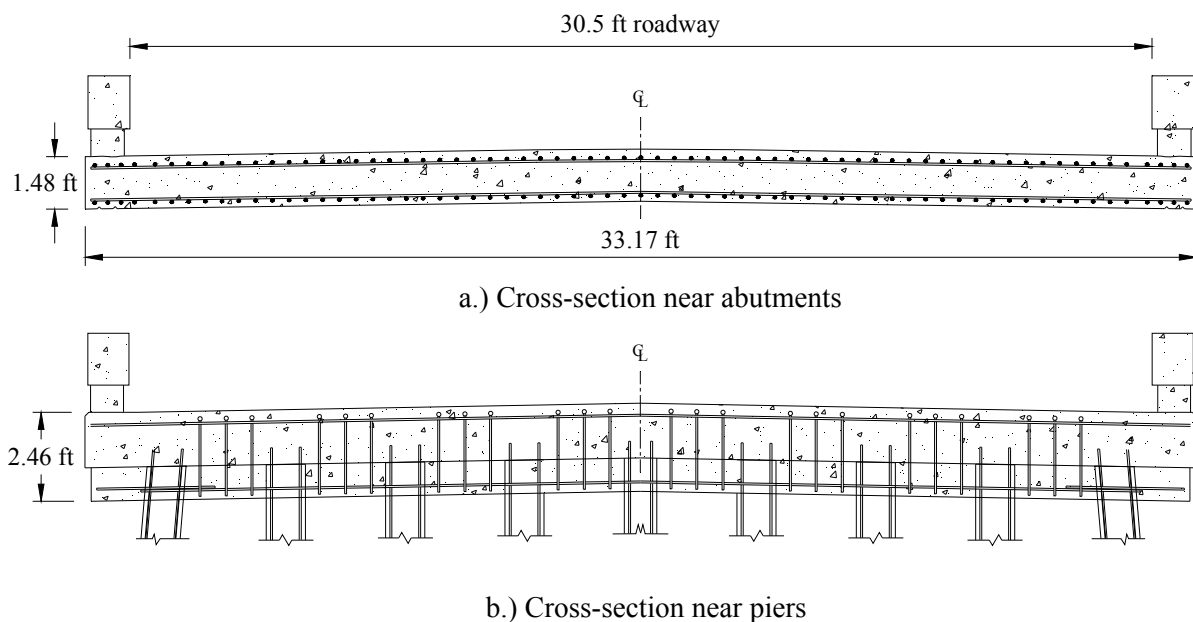
Figure 5-56. Replacement bridge deck for demonstration project in BC, Iowa.
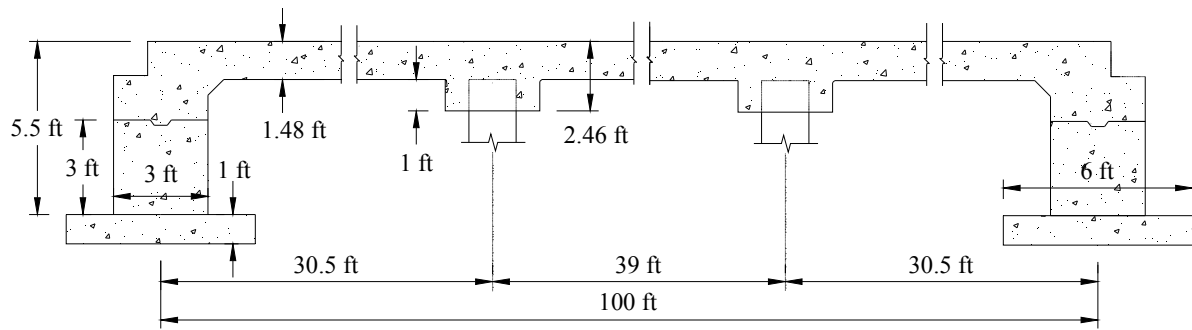
c.) Side view

Figure 5-56. (continued).

Abutment Foundation and Backfill Retaining System

The standard abutment for the J30C-87 required six driven piles to be used. ISU designed a system which replaced the piling with a 6 ft wide reinforced concrete spread footing that was supported by GRS retained (and further reinforced) by a steel sheet pile wall. A cross-section of the system is shown in Figure 5-57. The GRS system was created using 6 layers (1 ft vertical spacing) of biaxial geogrid with a granular backfill of 1.5 in. roadstone. A plan view of the abutment (both abutments have same layout) is shown in Figure 5-58; as previously stated, the abutment had a 30 degree skew.
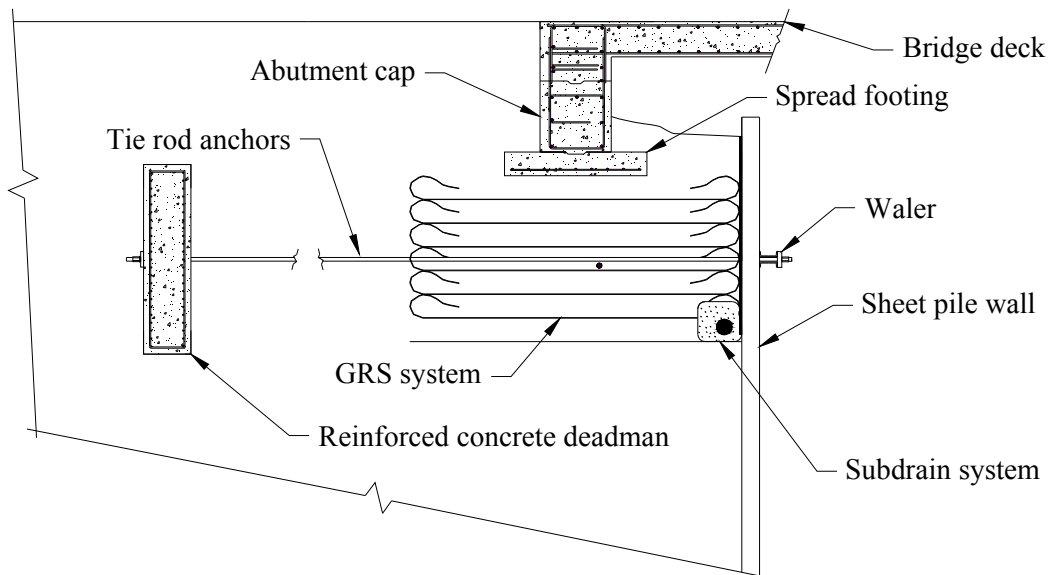
Figure 5-57. Cross-section of sheet pile abutment foundation system designed by ISU.
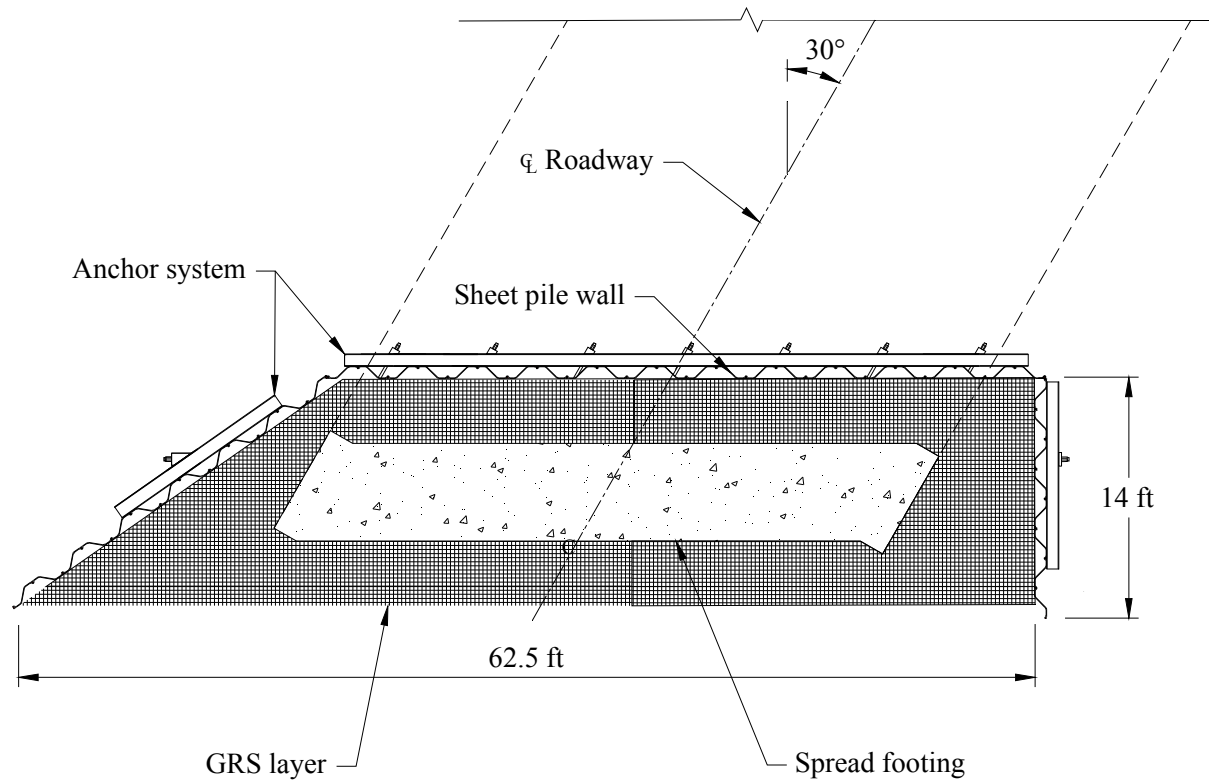
Figure 5-58. Plan view of GRS sheet pile abutment system.

Site Investigation

Field Investigation

Cone Penetrometer Testing

CPT soundings were performed approximately 15 ft east and west of the center of the bridge abutments on June 10, 2008. The CPT sounding locations are shown in Figure 5-59. CPT 1 and CPT 2 were advanced to depth of 45.6 ft and 44.1 ft, respectively, below existing grades. Logs of the soundings, showing cone tip stress and sleeve friction for both CPT 1 and CPT 2, are presented in Figure 5-60.
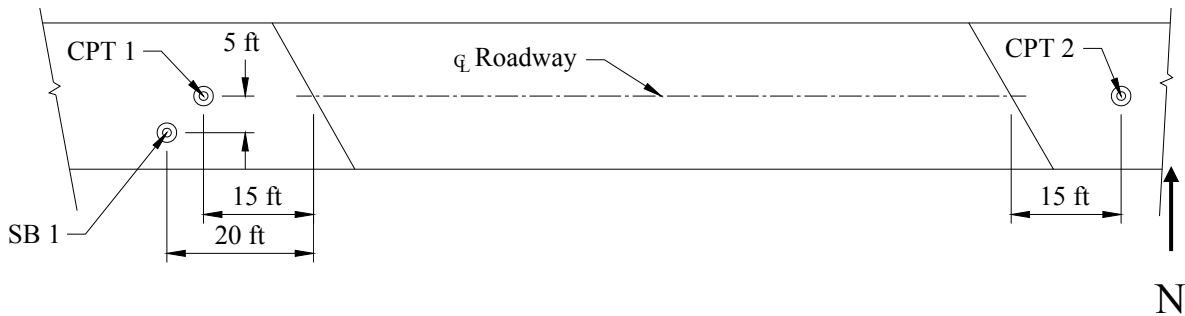
Figure 5-59. Plan view of CPT and soil boring locations for demonstration project in BC, Iowa.

Soil behavior types determined from CPT 1 and CPT 2 are presented in Figure 5-61; as can be seen, the majority of materials present are cohesive soils underlain by a granular base. Dense granular materials and over-consolidated fine grained soil deposits were determined to be present below depths of 34 ft in both soundings due to a relatively large decrease in pore water pressure (caused by soil fracturing and dilatency). Soil shear strength and SPT resistance estimates from correlations presented by Lunne, Powell, and Robertson (1997) for both CPT's are presented in Figure 5-62.
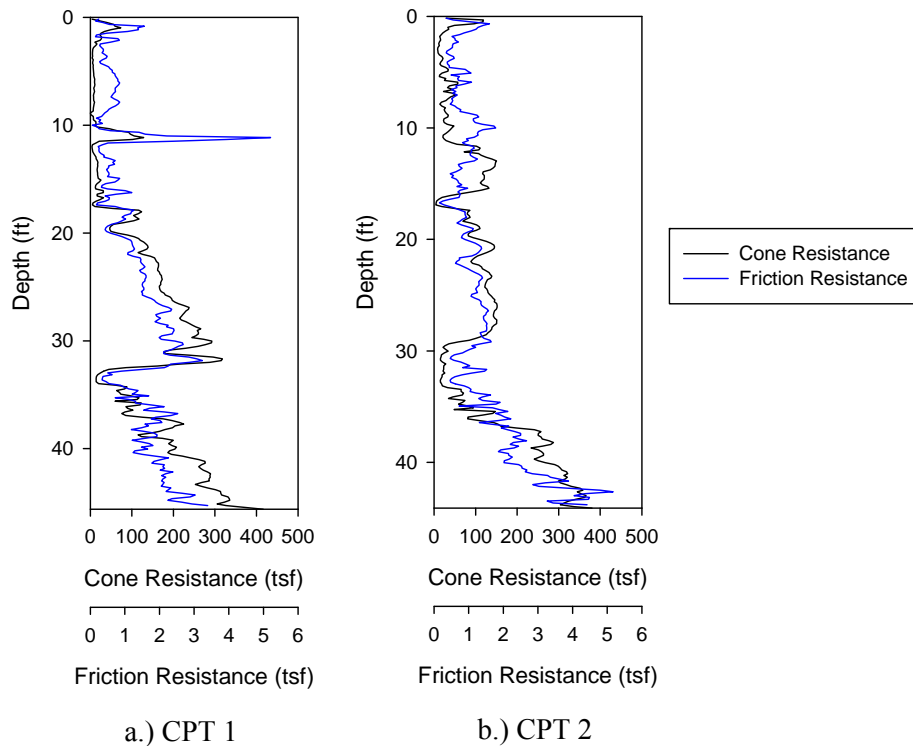
Figure 5-60. Results of CPT's showing cone tip and friction resistance.
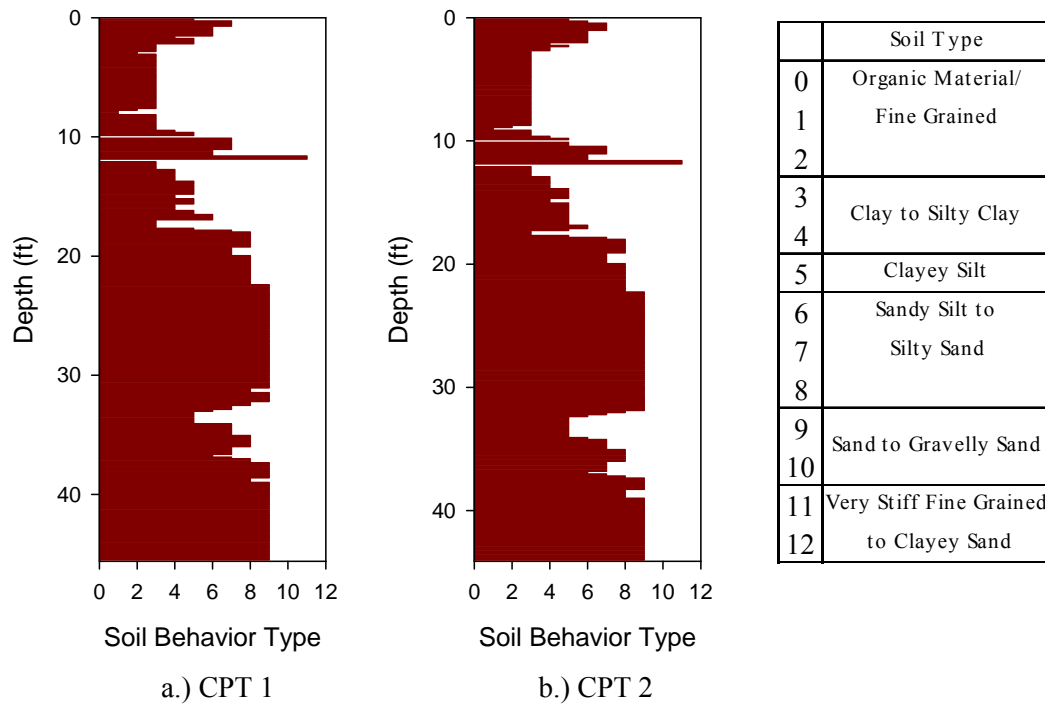
Figure 5-61. Soil behavior types determined from CPT's.
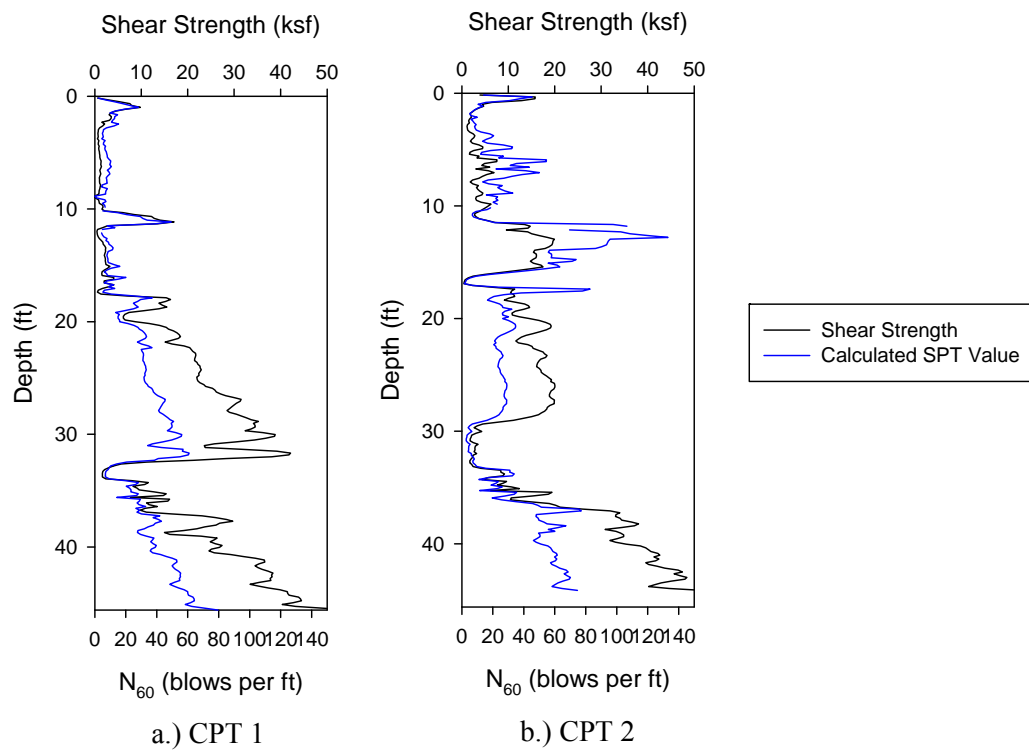
Figure 5-62. Shear strength and SPT correlations for CPT's.

Soil Borings

A soil boring was performed by members of the ISU research team on July 11, 2008. The location of the boring is shown in Figure 5-59; the boring log is provided in Figure B7 of Appendix B.

Laboratory Testing

Unconfined compression tests were performed to determine the shear strength of the selected undisturbed soil samples. As can be seen from the results presented in Table 5-15, the strength of the soil decreases significantly with increasing depth. The results of the Atterberg tests, the percentage of soil passing the No. 200 sieve (percent fines), and the USCS classification for select samples are presented in Table 5-16; as can be seen, the soil primarily consists of clay.

Table 5-15. Unconfined compression test results on select soil samples from SB 1.

Depth Range (in.)	Undrained Shear Strength (psf)
36 - 60	1645
72 - 96	1100
102 - 126	955
144 - 168	350

Table 5-16. Atterberg test and gradation results for select boring ranges.

Depth Range (in.)	LL (%)	PL (%)	PI (%)	Passing No. 200 (%)	Soil Type (USCS)
36 – 48	31.5	20.8	10.7	72	ML
72 – 96	41.5	24.8	16.7	78	CL
120	26.5	18.4	8.1	31	SC
144 – 168	25.7	18.2	7.5	74	CL
240	-*	-	-	26	SM

* No data available

Site Conditions

Geologic Setting

The project site is located on the "Des Moines Glacial Lobe", a region formed by significant glacial activity. According to GSI (see Figure B6 for CPT report), the predominant surficial sediment, which was deposited by the Wisconsinan glacier, is glacial drift. Soils commonly encountered within 15 ft of the ground surface are variable and usually consist of very silty sandy clay with interbedded sand

seams, layers, and pockets. The underlying materials (deposited beneath advancing glacial ice) tend to be homogenous compositions of silty sandy clay materials. Overburden deposits within the stream valleys generally consist of colluvium (slopewash) overlying alluvium of varying thickness which is underlain by the glacial till soils over bedrock. The colluvial deposits are derived from parent soil materials on hillsides while the underlying alluvium may consist of cohesive clayey silt and silty clay soils and/or deposits. This project is located on a creek upland of the Des Moines River floodplain which may have deposited alluvium consisting of interbedded sand and clay soils.

Soil Conditions

During soil boring, light gray clayey sand material (used as fill for the previous bridge) was found for the first 3 ft of depth. Very stiff black and light gray silty clays were discovered from depths of approximately 3 ft to 11 ft. Very stiff tan and light gray sandy clays or clayey sands were encountered after 11 ft of depth. From approximately 15 ft of depth to the end of the boring (20 ft) primarily tan silty sand was encountered.

Groundwater Observations

During the soil boring advancement and sampling operations, observations for free groundwater were made. Information regarding water level observations is recorded in the "Stratigraphy" column on the soil boring log. Groundwater was encountered at depths below existing grade of approximately 16 ft in soil boring SB 1. From the CPT soundings, the observed drop in tip stress and sleeve friction near depths of 15 ft to 17 ft likely coincides with the ground water surface.

Design

As previously mentioned, the design of the superstructure and piers was performed by the BC Engineer's Office; the design selected was the county bridge standard J30C-87. ISU designed a GRS sheet pile abutment and backfill retaining system that was used in place of the driven piling (six HP10x42's driven to a 25 ton bearing capacity) specified in the J30C-87 county bridge standard. The abutment cap for the county bridge standard was designed to bear on a reinforced concrete spread footing on a GRS system (6 layers of Tensar® BX1200 biaxial geogrid placed as shown in Figure B2 and Figure B3) retained by a sheet pile wall with an anchor system. Detailed design plans of the GRS sheet pile abutment and backfill retaining system are provided in Figure B1 through Figure B5.

The GRS sheet pile abutment and backfill retaining system was designed for HL-93 loading (AASHTO Section 3.6.1.2, 1998) of the superstructure using the critical load factors and load combinations presented in AASHTO (1998) Section 3.4.

GRS Sheet Pile Abutment and Backfill Retaining System Design

The sheet pile wall and reinforced concrete deadman anchor system were designed to resist all loads (including bridge and backfill surcharge loading), neglecting the contribution of the GRS system due to the limited existing research on long-term performance of such systems.

Loads transferred through the abutment cap to the spread footing were assumed to distribute evenly across the surface area. Dead loads were assumed to distribute over the entire length of the footing while the live loads were distributed over a 10 ft long strip. The spread footing was designed to be 6 ft wide to reduce the bearing pressure to a maximum factored load of 3500 psf. The surcharge loads were applied as lateral earth pressures to the sheet pile wall according to AASHTO (1998) Section 3.11.6.1. The sheet pile section required to resists design earth pressure loads was the PZ 22. The required depth of the sheet pile wall for stability (accounting for a 6 ft depth of scour) was approximately 25 ft; sheet pile sections were ordered 30 ft long as an additional factor of safety.

The tie rod anchors were placed at 6 ft below the top of the sheet pile wall and were required to resist a total force of approximately 1000 kips; seven #14, Grade 75 steel, fully-threaded epoxy-coated tie rods (obtained from Dywidag Systems International, Inc.) were used to provide anchorage for the wall. The tie rods were anchored to a 35 ft x 8 ft x 2 ft reinforced concrete deadman that was approximately 45 ft from the main wall at the nearest point (distance varied due to skew as seen in Figure B1). The method for transferring anchorage forces from the tie rods to the sheet pile wall were through the waler system described later in this thesis. The waler system consisted of two back-to-back C9x20 shapes with bearing plates constructed to account for the skew of the abutment. The abutment skew created greater loads in the tie rods as well as requiring welds to be made between the bearing plates, waler, and sheet pile wall to resist translational forces induced. Details on design calculations are provided in Appendix B.

Construction

The contractor selected for construction of the demonstration project was Graves Construction Co., Incorporated of Spencer, Iowa. The primary bridge crew consisted of five construction workers. Construction activities commenced on June 29, 2009 and were completed in approximately 18 weeks. A chronology of significant construction events is presented in Table 5-17; details of each event are given in this section of the report.

Table 5-17. Chronology of significant construction events for the BC, Iowa demonstration project.

Event description	Start date	Working Days Between Events
Demolition	06/29/09	7
Pier construction (west)	07/08/09	10
Abutment construction (west)	07/22/09	4
Abutment backfilling (west)	07/28/09	3
Anchor system const. (west)	07/31/09	3
Abutment flooding (west)	08/05/09	8
Pier Construction (east)	08/17/09	6
Abutment demolition (east)	08/25/09	4
Deck falsework assembly	08/31/09	1
Abutment construction (east)	09/01/09	5
Abutment backfilling (east)	09/08/09	3
Anchor system const. (east)	09/11/09	4
Abutment flooding (east)	09/17/09	3
Deck reinforcement placement	09/22/09	11
Concrete deck pour	10/07/09	3
Casting of guardrails	10/12/09	5
Removal of falsework	10/19/09	9
Finishing earthwork	10/30/09	7
Open for service	11/10/09	-
Bridge Load Testing	11/13/09	-

Demolition of Existing Structure

Initial construction activities involved assembly of cranes and clearing and grubbing of the project site. Removal of the superstructure and the west abutment were the first tasks of the demolition and required approximately 7 work days to complete. The west piers were also removed but the east pier and abutment were left in place for later demolition after equipment was moved to the east side of the creek. The superstructure was demolished by removing the timber decking and torch cutting sections of the steel girders for removal (see Figure 5-63). Timber piles (in the abutment and piers) were

pulled if possible or cut off below ground level. Complete removal of the superstructure and the west pier was completed in less than 3 days.

a.) Timber decking removed (exposing steel girders)

b.) Superstructure removed

Figure 5-63. Demolition of existing structure for the BC, Iowa demonstration project.

Pier Construction

Each pier consisted of 8, HP10x42, 80 ft long steel piles which were encased in reinforced concrete for the upper 18 ft and cast monolithic with the bridge deck. Since the concrete encasements extended below the existing stream bed elevation cofferdams were constructed for placement of the piles (see Figure 5-64a). The piles were driven in 40 ft sections using a single-acting diesel hammer and were specified a minimum 34 ton bearing capacity (approximately 0.30 in. penetration per hammer blow). One of the battered piles being driven while the other is being held in place after splicing on the second section is shown in Figure 5-64b. Piles were spliced by beveling the edges with a grinder (seen in Figure 5-65a) in preparation for the full-penetration groove welds to be made by the contractor's certified welder (see Figure 5-65b). After all piles were driven beyond specified bearing capacity, reinforcement and forms were placed for the 18 ft long encasement.
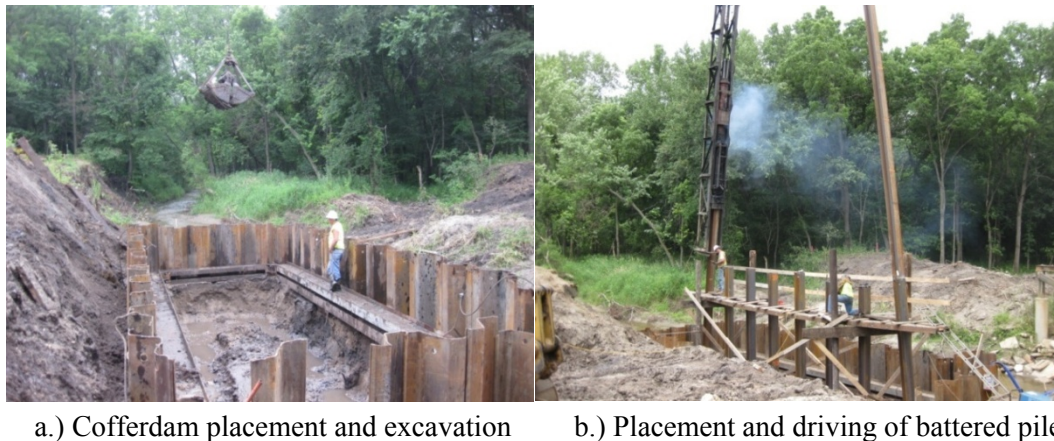
a.) Cofferdam placement and excavation   b.) Placement and driving of battered piles

Figure 5-64. Pier construction activities for the BC, Iowa demonstration project.
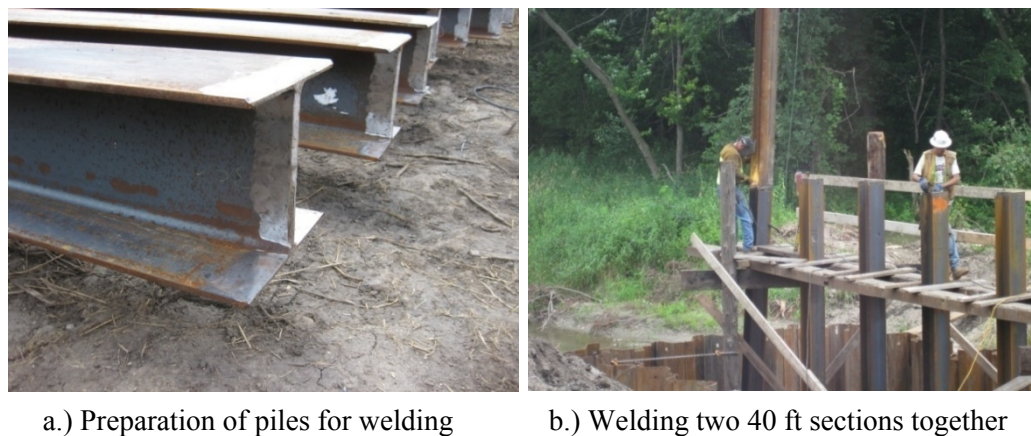
a.) Preparation of piles for welding   b.) Welding two 40 ft sections together

Figure 5-65. Splicing of H-Pile sections for bridge piers.

Sheet Pile Driving

After excavation to the base elevation of the backfill zone on the west abutment, the ISU research team inspected and approved the existing material by performing a dynamic cone-penetrometer (DCP) test as per ASTM D6951 (2003); the resulting data from a DCP test are an empirical value known as the California bearing ratio (CBR) and is an indicator of the level of compaction of soil. For the east abutment, DCP testing concluded that the existing material was unsuitable for construction; improvement was achieved by replacing 18 in. of the existing material with 1.5 in. roadstone placed in 9 in. lifts.

After approving the base material, 30 ft long sheet pile sections (PZ 22) were driven with a vibratory pile driver to design elevations (shown in Figure 5-66a). No pile bearing capacity was specified as the sheet pile sections act as a backfill retention and scour protecting structure in this application. As an alternative to construction of a guide rack, sheet pile sections were initially set and held during driving with the excavator boom as shown in Figure 5-66b.

a.) Vibratory pile driving   b.) Initially set and held with excavator boom

Figure 5-66. Placement of sheet pile sections.

One issue encountered during driving was, due to friction in between the interlocks of adjacent sheets, driving one pile would occasionally drive an adjacent pile further (past its design elevation); this issue was overcome by driving future piles at a reduced rate. The west abutment after all sheet piling (including the 35 degree and 90 degree wingwalls) had been driven to design elevations is shown in Figure 5-67.

Figure 5-67. West abutment after all sheet piling in place.

<u>Abutment Backfilling and Placement of GRS System</u>

Backfilling operations began after the sheet pile walls had been driven and the subdrain system was in place. The subdrain consisted of a rigid perforated PVC pipe surrounded by porous backfill and wrapped in engineering fabric to prevent soil fines from plugging the perforations. The subdrain system also utilized a wick drain installed along the backfill side of the sheet pile wall as a means of quickly draining any water that came in contact with the sheet pile wall. A single layer of the wick drain is displayed in Figure 5-68a; subsequent layers were placed with a slight overlap to provide continuous drainage and prevent the entrance of fines. The subdrain pipes exited through the south wingwalls in both abutments and were terminated with a 6 ft long, 6 in. diameter corrugated metal pipe (with a rodent guard) that drained on the downstream side of the bridge.

The backfill material used within the GRS zone was 1.5 in. crushed roadstone. The geogrid material (Tensar $^®$ BX1200 biaxial geogrid) was delivered to the jobsite in 9.8 ft by 164 ft long rolls. The geogrid consisted of essentially a sheet of polypropylene material with 1in. by 1in. apertures to form a grid (see Figure 5-69).

Before placement of any backfill, a layer of engineering fabric (to be placed around all sides of the GRS mass) was placed over the base of the excavation for erosion protection (see Figure 5-68a). Backfill material was placed in 6 in. lifts and compacted to a minimum of 98% of standard effort compaction test (ASTM D698, 2000) within 2% of optimum moisture content using several passes of the remote-operated vibratory compactor as shown in Figure 5-70b. After two lifts of backfill material (1 ft) a layer of geogrid was placed; a total of 6 layers of geogrid were placed in each abutment. Geogrid layers were installed by placing strips of the material (9.8 ft wide) perpendicular to the abutment to cover the GRS zone shown in Figure B3. Each strip placed was lapped a minimum of 12 in. over the adjacent strip to provide continuous reinforcement (see Figure 5-69). Sufficient length (approximately 3 ft) was provided so the ends of each layer could be wrapped over the next layer of backfill as depicted in Figure 5-70.

a.) Engineering fabric placement

b.) Vibratory compaction

Figure 5-68. Base layer of backfilling for west abutment.

Figure 5-69. Geogrid material for GRS abutment system in west abutment.

a.) View of geogrid wrapping around
layer of backfill
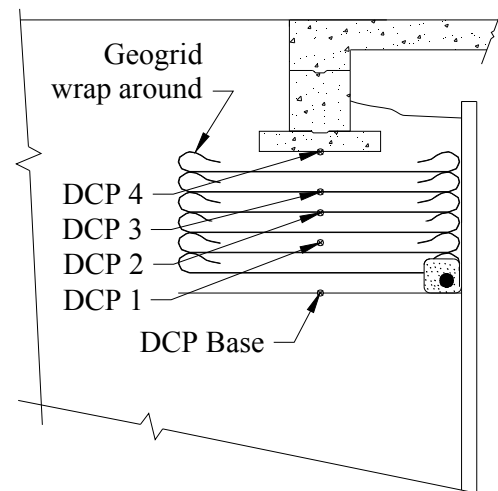
b.) Cross-section of west abutment
depicting locations of DCP tests

Figure 5-70. Geogrid from lower layer wrapped around backfill into upper lift.

Before backfilling of the each abutment, soils at the base of the excavation were investigated to determine adequacy for construction of the abutments by performing DCP tests. The DCP testing provided a value of the penetration index (PI) in terms of millimeter per hammer blow; the value for the CBR is determined as follows (Iowa Statewide Urban Design and Specifications, 2009):

$$\mathrm{CBR} = \left(\frac{292}{\mathrm{PI}}\right)^{1.12}$$

The results for the west abutment (see Figure 5-71a) showed steadily increasing strength with depth and was determined to be adequate. The results for the east abutment (see Figure 5-71b) showed no increase in strength with depth; ISU required that an 18 in. layer of the base material be removed and replaced with 1.5 in. compacted roadstone to increase strength.

During backfilling, several DCP tests were performed to verify compaction efforts were meeting the specified requirements. The locations of the DCP tests performed were depicted previously in Figure 5-70b with depths below the footing presented in Table 5-18. Through an analysis of the results of the DCP testing of the west abutment backfill, which is presented in Figure 5-72, it was determined the backfill met the required specifications for compaction.

a.) West abutment   b.) East abutment
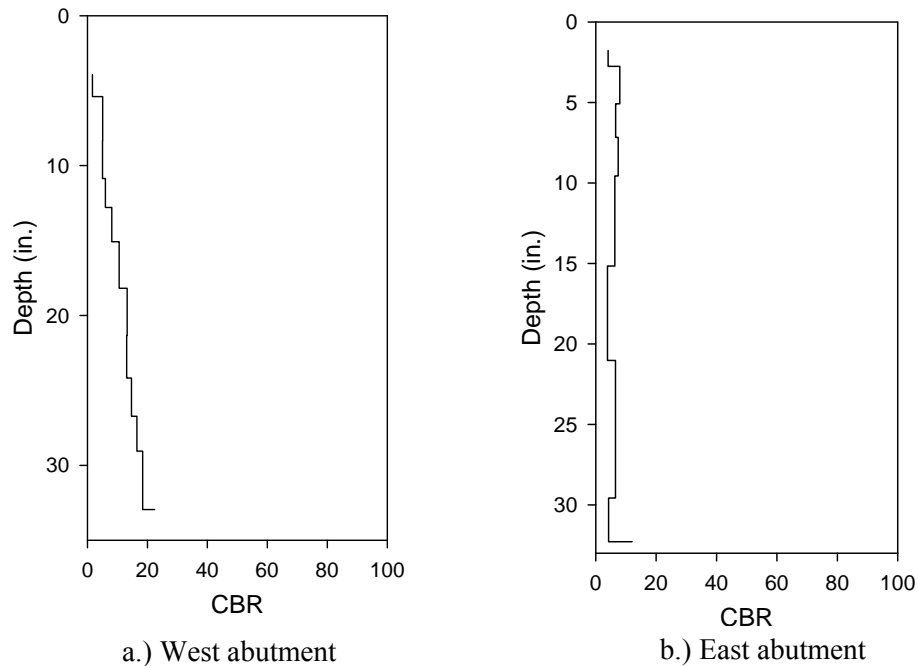
Figure 5-71. DCP testing results for base soils to determine adequacy for abutment construction.

Table 5-18. DCP test results for west abutment with reference to Figure 5-70b.

DCP Location	Depth below footing (ft)
Base	7.0
1	4.5
2	3.0
3	2.0
4	0.0
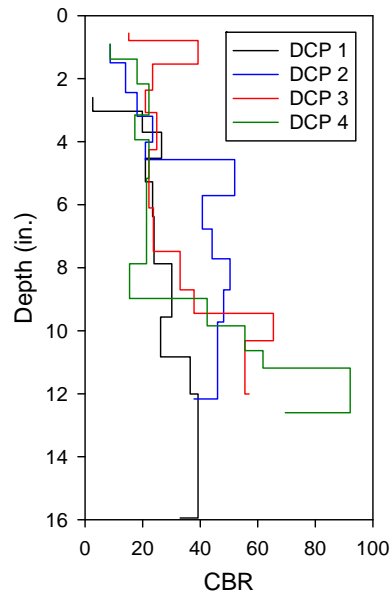
Figure 5-72. DCP test results for west abutment backfill material.

In the backfill of the west GRS sheet pile abutment system, several earth pressure cells were installed for measuring horizontal and vertical earth pressure. Each cell was placed in a pocket of fine silica sand and surrounded by course sand as shown in Figure 5-73. An overview of all instrumentation and locations is presented in the next section of this report.

a.) Fine silica sand bedding for earth pressure cell

Figure 5-73. Placement of earth pressure cells in west abutment backfill.

b.) Coarse sand bedding for earth pressure cell

Figure 5-73. (continued).

Deadman Anchor System

The anchor systems used on each abutment were anchored to a large, 35 ft x 8 ft x 2 ft reinforced concrete deadman placed approximately 50 ft behind the sheet pile wall and 6 ft below grade (see Figure B1 and Figure B2 for details). The deadman was cast in formwork placed in a large trench excavated 4 ft deep. The reinforcement in the deadman is shown in Figure 5-74. The deadman after formwork was removed is shown in Figure 5-75a. Flowable grout was poured into the excavated trench of the deadman (instead of using soil) to minimize the mobilization required to achieve full strength of the deadman (see Figure 5-75b). The deadman was perpendicular to the centerline of the roadway and thus the distance from the sheet pile wall to the deadman varied due to the skew of the bridge.

Each abutment was anchored to the deadman by seven 1.75 in. diameter tie rods (grade 75 steel) that were fully threaded and epoxy-coated (see Figure 5-76a). The bars came in two sections and required couplers to attain full length. The tie rods provided anchorage to the sheet pile wall through a waler system that consisted of two C9x20's placed back-to-back with a 3 in. gap between them for the rod to pass through (see Figure 5-76b and Figure 5-76c). Because of the skew of the abutment, the waler

needed to be welded to the sheet pile wall with a minimum of 6 in. welds at every contact point between the waler and the sheet pile to resist the translational force component (t) of the developed tie rod force (T) depicted in Figure 5-76d. A cross-section of the waler is provided in Figure 5-76e. This also required the bearing plates (which were constructed as shown in Figure 5-76f to compensate for the skew of the abutment wall) to be fully welded to the waler. The wingwalls were tied together using a 2.25 in. diameter epoxy-coated threaded tie rod and a waler system similar to that used for the wall (with differing skews); see Figure B1 for additional details.

a.) Overview of deadman trench   b.) Reinforcement and formwork being placed

Figure 5-74. Reinforcement placement for concrete deadman.

a.) Initial cast of deadman   b.) Placement of flowable grout

Figure 5-75. Reinforced concrete deadman in west abutment.

a.) Deadman and tie rods anchoring the west abutment sheet pile wall

b.) Side view of waler system

c.) Skewed bearing plate for tie rod connection
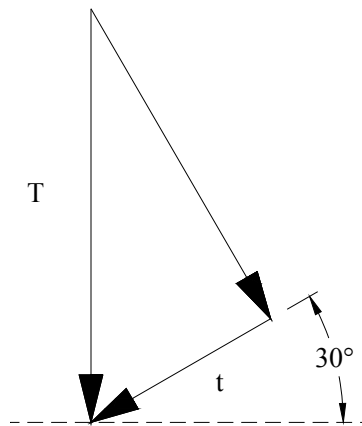
d.) Diagram of translational force component from tie rod

Figure 5-76. Details of anchorage system for BC, Iowa demonstration project.
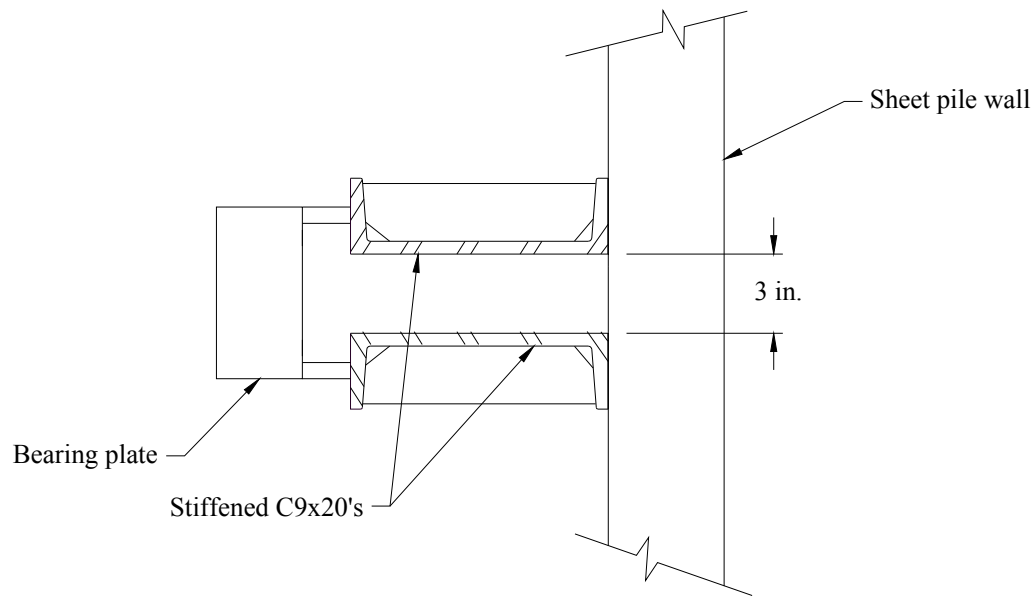
e.) Cross-section of waler
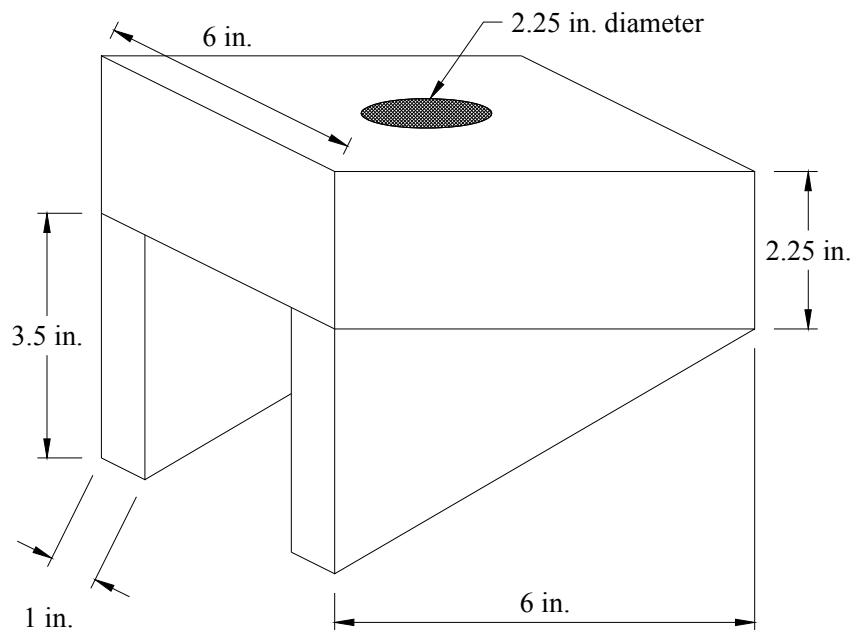
f.) Isometric view of bearing plate

Figure 5-76. (continued).

Due to the construction techniques used, the alignment of the sheet pile wall and both wingwalls were not straight which resulted in gaps between the waler and sheet piling wall in locations needed to be in contact (see Figure 5-77). Consequently, the minimum welding requirements between the waler and sheet pile wall previously mentioned could not be made. Attempts were made by the contractor

to eliminate the gaps using a winch, however only 2 of the 13 gaps were eliminated; the gaps varied in thicknesses from 0.5 in. to 13 in. The solution for eliminating the remaining gaps was to order plates to fill each gap and subsequently welding the plates to the sheet pile wall and the waler. For any gaps over 2 in., H-Pile sections were used instead of ordering custom bearing plates. According to the BC Engineer's Office, the cost of this solution was approximately $2,500. Contact between the waler and sheet pile wall was not an issue on the east abutment as a greater effort was made to ensure proper alignment during pile driving.
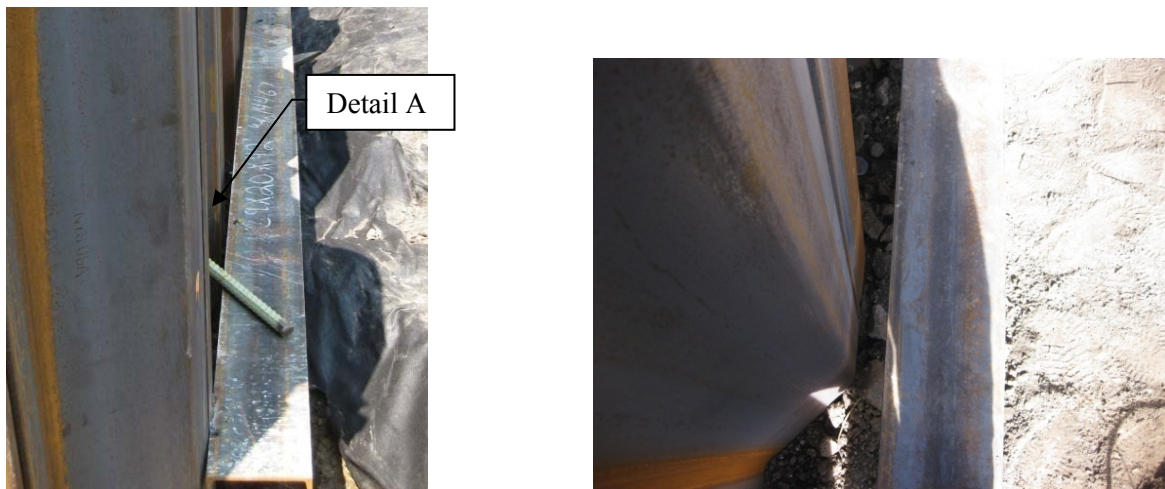
a.) Bottom waler channel welded to sheet pile wall   b.) Detail A

Figure 5-77. Waler not in contact on all sheet piles in west abutment.
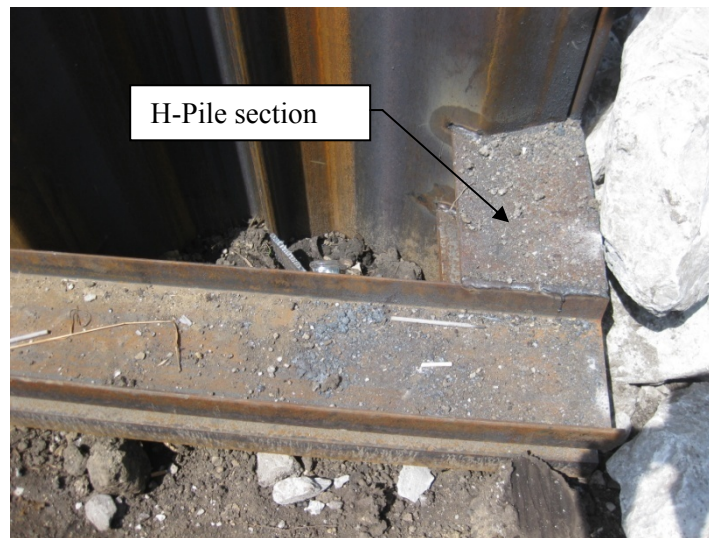
Figure 5-78. H-pile splice used on 90 degree wingwall waler of west abutment.

Abutment Finishing and Footing Construction

Several tasks were required to complete construction of the abutments. After backfilling was completed to the design elevation, the abutment was flooded with water pumped from the stream to reduce the amount of voids in the backfill material (to minimize settlement) and test the drainage system. Flooding of the abutment and the water successfully draining into the stream is shown in Figure 5-79a and Figure 5-79b, respectively.

<table>
<tr><td>a.) Pumping water from stream</td><td>b.) Water draining from abutment</td></tr>
</table>

Figure 5-79. Flooding of the west abutment.

After the abutments were backfilled and compacted to the design elevation, ISU researchers performed DCP and light weight deflectometer (LWD) testing (shown in Figure 5-80a) as per ASTM E2583 (2007) to determine the adequacy of the backfill soil which was to support the bridge abutment foundation. Seven LWD tests and three DCP tests were completed; the location of each test is shown in Figure 5-81 with reference to the coordinates given in Table 5-19.

LWD testing was performed by dropping a hammer (weight approximately 22 lbs) from a specified height several times onto a 300 mm square plate while monitoring the vertical displacement into the soil (see Figure 5-80). The results of the LWD testing (which provides an estimate of the elastic modulus of the soil) are presented in Table 5-20. The test performed at location LWD 7 (shown in Figure 5-80b) was on the material present at the site (instead of the compacted backfill) to provide a comparison for the data. The results revealed that elastic settlements were reduced more than 90% (comparing relative modulus of elasticity) on average through the use of quality, compacted backfill material over existing soils. The DCP testing involved dropping a 17.6 lb weight (from a height of

22.6 in.) to drive a 20 mm diameter cone into the soil while recording the observed penetration. A CBR value of approximately 50 was desired for the abutment backfill at the level of the footing. The DCP testing results for the west and east abutments at the level of the spread footing are presented in Figure 5-82a and Figure 5-82b, respectively. After analyzing the results of the DCP testing, the abutment backfill was considered adequate for the construction of the footings.

a.) Testing on abutment backfill at base of spread footing

b.) Testing on east abutment existing soil

Figure 5-80. LWD testing of backfill soil at spread footing location on east abutment.
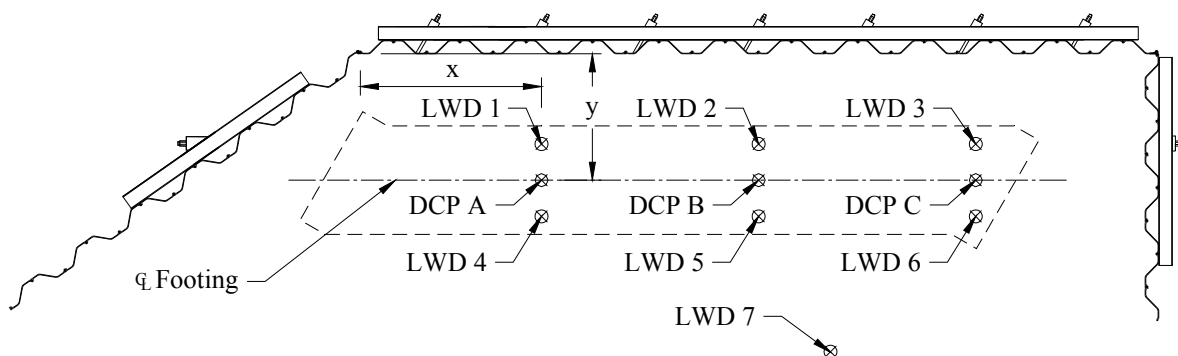
Figure 5-81. Dimensions of backfill LWD and DCP test locations (see Table 5-19) on abutments.

Table 5-19. Locations of backfill LWD and DCP test locations with reference to coordinates in Figure 5-81.

Test point	Location			
	West abutment		East abutment	
	x (ft)	y (ft)	x (ft)	y (ft)
LWD 1	4.0	5.0	12.0	5.0
LWD 2	18.0	5.0	24.0	5.0
LWD 3	40.0	5.0	36.0	5.0
LWD 4	4.0	9.0	12.0	9.0
LWD 5	18.0	9.0	24.0	9.0
LWD 6	40.0	9.0	36.0	9.0
LWD 7	-	-	26.0	16.5
DCP A	4.0	7.0	12.0	7.0
DCP B	18.0	7.0	24.0	7.0
DCP C	40.0	7.0	36.0	7.0

Table 5-20. LWD testing results.

LWD Location	Modulus of Elasticity (MN/m^2)	
	West abutment	East abutment
1	52.0	102.3
2	71.9	106.4
3	59.6	105.6
4	64.5	84.3
5	55.9	77.6
6	68.3	107.1
7	N/A	6.8

a.) West abutment   b.) East abutment
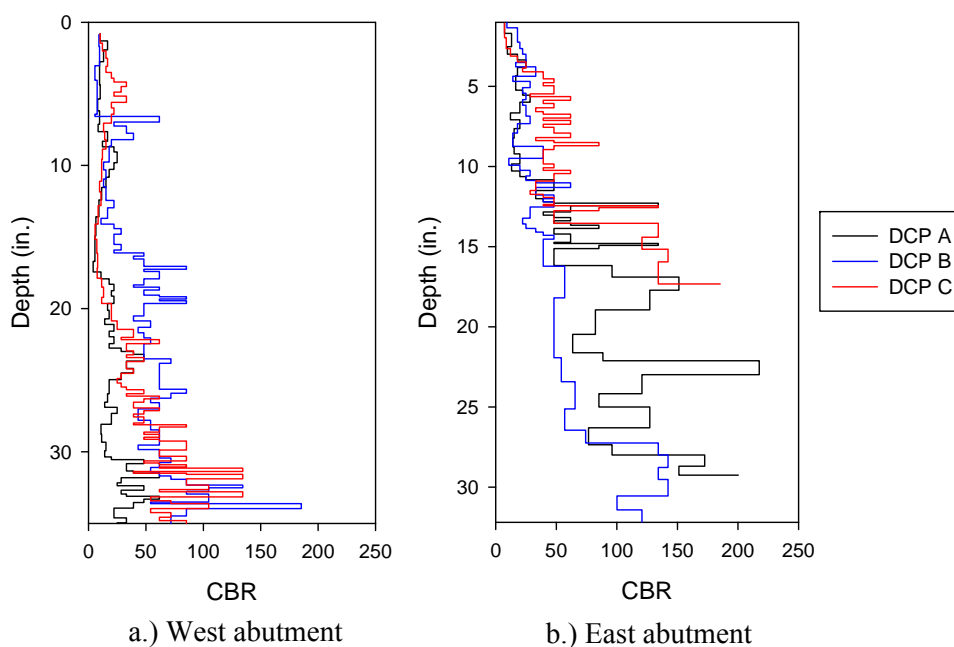
Figure 5-82. DCP results for backfill testing at footing elevation.

The reinforced concrete spread footing (designed by ISU) was 6 ft wide and 1 ft thick and was constructed to provide a larger bearing surface area for the abutment caps of the J30-87 county bridge standard which were originally designed for use with driven piling. The construction of the footing is shown in Figure 5-83 with dimensions and reinforcement details provided in Figure B1.

Figure 5-83. Reinforced concrete spread footing on west abutment.

With the use of driven piles for the pier footings there will likely be negligible settlement; with spread footings for the abutments on engineered fill there are some concerns about settlements. Although steps were taken to minimize abutment settlements (compaction, flooding, etc.), ISU designed a system to provide a means of counteracting excessive settlement. The joint between the abutment cap and the footing was constructed to provided translational resistance (through use of shear keys as depicted in Figure B2) without rotational resistance; this was accomplished by placing a layer of tar paper between the footing and the abutment cap. Although the footing-abutment cap interface was designed to prevent bending moment transfer from the superstructure to the footing, it also provided the ability for the abutment cap and footing to be separated. Four blockouts were formed in each abutment to provide a space for the placement of hydraulic jacks as shown in Figure 5-84a. The spacing between the longitudinal reinforcement in the abutment cap (shown in Figure 5-84b) is sufficient to accommodate a typical 60 ton hydraulic jack.

If significant differential settlements are observed, four 60 ton jacks will be placed in the blockout regions to lift the abutment cap so that shims (e.g., steel plates) can be inserted between the cap and

footing to return the structure to a state of acceptable differential settlement. Through a stress analysis of the bridge deck, it was determined that a maximum acceptable level of differential settlement is 0.875 in. to prevent cracking of the bridge deck over the piers. Settlements of the abutment caps will be monitored through use of a total station; four PVC pipes were cast into the east and west ends the bridge deck (one at the north edge and one at the south edge) at each abutment (see Figure 5-85) to provide a consistent reference point for future surveys.

a.) Overview of abutment cap and footing   b.) Blockout in abutment
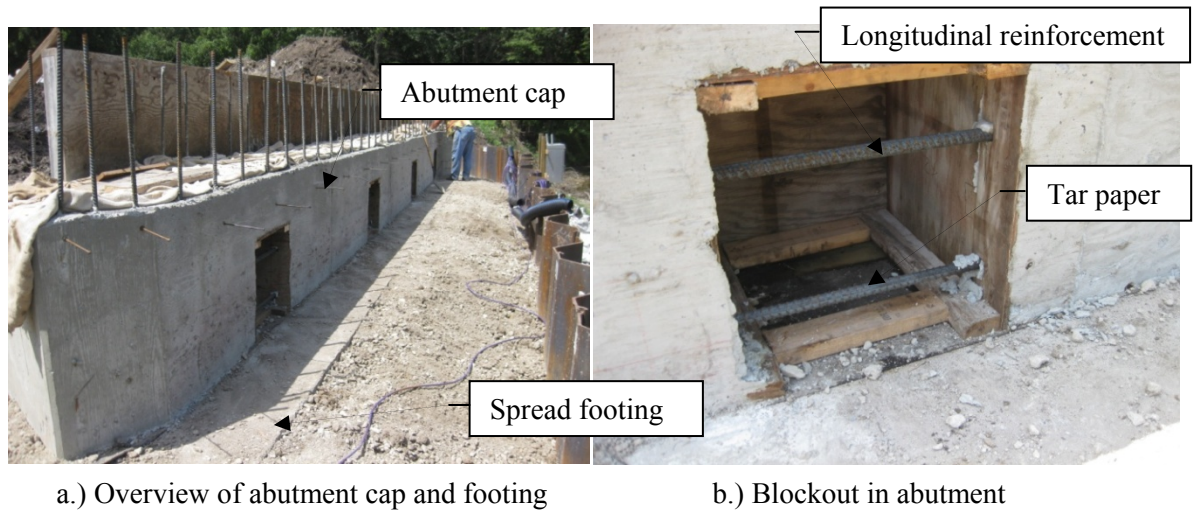
Figure 5-84. Blockouts in west abutment for placement of hydraulic jacks to raise abutment in the event of excessive differential settlement (relative to bridge piers).

a.) Before placement of the bridge deck   b.) After placement of the bridge deck
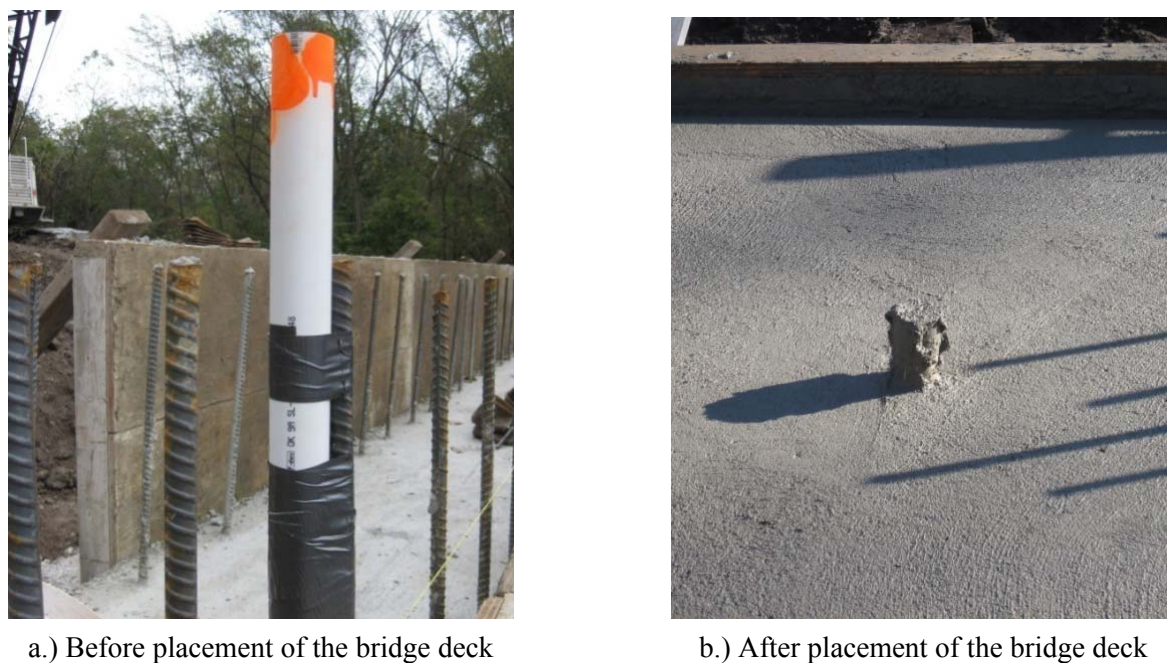
Figure 5-85. PVC pipe placement on east abutment for measuring differential settlement.

The remaining task for completion of the bridge abutments was the placement of Class E limestone revetment around the sheet pile abutment wall for erosion protection. A total of 865 tons of revetment was used on the project. A layer of engineering fabric was placed over the existing soil and revetment was subsequently placed in a layer of approximately 2 ft thickness. An overview of the completed west abutment and pier is shown in Figure 5-86.

Figure 5-86. Finished west abutment and pier.

Reinforced Concrete Bridge Deck Construction

After completion of the west abutment, construction began on the east abutment as well as the assembly of falsework for the bridge deck (starting from the west abutment as shown in Figure 5-87). Timber piles were driven for support of the falsework structure. The falsework for the west span and midspan of the bridge was assembled by an independent crew specializing in deck formwork; after completion of the east abutment, the regular bridge crew on site completed the formwork for the east end span.

Figure 5-87. Construction of falsework for placement of bridge deck.

Placement of the bridge deck reinforcement (see Figure 5-88) was also performed by and independent crew and only required 1 day to complete. Bridge deck reinforcement was not epoxy-coated as the BC Engineer's Office will not be using de-icing salts on a gravel roadway. For further information on bridge deck reinforcement and other superstructure details, a copy of the county bridge standard J30C-87 may be obtained from the Iowa DOT or the BC Engineer's Office.

Figure 5-88. Reinforcement in place for continuous concrete slab bridge.

Placing concrete in the bridge deck was performed on October 7, 2009 and required one day to complete. The entire bridge deck required 206 cy of concrete for completion. The deck was poured using a concrete pump truck as shown in Figure 5-89; three bridge crews were present on the day of the pour.

Figure 5-89. Concrete pumping for continuous concrete slab.

Concrete trucks delivered concrete in 10 cy loads on a schedule of approximately 20 minutes per delivery. The concrete was discharged into the hopper of the concrete pump truck and pumped to the desired location on the deck as shown in Figure 5-90. One worker guided the pump hose, one remotely controlled the rate of placement, while two others vibrated the concrete; placement proceeded from the east end of the bridge to the west end.

Figure 5-90. Concrete placement near east abutment with pump truck.

Once in place, the concrete was screeded to the specified crown of 1% using the system shown in Figure 5-91. The screeder (spinning in the opposite direction it was moving) passed back and forth along the rail structure which varied in height to form the crown of the bridge. The plate attached to the roller assembly assisted in finishing the concrete surface. Workers finished some areas of the deck surface by hand and subsequently raked the surface for additional roughness.

a.) Unfinished concrete after placement   b.) Screeded to form 1% crown

Figure 5-91. Method for forming finished 1% crown of bridge deck.

The contractor placed a curing compound on the finished deck surface as an alternative to covering the exposed concrete with wetted burlap sheets; as may be seen in Figure 5-92, the white curing compound is in place. The finishing of the west end of the bridge is shown in Figure 5-92b.

a.) East end

Figure 5-92. Curing compound in place.

b.) West end

Figure 5-92. (continued).

Bridge Finishing

Construction activities remaining to finish the bridge were placement of the guardrail, removal of falsework, backfilling behind the abutment caps, and earthwork around project site. Backfilling and earthwork were performed by a separate contractor. The finished bridge is presented in Figure 5-93.

a.) Side view   b.) End view

Figure 5-93. Finished BC demonstration bridge.

Instrumentation and Monitoring System

The bridge was instrumented with semiconductor earth pressure cells and strain gages as well as displacement transducers. The earth pressure cells (as well as several strain gages on the sheet piling and tie rods) were installed at the site for recording long-term data. Several strain and displacement transducers were installed for the live load test of the structure and were subsequently removed.

Permanent System

Strain gages were placed on one sheet pile (near centerline of the roadway) and on each tie rod in the west sheet pile abutment system. At each instrumented location on the piles, two gages were placed on opposite sides of the sheet pile so that axial and flexural strains (stresses) in the section could be determined. Strain gage locations on the instrumented pile are presented in Figure 5-94b; odd numbered gages denote backfill side of wall while even numbers denote stream side. Strain gages were welded on the flanges at four locations along the pile. Sections of angle iron were then welded over the gages to provide protection during pile driving (shown previously in Figure 5-33). Bending moments in the pile sections were calculated from the flexural strains (stresses) determined by the gages using a section modulus that included the contribution of the angle iron to the stiffness of the section.

A total of 10 semiconductor earth pressure cells were placed in the backfill of the west sheet pile abutment system to measure both vertical and lateral earth pressures. Three 24 in. diameter cells were placed beneath the abutment footing (at centerline of roadway) and were oriented to measure vertical earth pressure (Cells D1 through D3). The remaining cells were oriented for measuring lateral earth pressure. Positions of the cells near the centerline of the roadway in a side view are shown in Figure 5-95; the labeling system for each cell is alphanumeric. Two other pressure cells were placed near the reinforced concrete deadman (Cell X1 located 24 in. below the top of the deadman) and at the face of the wingwall (Cell X2 located 24 in. below the elevation of the bottom of the abutment footing); the location of these cells in plan view is shown in Figure 5-94a. The pile section instrumented is shown in Figure 5-94a with the locations of the gages along the pile given in Figure 5-94b. The piezometer was placed at an elevation of 18 ft below the bottom of the bridge deck; the location of the piezometer is near the east pier (third pile from the north edge of the bridge).

Measurements of the permanent instrumentation system were recorded using a Campbell Scientific, Inc., CR9000x datalogger. This system was used for long-term monitoring of the abutment as well as short-term datalogging during the live load test. Data were recorded at a rate of 10 hz during the live load testing while long-term readings were to be taken 4 times per day for several months.
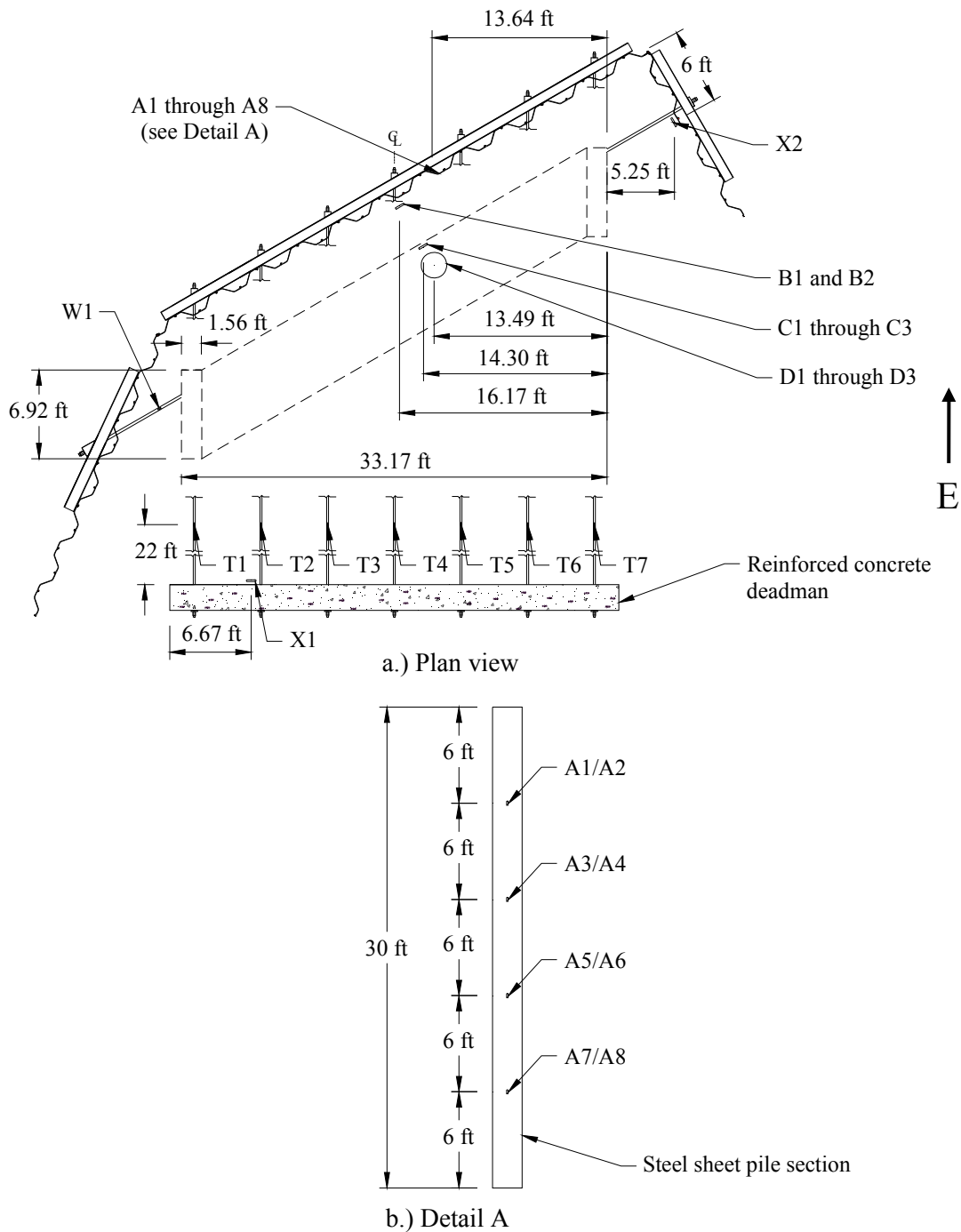
Figure 5-94. Location of instrumentation in west sheet pile abutment system in BC, Iowa.
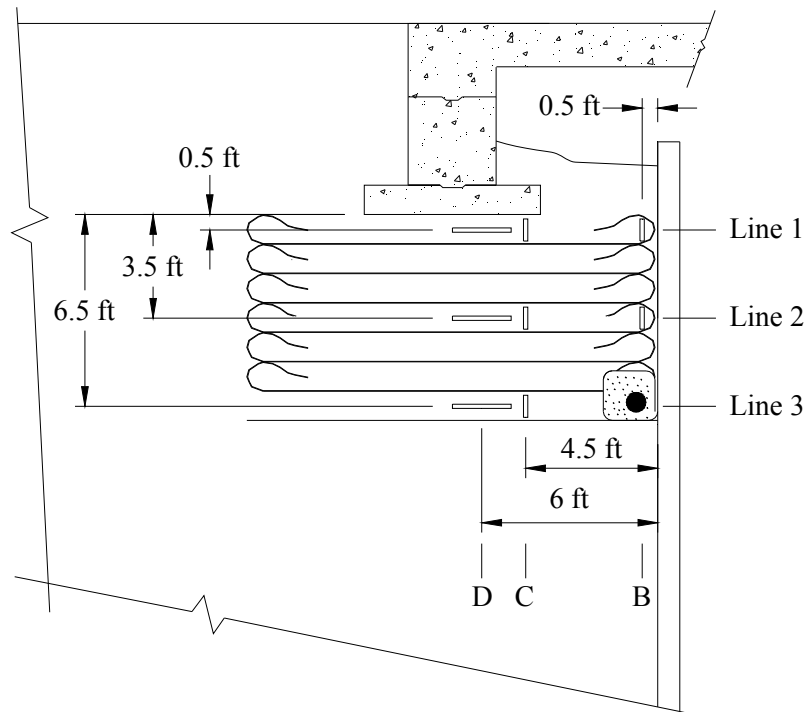
Figure 5-95. Location of earth pressure cells in west sheet pile abutment system in BC, Iowa.

Temporary Instrumentation System

To obtain structural displacements of the sheet pile wall as well as strains in the superstructure, a second (temporary) instrumentation system was installed after construction of the bridge was complete. Deflection and strain transducers were attached to the structure and measurements were recorded with a datalogger at a rate of 10 hz (the same rate used for the permanent system during the live load test).

Four strain gages were placed over the west pier (on the driving surface of the roadway 30.5 ft from the west abutment centerline) and four strain gages were placed on the bottom of the bridge 10 ft from the west abutment centerline to measure the approximate maximum negative and positive bending moments in the bridge, respectively; locations of the gages are shown in Figure 5-96. The strain gages on the bottom of the bridge deck were incorrectly installed perpendicular to the abutment centerline as shown in Figure 5-97 (at a skew of 30 degrees) thus requiring a factor of 0.866 to be applied to the measured strains (stresses) to determine the equivalent values if they were oriented along the centerline of the roadway. Deflection transducers (three at each abutment) were placed on

the sheet pile walls of both abutment systems with four strain gages also placed on the west sheet pile abutment system as shown in Figure 5-98.

Coordination between datalogging systems was achieved by using an instrument to provide a marked location in the data whenever the trucks were at the desired positions.
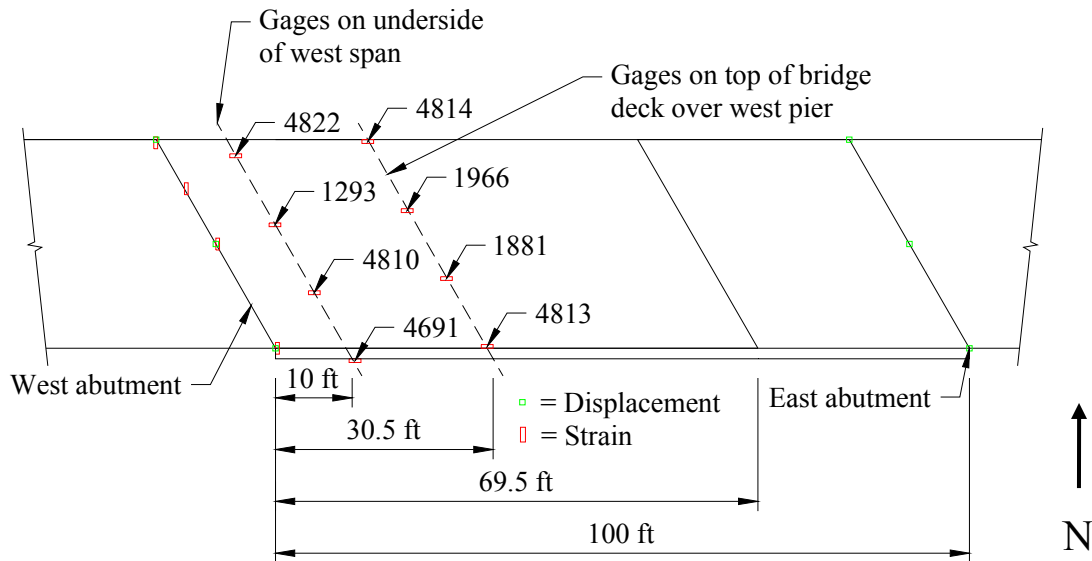
Figure 5-96. Plan view of instrumentation locations for temporary system used during live load testing (see Figure 5-98 for instrumentation on the abutments).
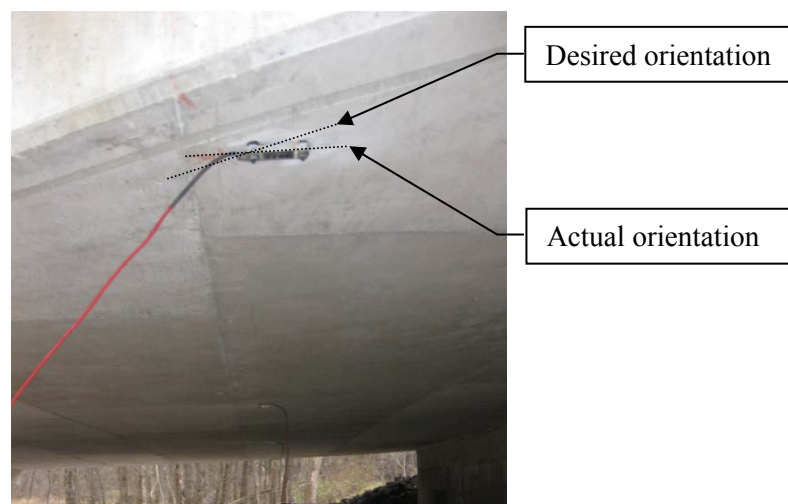
Figure 5-97. Installation error for strain transducers attached to bottom of bridge deck in BC.

a.) Facing west abutment

b.) Facing east abutment
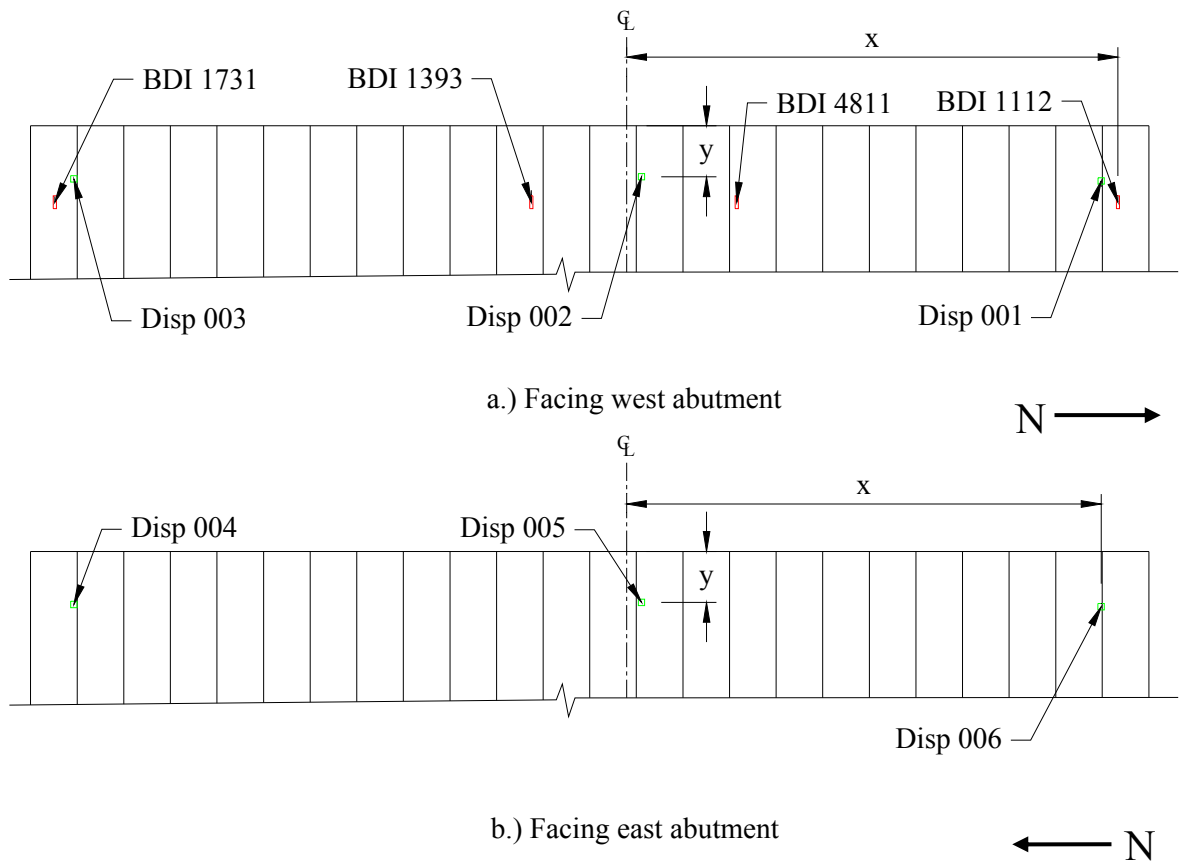
Figure 5-98. Locations of instrumentation on sheet pile walls for temporary system during live load testing.

Table 5-21. Location of instrumentation for temporary system used during live load testing with respect to coordinate system presented in Figure 5-98.

Instrument	x (ft)	y (ft)
BDI 1112	19.33	3.00
BDI 4811	4.33	3.00
BDI 1393	3.75	3.00
BDI 1731	22.50	3.00
Disp 001	18.67	2.17
Disp 002	0.58	2.00
Disp 003	21.75	2.08
Disp 004	21.75	2.08
Disp 005	0.58	2.00
Disp 006	18.67	2.17

Monitoring of Abutment System Movement

Displacement of the sheet pile walls and settlement of the bridge abutment footings were monitored through surveys performed with a total station. Utilizing several benchmarks placed around the project site, positions of the sheet pile walls on both abutments were recorded at various stages during construction. The positions of the walls were recorded using prisms fixed to the sheet piles at the centerline of each abutment as depicted in Figure 5-99; each had 3 prisms placed at 2 ft, 4 ft, and 6 ft below the top of the sheet pile.

The settlements of the bridge abutment footings were monitored using two points on each abutment. The PVC pipe installed during the placement of the bridge deck concrete (previously shown in Figure 5-85) allowed for placement of a surveying rod. A survey of the bridge was performed on March 22, 2010; results of the survey, providing settlement at each corner of the bridge abutments (relative to a survey performed after live load testing in November 2009), are presented in Table 5-22. Long-term movements of the sheet pile wall were negligible and are not presented.

Figure 5-99. Prisms for surveying displacement of sheet pile wall.

Table 5-22. Settlement of abutments relative to elevations recorded in November 2009.

Abutment corner	Settlement – March 2010 (in.)	Settlement – July 2010 (in.)
Northwest	0.159	0.249
Southwest	0.199	0.210
Northeast	0.000	0.026
Southeast	0.040	0.013

As previously mentioned, the maximum allowable settlement for each abutment was 0.875 in. to prevent cracking of the concrete over the bridge piers. Since all settlements were within acceptable limit no lifting of the abutments was required at the time of the surveys. Future surveys are recommended to ensure settlements remain within the acceptable limit.

Bridge Load Testing

Compaction Test

During backfilling of the west abutment, testing was performed to determine the effects of compaction on the sheet pile bridge abutment system; this testing occurred during compaction of the final layer of backfill (the layer on which the bridge abutment footing was cast). Readings were taken of all instrumentation before and after compaction of the final layer of backfill. Changes in earth pressure for selected cells (refer to Figure 5-95 for the location of each pressure cell) after compaction of the final layer of backfill are presented in Table 5-23; a negative value representing a decrease in earth pressure. High-sampling rate data (333 hz) were also taken as the compaction equipment passed over Pressure Cells D1, D2, and D3 (oriented to measure vertical earth pressure); data results are presented in Figure 5-100.

Table 5-23. Change in earth pressures after performing compaction of final backfill layer on west abutment.

Pressure Cell	Earth pressure change due to compaction (psf)
D1	75
D2	15
D3	20
C1	30
C2	-5
C3	0
B1	25
B2	-25
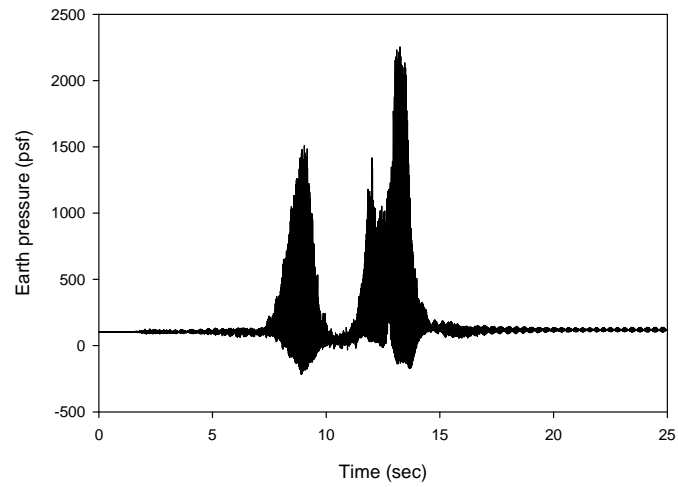
a.) Pressure Cell D1
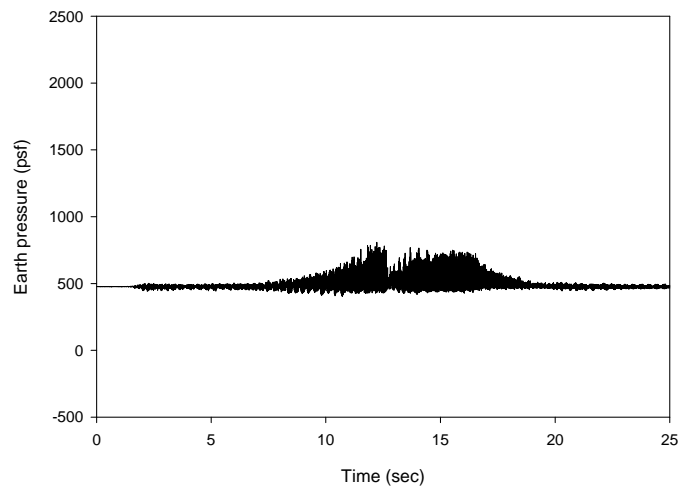
b.) Pressure Cell D2
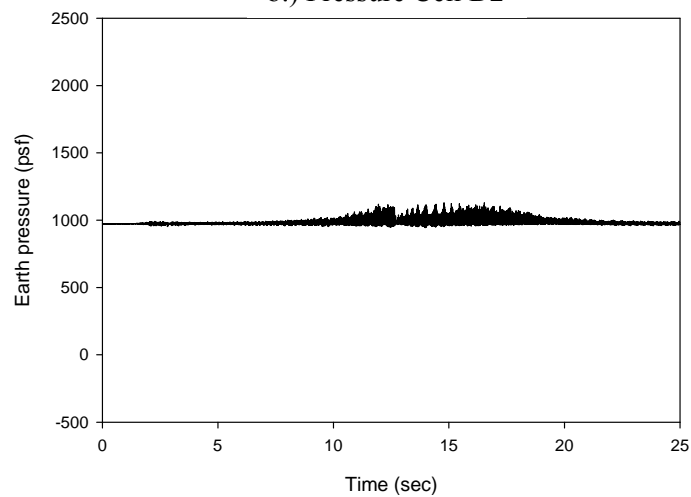
c.) Pressure Cell D3

Figure 5-100. Changes in earth pressure as compaction equipment passed over cells.

Pressure Cell D1 experienced the maximum fluctuation in vertical earth pressure, approximately 2400 psf, as the compaction equipment passed over it. Cells D2 and D3 (below Cell D1) experienced fluctuations of approximately 400 psf and 180 psf, respectively; as shown in Figure 5-95, Cell D2 is 3 ft below D1 and D3 is 6 ft below D1. As a result of compaction of the final layer, the only significant increase in earth pressures was seen in the cells within the compacted layer (D1, C1, and B1). Although a vertical pressure increase of approximately 20 psf occurred in Cells D2 and D3, the increase can be attributed to the weight of the added backfill material. Cells C1 and B1 (measuring horizontal earth pressure in the upper layer of backfill) recorded earth pressure increases of approximately 30 psf and 25 psf, respectively; this indicates the geogrid material effectively reduces lateral pressure applied to the sheet pile wall. The decrease in horizontal earth pressure that occurred in Cells C2, C3, and B2 (below the layer of backfill being compacted) indicates movement of the sheet pile wall during compaction of the final layer; movement of the wall away from the backfill would reduce earth pressure in previously compacted layers.

Permanent tensile strains (stresses) induced in the tie rods (due to compaction of the backfill soil) were a maximum of 0.09 ksi and thus considered negligible. Flexural strains (stresses) induced in the instrumented sheet pile element (located near the centerline of the roadway) were a maximum of 0.08 ksi and thus were also considered negligible.

<u>Live Load Test</u>

Test Procedure

Test truck axle weights are given in Table 5-24; test truck dimensions are given in Table 5-25 along with the truck diagrams shown in Figure 5-101.

Table 5-24. Test truck axle loads and total weight.

Load type	*Truck 228 (lbs)*	*Truck 229 (lbs)*
Front axle	15,400	15,420
Tandem axle	34,820	40,480
Total weight	50,220	55,900

Table 5-25. Test truck dimensions.

Dimension	Truck 228 (ft)	Truck 229 (ft)
A	6.88	6.83
B	6.17	6.17
C	16.08	15.13
D	20.67	19.54

a.) Front view   b.) Rear view   c.) Side view
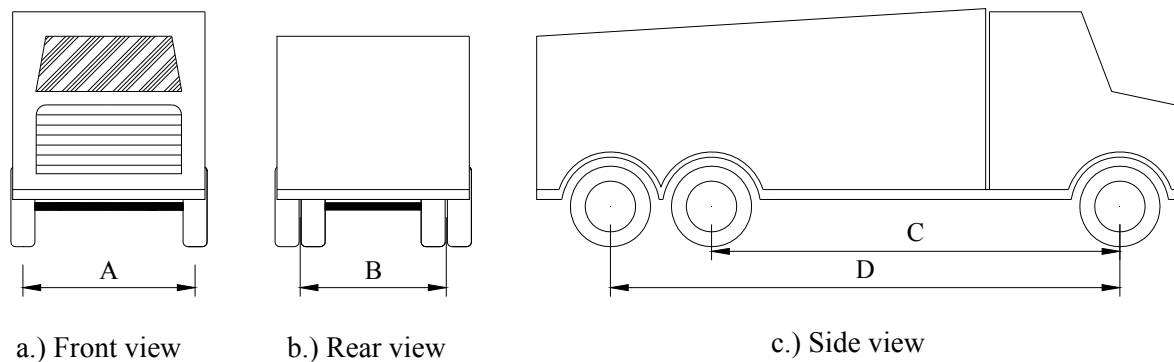
Figure 5-101. Diagram of test trucks.

The live load test consisted of the four different runs shown in Figure 5-102. Each test run involved the truck travelling from west to east and stopping at predetermined locations (10 ft spacing between each location) along the bridge. Test locations along the bridge from west to east are labeled by a letter (corresponding to a test run in Figure 5-102) and a location number according to position along the bridge; location numbers are presented in Figure 5-103. In Run A, readings were taken when the centerline of the south tandem was positioned over the marked locations. In Runs B, C and D readings were taken when the centerline of the north tandems were positioned over the marked locations; this is illustrated in Figure 5-103.

a.) Test Run A
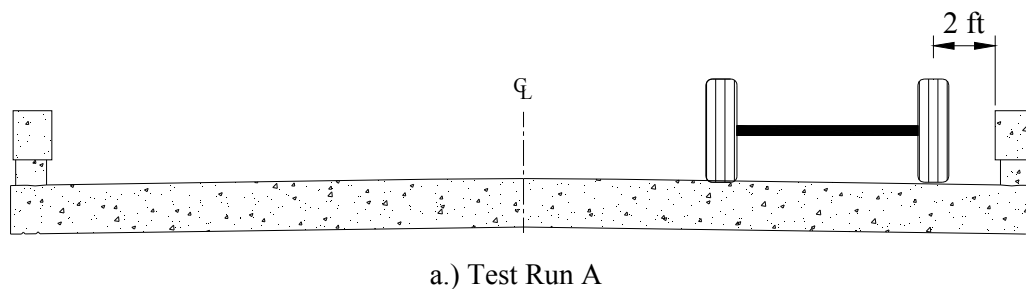
Figure 5-102. Transverse location of truck(s) in live load tests.

b.) Test Run B

c.) Test Run C

d.) Test Run D
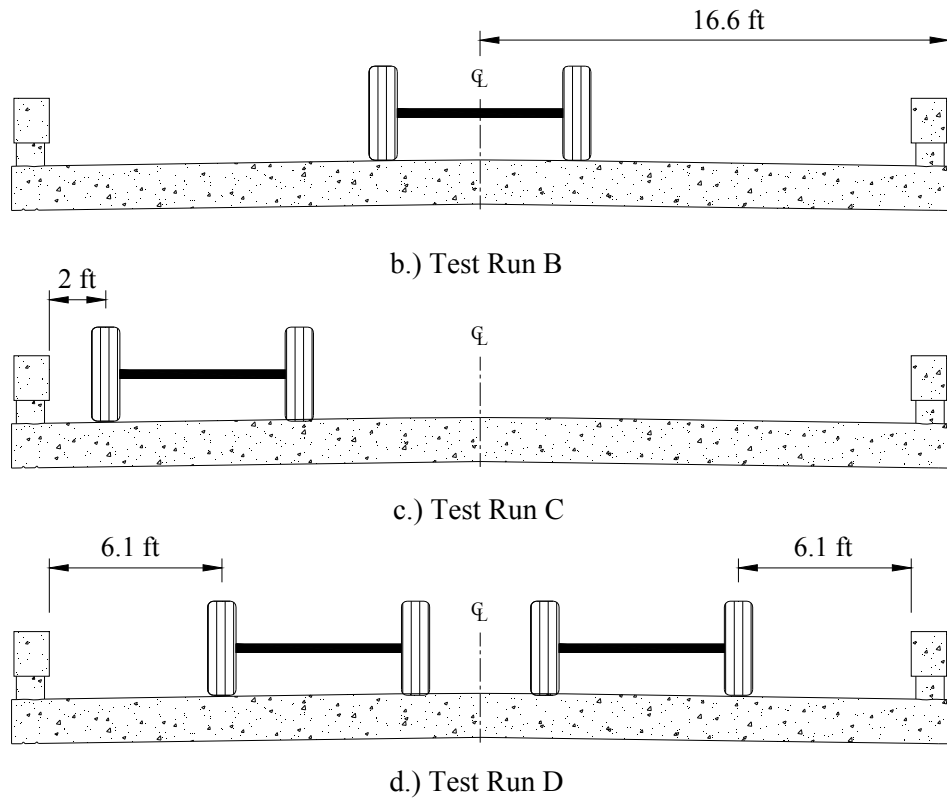
Figure 5-102. (continued).
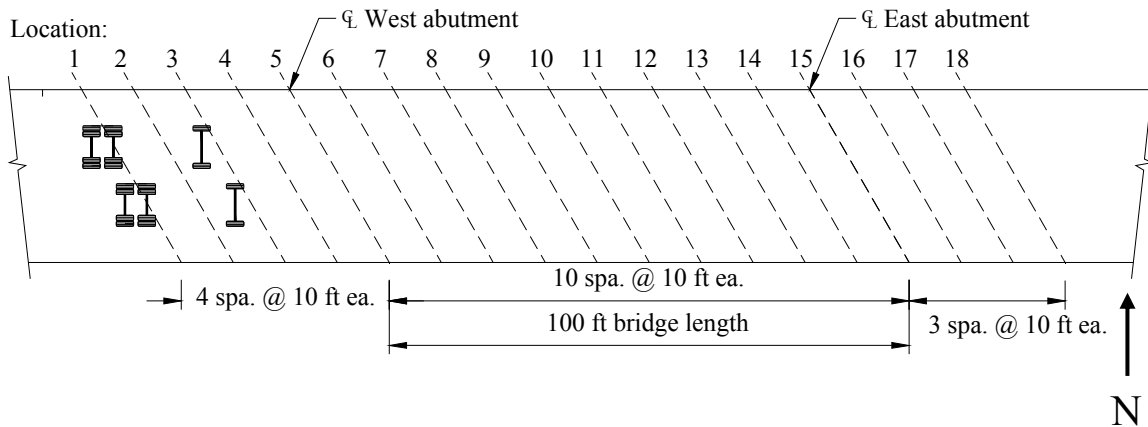
Figure 5-103. Locations of truck axles along the bridge (west to east).

Data Analysis and Results

Results from the live load test are presented in terms of loads and deflections due to live load only (zero readings taken just before live load testing began) and loads and deflections due to Load 1, a loading in which data are presented relative to a zero reading taken after completion of the west

abutment construction as shown in Figure 5-104; this loading includes test truck loads and the weight of the superstructure but does not include the weight of the spread footing and abutment cap.

Figure 5-104. State of completion of the west abutment when zero readings were taken to determine loads and deflections for Load 1.

Analyses were performed for six different positions of the truck(s). In Run D (both trucks traveling from west to east along driving lanes of the bridge; see Figure 5-105), analyses were performed for Locations 5, 6, and 10 which were selected to investigate the maximum load on the west abutment footing, approximate maximum positive bending moment in the west end span of the bridge, and the maximum negative moment over the west pier of the bridge, respectively. The remaining three test locations investigated were for Runs A, B, and C with Truck 229 positioned at Location 5 (maximum load on west abutment). The results of the analyses (expected loads and deflections) and the live load test data (measured loads and deflections) for the selected test locations are presented in Table 5-26 through Table 5-31.

Figure 5-105. Live load test Run D (trucks in approximated driving lanes) for BC.

Table 5-26. Live load test data and analysis results from Run D at Location 5.

Load or deflection	Live load only		Load 1	
	Expected	*Measured*	*Expected*	*Measured*
Vertical earth pressure				
D1	560 psf	410 psf	1435 psf	1985 psf
D2	450 psf	190 psf	1155 psf	1000 psf
D3	305 psf	125 psf	785 psf	515 psf
Horizontal earth pressure				
C1	180 psf	50 psf	420 psf	590 psf
C2	145 psf	0 psf	335 psf	205 psf
C3	95 psf	-20 psf	225 psf	-280 psf
B1	75 psf	15 psf	160 psf	920 psf
B2	225 psf	20 psf	550 psf	520 psf
X1 (deadman)	400 psf	5 psf	640 psf	365 psf
X2 (wingwall)	60 psf	20 psf	140 psf	205 psf
Wall flexural stress				
A1/A2	0.37 ksi	0.03 ksi	0.79 ksi	0.59 ksi
A3/A4	2.61 ksi	0.08 ksi	6.43 ksi	0.33 ksi
A5/A6	2.41 ksi	0.04 ksi	5.95 ksi	0.25 ksi
A7/A8	1.22 ksi	0.00 ksi	3.00 ksi	0.08 ksi
2 ft below top of wall	0.00 ksi	0.02 ksi	-	-
Tie rod axial stress				
main wall (max)	5.52 ksi	0.23 ksi	11.28 ksi	11.83 ksi
wingwall	6.18 ksi	0.02 ksi	14.80 ksi	- 5.23 ksi
Bridge deck stress				
over pier (max)	0.01 ksi	0.10 ksi	-	-
west span (max)	0.05 ksi	0.16 ksi	-	-
Wall displacements				
west (max)	0.100 in.	0.000 in.	-	-
east (max)	0.000 in.	0.000 in.	-	-

Test Run D
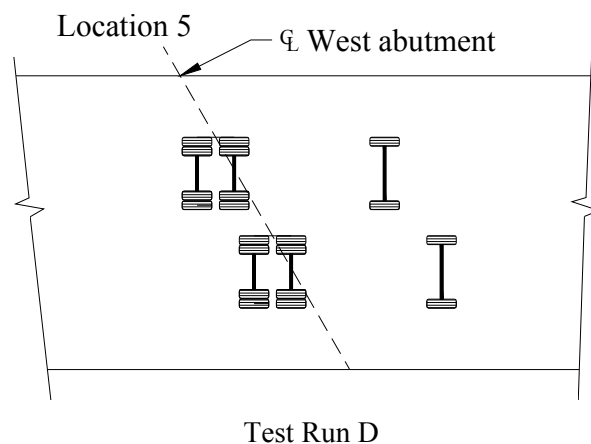
Table 5-27. Live load test data and analysis results from Run D at Location 6.

Load or deflection	Live load only		Load 1	
	Expected	*Measured*	*Expected*	*Measured*
Vertical earth pressure				
D1	435 psf	310 psf	1305 psf	1880 psf
D2	350 psf	110 psf	1050 psf	920 psf
D3	235 psf	80 psf	715 psf	470 psf
Horizontal earth pressure				
C1	115 psf	30 psf	355 psf	570 psf
C2	95 psf	-5 psf	285 psf	205 psf
C3	65 psf	-25 psf	195 psf	-285 psf
B1	40 psf	10 psf	125 psf	915 psf
B2	160 psf	15 psf	485 psf	520 psf
X1 (deadman)	185 psf	5 psf	555 psf	365 psf
X2 (wingwall)	40 psf	10 psf	125 psf	200 psf
Wall flexural stress				
A1/A2	0.28 ksi	0.04 ksi	0.85 ksi	0.60 ksi
A3/A4	1.74 ksi	0.03 ksi	5.04 ksi	0.28 ksi
A5/A6	1.58 ksi	0.03 ksi	4.44 ksi	0.24 ksi
A7/A8	0.79 ksi	0.02 ksi	2.22 ksi	0.10 ksi
2 ft below top of wall	0.00 ksi	0.01 ksi	-	-
Tie rod axial stress				
main wall (max)	3.31 ksi	0.08 ksi	9.85 ksi	11.68 ksi
wingwall	4.34 ksi	0.07 ksi	12.93 ksi	-5.18 ksi
Bridge deck stress				
over pier (max)	0.03 ksi	0.12 ksi	-	-
west span (max)	0.18 ksi	0.55 ksi	-	-
Wall displacements				
west (max)	0.062 in.	-0.003 in.	-	-
east (max)	0.000 in.	0.001 in.	-	-

Test Run D
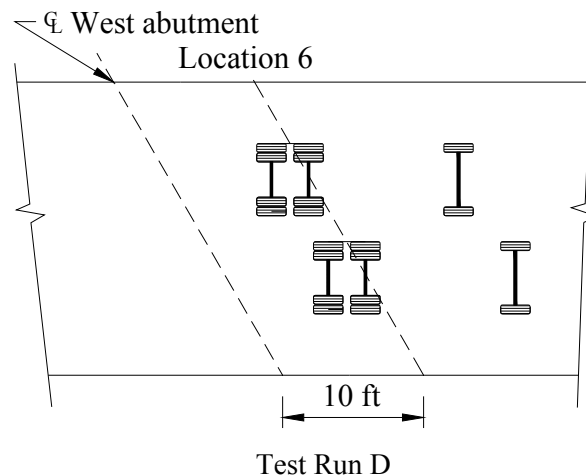
Table 5-28. Live load test data and analysis results from Run D at Location 10.

Load or deflection	Live load only		Load 1	
	Expected	*Measured*	*Expected*	*Measured*
Vertical earth pressure				
D1	-70 psf	-55 psf	805 psf	1515 psf
D2	-55 psf	-30 psf	645 psf	780 psf
D3	-40 psf	-15 psf	440 psf	375 psf
Horizontal earth pressure				
C1	-20 psf	-10 psf	220 psf	530 psf
C2	-15 psf	15 psf	175 psf	220 psf
C3	-10 psf	10 psf	120 psf	-250 psf
B1	-5 psf	-5 psf	80 psf	900 psf
B2	-25 psf	0 psf	300 psf	500 psf
X1 (deadman)	-30 psf	5 psf	350 psf	365 psf
X2 (wingwall)	-5 psf	15 psf	75 psf	205 psf
Wall flexural stress				
A1/A2	0.05 ksi	0.02 ksi	0.53 ksi	0.58 ksi
A3/A4	0.29 ksi	0.04 ksi	3.25 ksi	0.29 ksi
A5/A6	0.26 ksi	0.03 ksi	2.93 ksi	0.24 ksi
A7/A8	0.13 ksi	0.00 ksi	1.48 ksi	0.08 ksi
2 ft below top of wall	0.00 ksi	0.01 ksi	-	-
Tie rod axial stress				
main wall (max)	-0.54 ksi	-0.05 ksi	6.16 ksi	11.55 ksi
wingwall	-0.71 ksi	-0.10 ksi	8.08 ksi	-5.35 ksi
Bridge deck stress				
over pier (max)	0.05 ksi	0.27 ksi	-	-
west span (max)	0.04 ksi	-0.18 ksi	-	-
Wall displacements				
west (max)	0.015 in.	0.003 in.	-	-
east (max)	0.015 in.	0.000 in.	-	-

Test Run D
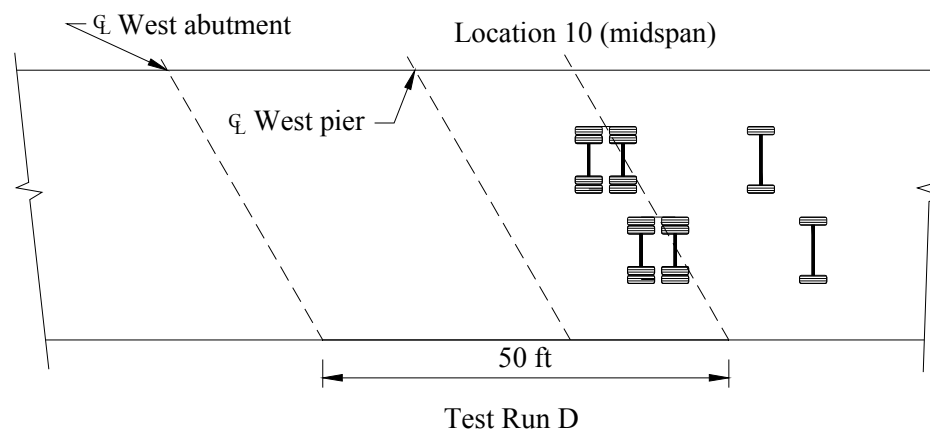
Table 5-29. Live load test data and analysis results from Run A at Location 5.

Load or deflection	Live load only		Load 1	
	Expected	*Measured*	*Expected*	*Measured*
Vertical earth pressure				
D1	600 psf	195 psf	1475 psf	1770 psf
D2	480 psf	75 psf	1185 psf	885 psf
D3	330 psf	45 psf	805 psf	430 psf
Horizontal earth pressure				
C1	165 psf	30 psf	400 psf	570 psf
C2	135 psf	-10 psf	325 psf	200 psf
C3	90 psf	-10 psf	220 psf	-270 psf
B1	60 psf	10 psf	145 psf	915 psf
B2	225 psf	20 psf	550 psf	525 psf
X1 (deadman)	265 psf	-10 psf	660 psf	350 psf
X2 (wingwall)	45 psf	0 psf	110 psf	190 psf
Wall flexural stress				
A1/A2	0.42 ksi	0.03 ksi	1.00 ksi	0.59 ksi
A3/A4	2.45 ksi	0.02 ksi	5.97 ksi	0.27 ksi
A5/A6	2.22 ksi	0.02 ksi	5.43 ksi	0.23 ksi
A7/A8	1.12 ksi	0.00 ksi	2.73 ksi	0.08 ksi
2 ft below top of wall	0.00 ksi	0.01 ksi	-	-
Tie rod axial stress				
main wall (max)	4.74 ksi	0.08 ksi	11.69 ksi	11.68 ksi
wingwall	6.22 ksi	0.13 ksi	15.35 ksi	-5.12 ksi
Bridge deck stress				
over pier (max)	0.01 ksi	0.10 ksi	-	-
west span (max)	0.03 ksi	0.38 ksi	-	-
Wall displacements				
west (max)	0.087 in.	-0.002 in.	-	-
east (max)	0.000 in.	0.000 in.	-	-

Test Run A
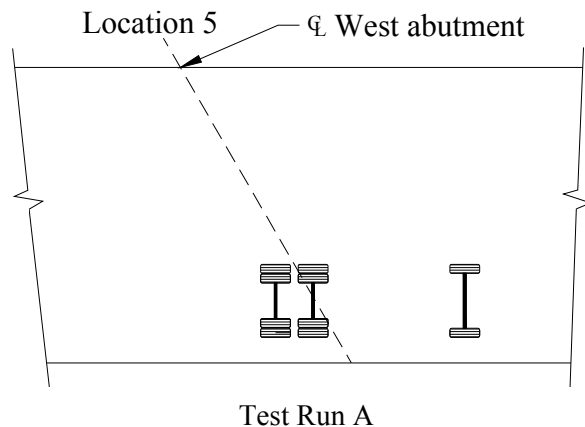
Table 5-30. Live load test data and analysis results from Run B at Location 5.

Load or deflection	Live load only		Load 1	
	Expected	Measured	Expected	Measured
Vertical earth pressure				
D1	600 psf	185 psf	1475 psf	1760 psf
D2	480 psf	80 psf	1185 psf	890 psf
D3	330 psf	60 psf	805 psf	445 psf
Horizontal earth pressure				
C1	185 psf	15 psf	420 psf	555 psf
C2	145 psf	5 psf	335 psf	210 psf
C3	100 psf	-20 psf	225 psf	-280 psf
B1	70 psf	15 psf	155 psf	920 psf
B2	235 psf	10 psf	560 psf	515 psf
X1 (deadman)	280 psf	-5 psf	660 psf	360 psf
X2 (wingwall)	50 psf	15 psf	110 psf	205 psf
Wall flexural stress				
A1/A2	0.48 ksi	0.02 ksi	1.05 ksi	0.58 ksi
A3/A4	2.51 ksi	0.02 ksi	6.03 ksi	0.27 ksi
A5/A6	2.28 ksi	0.03 ksi	5.49 ksi	0.24 ksi
A7/A8	1.15 ksi	0.00 ksi	2.76 ksi	0.08 ksi
2 ft below top of wall	0.00 ksi	0.01 ksi	-	-
Tie rod axial stress				
main wall (max)	4.97 ksi	0.06 ksi	11.66 ksi	11.66 ksi
wingwall	6.52 ksi	-0.22 ksi	15.30 ksi	-5.47 ksi
Bridge deck stress				
over pier (max)	0.01 ksi	0.10 ksi	-	-
west span (max)	0.03 ksi	0.36 ksi	-	-
Wall displacements				
west (max)	0.089 in.	-0.003 in.	-	-
east (max)	0.000 in.	0.000 in.	-	-

Test Run B
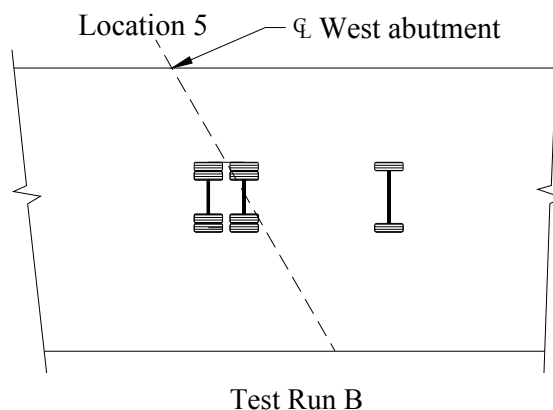
Table 5-31. Live load test data and analysis results from Run C at Location 5.

Load or deflection	Live load only		Load 1	
	Expected	*Measured*	*Expected*	*Measured*
Vertical earth pressure				
D1	600 psf	205 psf	1475 psf	1780 psf
D2	480 psf	75 psf	1185 psf	885 psf
D3	330 psf	50 psf	805 psf	435 psf
Horizontal earth pressure				
C1	165 psf	35 psf	405 psf	570 psf
C2	135 psf	-15 psf	325 psf	195 psf
C3	90 psf	-30 psf	220 psf	-290 psf
B1	65 psf	15 psf	145 psf	920 psf
B2	230 psf	15 psf	550 psf	520 psf
X1 (deadman)	260 psf	5 psf	640 psf	370 psf
X2 (wingwall)	45 psf	-10 psf	105 psf	180 psf
Wall flexural stress				
A1/A2	0.39 ksi	0.01 ksi	0.97 ksi	0.57 ksi
A3/A4	2.41 ksi	0.03 ksi	5.94 ksi	0.28 ksi
A5/A6	2.19 ksi	0.02 ksi	5.39 ksi	0.23 ksi
A7/A8	1.10 ksi	0.02 ksi	2.71 ksi	0.10 ksi
2 ft below top of wall	0.00 ksi	0.01 ksi	-	-
Tie rod axial stress				
main wall (max)	4.60 ksi	0.07 ksi	11.29 ksi	11.67 ksi
wingwall	6.03 ksi	-0.01 ksi	14.82 ksi	-5.26 ksi
Bridge deck stress				
over pier (max)	0.01 ksi	0.16 ksi	-	-
west span (max)	0.03 ksi	0.31 ksi	-	-
Wall displacements				
west (max)	0.086 in.	-0.001 in.	-	-
east (max)	0.000 in.	0.000 in.	-	-

Test Run C
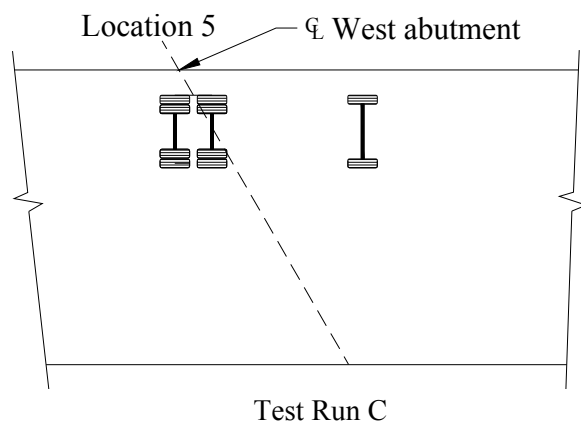
During the live load testing severe rutting in the east approach occurred (see Figure 5-106) and grading of the roadway was necessary after the testing; proper compaction of approach fill would have likely reduced or prevented this rutting.

Figure 5-106. Rutting of bridge approaches due to live load testing.

In general, the loads and deflections measured during live load testing were significantly less than those expected by the analyses performed which utilized the same methods and assumptions used in the design of the sheet pile bridge abutment systems.

Maximum loading of the west sheet pile bridge abutment system was expected during Run D when the trucks were positioned at Location 5 (north tandem of Truck 229 positioned over centerline abutment bearing). Vertical earth pressures (due to live loads only) recorded in Cells D1, D2, and D3 during live load test Run D are presented in Figure 5-107; the results confirmed that maximum loading of the west sheet pile bridge abutment system was experienced with the load at Location 5. The effect of uplift on the west abutment due to truck loads positioned in the midspan of the bridge is also apparent in Figure 5-107; negative earth pressures are recorded as the dead load of the bridge on the west abutment is reduced due to the deformation of the bridge superstructure. Lateral earth pressures recorded during test Run D are presented in Figure 5-108 and Figure 5-109; the lateral earth pressures recorded were lower than expected and diminished significantly towards the sheet pile wall, suggesting the geogrid was effective in minimizing lateral loading of the sheet piling.

It should be noted that, during maximum loading of the west sheet pile abutment system, a reduction in earth pressure (negative value) occurred in Cells C2 and C3. A potential explanation for this phenomenon is the load path of the earth pressure in the backfill. As depicted in Figure 5-110, the surcharge loads from the superstructure may be distributed to the geogrid and sheet pile wall in a path that does not significantly include Cells C2 and C3. As load is applied to the wall near the top, the deformation of the sheet pile wall (outward towards stream) reduces pressure on the backfill in the lower region containing Cells C2 and C3, resulting in the negative earth pressures recorded.
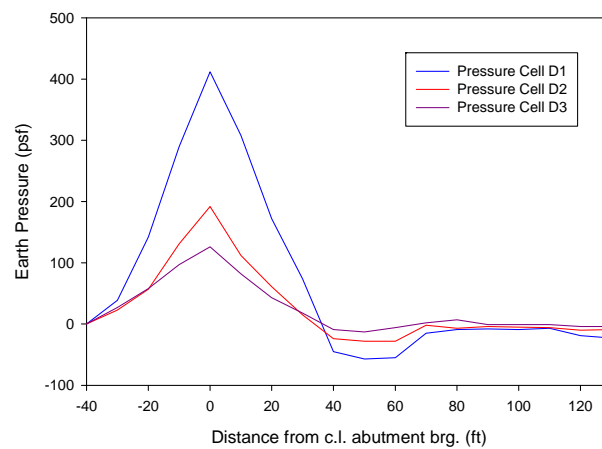
Figure 5-107. Vertical earth pressures recorded in Cells D1, D2, and D3 during test Run D (live load only).
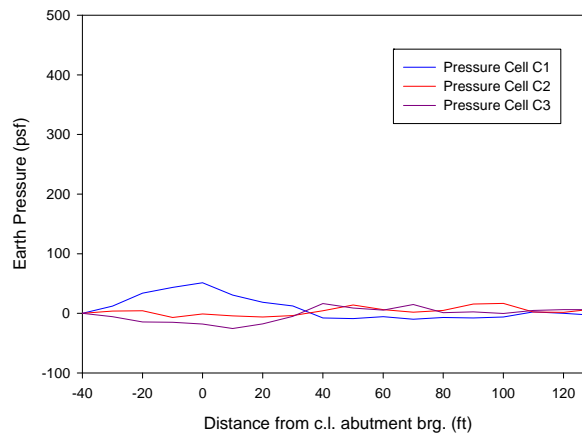
Figure 5-108. Lateral earth pressures recorded in Cells C1, C2, and C3 during test Run D (live load only).
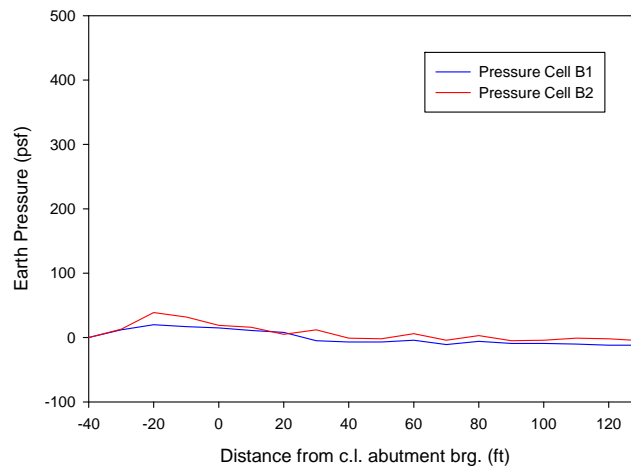
Figure 5-109. Lateral earth pressures recorded in Cells B1 and B2 during test Run D (live load only).
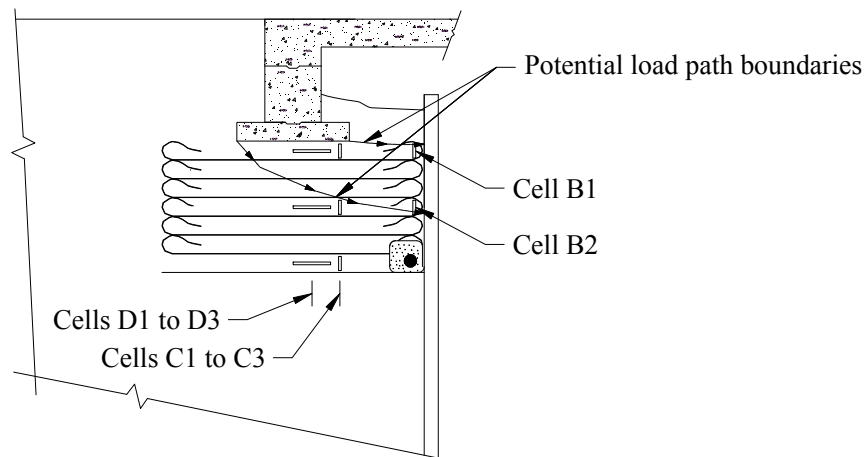
Figure 5-110. Potential bridge surcharge load path through backfill.

In terms of loading relative to completion of construction of the west sheet pile bridge abutment system (Load 1), Cells D1, C1, and B1(all located at an elevation 6 in. below the spread footing) recorded earth pressures greater than those expected by analysis for all of the test locations investigated. Since these earth pressures cells are located above any geogrid reinforcement, the results suggest that the long-term dead load surcharge of the superstructure, abutment cap, and footing is significantly concentrated in the upper layer of the backfill (the path of least resistance) due to the geogrid below; lateral deformation of (and thus earth pressure developed within) the backfill soil is more significantly resisted in the geogrid reinforced layers.

During live load testing, the strain gages attached to the primary tie rods recorded increases in strain (stress) that, at a maximum, were 4.2 % of the expected values by analysis; thus, the stresses developed in the tie rods due to live loads were negligible. In terms of Load 1, however, the primary tie rod stresses developed since completion of the west sheet pile bridge abutment system were significant. The recorded stresses were approximately (and in some cases greater than) those predicted by analysis. In the wingwall tie rod, tensile stress increase due to live load only was also significantly lower than predicted by analysis, while Load 1 stress results recorded a reduction in stress of approximately 5 ksi. The reduction in stress suggests the wingwalls had moved inward after construction of the superstructure; a potential explanation of this phenomenon was discussed in the BHC project (see Figure 5-45a).

Primary tie rod stress results indicate that, although significantly over-designed in terms of vehicular load resistance, the tie rod anchorage system (in the size designed) was necessary for construction of the bridge. The designed size of the wingwall tie rod was significantly conservative as the tie rod experienced a *reduction* in stress after construction of the superstructure and relatively negligible stress increase during live load testing.

The minimal transfer of load (due to live load only) to the wingwalls and deadman are also confirmed by the earth pressures recorded in Cells X1 (at the face of the concrete deadman) and X2 (in the upper layer of backfill at the face of the southwest wingwall). In terms of Load 1 stress in the wingwall pressure cell, however, the recorded earth pressures were larger than expected. This stress increase may also be explained by inward movement of the wingwalls (a behavior not taken into account in the analysis) as such movement would increase lateral earth pressure in the backfill at the face of the sheet pile wingwall.

Flexural strains (stresses) in the instrumented sheet pile near the centerline of the roadway recorded were significantly less than the values expected in design (due to both live load only and Load 1). In the analysis, maximum flexural stress in the sheet pile section was assumed to occur in the gages 6 ft below the tie rod anchor height (Gages A3 and A4) thus it can be determined that the profile of the wall is bending outward below the anchor with the upper portion displacing inward toward the footing. Measured flexural stresses during live load testing recorded maxima *at the location of the tie rod anchor* (Gages A1 and A2), thus the top of the wall is displacing outward (away from the footing); this behavior is confirmed by displacement transducers on the west sheet pile bridge

abutment system wall. Displacement transducers on both abutments recorded displacements significantly lower than expected by analysis; displacements for all transducers during test Run D are presented in Figure 5-111.
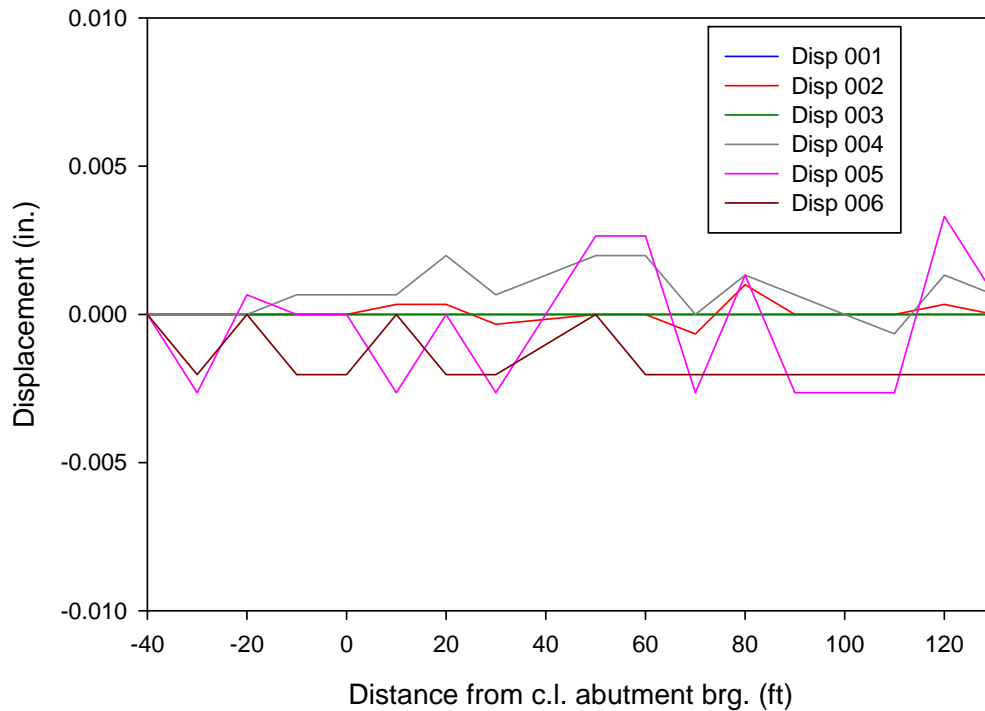
Figure 5-111. Displacements of the sheet pile wall during live load test Run D in BC.

Bridge deck strains (stresses) were also measured during live load testing; gages were placed to measure strains (stresses) over the west pier (top of deck, maximum negative moment) and on the bottom of the deck, 10 ft from the west abutment centerline of bearing (approximate maximum positive moment). In Figure 5-112, the location of bending moment maxima in analysis are verified; positive bending maximum moment was attained in test Run D, Location 6 (+10 ft from centerline abutment bearing) and maximum negative bending moment was attained in test Run D, Location 10 (+50 ft from centerline abutment bearing). For all test runs, the strains measured were higher than those expected by the analysis which utilized design assumptions that distributed lane loads over 10 ft width (see Appendix B for example analysis calculations); this would suggest that, in the superstructure only, the 10 ft distribution assumption is unconservative.

At Location 10 in test Run D, uplift forces on the west bridge abutment (due to deformation of the superstructure with the trucks placed at midspan) reduced dead load surcharge on the west sheet pile abutment system backfill and subsequently reduced vertical and lateral earth pressures (as well as other loads and deformations); see Table 5-28 for results from this test location. The mechanism by which dead load surcharge is reduced is depicted (significantly exaggerated) in Figure 5-113. The effect of live load on the deflection is shown; in the actual bridge there would be no net uplift since live load would be acting in combination with the dead load.
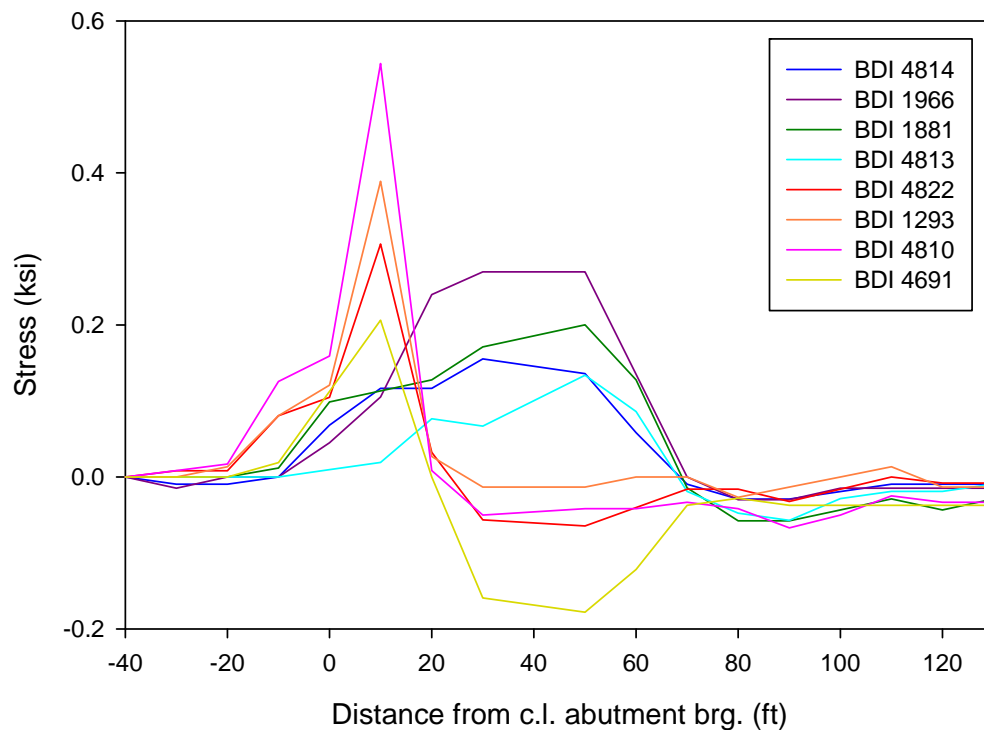
Figure 5-112. Bridge deck strains (stresses) during live load test Run D (refer to Figure 5-96 for instrumentation locations).
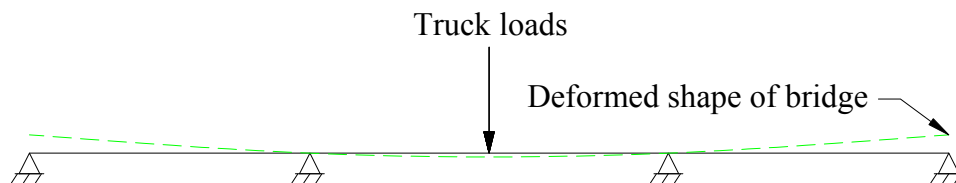
Figure 5-113. Simulated deformation of bridge superstructure with trucks at midspan causing reduction in reaction force at abutments.

To investigate the effects of pattern loading on the strain (stress) at the west span and over the west pier, the trucks were positioned at the two locations presented in Figure 5-114. The maximum negative bending stress over the west pier (due to the pattern loading shown in Figure 5-114a) was 0.13 ksi and the maximum positive bending stress in the west span (due to the pattern loading shown in Figure 5-114b) was 0.17 ksi; the stresses at these locations during test Run D (with both trucks) were greater than what was measured during the pattern loading test.
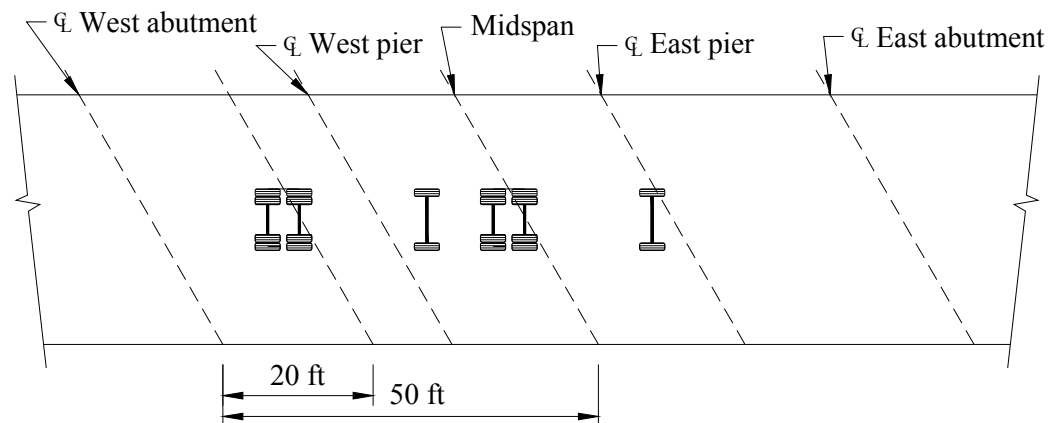
a.) Negative bending over west pier
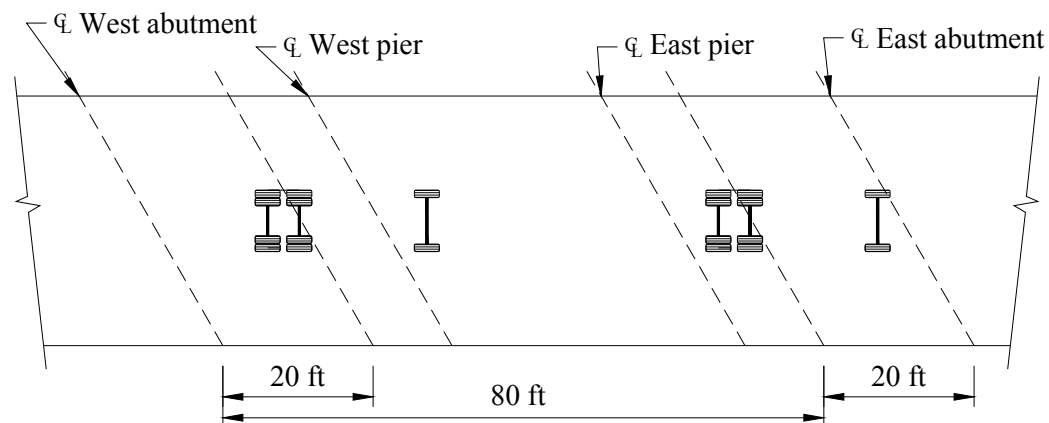
b.) Positive bending in bottom of west span

Figure 5-114. Truck locations providing pattern loading strains (stresses).

Test Runs A, B, and C were only analyzed for Location 5. The corresponding results from these test locations differed minimally, suggesting effective load distribution through the superstructure, abutment cap, and spread footing; the design assumption of 10 ft lane distribution for superstructure live loads is conservative.

<u>Long-Term Monitoring</u>

Due to a failure of the datalogging system during recording, all long-term data was lost and is thus
absent from this report. Earth pressures were manually recorded in May of 2010 using a voltmeter to
provide the only long-term data of the structure that were available (strains were unable to be
recorded without the datalogger); changes in backfill earth pressures between November of 2009
(after live load testing of the bridge) and May of 2010 are presented in Table 5-32.

Table 5-32. Change in earth pressure from November 2009 to May 2010 in BC, Iowa.

Pressure Cell	Long-term change in earth pressure (psf)
D1	-640
D2	-5
D3	10
C1	-95
C2	155
C3	190
B1	85
B2	-120
X1	145
X2	85

A significant decrease (negative change) in earth pressure occurred in Cells D1, C1, and B2. Several
factors may be involved in causing this effect: frost heave of the soil during the winter, arching of the
load path around the cells, and creep of the geogrid material; it is difficult to determine the exact
cause of the decreases in earth pressure. Increases in Cells X1 and X2 (placed near the deadman and
the wingwall, respectively) are likely due to long-term creep in the geogrid and settlement of the
backfill, transferring lateral loads to the sheet pile wall.

Key Findings

Through the construction and structural monitoring of the BC demonstration bridge, geosynthetically
reinforced earth steel sheet pile bridge abutment systems have been shown to be a potential
alternative for LVR bridge abutments. Several improvements and further research, however, are
necessary before sheet pile bridge abutment systems similar to the BC project are economically
feasible. The total cost of the construction of the BC demonstration project was approximately

$591,000, with a typical 100 ft, three-span county road J30C-87 standard bridge (with steel H-pile abutments) expected to cost $397,000; total construction time required approximately 18 weeks.

Analyses of the live load test results concluded that the design methods used, in general, were significantly conservative when compared to the stresses experienced due to vehicular traffic. The Maximum flexural stress experienced in the sheet pile elements were 0.08 ksi (3% of the expected value by analysis). Vertical and horizontal earth pressures in the backfill (with maxima of 410 psf and 50 psf, respectively) were also lower than expected and were 73% and 28% of estimated values, respectively. The maximum lateral earth pressure experienced at the face of the sheet pile wall was 20 psf and was 10% of the value estimated without including the geosynthetic reinforcement in the analysis; these results indicate a significant contribution of the geosynthetic reinforcement in reducing lateral earth pressures on the wall. The anchorage system, which increased the overall cost of the project significantly due to extra construction time, special materials ($70,000 approximately), etc., was determined to be resisting negligible loads during live load testing (4% of expected load); this suggests there are potential cost savings with a reduced (or eliminated) permanent anchorage system. The stresses due to Load 1 on the anchorage system, however, were significant and thus the system (or some alternative method of providing lateral restraint) was necessary for construction of the bridge superstructure.

Stresses in the wingwall tie rod (from live load only and Load 1) were negligible and thus provide potential for reduced material costs. Behavior of the wingwalls was not accurately accounted for by the design methods used.

Due to the inherent potential for settlement of spread footings, use of this type of sheet pile bridge abutment system for multiple span (statically indeterminate) structures must include strict requirements for compaction and reduction of voids in the backfill material (such as the flooding technique used for the abutments in the BC bridge). The demonstration project constructed in Tama County, Iowa presents the use of a similar sheet pile bridge abutment system for a single span bridge in which significant differential abutment settlements are not detrimental to the superstructure.

Tama County

Project Details

The third demonstration project was constructed in Tama County (TC), Iowa. The site that was selected was a low volume road bridge (servicing one residence) on MM Avenue near 380th Street crossing Richland Creek (a tributary of the Iowa River); the location of the bridge is shown in Figure 5-115.

This project was undertaken to investigate the feasibility of using sheet piling combined with a GRS system for the primary abutment foundation element and backfill retaining system. Construction of the new bridge was initiated on June 29, 2009 and was not completed at the time of this thesis which presents information on the design of the new sheet pile abutment system and its construction. Information on the instrumentation installed, load testing, and data analysis will be presented in a future report (TR-568). The following sections give an overview of the previous structure and the new sheet pile abutment bridge system.
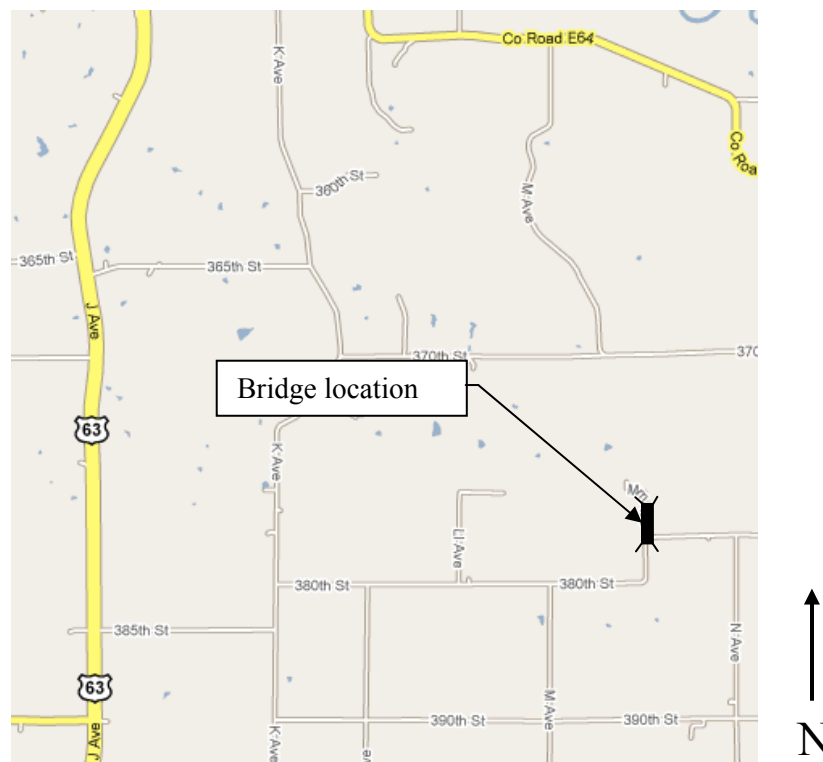
Figure 5-115. Location of demonstration project in TC, Iowa.

<u>Previous Bridge Structure</u>

The structure that was replaced was an 18 ft wide, 60 ft long two-span bridge originally constructed in 1970. The bridge (constructed approximately 16 ft above stream level) had a timber deck on steel girders with timber pile abutments and a timber pier (see Figure 5-116).

| a.) Side view | b.) End view |

Figure 5-116. Previous bridge structure at demonstration project site in TC, Iowa.

<u>New Sheet Pile Abutment Bridge System Overview</u>

Superstructure

The new bridge structure in TC utilizes two 89 ft long railroad flatcars (RRFC's) for the superstructure. A 10 ft x 10 ft footing (consisting of twelve, 10 ft long 10 in. x 10 in. timbers) was bolted to both ends of each RRFC. The timber footings were attached so the RRFC's could be used as a temporary bridge during construction of the abutments and subsequently moved into their final position without the need to create two separate footings. Once in place, the RRFC's were to be bolted together transversely and filled with roadstone to provide a driving surface on the bridge.

For more information on the research, design, application, construction, and performance of RRFC bridge structures refer to research projects TR-444 "Demonstration Project Using Railroad Flatcars for Low-Volume Road Bridges" and TR-498 "Field Testing of Railroad Flatcar Bridges."

a.) Midspan

b.) Over timber footing
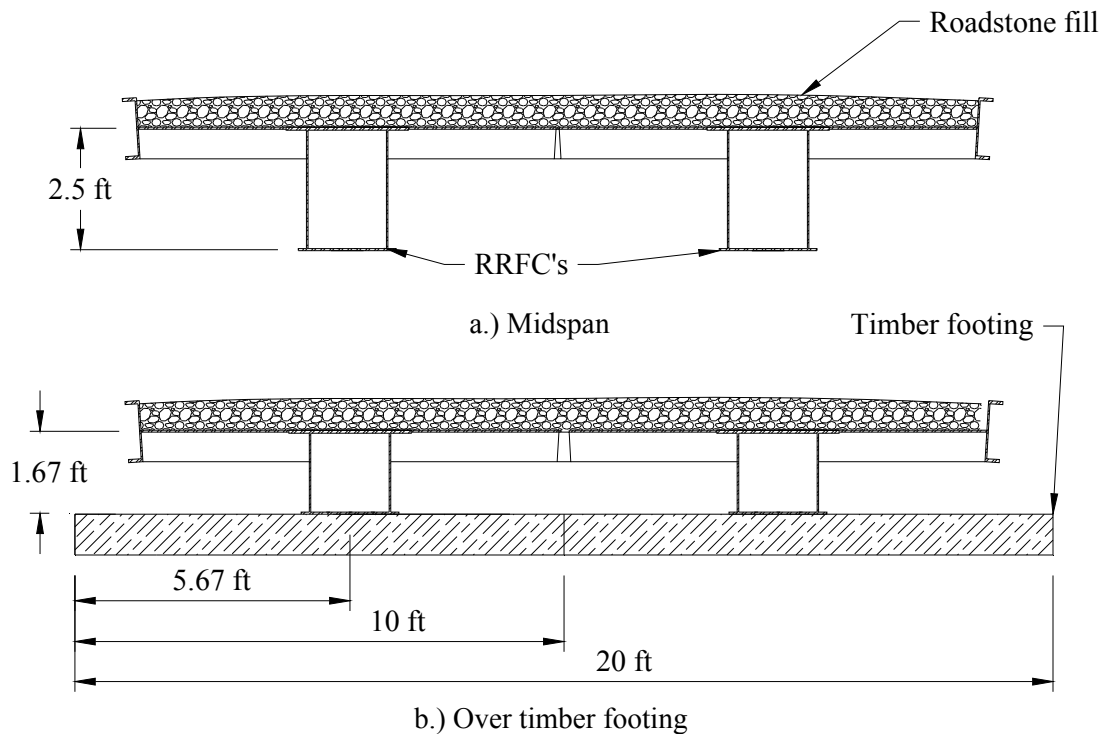
Figure 5-117. Cross-section of new RRFC bridge superstructure for demonstration project in TC, Iowa.

Abutment Foundation and Backfill Retaining System

The substructure for the bridge utilizes a GRS system with a steel sheet pile retaining and scour protecting wall similar to the project in BC, Iowa. The project in TC, however, utilizes PZC 13 sheet pile sections which are lighter and stronger than the traditional PZ 22 section. The project also avoids the significant earthwork required from a reinforced concrete deadman by attaching the tie rods to the RRFC superstructure as shown in Figure 5-118. With this system, the sheet pile wall is anchored by developing axial compressive forces in the RRFC superstructure.

The replacement structure is to be constructed in front of the existing timber abutments (left in place) which subsequently requires less demolition work. The GRS system is to have 7 layers of BX1200 geogrid and is to be constructed approximately 20 ft x 40 ft in plan (see Figure 5-119). Unlike the structure in BC, the design of the sheet pile abutment retaining system in TC considers the contribution of the GRS system and requires significantly smaller sheet pile sections and anchorages than would have been traditionally required. For additional details on the structure, design plan sheets developed by ISU are presented in Figure C1 through Figure C5 in Appendix C.

Documentation on construction of the bridge structure and subsequent load testing and analysis are to be provided in the final report for IHRB project TR-568. The following sections provide information on the site investigation and design of the bridge structure.
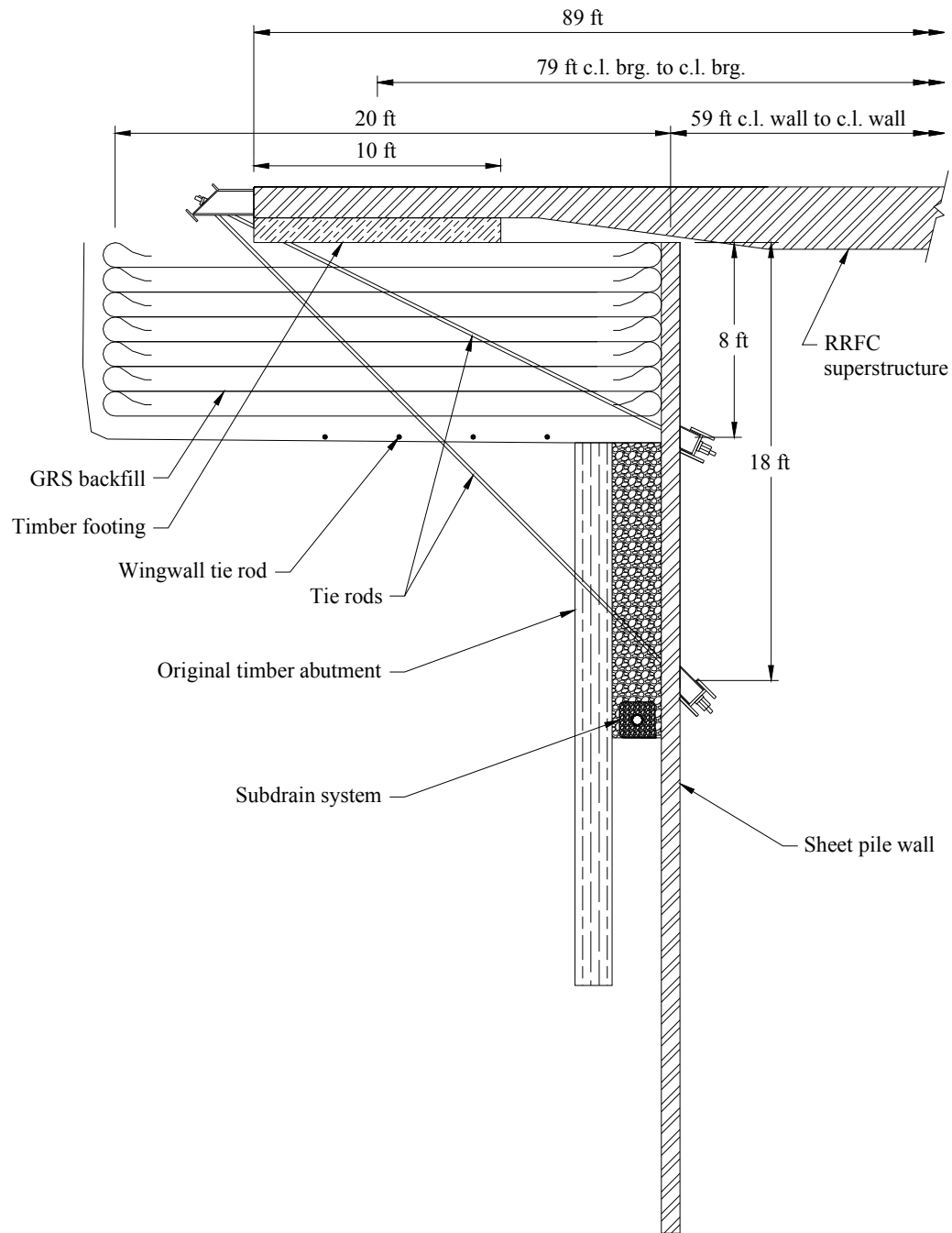
Figure 5-118. Design detail cross-section of TC, Iowa sheet pile bridge abutment and backfill retaining system for demonstration project.
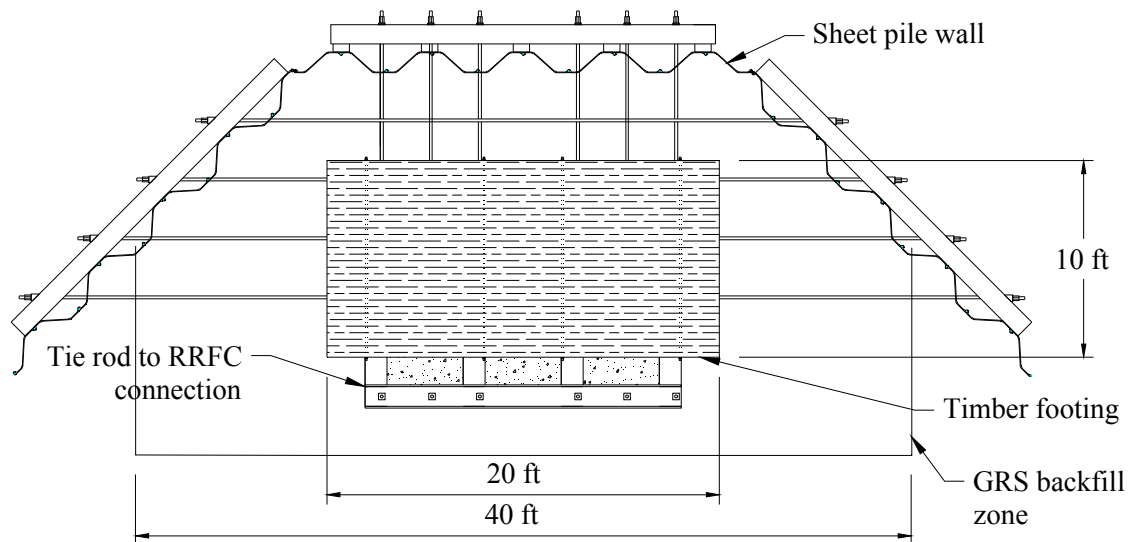
Figure 5-119. Design detail plan view of TC, Iowa sheet pile abutment and backfill retaining system for demonstration project (superstructure not shown).

Site Investigation

Field Investigation

Cone Penetrometer Testing

Two CPT soundings were performed approximately 15 ft south and north of the center of the bridge abutments on June 9, 2008. The CPT soundings were completed by GSI located in Des Moines, Iowa.

CPT 1 and CPT 2 were advanced to depths of 55.5 ft and 55.8 ft, respectively, below existing grades. Logs of the soundings, showing cone tip stress and sleeve friction, are presented in Figure 5-120. Soil behavior types determined from CPT 1 and CPT 2 are presented in Figure 5-121. As can be seen in this figure, the majority of materials present are cohesive soils underlain by a granular base with very soft material in the upper 6 ft to 20 ft of each sounding. After the soft material, the profile transitions to granular deposits that extend to approximately 37 ft below existing grades in both soundings. Fine-grained, Pre-Illinoian glacial till was present in the remaining lower portion of each sounding (approximately 18 ft to 19 ft). Presented in Figure 5-122 are the soil shear strength and SPT resistance estimates from correlations presented by Lunne, Powell, and Robertson (1997).
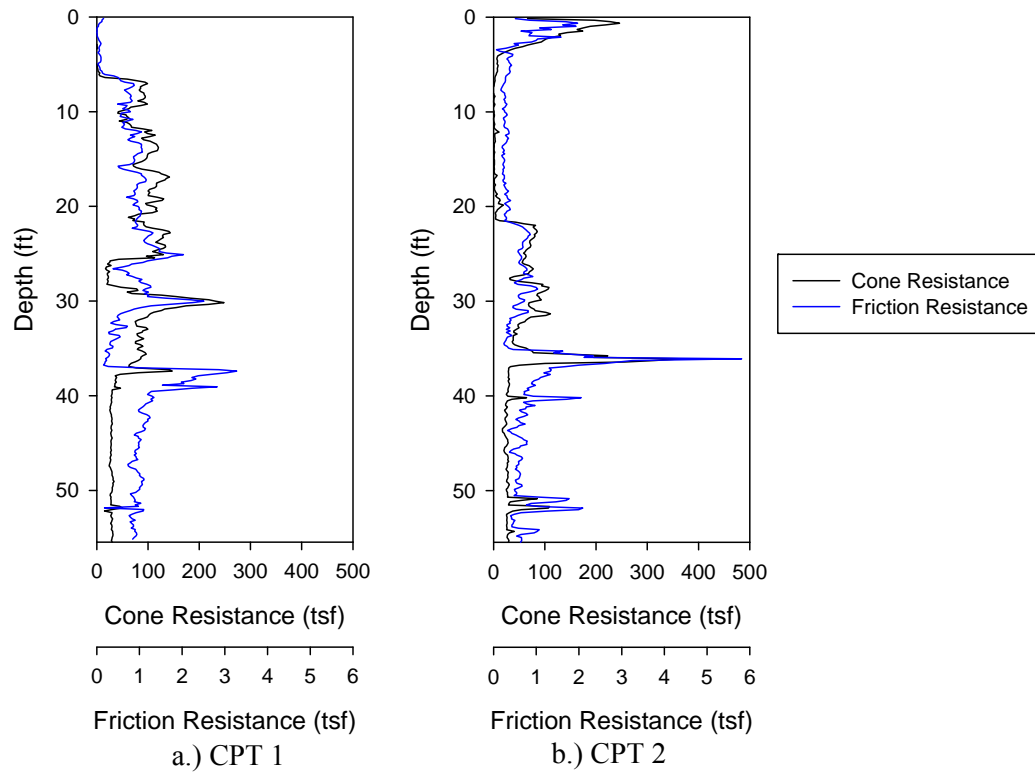
Figure 5-120. Results of CPT's showing cone tip and friction resistance.
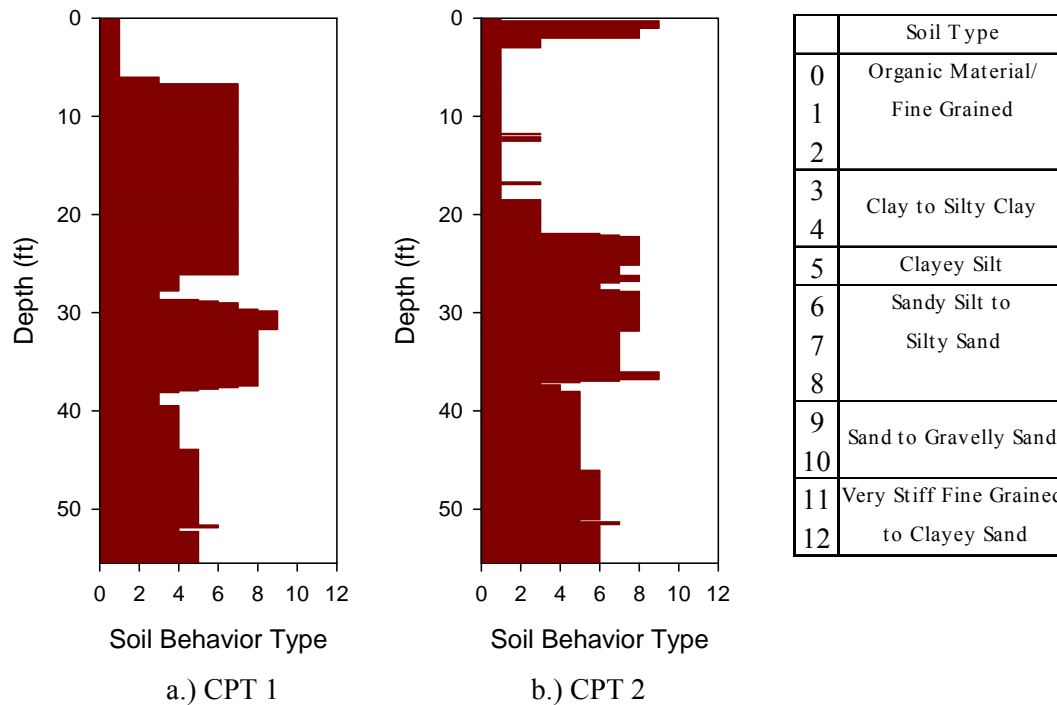
Figure 5-121. Soil behavior types determined from CPT's.
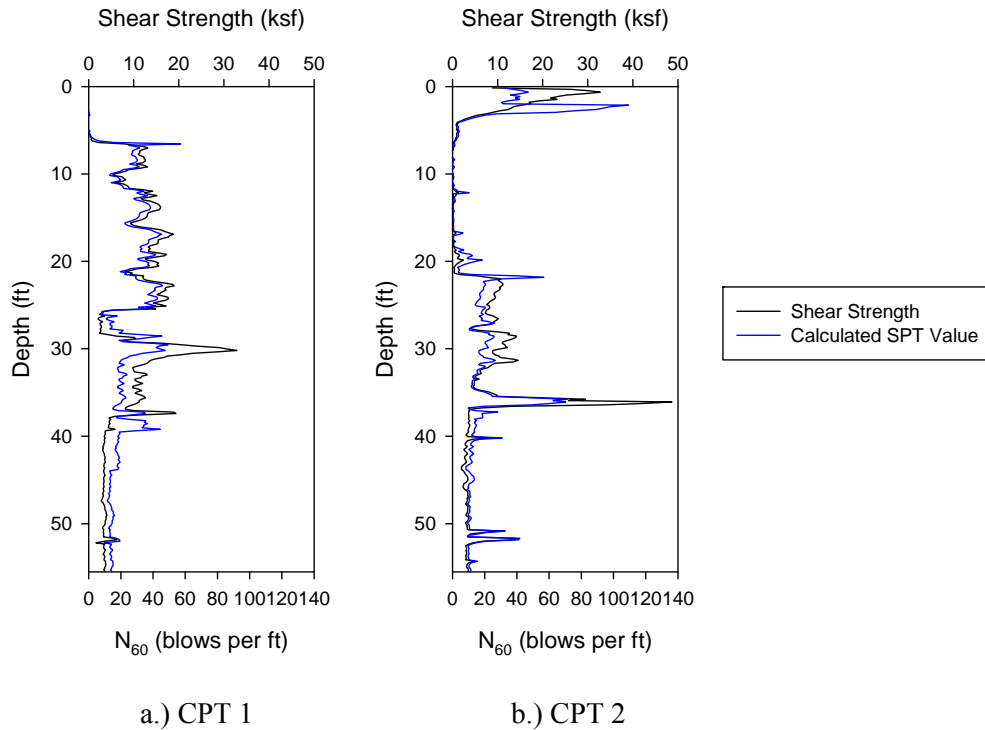
Figure 5-122. Shear strength and SPT correlations for CPT's.

Soil Borings

The two soil borings were completed by members of the ISU research team on August 1, 2008. The location of each boring as well as the location of the CPT soundings is shown in Figure 5-123; the boring logs are provided in Figure C12 and Figure C13 of Appendix C.
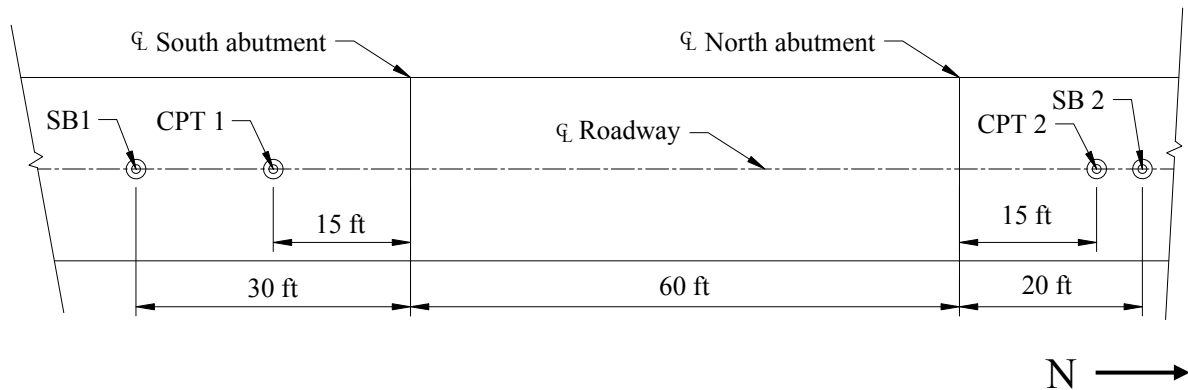
Figure 5-123. Plan view of CPT and soil boring locations for TC, Iowa demonstration project.

Laboratory Testing

Undrained shear strengths were determined by performing UU compression tests with varying confining pressures to approximate in situ conditions for each sample. As can be seen from the results presented in Table 5-33, the strength of the soil decreases significantly with increasing depth (which is also seen in the CPT soundings). Moisture content and dry densities were also determined for each of the samples and are provided in Table 5-33 as well.

The results of the Atterberg tests, the percentage of soil passing the No. 200 sieve (percent fines), and the USCS classification for select samples are presented in Table 5-34.

Table 5-33. Test results on select soil samples.

Boring	Sample Depth (in.)	Confining Pressure (psf)	Undrained Shear Strength (psf)	Moisture Content (%)	Dry Density (pcf)
SB 2	72	700	6590	29.7	94.4
SB 2	120	1100	4475	28.5	95.3
SB 2	144	1400	4270	16.7	109.3
SB 2	180	1750	2585	45.6	75.5

Table 5-34. Atterberg test and gradation results for select soil boring ranges.

Boring	Depth Range (in.)	LL (%)	PL (%)	PI (%)	Passing No. 200 (%)	Soil Type (USCS)
SB 1	36 – 42	50	20	30	98	CH
SB 1	90 – 96	40	17	23	87	CL
SB 1	108 – 156	-*	-	-	24	SM
SB 2	60 – 84	32	25	7	98	ML
SB 2	132 – 156	28	20	8	72	CL
SB 2	216 – 240	35	18	17	59	CL
SB 2	240	-	-	-	17	SM

* No data available

Void ratio and coefficient of consolidation versus pressure (with pressure on a logarithmic scale) plots were created for the three samples tested and are presented in Figure C14 through Figure C16. Preconsolidation pressures were estimated from the void ratio versus pressure plots and are given in Table 5-35.

Table 5-35. Estimated preconsolidation pressure of select samples from SB 2.

Sample depth (in.)	Preconsolidation pressure (psf)
94	1820
107	1880
179	2170

Site Conditions

Geologic Setting

The project site is located in the Iowa River floodplain. According to GSI, topography in this floodplain is essentially horizontal and is typified by surficial soils of alluvial silt and clay. Below the surficial soils, a transition to sand and gravel deposits occurs. The alluvial deposits may be underlain by cohesive glacial till or clay shale and limestone bedrock (deposited by the Pre-Illinoian or Devonian glacial advances, respectively). The surficial profile is highly variable due to construction activities associated with floodplain reclamation events in the area.

Soil Conditions

Soil boring SB 1on the south end of the bridge encountered stiff, tan and light gray silty clays for the first 8 ft. From 8 ft to the end of the boring (approximately 13 ft) tan silty sands were encountered. On the north end of the bridge in SB 2, light gray sandy gravel was encountered in the first 3 ft of soil exploration. For depths of 3 ft to 21 ft, primarily loose, light gray clayey silt was encountered. The boring was terminated at the 23 ft depth after encountering tan silty sands below the water table that could not be sampled with the Shelby tube.

Groundwater Observations

During the soil boring advancement and sampling operations, observations for free groundwater were made. Information regarding water level observations is recorded in the "stratigraphy" column on the soil boring log. Groundwater was encountered at a depth below existing grade of approximately 17.5 ft in soil boring SB 2. From the CPT soundings, the observed drop in tip stress and sleeve friction near depths of 20 ft likely coincides with the ground water surface.

Design

As previously noted, the design of the superstructure was performed by the TC Engineer's Office; the design consisted of two 89 ft long RRFC's (bolted together) that are set on a 20 ft x 10 ft x 10 in. timber spread footing. ISU designed a GRS sheet pile abutment and backfill retaining system that provided a design bearing capacity of 2500 psf for the spread footing of the superstructure.

The GRS system (7 layers of Tensar® BX1200 biaxial geogrid placed as shown in Figure C1 and Figure C2) was retained by a sheet pile wall with an anchor system that provided anchorage without a deadman by developing a compressive force in the RRFC superstructure. Detailed design plans of the GRS sheet pile abutment and backfill retaining system are provided in Figure C1 through Figure C5.

The GRS sheet pile abutment and backfill retaining system was designed for HL-93 loading (AASHTO Section 3.6.1.2, 1998) of the superstructure using the critical load factors and load combinations presented in AASHTO (1998) Section 3.4. Detailed design calculations are provided in Appendix C.

GRS Sheet Pile Abutment and Backfill Retaining System Design

The sheet pile wall and anchor system were designed to resist all loads (including bridge and backfill surcharge loading) but considered the contribution of the GRS system to prevent lateral loads being applied to the abutment over the extent of the GRS system. The design profile for the sheet pile wall is shown in Figure C19; it was analyzed as a simply supported beam with pinned supports at the location of the anchors.

Loads transferred through the abutment cap to the spread footing were assumed to distribute evenly across the surface area. Dead loads were assumed to distribute over the entire length of the footing while the live loads were distributed over a 10 ft long strip. The spread footing was designed to be 6 ft wide to reduce the bearing pressure to a maximum factored load of 3500 psf. Surcharge loads were applied as lateral earth pressures to the sheet pile wall according to AASHTO (1998) Section 3.11.6.1. The sheet pile section selected to resist design earth pressure loads was the PZC 13. For stability of the sheet pile wall, the required depth of penetration (accounting for a 10 ft depth of scour) was 40 ft.

The controlling factor in the design of the sheet pile section was the location of the bottom anchor relative to the top of the wall. For full resistance to HL-93 loading, the anchor must be located 20 ft below the sheet pile wall; this may not be feasible due to constructability issues associated with the stream elevation. After performing several analyses of different anchor locations as well as reducing the factor of safety on the loads due to the retained soil and live load surcharge, it was determined that the minimum specified bottom anchor depth would be 18 ft below the top of the sheet pile wall. Monitoring of wall stresses and movements during the bridge live load test (as well as long-term monitoring) will be performed to ensure the bridge abutment design is satisfactory.

The original design for the project in TC was desired to be an axially-loaded combination sheet pile wall (see Figure 3-4 for an example). Due to the poor soil conditions and relatively large abutment height required from the profile of the site, the use of axially-loaded sheet piling would have required sections over 70 ft long; this alternative was not feasible for the project site. Other alternatives were also investigated before the final design was selected. One design utilized a system similar to the BC project (a GRS system with reinforced concrete deadman anchor) but required 50 ft long PZ 35 sections and thus it was not economical. A second alternative (depicted in Figure 5-124a) utilized a series of struts to provide lateral resistance to the wall. The bottom strut, which was to span the entire stream (approximately 60 ft), would have consisted of steel beams spliced together and mechanically attached to the sheet pile wall. In the design of this system, it was discovered that the location of the bottom strut had a significant influence on the design bending moment in the sheet pile wall; variation in maximum bending moments with the distance of the bottom strut from the top of the sheet pile wall is shown in Figure 5-125. The top of the sheet pile wall was to be braced with a small strut bolted to the RRFC superstructure. Due to the constructability issues inherent with performing extensive work in the stream, as well as debris collection and additional scour induced by the in-stream strut, this alternative was not selected. Another alternative considered for the design utilized a combination wall (50 ft long) and a reinforced concrete deadman (see Figure 5-124b). Although a final design was completed for this alternative (full design plan sheets are presented in Figure C6 through Figure C10) it was not selected due to the cost and construction difficulties associated with the combination W-shape and sheet pile wall design.
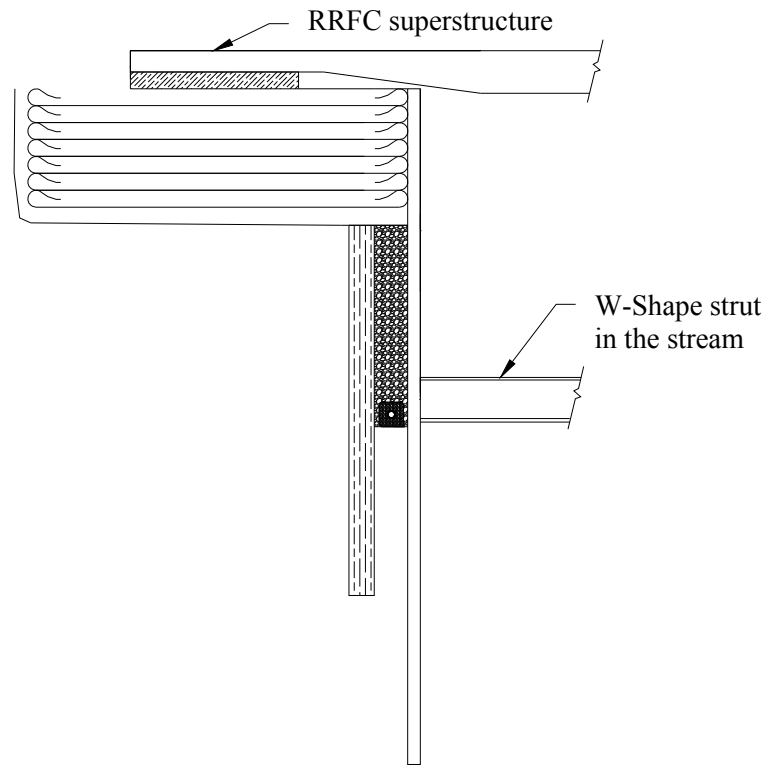
a.) Stream strut alternative
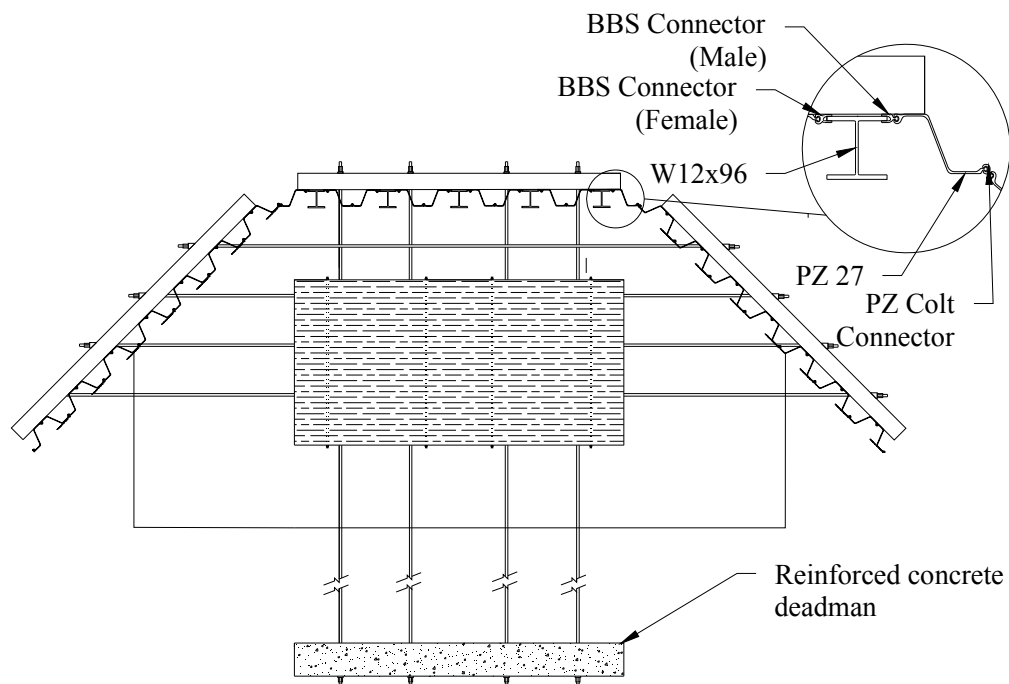
b.) Combination wall alternative

Figure 5-124. Design alternatives for demonstration project in TC, Iowa.
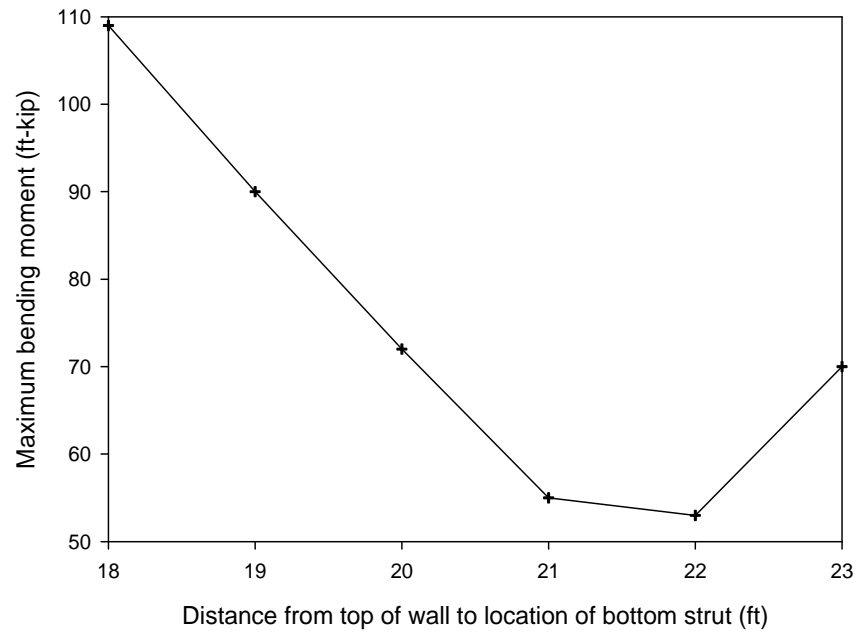
Figure 5-125. Variation of design bending moment with distance from top of sheet pile wall to bottom strut for the design alternative shown in Figure 5-124a.

CHAPTER 6. SUMMARY AND CONCLUSIONS

Iowa Highway Research Board Project TR-568, initiated in January 2007, has investigated the use of steel sheet piling as an alternative foundation component for LVR bridges through a review of existing research as well as the development of designs, documentation of construction, and analysis of live load test data for three demonstration projects utilizing different experimental abutment systems. As of September 2010, bridge construction and analysis of live load test data for the demonstration projects in Black Hawk County and Boone County were completed. Construction of the demonstration project in Tama County was completed with live load testing scheduled for October 2010.

The demonstration project in Black Hawk County, Iowa investigated the viability of axially-loaded sheet pile bridge abutments.   The project involved construction of a 40 ft, single-span bridge utilizing axially-loaded steel sheet piling as the primary foundation component. An instrumentation system (consisting of strain gages, deflection transducers, earth pressure cells, and piezometers) was installed on the bridge for obtaining live load test data as well as long term performance data. Live load testing of the bridge structure was performed on November 3, 2008 by placing two loaded trucks (approximately 24 ton each) at various locations on the bridge and recording data. Maximum axial stresses occurring in the piles were approximately 0.5 ksi and were comparable to estimates made by analysis for a load distribution width of 10 ft. Flexural stresses, in general, were significantly less than those estimated by analysis and maximum values were approximately 0.2 ksi. Earth pressures recorded during live load testing (with maxima of approximately 100 psf) were also significantly lower than earth pressures estimated by analysis. These results suggest the method of analysis for lateral earth pressures applied to the sheet pile wall was conservative. Long-term monitoring of the bridge from November 2008 through February 2009 was also performed; the datalogging system was damaged by flooding in March 2009 and subsequent long-term monitoring was terminated. Variations in earth pressure over time were observed with the largest variations in earth pressure occurring behind the abutment cap. The earth pressures experienced cycles that varied in magnitude from 50 psf to 1500 psf, suggesting long-term loading due to freeze/thaw cycles of the soil and the thermal deformation of the superstructure elements may be the critical factors in the design of sheet pile abutment and backfill retaining systems rather than vehicular live loads. Through the construction and structural monitoring of the demonstration project, axially-loaded steel sheet piling have been shown to be a feasible alternative for bridge abutments with site conditions similar to

Black Hawk County (i.e., shallow bedrock). Although the project required approximately 10 weeks for construction, the construction time could be significantly shortened if critical to the project timeline. According to the Black Hawk County Engineer's Office, the total cost of the project (including labor and materials) was $151,230. The Black Hawk County Engineer's Office believes that a significant portion of the cost can be attributed to the labor and equipment time involved in developing a new method of construction for this type of bridge as well as the many associated equipment breakdowns. Future projects utilizing a similar design and construction method with comparable site conditions could be performed at a reduced cost.

The demonstration project in Boone County was designed using a geosynthetically reinforced soil backfill with a steel sheet pile backfill retention system for the bridge abutments. The bridge superstructure, a 100 ft long three span J30C-87 standard continuous concrete slab, was supported by reinforced concrete spread footings at each end bearing on the geosynthetically reinforced backfill. Live load testing was performed on November 13, 2009. Analyses of the live load test results concluded that the design methods used, in general, were significantly conservative when compared to the stresses and deflections experienced due to vehicular traffic. Maximum flexural stress experienced in the sheet pile elements were 0.08 ksi (3% of the expected value by analysis). Vertical and horizontal earth pressures in the backfill (with maxima of 410 psf and 50 psf, respectively) were also lower than expected and were 73% and 28% of estimated values, respectively. The maximum lateral earth pressure experienced at the face of the sheet pile wall was 20 psf and was 10% of the value estimated without including the geosynthetic reinforcement in the analysis; these results indicate a significant contribution of the geosynthetic reinforcement in reducing lateral earth pressures on the wall. The anchorage system, which increased the overall cost of the project significantly due to extra construction time, special materials ($70,000 approximately), etc., was determined to be resisting negligible loads during live load testing (4% of expected load); this suggests there are potential cost savings with a reduced (or eliminated) permanent anchorage system. The stresses due to Load 1 on the anchorage system, however, were significant and thus the system (or some alternative method of providing lateral restraint) was necessary for construction of the bridge superstructure. Stresses in the wingwall tie rod (from live load only and Load 1) were negligible and thus provide potential for reduced material costs. Through the construction and structural monitoring of the BC demonstration bridge, geosynthetically reinforced earth steel sheet pile bridge abutment systems have been shown to be a potential alternative for LVR bridge abutments. Several improvements and further research, however, are necessary before sheet pile

bridge abutment systems similar to the BC project are economically feasible. The total cost of the construction of the BC demonstration project was approximately $591,000, with a typical 100 ft, three-span county road J30C-87 standard bridge (with steel H-pile abutments) expected to cost $397,000; total construction time required approximately 18 weeks.

The Tama County demonstration project utilized a geosynthetically reinforced sheet pile abutment system similar to Boone County with the exception that, instead of using a large reinforced concrete deadman for anchoring the sheet pile wall, the tie rods were anchored to the superstructure (two 89 ft railroad flatcars bolted together). The railroad flatcars are supported by 10 ft by 20 ft spread footings constructed with several 10 in. thick timbers; each spread footing was designed to bear on the geosynthetically reinforced backfill. The project in Tama County completed construction in August 2010 with subsequent live load testing scheduled in October 2010.

CHAPTER 7. RECOMMENDATIONS

Several improvements for sheet pile bridge abutment systems were determined during the construction and load testing of the demonstration projects. It is recommended that pile lengths determined from site investigation results be ordered a minimum of 5 ft longer than expected as splicing of sheet pile sections will result in greater costs (associated with materials and construction delays) if the subsurface profile is more variable than predicted.

Although the tie rod stresses were shown to be negligible once the superstructure is constructed, the use of some form of lateral restraint is needed to resist the loads developed during abutment construction. Tie rods are one alternative and will also provide overall system stability during large lateral loading events that may occur. If tie rods are used, they must be attached to a relatively stiff deadman to provide adequate anchorage to the wall; the use of a driven pile as a deadman is not recommended as it is too flexible to develop sufficient resistance without excessive movement of the wall.   Due to the high costs of deadman anchored tie rods, temporary bracing systems should be investigated as an alternative method of lateral restraint during construction. Additional research is recommended to investigate the development of an economical anchorage system. Recommendations for such research included testing of a full-scale, field constructed model with no anchorage system (or temporary construction bracing) that could be tested to determine ultimate strength and behavior under load of a GRS sheet pile bridge abutment system; the presence of an anchorage system significantly alters the behavior of sheet pile wall systems.

When driving piles into bedrock, the use of a forged pile driving cap for sheet piling is another recommendation as significant time and labor was spent repairing the custom made, welded cap used by BHC. The width of guide racks for setting and driving of sheet pile sections should be minimized to reduce the potential for misalignment; a width of 0.25 in. to 0.5 in. greater than the width of a sheet pile section is recommended.

Instrumentation of sheet pile sections should be protected by welding steel angles on the inside of the sheet pile flanges to minimize the influence on flexural stress (by minimizing the increase in flexural stiffness of the pile) as well as improve constructability of the sheet pile wall. Redundancy of instrumentation is important for all critical information desired; damage to some instrumentation should be expected during construction.

For all projects utilizing steel sheet piling, the use of PZC sections is recommended. PZC sections have a greater flexural resistance and require less steel per ft of wall compared to traditional PZ sections.

For axially-loaded sheet pile structures, the use of a wall sawing service for the trimming to grade of the sheet pile wall is recommended as it saves construction time and is economical versus torch cutting and grinding.

Although the bridge test results showed significantly lower stresses and deflections than expected, further testing is recommended to determine the nature of earth pressure development behind sheet pile abutments. Development of a more accurate analysis method for sheet pile wingwalls has the potential for significant cost savings through the reduction in sheet pile resistance as well as anchorage systems required.

Due to the inherent potential for settlement of spread footings, utilization of a GRS sheet pile bridge abutment system in multiple span (statically indeterminate) structures must include strict requirements for compaction and reduction of voids in the backfill material (such as the flooding technique used for the abutments in the BC bridge); use in simple-span bridges is ideal as significant differential abutment settlements are not detrimental to the superstructure.

REFERENCES

Abu-Hejleh, N., Hearn, G., McMullen, M., and Zornberg, J. (2001a). "Design and Construction Guidelines for MSE Walls with Independent Full-height Facing Panels." *Report No. CDOT-DTD-R-2001-05,* Colorado Department of Transportation.

Abu-Hejleh, N., McMullen, M., Outcalt, S., and Zornberg, J. (2001b). "Results and Recommendations of Forensic Investigation of Three Full-Scale GRS Abutment and Piers in Denver, Colorado." *Report No. CDOT-DTD-R-2001-6*, Colorado Department of Transportation.

Abu-Hejleh, N., McMullen, M., Outcalt, S., Wang, T., and Zornberg, J. (2001c). "Performance of Geosynthetic-Reinforced Walls Supporting the Founders/Meadows Bridge and Approaching Roadway Structures, Report 2: Assessment of the Performance and Design of the Front GRS Walls and Recommendations for Future GRS Abutments." *Report No. CDOT-DTD-R-2001-12*, Colorado Department of Transportation.

Abu-Hejleh, N., Hanneman, D., Ksouri, I., Wang, T., and White, D. J. (2006). "Flowfill and MSE Bridge Approaches: Performance, Cost, and Recommendations for Improvements." *Report No. CDOT-DTD-R-2006-2,* Colorado Department of Transportation.

American Association of State Highway and Transportation Officials. (1998). "Load and Resistance Factor Design Bridge Design Specifications." 2nd ed.

American Institute of Steel Construction, Inc. (2005). "Steel Construction Manual." USA. 13th ed.

American Society of Civil Engineers. (1996). "Design of Sheet Pile Walls." *Technical Engineering and Design Guides as Adapted from the US Army Corps of Engineers*, no. 15.

Askar, Y. I. (1988). "Safety Rating of Steel Sheet Pile Structures (Thesis)." Ames: Iowa State University.

ASTM Standard D421. (2007). "Standard Practice for Dry Preparation of Soil Samples for Particle-Size Analysis and Determination of Soil Constants." *ASTM International*. West Conshohocken, PA, 2007, DOI: 10.1520/D421-85R07, www.astm.org.

ASTM Standard D422. (2007). "Standard Test Method for Particle-Size Analysis of Soils." *ASTM International*. West Conshohocken, PA, 2007, DOI: 10.1520/D422-63R07, www.astm.org.

ASTM Standard D1452. (2009). "Standard Practice for Soil Exploration and Sampling by Auger Borings." *ASTM International*. West Conshohocken, PA, 2009, DOI: 10.1520/D1452-09, www.astm.org.

ASTM Standard D1587. (2008). "Standard for Thin-Walled Tube Sampling of Soils for Geotechnical Purposes." *ASTM International*. West Conshohocken, PA, 2008, DOI: 10.1520/D1587-08, www.astm.org.

ASTM Standard D2166. (2006). "Standard Test Method for Unconfined Compressive Strength of Cohesive Soil." *ASTM International*. West Conshohocken, PA, 2006, DOI: 10.1520/D2166-06, www.astm.org.

ASTM Standard D2216. (2005). "Standard Test Methods for Laboratory Determination of Water (Moisture) Content of Soil and Rock by Mass." *ASTM International*. West Conshohocken, PA, 2005, DOI: 10.1520/D2216-05, www.astm.org.

ASTM Standard D2435. (2004). "Standard Test Methods for One-Dimensional Consolidation Properties of Soils Using Incremental Loading." *ASTM International*. West Conshohocken, PA, 2004, DOI: 10.1520/D2435-04, www.astm.org.

ASTM Standard D2850. (2007). "Standard Test Methods for Unconsolidated-Undrained Triaxial Compression Test on Cohesive Soils." *ASTM International*. West Conshohocken, PA, 2007, DOI: 10.1520/D2850-03AR07, www.astm.org.

ASTM Standard D4318. (2005). "Standard Test Methods for Liquid Limit, Plastic Limit, and Plasticity Index of Soils." *ASTM International*. West Conshohocken, PA, 2005, DOI: 10.1520/D4318-05, www.astm.org.

ASTM Standard D5778. (2007). "Standard Test Method for Electronic Friction Cone and Piezocone Penetration Testing of Soils." *ASTM International*. West Conshohocken, PA, 2007, DOI: 10.1520/D5778-07, www.astm.org.

ASTM Standard D6528. (2007). "Standard Test Method for Consolidated Undrained Direct Simple Shear Testing of Cohesive Soils." *ASTM International*. West Conshohocken, PA, 2007, DOI: 10.1520/D6528-07, www.astm.org.

ASTM Standard D6951. (2003). "Standard Test Method for Use of Dynamic Cone Penetrometer in Shallow Pavement Applications." *ASTM International*. West Conshohocken, PA, 2003, DOI: 10.1520/D6951-03, www.astm.org.

ASTM Standard D698. (2000). "Standard Test Methods for Laboratory Compaction Characteristics of Soil Using Standard Effort." *ASTM International*. West Conshohocken, PA, 2000, DOI: 10.1520/D698-00AE1, www.astm.org.

ASTM Standard E2583. (2007). "Standard Test Methods for Measuring Deflections with a Light Weight Deflectometer." *ASTM International*. West Conshohocken, PA, 2007, DOI: 10.1520/E2583-07, www.astm.org.

Bigelow, J., Bowers, R., Klaiber, F. W., Phares, B., and Wipf, T. J. (2009). "Precast Concrete Elements for Accelerated Bridge Construction: Laboratory Testing, Field Testing, Evaluation of a Precast Concrete Bridge, Madison County Bridge." *Report No.TR-561,* Iowa Highway Research Board. Ames, IA.

Braun, K., Nottingham, D., and Thieman, D. (2002). "Design, Construction, and Performance of Open Cell Sheet Pile Bridge Abutments." *Cold Regions Engineering: Cold Regions Impacts on Transportation and Infrastructure (Proceedings of the 11th International Conference), 11,* 436-447.

Carle, R. J. and Whitaker, S. S. (1989). "Sheet Piling Bridge Abutments." *Realizing DFI's Potential, a Parallel to Baltimore's Renaissance*, 25.

Coduto, Donald P. (2001). "Foundation Design: Principles and Practices." 2nd edition.

Chung, H. I., Kim, B., Oh, I. K., and Yoo, J. (2004). "Application of Steel Sheet Pile Embedded Retaining Wall as a Bridge Abutment." *Geotechnical Engineering for Transportation Projects, 2,* 2186-2194.

Das, Braja M. (2006). "Principles of Foundation Engineering." 6th ed.

Davis, S. R. and Richardson, E. V. (2001). "Evaluating Scour at Bridges." *Hydraulic Engineering Circular No. 18.* 4th ed.

Dondelinger, M. and Sommerfield, W. J. (1986). "The World in Steel Sheet Piling." *Proceedings of the First International Conference on Piling and Deep Foundations*, 636, 52-63.

Duncan, J. M., Seed, R. B., Sehn, A. L., and Williams, G. W. (1991). "Estimation Earth Pressures due to Compaction." *Journal of Geotechnical Engineering, American Society of Civil Engineers.* Vol. 117, No. 12, 1833-1847.

Dutta, P. K. and Vaidya, U. (2003). "A Study of the Long-Term Applications of Vinyl Sheet Piles." *Cold Regions Research and Engineering Laboratory*. Hanover, NH.

Engle, R., Masada, T., and Sargand, S. M. (1999). "Spread Footing for Highway Bridge Applications." *Journal of Geotechnical and Geoenvironmental Engineering.* Vol. 125, No. 5, 373-382.

Federal Highway Administration. (2008). *National Bridge Inventory: Deficient Bridges by State and Highway System.* Office of Bridge Technology. Retrieved June 12th, 2009, from http://www.fhwa.dot.gov/bridge/deficient.cfm

Geokon, Incorporated. (2006). "Geotechnical Instrumentation (Product Guide)." Lebanon, NH.

Gilman, J. F., Nottingham, T. S., & Pierce, D. M. (2001). "Open Cell Wharf Structures –Applications from Coast to Coast." *Proceedings of Ports 2001, American Society of Civil Engineers.*

Greimann, L.F. (1987). "Pile Design and Tests for Integral Abutment Bridges: Final Report." *Iowa State University. Engineering Research Institute.* Ames, Iowa.

Iowa Statewide Urban Design and Specifications. (2009). Chapter 6E-1: Subgrade Design and Construction. *Design Manual.*

Kort, D. A. (2002). "Steel Sheet Pile Walls in Soft Soil." Netherlands: DUP Science.

Lunne, T., Powell, J. J. M., and Robertson, P. K. (1997). "Cone Penetration Testing in Geotechnical Practice." New York, NY: Routledge.

McShane, G. (1991). "Steel Sheet Piling used in the combined role of Bearing Piles and Earth Retaining Members." *Proceedings of the 4th International Deep Foundations Institute Conference on Piling and Deep Foundations*, Stresa, Italy, 415-420.

North American Steel Sheet Piling Association. (2005). "North American Steel Sheet Piling Association Best Practices Sheet Piling Installation Guide." USA.

Robertson, P. K. (1989). "Soil Classification using the Cone Penetration Test." *Department of Civil Engineering, The University of Alberta.* Edmonton, Alta., Canada.

QCONBridge. (2005). "Live Load Analysis Program for AASHTO LRFD Bridge Design Specification HL93 Live Load Model." *Washington State Department of Transportation.* Version 1.3. May 11, 2005.

STAAD. (2008). "Structural Analysis and Design Software." *Bentley Systems, Incorporated.* STAAD.Pro Version V8i. Copyright 2008.

Steel Construction Institute. (1998). "Design Guide for Steel Sheet Pile Bridge Abutments." United Kingdom.

United States Steel. (1974). "Steel Sheet Piling Design Manual." USA.

APPENDIX A: BLACK HAWK COUNTY

EXPERIMENTAL BRIDGE 1
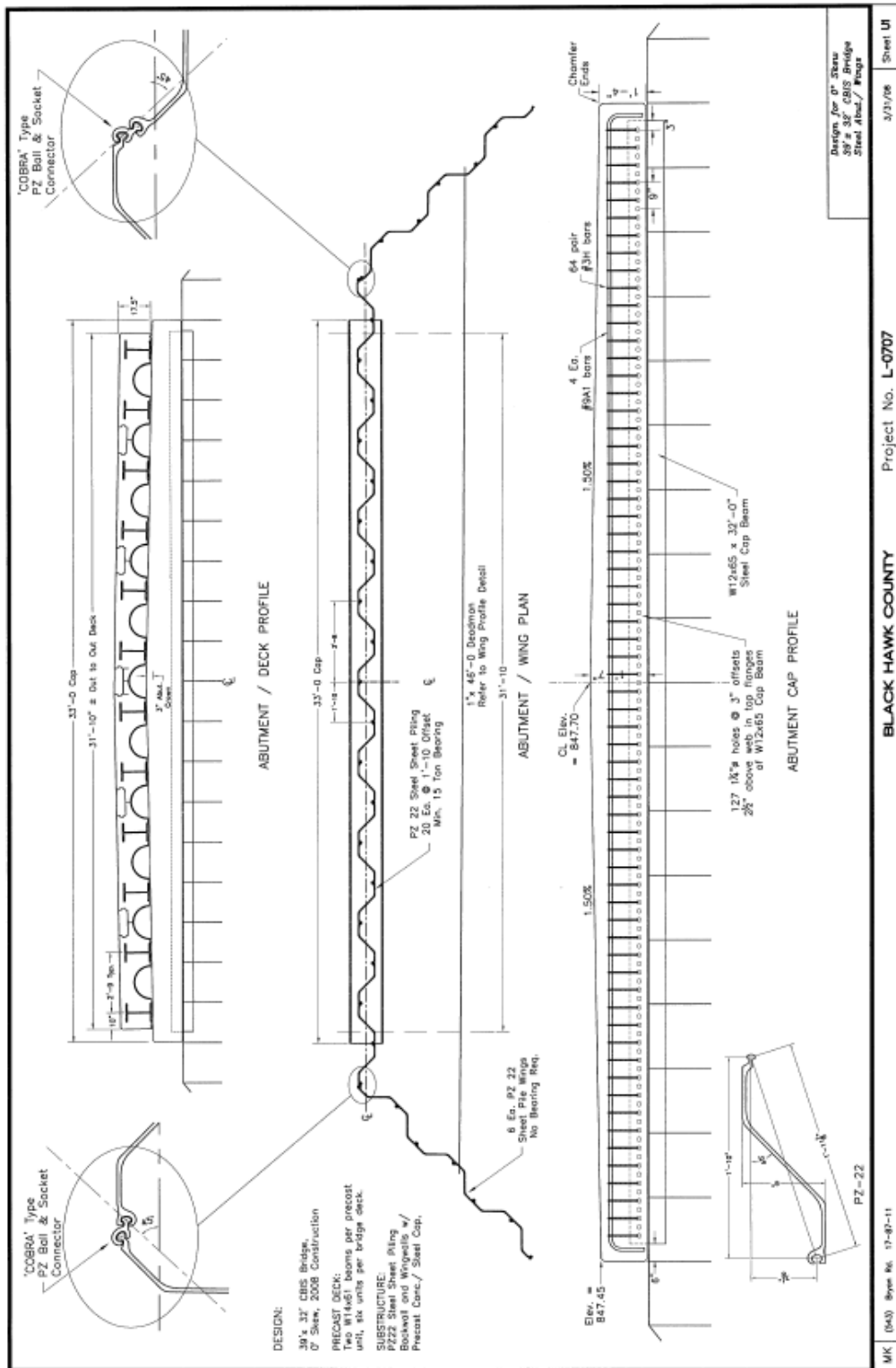
Figure A1. Plan and section views of sheet pile abutment and backfill retaining system for demonstration project in BHC, Iowa.
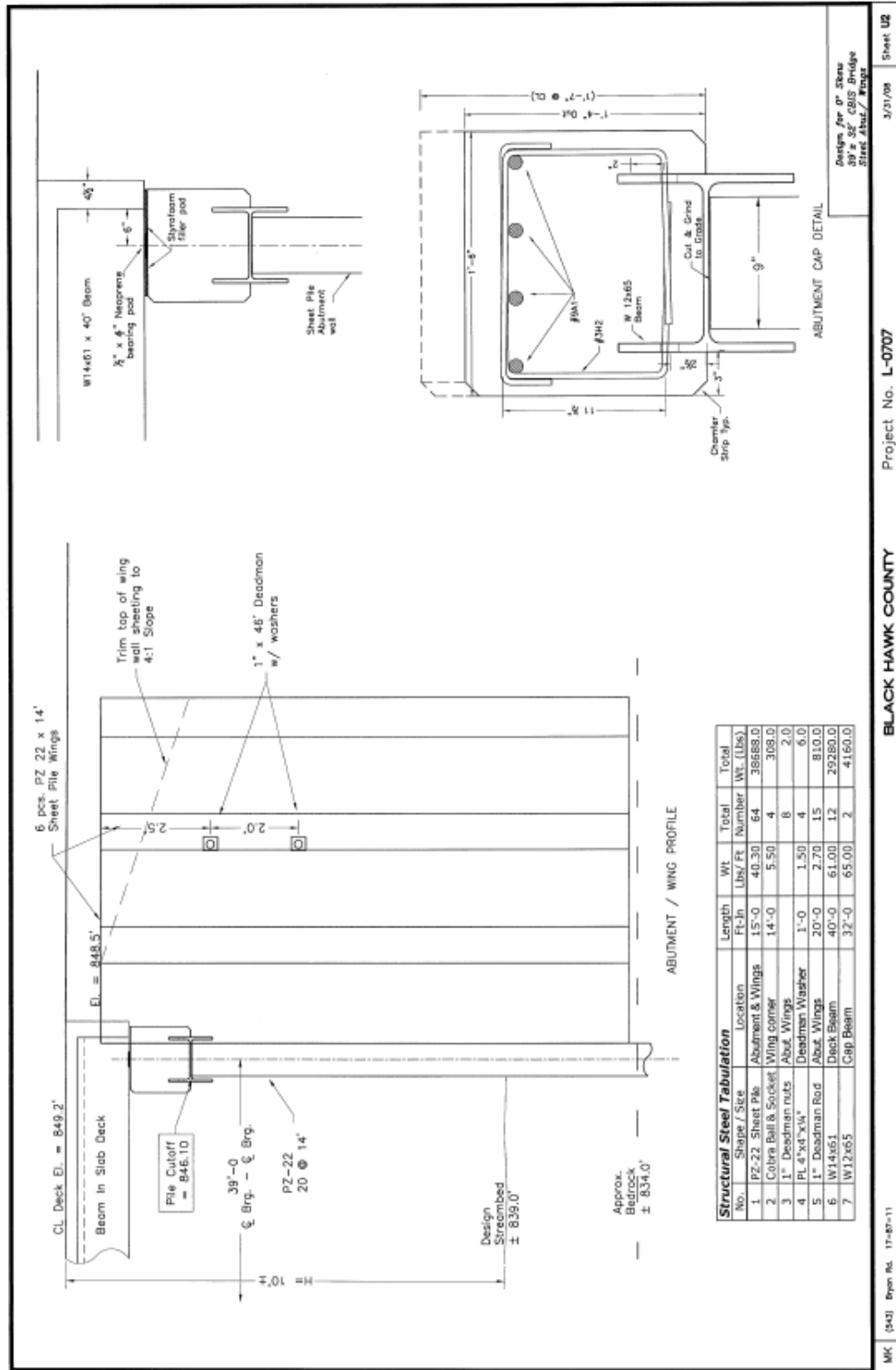
Figure A2. Abutment profile and cap detail of sheet pile abutment and backfill retaining system for demonstration project in BHC, Iowa.
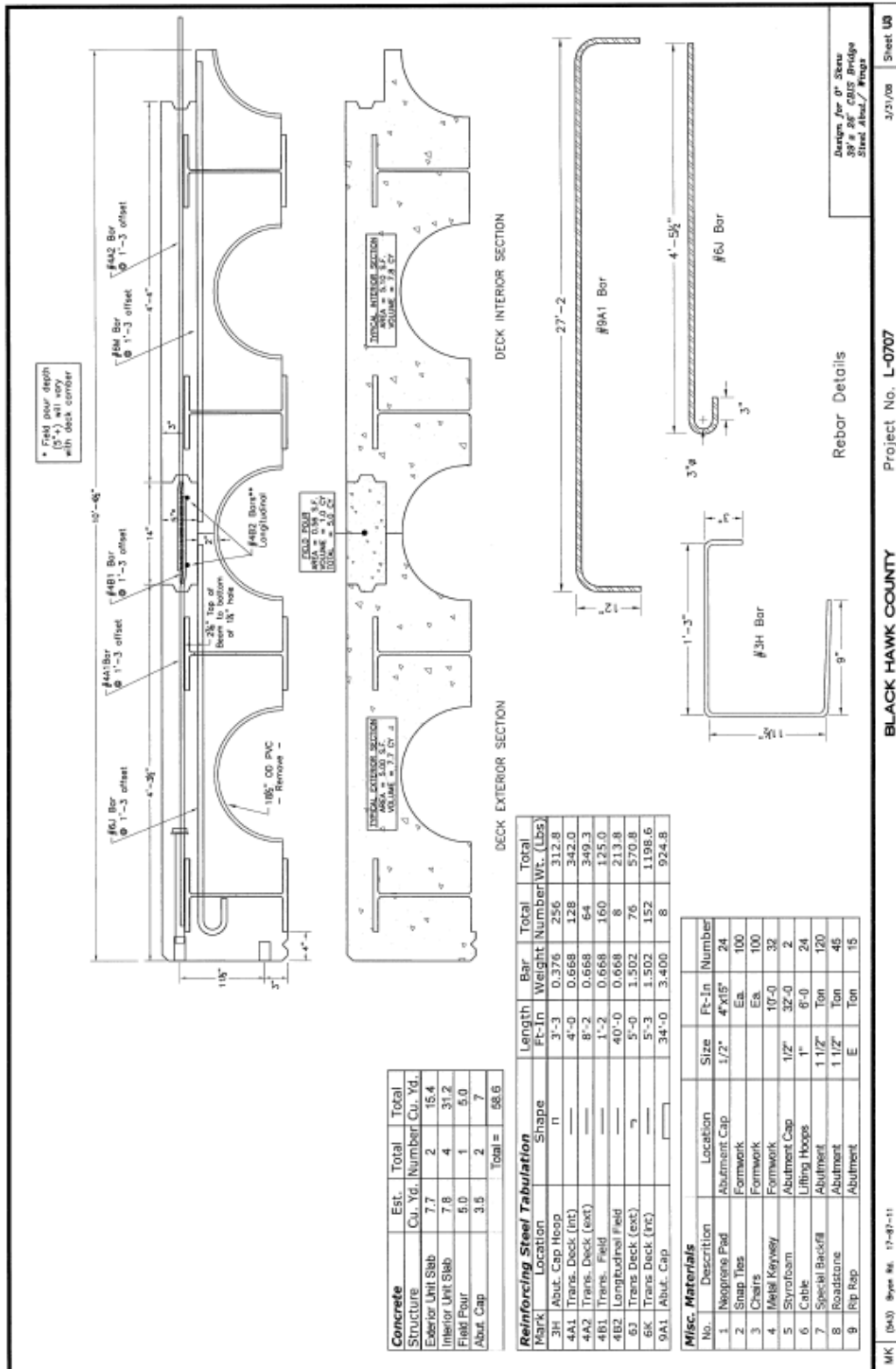
Figure A3. Section view and details of deck elements for demonstration project in BHC, Iowa.
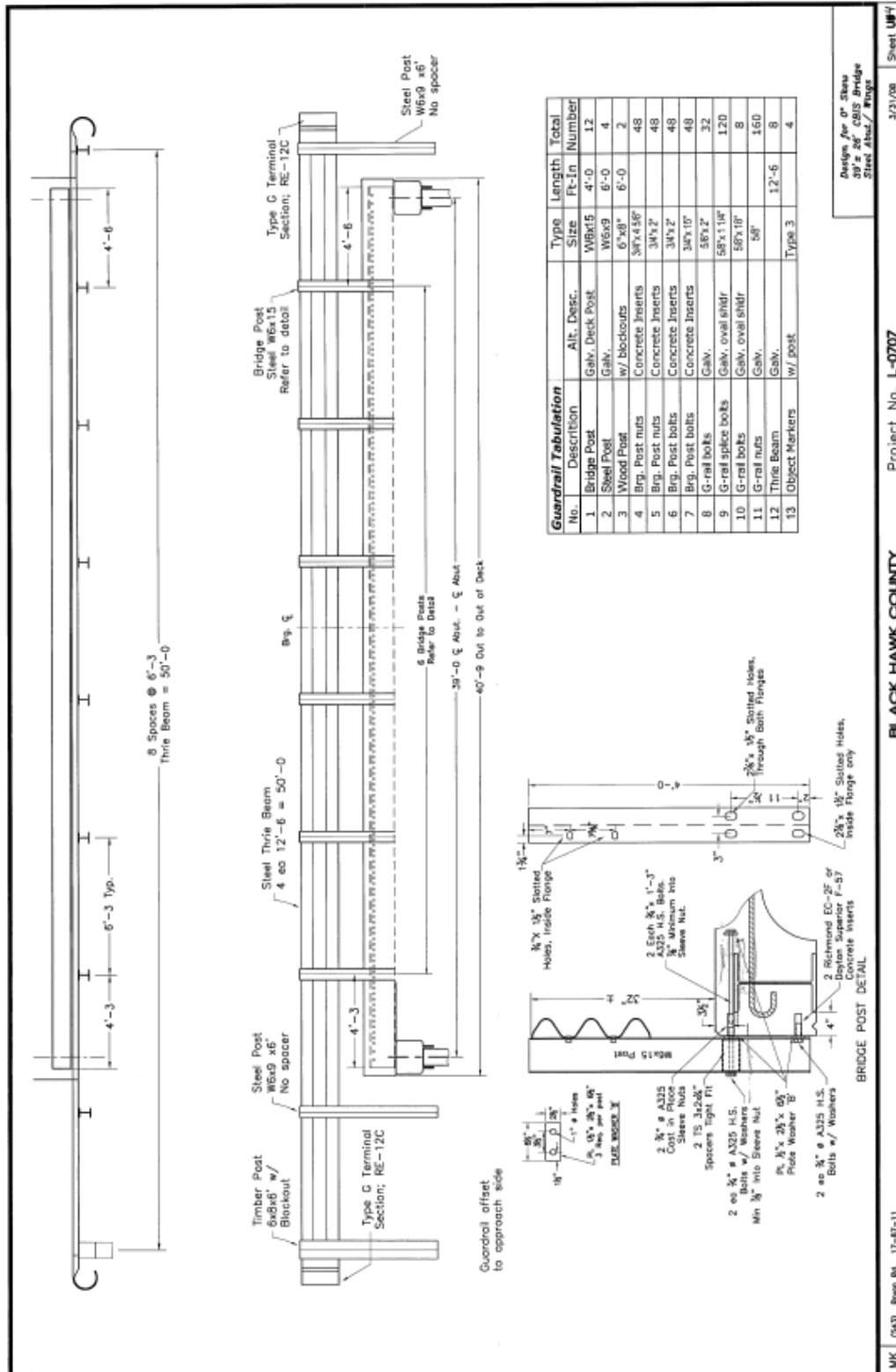
Figure A4. Guardrail details for demonstration project in BHC, Iowa.
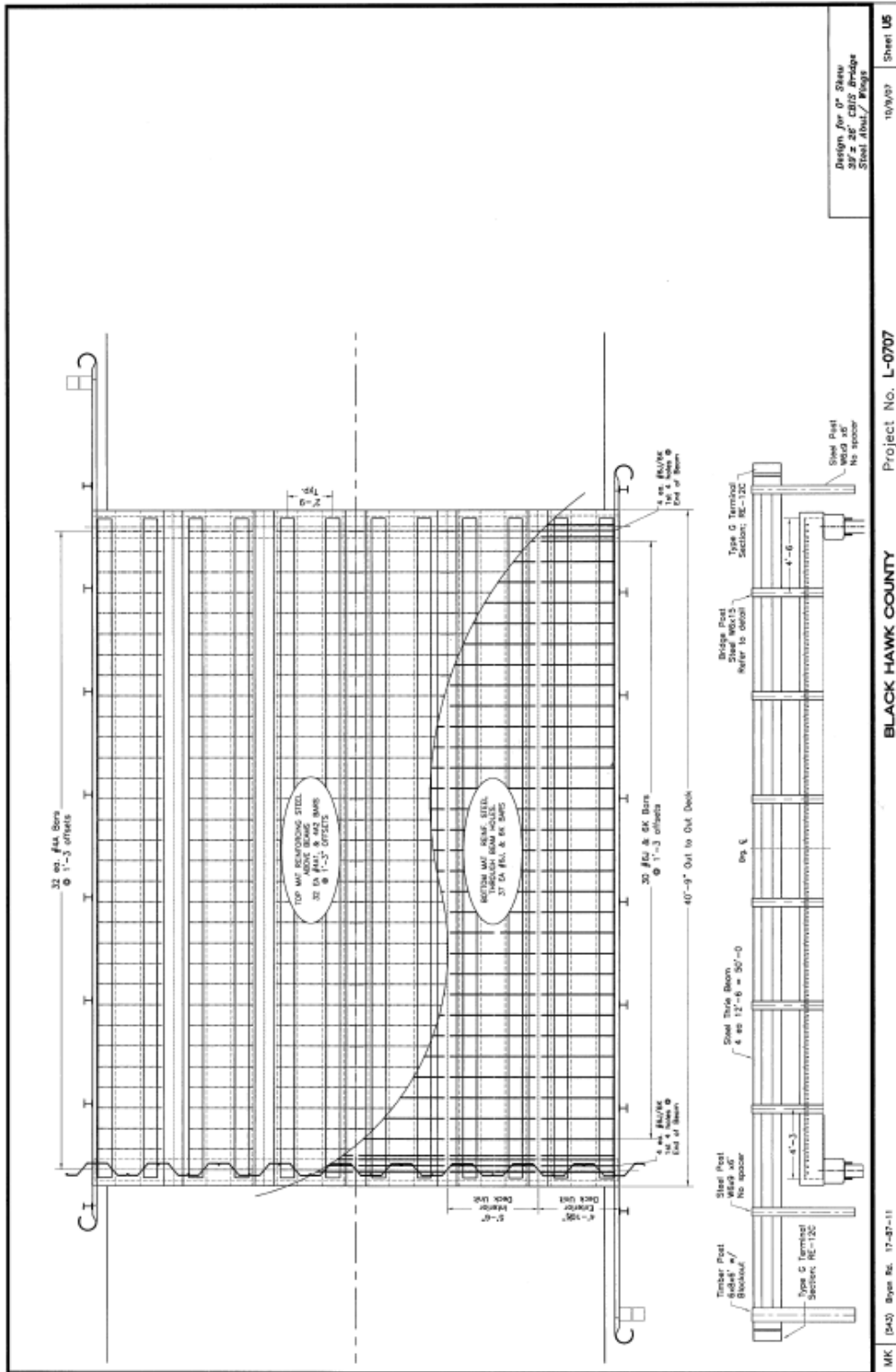
Figure A5. Plan view of reinforcement details of deck elements for demonstration project in BHC, Iowa.

Design Calculations

To design the sheet pile member, the loads on the element must be determined given the design profile below:
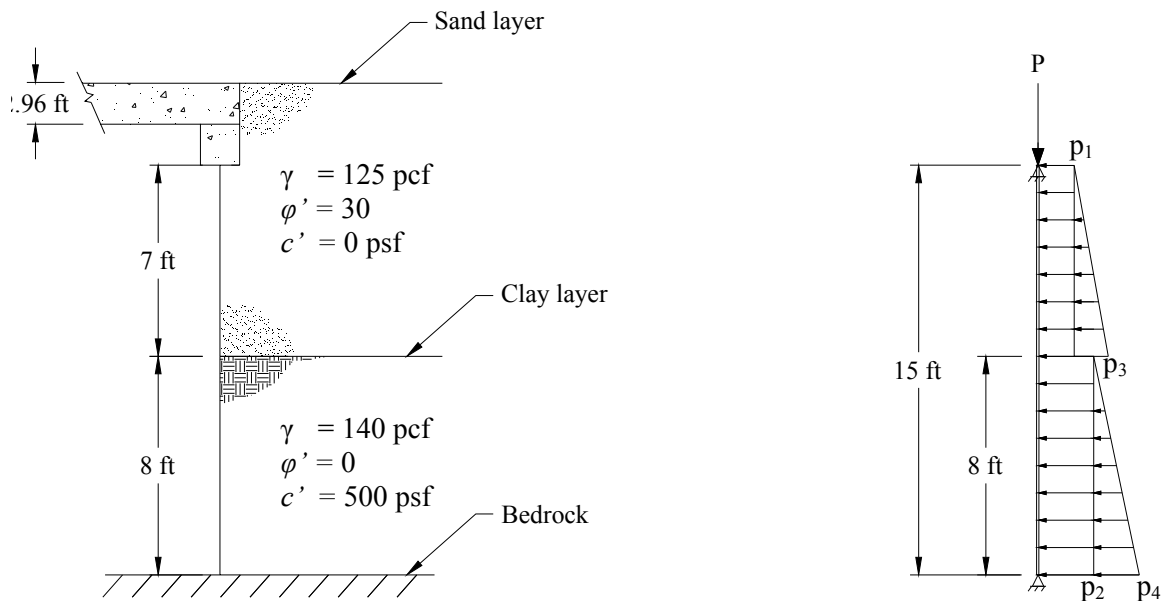
Load Estimation

<u>Lateral Earth Pressure Loads</u>

First, calculate the coefficient of lateral earth pressure, K_o, for both soil layers:

$$K_o = 1 - \sin \varphi'$$

$$K_{o1} = 1 - \sin 30° = 0.50 \text{ (sand layer)}$$

$$K_{o2} = 1 - \sin 0° = 1.0 \text{ (clay layer)}$$

Determine factored loads p_1 through p_4:

1. Pressure from soil surcharge (1.5 factor) above wall and live load surcharge (1.75 factor)
(continued)

$$p_1 = 1.50 * \gamma * z * K_{o1} + 1.75 * \text{LL surcharge}$$

$$\text{LL surcharge} = K_{o1} * \gamma * h_{eq} \qquad \text{(see Section 3.11.6.4-1, AASHTO, 1998)}$$

where $h_{eq} = 2.4$ ft (interpolated for abutment height)

$$p_1 = 1.50 * 0.125\text{kcf} * 2.96\text{ft} * 0.50 + 1.75 * 0.50 * 0.125\text{kcf} * 2.4\text{ft} = 0.540 \text{ ksf}$$

2. Surcharge in clay layer

$$p_2 = 1.50 * K_{o2} * \gamma * z + 1.75 * (\text{LL surcharge in clay}) + 1.50(K_{o2} * \gamma * 7 \text{ ft})$$
$$= 1.50(0.125 \text{ ksf})\left(\frac{17.5 \text{ in.} + 18 \text{ in.}}{12}\right)(1.0) + 1.75(0.150 \text{ ksf})\left(\frac{0.5}{1.0}\right)$$
$$+ 1.50(1.0)(0.125 \text{ kcf})(7 \text{ ft}) = 2.393 \text{ ksf}$$

3. Pressure due to retained backfill

$$p_3 = 1.50 * K_{o1} * \gamma * z = 1.50(0.5)(0.125 \text{ kcf})(7 \text{ ft}) = 0.656 \text{ ksf}$$

4. Pressure due to retained clay

$$p_4 = 1.50 * K_{o2} * \gamma * z = 1.50(1.0)(0.140 \text{ kcf})(8 \text{ ft}) = 1.680 \text{ ksf}$$

<u>Concentrated Loads from Superstructure</u>

The dead loads on the abutment were calculated with reference to the design plans provided by the BHC Engineer's Office (Figure A1through Figure A5). The weight of the deck elements (assuming a reinforced concrete weight of 150 pcf) was calculated to be 4.98 k/ft. The dead loads were subsequently distributed evenly across the 12 beams (2 beams per deck element) for analysis. The beam-in-slab deck elements had a total of 12 W14x61 beams which set on the abutment cap. Assuming 100 plf for guardrail weight, the total distributed dead load on the bridge (per beam) was:

$$w = \frac{4.98 \text{ k/ft}}{12 \text{ beams}} + \left(\frac{.100 \text{ k/ft}}{12 \text{ beams}} \text{ of guardrail}\right) + \left(0.061 \frac{k}{ft} \text{ beam weight}\right) = 0.48 \text{ k/ft per beam}$$

Using a 40.75 ft bridge length, each girder was determined to deliver a concentrated force of 9.78 k per abutment. Assuming a 20 psf future wearing surface, the force per girder was calculated to be 1.08 k per abutment. The weight of the abutment cap was 0.97 k per girder.

The factored dead loads, $P_{u_{DL}} = 1.25(9.78 \text{ k} + 0.97 \text{ k}) + 1.50(1.08 \text{ k}) = 15.06 \text{ k}$ (per girder, per abutment)

Live loads were determined by calculating the maximum AASHTO (1998) HL-93 loading effects using QConBridge (2005). For a 39 ft long bridge (between bearing centerlines) with both lanes loaded, the factored live load reaction at an abutment was determined to be 298.62 k. Live load distribution factors were calculated according to AASHTO (1998) Section 4.6.2. The critical distribution factor was for an interior beam with a single lane loaded ($g_{int} = 0.423$). The factored live load per girder, $P_{u_{LL}} = g_{int} * 298.62 \text{ k} = (0.423)(298.62 \text{ k}) = 126.32 \text{ k}$.

The BHC Engineer's Office checks all bridges for a special permit truck loading of five 10-ton axles spaced at 4.17 ft on center. An analysis of the bridge was performed using this loading, with an impact load factor of 1.33 and no lane load or live load factor applied, and it was determined that this permit truck did not control the design of the substructure.

Dead loads were assumed to distribute evenly across the sheet pile wall (33 ft wide abutment cap). Live loads were assumed to distribute over 3 piles (66 in. wide). The weight of a 15 ft long PZ 22 section was determined to be 0.33 k per ft width of wall. The concentrated load on the sheet piling per ft width of wall, P_u, was determined to be:

$$P_u = \frac{126.32 \text{ k}}{\frac{66}{12} \text{ ft}} + (15.06 \text{ k per beam})(12 \text{ beams})\left(\frac{1}{33 \text{ ft}}\right) + 0.33 \text{ k/ft} = 28.77 \text{ k/ft}$$

Analysis of the model was performed using STAAD (2008) software for a PZ 22 section. The results of the analysis showed a bending moment of 61.2 ft-kip per ft and a maximum lateral deflection, $\delta = 0.998$ in. (depicted in Figure A6). The compressive force on the wall from the superstructure induces a second order moment, M:

$$M = Pu * \delta = \left(28.77 \frac{\text{k}}{\text{ft}}\right)\left(\frac{0.998}{12} \text{ ft}\right) = 2.39 \text{ ft-kip per ft}$$

The total bending moment in the section, M = 61.2 ft-kip + 2.39 ft-kip = 63.6 ft-kip per ft. The design capacity of a PZ 22 section is 67.9 ft-kip per ft (considering elastic section modulus).
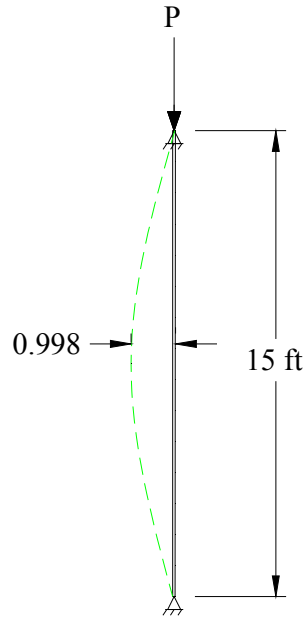
Figure A6. Lateral deflection determined for second-order moment calculation.

The compressive capacity was determined to be 243.1 k per ft of wall according to AASHTO (1998) Section 6.9.4.2. Flange-local and web-local buckling checks of the sheet pile sections were performed according to AISC (2005) Table B4.1 Case 14 and were determined to be sufficient. Element slenderness was also checked according to AISC (2005) and it was determined that the element was not slender and a fully elastic stress distribution will develop in the pile (allowing full bending moment capacity). Lateral-torsional buckling was not considered due to full bracing of compressive flanges by adjacent piles.

Interaction behavior of an element under flexural and compressive loads was checked according to AISC (2005) Equation H1-16. The interaction equation yielded a value less than 1.00 thus the PZ 22 section (Grade 50 steel) was sufficient for the assumed loading.

Design of the deadman and waler systems were performed by the BHC Engineer's Office and are not presented in this report.

GSI

August 17, 2007

Dr. David J. White, PhD
Associate Professor
Iowa State University
476 Town Engineering Building
Ames, IA 50011

RE: CONE PENETRATION TEST SOUNDING DATA AND INTERPRETATION
EXISTING CREEK CROSSING BRIDGE
BRYAN ROAD EAST OF COUNTY HIGHWAY V61, BLACK HAWK COUNTY, IOWA
GSI PROJECT NO. 076203

Dear Dr. White:

Geotechnical Services, Inc. (GSI) is pleased to submit the results of our cone penetration testing performed at the above referenced site on August 14, 2007. The work was authorized by Iowa State University Purchase Order No. I8 56064 00 and performed in accordance with our proposal dated August 10, 2007.

The project site consisted of single-span bridges over a tributary to the Cedar River. Bryan Road was surfaced with crushed limestone at the time of our field exploration. The bridge deck at the abutments was approximately 10 feet above the creek bed. We observed that the bridge is supported on a combination of timber and steel H-piles with relatively small wooden wing walls. We were provided with a boring log from the east abutment that indicates approximately 14 feet of predominately fine-grained soils underlain by limestone bedrock.

The electronic piezocone test (CPT$_u$) soundings were performed east and west of the bridge abutments. The test locations are described in the table below. Utility lines were located along the south side of Bryan Road and traffic across the posted narrow bridge could not be blocked.

CPT Sounding	CPT$_u$ Location
CPT 1	28' east and 7' north of center of east abutment
CPT 2	15' west and 6' north of center of west abutment

The investigation utilized a 20-ton capacity, truck-mounted rig hydraulically advancing a Hogentogler Type 2, 10-ton subtraction cone. The electronic cone has a 60° tip angle, tip area of 10 cm^2, a net area ratio of 0.8, and a friction sleeve area of 150 cm^2, and was advanced at a rate of approximately one inch per second. The data collection system recorded data at five centimeter intervals. The CPT$_u$ testing was performed in general accordance with ASTM D5778, "Performing Electric Friction Cone and Piezocone Penetration Testing of Soils." The uncorrected tip stress, sleeve friction, and pore pressure graphical results are provided with this report and the raw data have been attached to this report for your use in calculating soil parameters. The soil behavior

www.gsinetwork.com

2853 99th Street ♦ Des Moines, IA 50322-3858 ♦ (515) 270-6542 ♦ FAX (515) 270-1911

Figure A7. CPT report for BHC, Iowa demonstration project.

GSI

type is also shown on the attached graphs. These classifications are based on the Simplified Soil Classification Chart for Electric Friction Cone by Robertson and Campanella (1986) and are a general indication of the soils encountered at this site.

These CPT$_u$ soundings were used to provide a nearly continuous subsurface soil profile that will be used to obtain soil shear strength parameters. These parameters will then be used to model the soil-structure interaction of the bridge structure and the new sheetpile abutment system. Both soundings were advanced to practical refusal based on the equipment and our experience to depths of 15.9 and 17.4 feet below existing grades. The cone tip was covered with light tan weathered limestone after being withdrawn from the CPT 2 sounding hole.

The project site is located on the "Iowan Surface", a distinct geomorphic region limited to the northeastern portion of Iowa. Transected surficial drainage imparts the topography consisting of gently rolling hills with long slopes and gentle relief. Prominent isolated elliptical hills, termed "pahas", tend to be concentrated along the region's southern border and karst features, including sinkholes, are common to the northern portion of the Iowan Surface due to the thin overburden deposits underlain by limestone bedrock formations.

Overburden deposits within the stream valleys generally consist of colluvium (slopewash) overlying alluvium of varying thickness which is underlain by the glacial till soils over bedrock. The colluvial deposits are derived from parent soil materials on hillsides while the underlying alluvium may consist of both cohesive clayey silt and silty clay soils and/or deposits. This project is locally located on a creek channel and on an upland above the Cedar River floodplain which may have deposited alluvium consisting of interbedded sand and clay soils.

The profiles generally consist of fine-grained fill and alluvium underlain by over-consolidated fine-grained soils shown by a relatively large decrease in pore water pressure at depths of 13.7 and 14 feet, in CPT 1 and 2, respectively. The observed drop in tip stress and sleeve friction near depths of 10 feet likely coincides with the ground water surface. It appears that the soils below 10 feet contain sand seams as evidenced by the variability in the tip stress and sleeve friction data. We were able to push into the weathered limestone approximately one foot before refusal occurred.

GSI is proud to be part of Iowa State University's continued research in the field of geotechnical engineering and soil behavior. Please contact us at (515) 270-6542 if you have any questions on this job or if you would like our assistance on future projects.

Respectfully,
Geotechnical Services, Inc.

Zachary G. Thomas, P.E.
Project Engineer

Michael T. Lustig, P.E.
Principal Engineer

Attachments: Graphical CPT Logs (4), Electronic Raw Data Disk

Figure A7. (continued).

Geotechnical Services, Inc.

Operator: ZGT
Sounding: CPT 1
Cone Used: 233

CPT Date:Time: 08-14-07 09:19
Location: E Abutment
Job Number: 076203

Tp Resistance Qc (Ton/ft^2)	Local Friction Fs (Ton/ft^2)	Pore Pressure Pw (psi)	Soil Behavior Type* Zone: UBC-1983

Maximum Depth = 15.91 feet

Depth increment = 0.164 feet

1	sensitive fine grained	4	silty clay to clay	7	silty sand to sandy silt	10	gravelly sand to sand
2	organic material	5	clayey silt to silty clay	8	sand to silty sand	11	very stiff fine grained (*)
3	clay	6	sandy silt to clayey silt	9	sand	12	sand to clayey sand (*)

*Soil behavior type and SPT based on data from UBC-1983

Figure A7. (continued).

Geotechnical Services, Inc.

Operator: ZGT
Sounding: CPT 1
Cone Used: 233

CPT Date/Time: 08-14-07 09:19
Location: E Abutment
Job Number: 076203

Maximum Depth = 15.91 feet

Depth Increment = 0.164 feet

1	sensitive fine grained	4	silty clay to clay
2	organic material	5	clayey silt to silty clay
3	clay	6	sandy silt to clayey silt

7	silty sand to sandy silt	10	gravelly sand to sand
8	sand to silty sand	11	very stiff fine grained (*)
9	sand	12	sand to clayey sand (*)
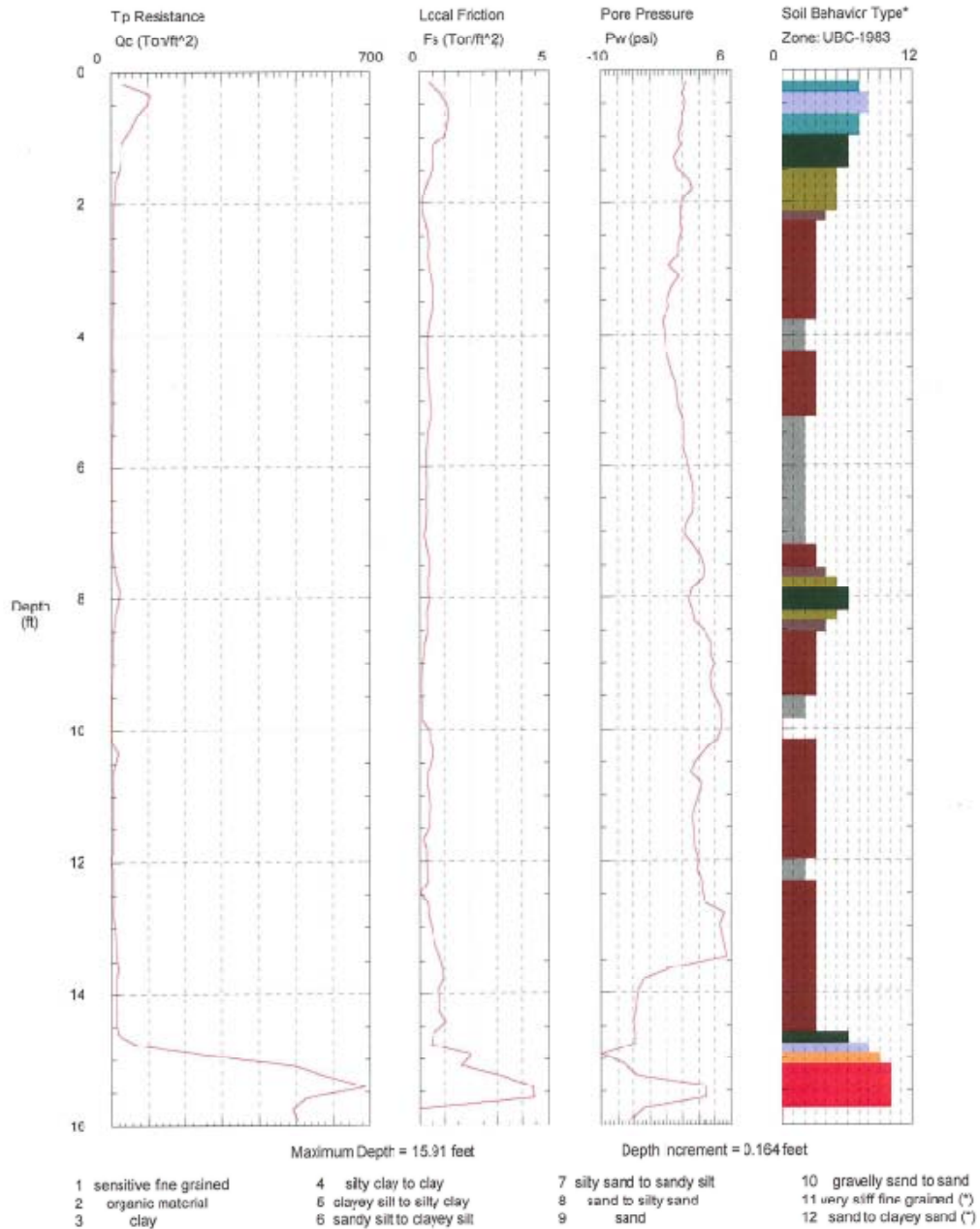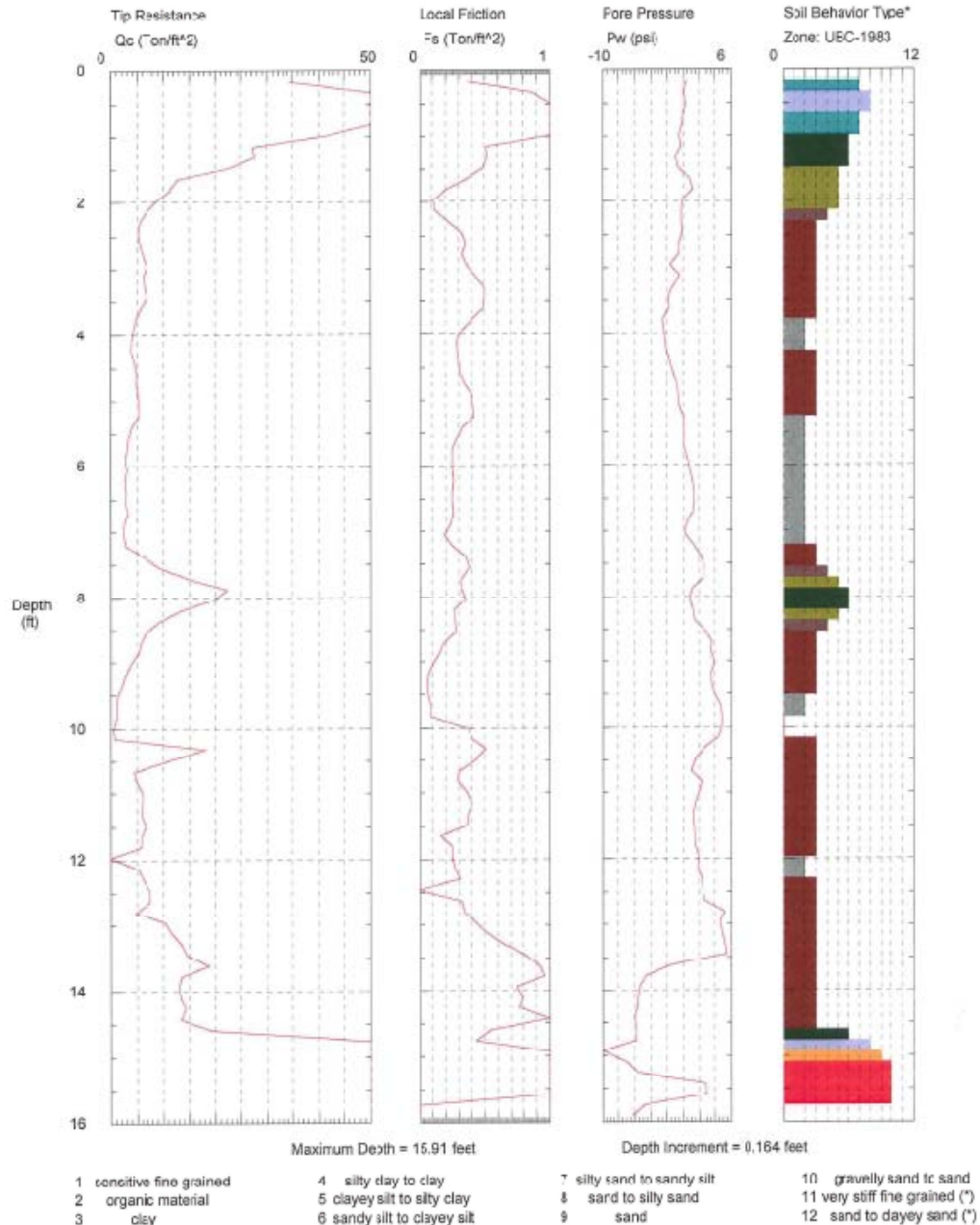
*Soil behavior type and SPT based on data from UBC-1983

Figure A7. (continued).

Geotechnical Services, Inc.

Operator: ZGT
Sounding: CPT 2
Cone Used: 233

CPT Date/Time: 08-14-07 09:52
Location: W Abutment
Job Number: 076203

Maximum Depth = 17.39 feet

Depth Increment = 0.164 feet

1	sensitive fine grained	4	silty clay to clay	7	silty sand to sandy silt	10	gravelly sand to sand
2	organic material	5	clayey silt to silty clay	8	sand to silty sand	11	very stiff fine grained (*)
3	clay	6	sandy silt to clayey silt	9	sand	12	sand to clayey sand (*)

*Soil behavior type and SPT based on data from UBC-1983

Figure A7. (continued).

Figure A7. (continued).

ctre
Center for Transportation Research and Education

| Log of Soil Boring No. | **SB 1** |

Project: *Bryan Road Bridge*
Location: *Black Hawk County, IA*
Sheet ___ of ___
Project No.: *BHC 01*

Logged By: Ryan Evans
Driller: H. Gieselman
Drill Rig: ___
Date: **September 7, 2007**

Client: *Iowa DOT/Black Hawk County*
Proj. Mgr.: *Ryan Evans*
GPS: Latitude ___ N
Longitude: ___ W

Depth (feet)	Sample Depth Range	Type	No.	Container	Recovery	Field Data (P) SPT OVA (tsf)	Visual Classification	Depth	Stratigraphy	Laboratory Assignments Depth	Assignment
	12" - 40"	ST	1			2.00	Sandy clay - dark gray		Sandy Clay		
5	42" - 61"	ST	2			1.25	ClaySilt Organic - dark gray/black				
	72" - 94"	ST	3			2.75	Sandy clay - dark gray				
10	102"-118'	ST	4			1.00	Sandy clay - dark gray*below water level		water level		
	124"	ST	5			N/A	Clay w/ gravel - dark gray (tube not full)				
	144" +					N/A	Sand with clay seams		Sand with Clay Seams		
15											
20											
25											

Boring Advancement		Boring Abandonment	Groundwater Information	Topsoil Depth / Surface Conditions:
Depth Range	Method	Cuttings ☐ Grout ☐	First Encountered: 10 feet	31' E of E abt, 6' N of d
___	___	Grout Mixture:	Rise: ___ after ___	
___	___	___	Static: after ___	Start Time: ___ Finish Time: ___

Figure A8. Log of soil boring SB 1 for demonstration project in BHC, Iowa.

Log of Soil Boring No. _SB 2_

CTRE		

Project: _Bryan Road Bridge_ Location: _Black Hawk County, IA_

Sheet _____ of _____

Project No.: _BHC 01_

Logged By: Ryan Evans Driller: H. Gieselman Drill Rig: _____ Date: **September 7, 2007**

Client: _Iowa DOT/Black Hawk County_ Proj. Mgr.: _Ryan Evans_ GPS: Latitude _____ N Longitude: _____ W

Depth (feet)	Sample					Field Data (P) (tsf)	Visual Classification	Depth	Stratigraphy	Laboratory Assignments	
	Depth Range	Type	No.	Container	Recovery					Depth	Assignment
									SandyClay		
5	24" - 50"	ST	6			1.35	Silty Clay/ Organic - dark gray black				
	63" - 87"	ST	7			2.25	Sandy clay - light brown and dark gray				
10	96"-124"	ST	8			1.30	Clay w/ Sand - dark gray and brown (water)		water level		
	124"-130"	ST	9				Saturated sand				
	156"	AG				N/A	Sand		Sand		
15	202"	ST	10			N/A	Sand silt-dark gray to bedrock		Bedrock - limestone		
20											
25											

Boring Advancement		Boring Abandonment	Groundwater Information	Topsoil Depth / Surface Conditions:
Depth Range	Method	Cuttings ☐ Grout ☐ Grout Mixture: _____	First Encountered: 11 feet Rise: _____ after _____ Static: _____ after _____	25' E, 6' N of E abt Start Time: _____ Finish Time: _____

Figure A9. Log of soil boring SB 2 for demonstration project in BHC, Iowa.

Log of Soil Boring No. _SB 3_

Sheet _____ of _____

Project: _Bryan Road Bridge_ **Location:** _Black Hawk County, IA_ **Project No.:** _BHC 01_

Logged By: _Ryan Evans_ **Driller:** _H. Gieselman_ **Drill Rig:** _____ **Date:** _September 7, 2007_

Client: _Iowa DOT/Black Hawk County_ **Proj. Mgr.:** _Ryan Evans_ **GPS:** Latitude _____ N Longitude: _____ W

Depth (feet)	Sample Depth Range	Type	No.	Container	Recovery	Field Data (P) SPT OVA (tsf)	Visual Classification	Depth	Stratigraphy	Laboratory Assignments Depth	Assignment
5	23"-50"	ST	11			2.30	Silty Clay - dark gray/black		Silty Clay		
	54"-74"	ST	12			1.30	Silty Clay w/ gravel - Dark gray				
10	90"-109"	ST	13			1.90	Mottled clay - gray/orange				
	114"-139'	ST	14				Mottled clay till - gray/orange		water level		
	144" +					N/A	Sand with clay seams				
15	150"-180'	ST	15			3.75	Orange Silty Clay		Clay		
	192"					3.25	Dark gray clay				
20											
25											

Boring Advancement		Boring Abandonment	Groundwater Information	Topsoil Depth / Surface Conditions
Depth Range	Method	Cuttings ☐ Grout ☐ Grout Mixture:	First Encountered: _12_ feet	12' W of bridge, 6' N of cl
_____	_____		Rise: _____ after _____	
_____	_____		Static: _____ after	Start Time: _____ Finish Time: _____

Figure A10. Log of soil boring SB 3 for demonstration project in BHC, Iowa.

Figure A11. Log of soil boring SB 4 for demonstration project in BHC, Iowa.

Figure A12. Direct shear test results on backfill material for demonstration project in BHC, Iowa.

Example Analysis Calculations for Live Load Test Data Comparison

This section of the Appendix provides the methods and assumptions used in calculating the estimated values in Table 5-12 through Table 5-14; calculations for test Run A at location 5 (tandem axle over centerline of abutment bearing) are presented to demonstrate the methods used.

It should be noted that the "estimated" values are calculated using the same approach that was used for the design of the bridge; this was done to provide a reference value (stress or deflection) for comparison of the data collected during the live load testing. Although the load distribution and analysis methods may not accurately predict the behavior of the structure, the comparison of the theoretical analysis to the live load test data will provide an indication of the adequacy (i.e., conservative or unconservative) of the design method utilized.

The dead loads of the superstructure (bridge deck elements and abutment cap) were determined to be approximately 3.8 k per ft width of the bridge. The cross-sectional area of a PZ 22 is 6.47 in^2/ft causing a dead load axial stress of 0.59 ksi in the sheet piling. The live loads of Truck 48 (31.4 kip tandem axle and 17.5 kip front axle) were positioned on the bridge according to Figure A13 for location 5; the loads on the bridge and the abutment backfill causing axial and flexural stresses in the sheet pile wall, respectively.
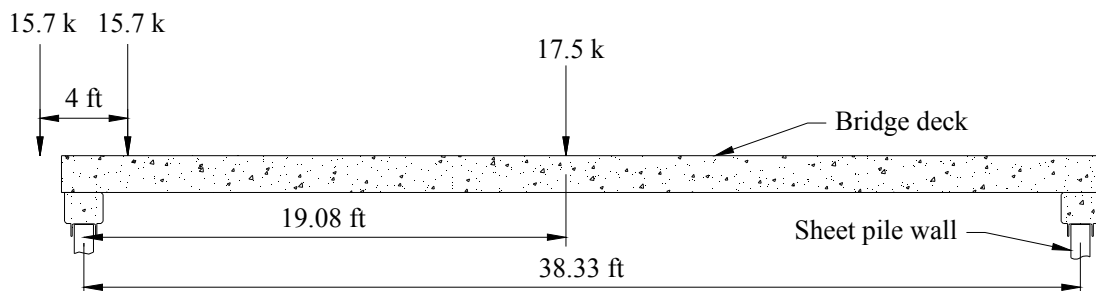
Figure A13. Location of Truck 48 wheel loads for Run A, location 5.

Analyzing the superstructure as a simply-supported beam, the reaction on the west abutment is determined to be 23 kips. Using a 10 ft wide load distribution (same as design), the resulting live load axial stress is determined to be 0.35 ksi.

Analysis of lateral loads was performed assuming the sheet pile wall was a rigid structure; this assumption was made due to the resistance of the superstructure to lateral movement of the top of the wall. For determining lateral earth pressure from the retained backfill, an earth pressure coefficient of 0.293 was used (assuming 45 degree angle of internal friction as determined from a direct shear test on the backfill material) with a soil unit weight of 120 pcf. Live load of the wheels on the backfill were assumed to act as a line load of 1.57 k/ft (15.7 kip wheel load distributed over 10 ft) acting 2 ft behind the centerline of the sheet pile wall according to AASHTO (1998) Section 3.11.6.1. The resulting lateral loads determined from the equation in AASHTO (1998) Section 3.11.6.1 were also used to estimate live load lateral earth pressures of 250 psf, 80 psf, and 30 psf for the earth pressure cells 1 ft, 3 ft, and 5 ft below TOC, respectively; the total loads on these cells were determined by adding backfill earth pressures of 65 psf, 135 psf, and 205 psf to the corresponding live load lateral earth pressures at cells 1 ft, 3 ft, and 5 ft below TOC, respectively. The resulting lateral loading diagram for the sheet pile wall (with pinned supports assumed to act at the bottom of the wall and the location of the tie rod) is presented in Figure A14.
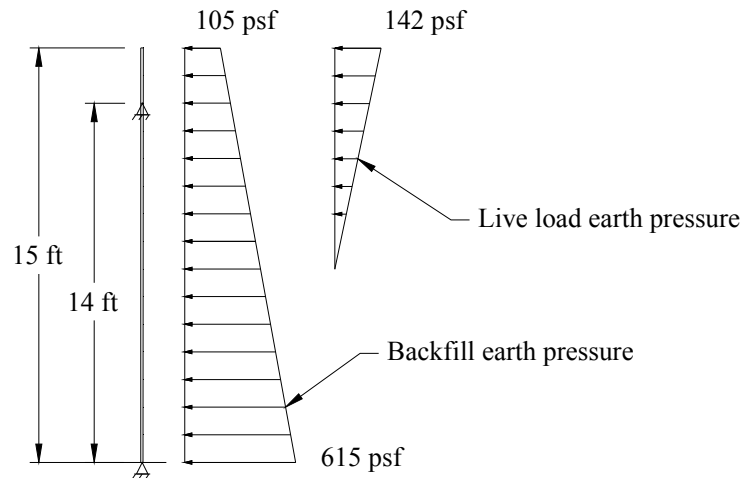
Figure A14. Lateral loading diagram for analysis of sheet pile wall.

Two analyses were performed, one analysis including both live load and dead load lateral earth pressures and the second analysis including only live load earth pressures; these resulted in maximum bending moments of 112.64 k-in and 10.56 k-in, respectively; wall deflections were also estimated by each analysis. Using the modified section modulus of 35.2 in^3/ft for an instrumented sheet pile, the flexural stresses due to total loads and live loads only are calculated to be 3.20 ksi and 0.30 ksi, respectively.

Stresses and deflections of the superstructure at midspan were calculated assuming the bridge acted as a simply-supported beam of 39.33 ft length (as-built length between centerlines of bearing locations). A section modulus and moment of inertia of 659.6 in^3 and 6330.91 in^4 were calculated for a 10 ft wide section (design distribution width) based on the repeating section values provided by the BHC Engineer's Office. Analysis of the structure resulted in a bending moment at midspan of 172.58 ft-k corresponding to a flexural stress (at the bottom flange of the steel beams) of 3.10 ksi; the vertical deflection at midspan was determined to be 0.23 in.

APPENDIX B: BOONE COUNTY EXPERIMENTAL BRIDGE 2
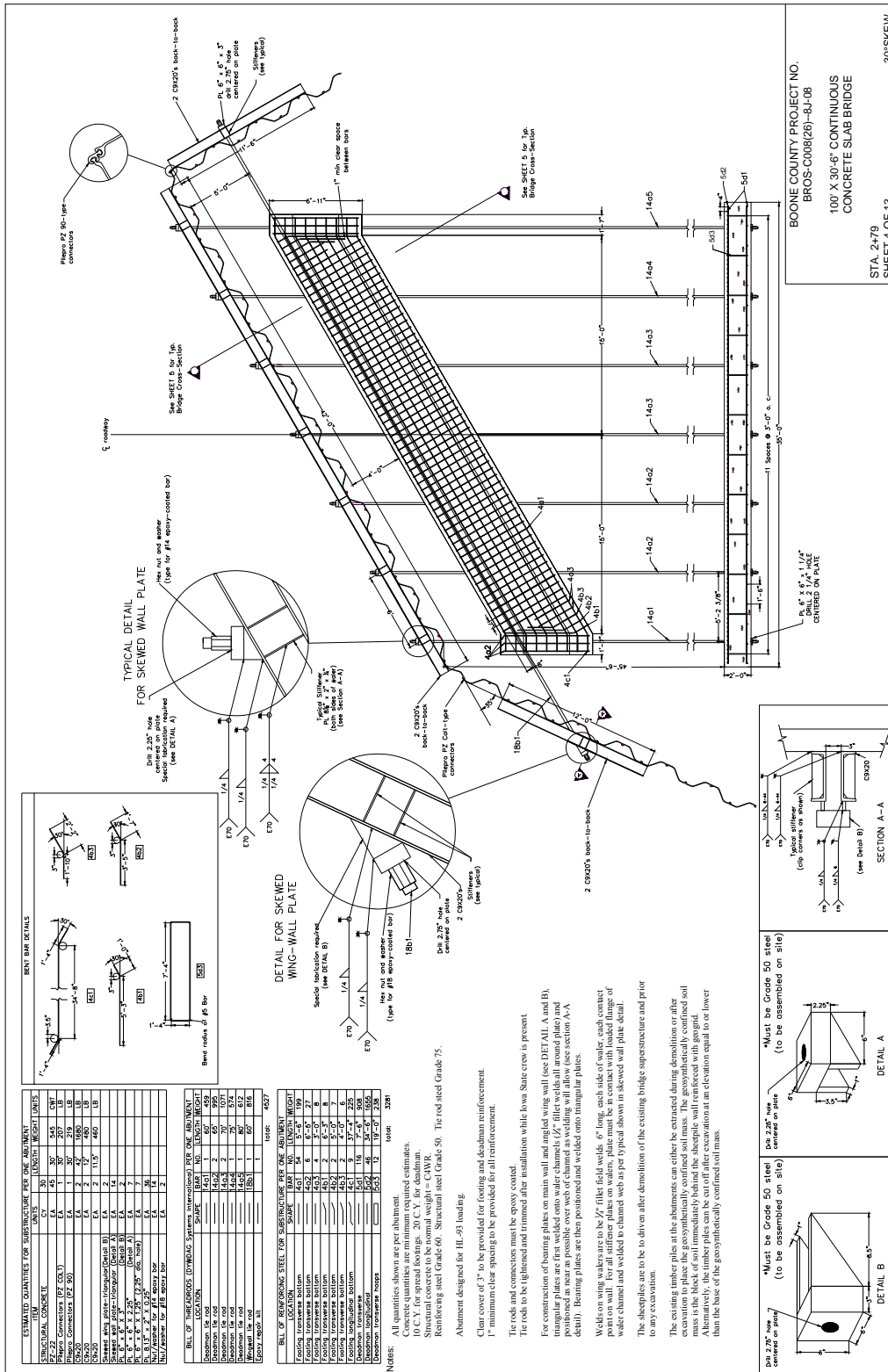
Figure B1. Plan view of abutment for demonstration project in BC, Iowa.
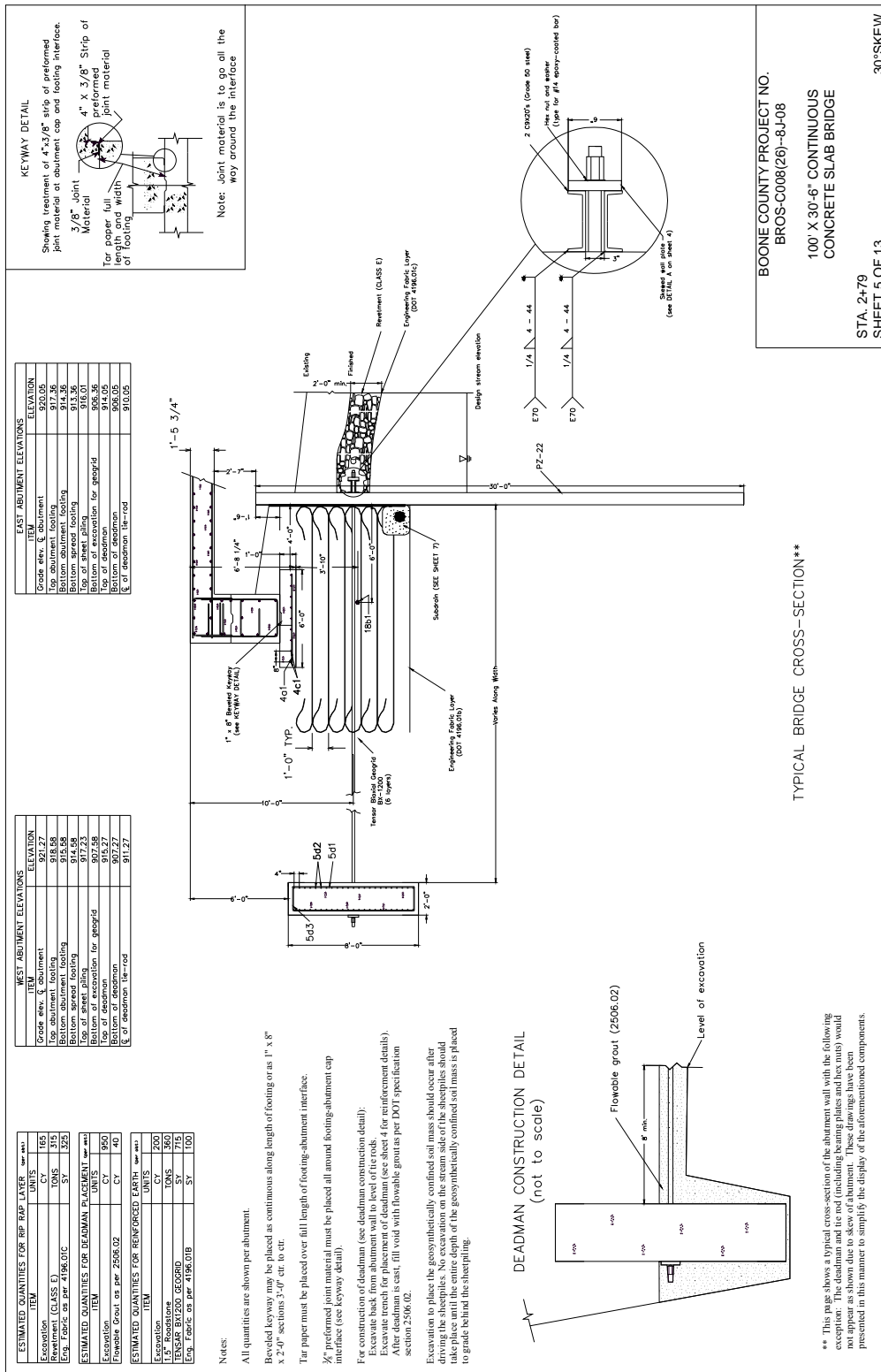
Figure B2. Cross-section of abutment for demonstration project in BC, Iowa.
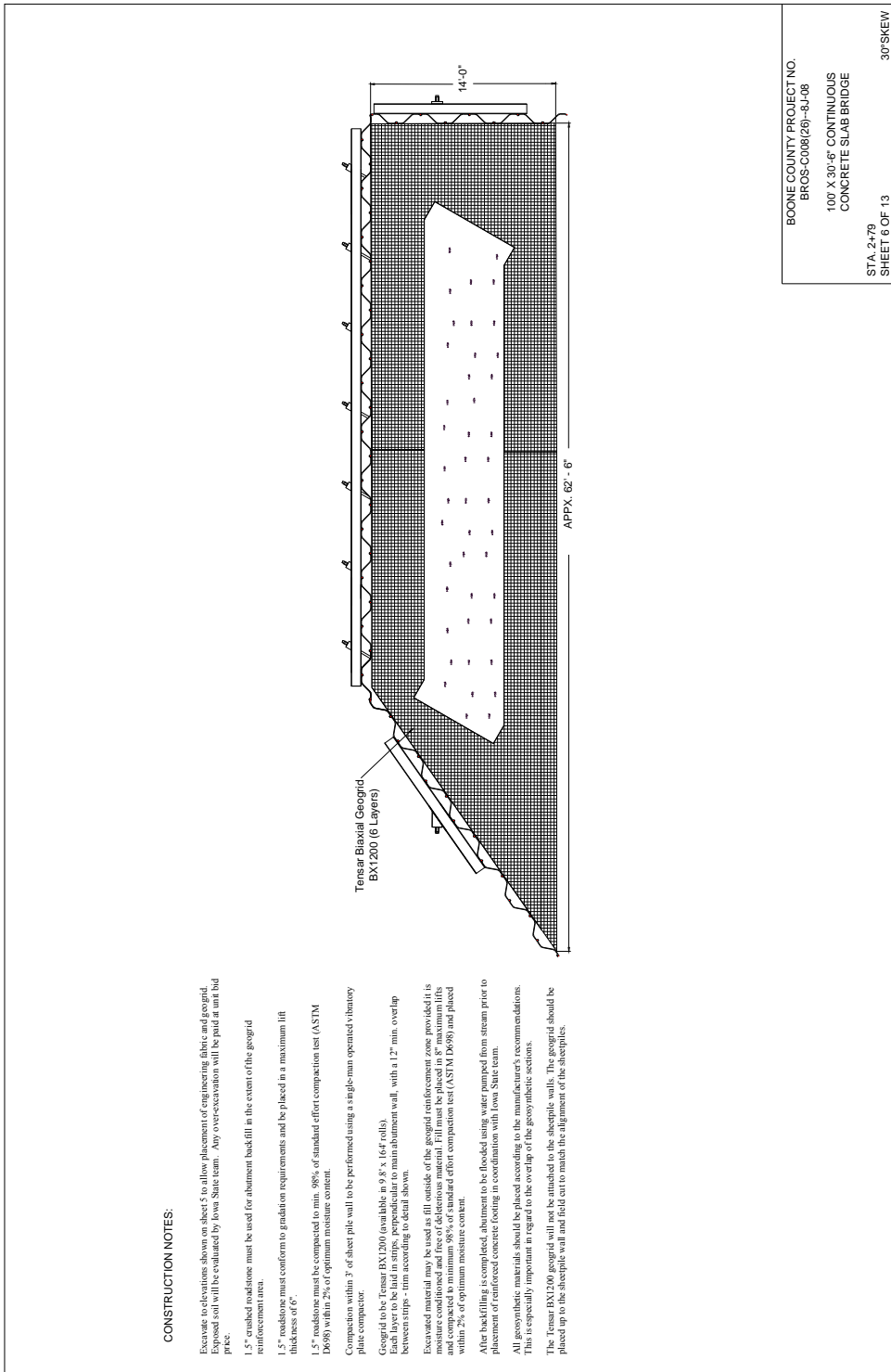
Figure B3. Plan view of abutment showing geogrid layout for demonstration project in BC, Iowa.

Figure B4. Drainage system details for demonstration project in BC, Iowa.
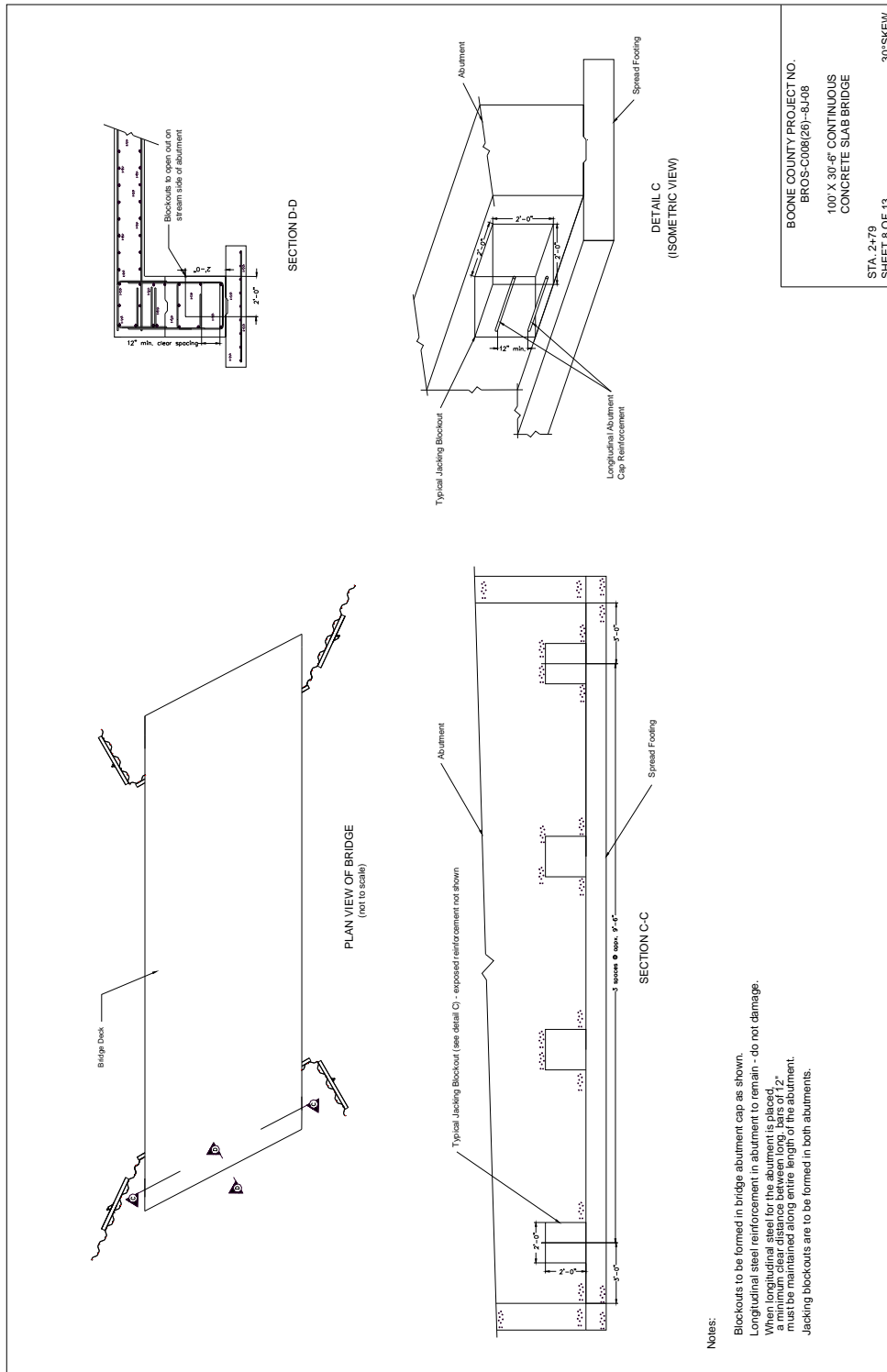
Figure B5. Details of blockout system in bridge abutments for demonstration project in BC, Iowa.

GSI

June 17, 2008

Dr. David J. White, PhD
Associate Professor
Iowa State University
476 Town Engineering Building
Ames, IA 50011

RE: CONE PENETRATION TEST SOUNDING DATA AND INTERPRETATION
       EXISTING CREEK CROSSING BRIDGE
       OWL AVENUE EAST OF 310TH STREET, BOONE COUNTY, IOWA
       GSI PROJECT NO. 086113

Dear Dr. White:

Geotechnical Services, Inc. (GSI) is pleased to submit the results of our cone penetration testing performed at the above referenced site on June 10, 2008. The work was authorized by Iowa State University Purchase Order No. I8 63293 00 and performed in accordance with GSI proposal P086121 dated May 18, 2008.

The project site consisted of a single-span bridge over Eversoll Creek which is a tributary to the Des Moines River. Owl Avenue was surfaced with crushed limestone at the time of our field exploration. We were provided with a boring log from the east abutment that indicates approximately 18 feet of predominately fine-grained soils underlain by sand with interbedded clay seams.

The electronic piezocone test (CPT$_u$) soundings were performed east and west of the bridge abutments. The test locations were approximately 15 feet east and west of the center of each abutment in order to avoid any rubble or ties between the wing walls.

This investigation utilized a 20-ton capacity, truck-mounted rig hydraulically advancing a Hogentogler Type 2, 10-ton subtraction cone. The electronic cone has a 60° tip angle, tip area of 10 cm^2, a net area ratio of 0.8, and a friction sleeve area of 150 cm^2, and was advanced at a rate of approximately one inch per second. The data collection system recorded data at five centimeter (2-inch) intervals. The CPT$_u$ testing was performed in general accordance with ASTM D5778, "Performing Electric Friction Cone and Piezocone Penetration Testing of Soils." The uncorrected tip stress, sleeve friction, and pore pressure graphical results are provided with this report. The soil behavior type is also shown on the attached graphs and is reported for the average of three reading intervals. These classifications are based on the Simplified Soil Classification Chart for Electric Friction Cone by Robertson and Campanella (1986) and are a general indication of the soils encountered at this site. Uncorrected tip stress, sleeve friction, and pore pressure have been converted to text data and will be included with this report.

Figure B6. CPT report for BC, Iowa demonstration project.

GSI

These CPT$_u$ soundings were used to provide a nearly continuous subsurface soil profile that will be used to obtain soil shear strength parameters. These parameters will then be used to model the soil-structure interaction of the bridge structure and the new sheetpile abutment system. Both soundings were advanced to practical refusal based on the equipment and our experience to depths of 45.6 and 44.1 feet below existing grades.

The project site is located within a geomorphic region referred to as the "Des Moines Glacial Lobe." This landform region was formed by extensive glacial activity including erosion, reworking, and deposition. Typically, the predominant surficial sediment is glacial drift deposited by the Wisconsinan glacier. Glacial soils commonly encountered within 15± feet of ground surface are classified as supraglacial sediments. The supraglacial materials are generally variable and can be stratified in composition consisting of very silty sandy clay interbedded with silt and sand seams, layers, and extensive pockets throughout. In contrast, the underlying subglacial soils, which were deposited beneath the glacial ice as it advanced, tend to be a more homogeneous composition of silty sandy clay materials.
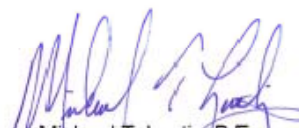
Overburden deposits within the stream valleys generally consist of colluvium (slopewash) overlying alluvium of varying thickness which is underlain by the glacial till soils over bedrock. The colluvial deposits are derived from parent soil materials on hillsides while the underlying alluvium may consist of both cohesive clayey silt and silty clay soils and/or deposits. This project is locally located on a creek channel and on an upland above the Des Moines River floodplain which may have deposited alluvium consisting of interbedded sand and clay soils.

The profiles encountered during CPT$_u$ sounding generally consist of cohesive soils underlain by predominately granular soil based on Robertson and Campenella's soil behavior types. The soil encountered near depths of 34 feet and below in each sounding generally consists of over-consolidated fine grained soil deposits and dense to very dense granular materials as evidenced by a relatively large decrease in pore water pressure due to fracturing and dilatency. The depth to ground water was observed to be approximately 15 to 17 feet based on the recorded pore water pressure.

GSI is proud to be part of Iowa State University's continued research in the field of geotechnical engineering and soil behavior. Please contact us at (515) 270-6542 if you have any questions on this job or if you would like our assistance on future projects.

Respectfully,
Geotechnical Services, Inc.

Zachary G. Thomas, P.E.
Project Engineer

Michael T. Lustig, P.E.
Principal Engineer

Attachments: Graphical CPT$_u$ Logs (2), Electronic Raw Data Disk

GSI No. 086113   2   June 17, 2008

Figure B6. (continued).

Figure B6. (continued).

Geotechnical Services, Inc.

Operator: DAH
Sounding: CPT 2
Cone Used: 233

CPT Date/Time: 06-10-08 09:50
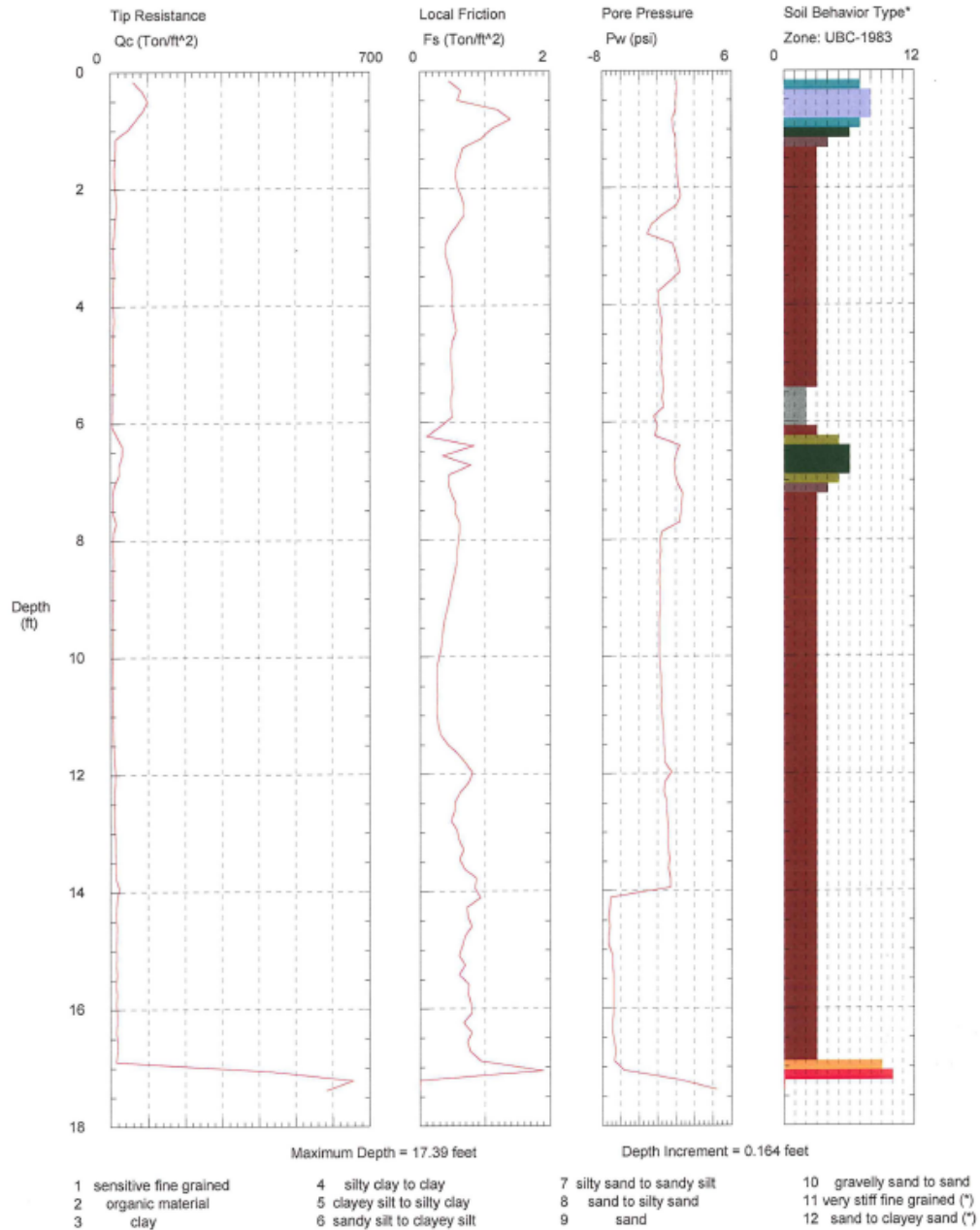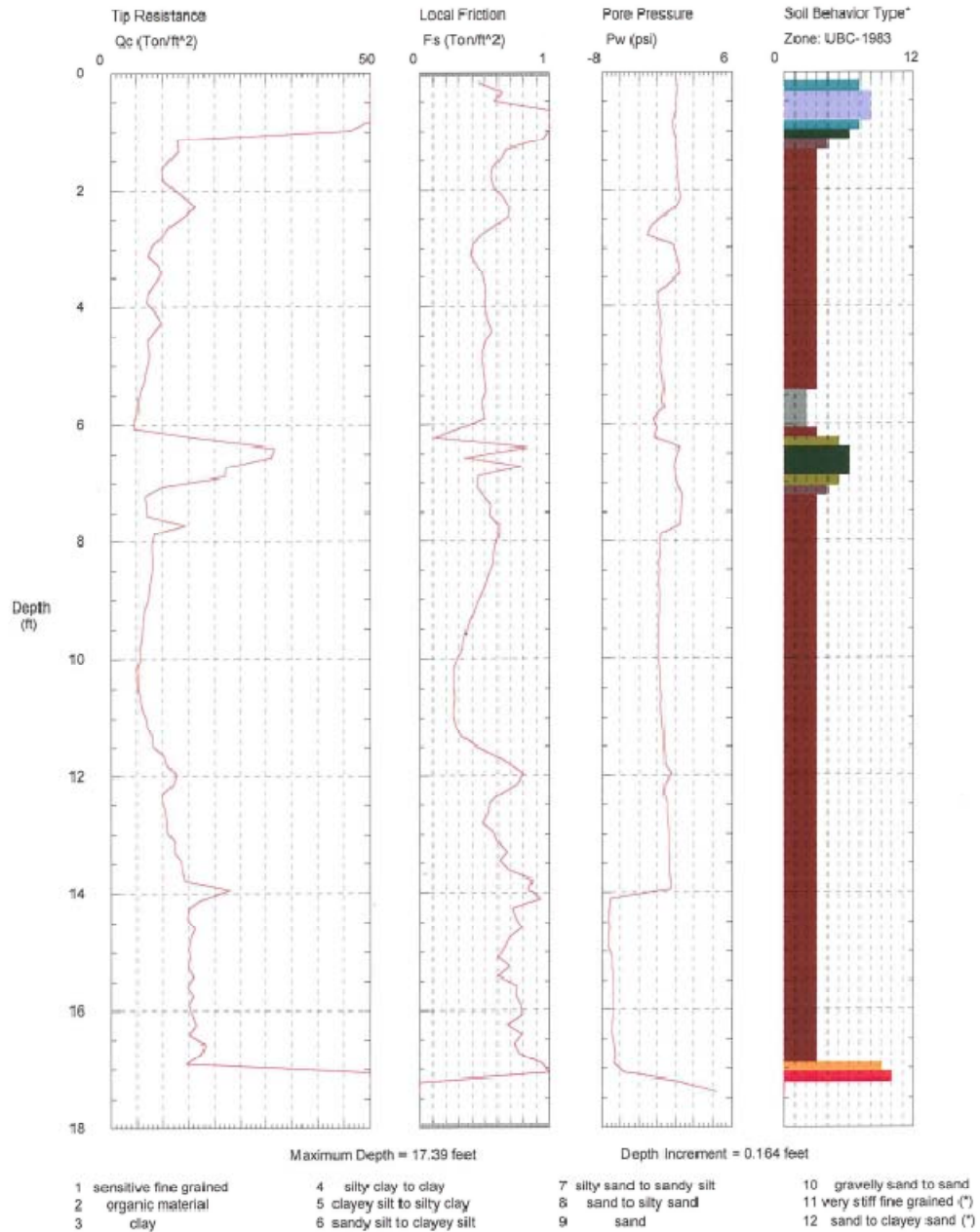Location: 15' E of E Abutment
Job Number: 086113

| Tip Resistance | Local Friction | Pore Pressure | Soil Behavior Type* |
| Qc (Ton/ft^2) | Fs (Ton/ft^2) | Pw (psi) | Zone: UBC-1983 |

Maximum Depth = 44.13 feet

Depth Increment = 0.164 feet

1 sensitive fine grained	4 silty clay to clay	7 silty sand to sandy silt	10 gravelly sand to sand
2 organic material	5 clayey silt to silty clay	8 sand to silty sand	11 very stiff fine grained (*)
3 clay	6 sandy silt to clayey silt	9 sand	12 sand to clayey sand (*)
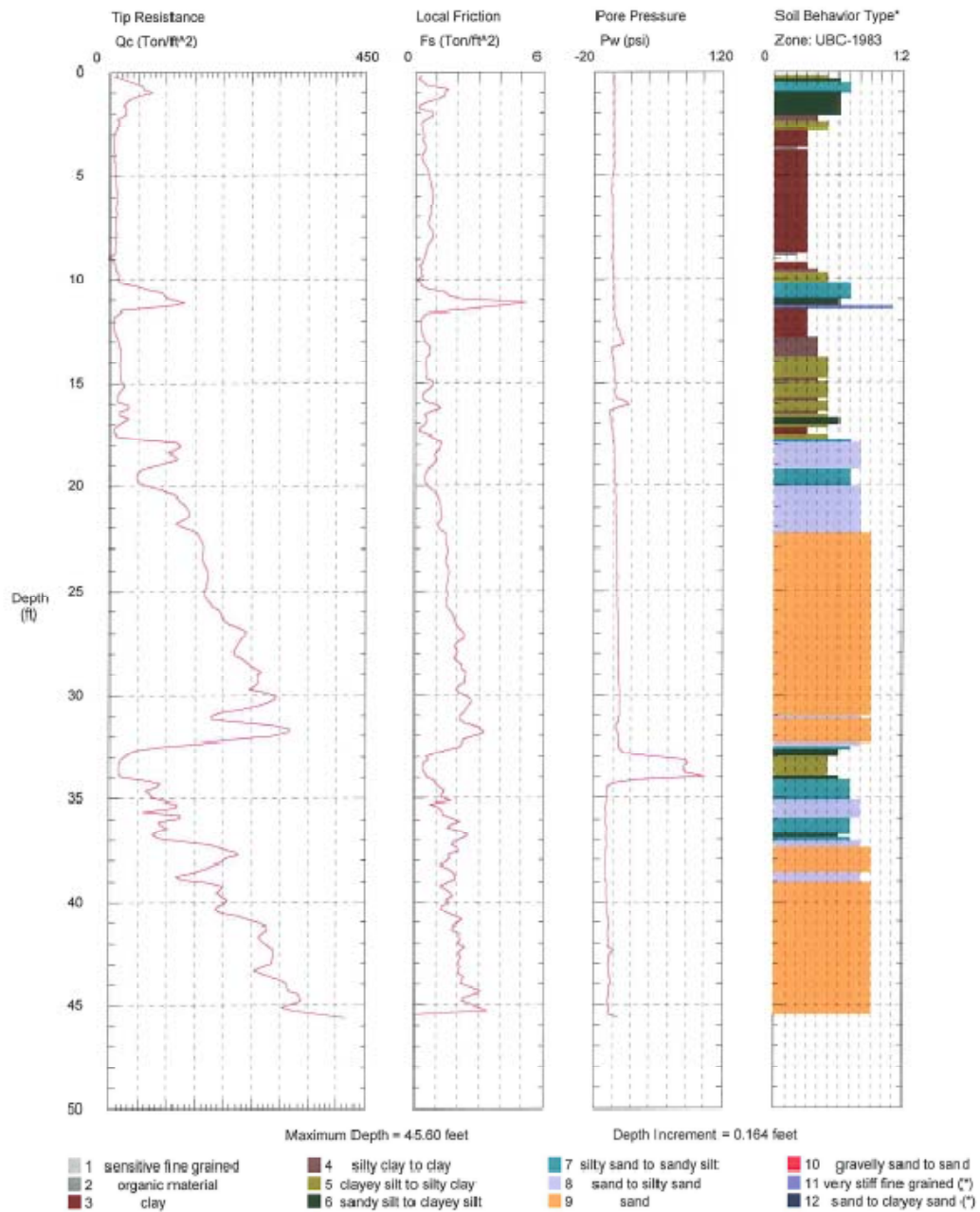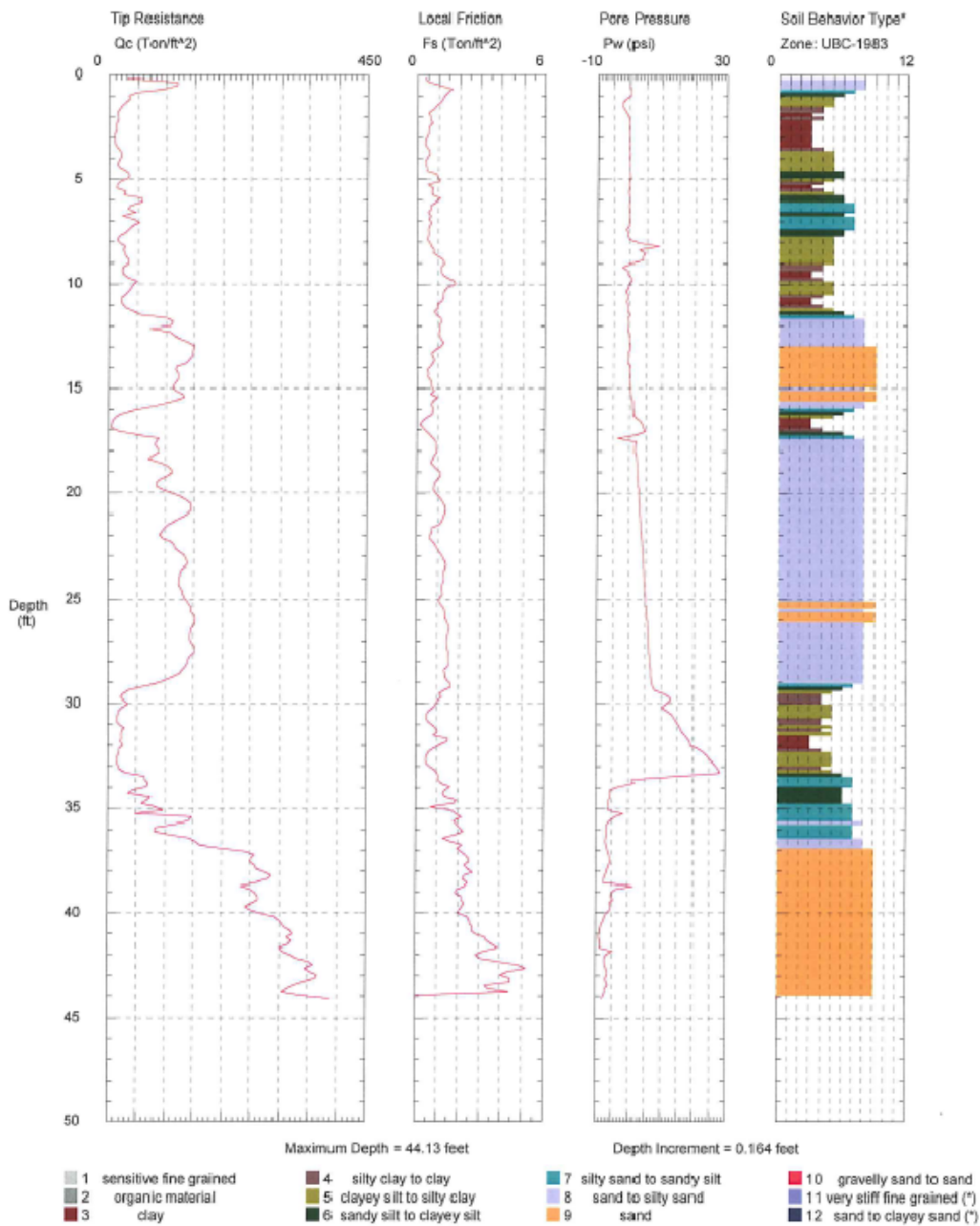
*Soil behavior type and SPT based on data from UBC-1983

Figure B6. (continued).

Log of Soil Boring No. *SB 1*

Sheet 1	of 1

Project: *Owl Ave. Bridge* **Location:** *Boone County, IA* **Project No.:** *BROS-C008(26)--8J-*

Logged By: Ryan Evans **Driller:** Brian **Drill Rig:** JIMCO **Date:** **July 11, 2008**

Client: *Iowa DOT/Boone County* **Proj. Mgr.:** *Ryan Evans* **GPS: Latitude** N **Longitude:** W

Depth (feet)	Sample Depth Range	Type	No.	Container	Recovery	Field Data (P) SPT OVA	Visual Classification	Depth	Stratigraphy	Lab Depth	Assignment
	0" - 12"	A		B			Tan Sandy Gravel		Tan sandy gravel fill		
	12" - 24"	A		B			Light gray clayey sand		Light gray clayey	2'	water content,
	24" - 36"	A		B			Light gray clayey sand fill		sand fill		grain size dist.
5	36" - 60"	T		T		2.5 tsf	Black and light gray silty clay w/ possible organic material (very stiff)		Very stiff black and light gray silty clay	3'-5'	UC, AL
	72" - 96"	T		T		2.0 tsf	Black and light gray silty clay w/ possible organic material			6'-8'	UC, AL
10	102" - 126"	T		T		2.0 tsf	Black and light gray silty clay w/ possible organic material *cobble at 10.5 ft		Very stiff tan and light gray sandy clay or	8.5'-10.5'	UC, AL
	144" - 168"	T		T		2.75 tsf	Very stiff tan sandy clay or clayey sand		clayey sand	14'	
15	180" - 192"	A		B					Tan silty sand to slighty		dry out direct shear
	192" - 216"	T		T		N/A	Wet sand		silty sand		50, 100, 150 kpa
20	240"	A		B							
25											

Boring Advancement		Boring Abandonment	Groundwater Information	Topsoil Depth / Surface Conditions:
Depth Range	Method	Cuttings ☒	First Encountered: 16 feet	Gravel Road, west of west abutment
0 - 20 ft	Cont. flight Ag	Grout ☐ Grout Mixture:	Rise: after	
			Static: after	Start Time: Finish Time:

Figure B7. Soil boring log SB 1 for demonstration project in BC, Iowa.

Design Calculations

Loading summary

Preliminary design assumptions for loading calculation:

- Weight of reinforced concrete = 150 pcf

- Future wearing surface = 20 psf (unlikely to be used on gravel road bridge)

- 6 ft wide, 12 in. thick spread footing

- 4 in. thick gravel surface for roadway with unit weight of 110 pcf

- backfill soil weight, γ_s = 120 pcf

- backfill friction angle, $\varphi' = 35°$

AASHTO (1998) Section 3.4 specifies the following maximum load factors for Strength I limit state design (the critical limit state determined for this design):

- Dead loads of structural components (DC): 1.25

- Dead loads of wearing surfaces and utilities (DW): 1.50

- Horizontal earth pressure (EH): 1.50 active and 1.35 at-rest

- Earth surcharge load (ES): 1.50

- Vertical pressure from earth dead load (EV): 1.35 for retaining structures

- Vehicular live load (LL): 1.75

- Live load surcharge (LS): 1.75

DC and DW Load Estimates

Abutment cap: $\left[\frac{(30\text{ in.}+36\text{ in.})(36\text{ in. wide})}{144\text{ in}^2\text{ per ft}}(33.2\text{ ft wide bridge})(0.150\text{ kcf})\right] = 82.2\text{ k (each abt.)}$

Barrier rail: $2(2.84\text{ ft}^2\text{ area})(0.150\text{ kcf}) = 0.852\text{ klf (assumed F-shape barrier rail)}$

Wearing surface: $0.020\text{ ksf}(30.5\text{ ft wide roadway}) = 0.61\text{ klf}$

Spread footing: $(6\text{ ft wide})(1\text{ ft thick})(0.150\text{ kcf})(35\text{ ft wide}) = 31.5\text{ k (each abt.)}$

Roadway gravel: $\left(\frac{4}{12}\text{ ft thick}\right)(0.110\text{ kcf})(30.5\text{ ft wide roadway}) = 1.12\text{ klf}$

Superstructure: $0.150\text{ kcf}(49.11\text{ ft}) = 7.37\text{ klf}$

LL Estimates

The live loads applied to the abutment through the spread footing were estimated by analyzing the superstructure for HL-93 loading using the computer program QConBridge (2005). After calculating the live load envelopes for the bridge (by incrementally stepping HL-93 loads across the bridge spans), maximum live load calculated at an abutment was 72.3 kips per lane.

For live load surcharge on the retained backfill (due to vehicles approaching the superstructure), AASHTO (1998) Section 3.11.6.4 recommends the use of the following empirical formula:

LS:

$$p_{ll} = k * \gamma_s * h_{eq} = 0.271(0.120\text{ kcf})(2.0\text{ ft}) = 0.110\text{ ksf equivalent lateral earth pressure}$$

where:

$$k = \text{coefficient of lateral earth pressure (active)} = \tan(45° - \frac{\varphi'}{2})^2 = 0.271$$

and:

h_{eq} = equivalent height of backfill = 2.0 ft (for retaining walls higher than 20 ft)

Factored-level Loads

Dead load on abutment, $P_{U_{DL}} = 1.25(82.2 \text{ k} + 31.5 \text{ k}) = 142.1 \text{ k}$ (per abutment)

Live load on abutment, $P_{U_{LL}} = 1.75(72.3 \text{ k}) = 126.5 \text{ k}$ (per lane)

Distributed load on bridge (DC + DW):

$$w_U = 1.25(7.4 \text{ klf} + 0.85 \text{ klf} + 1.12 \text{ klf}) + 1.50(0.61 \text{ klf}) = 12.63 \text{ klf}$$

To determine the amount of distributed load (w_U) transferred to the abutment, an analysis was performed using STAAD (2008) with a model consisting of rigid supports at the abutment and piers and a beam element (rigidity of a 1.46 ft deep x 33.17 ft wide reinforced concrete beam) for the bridge deck. The results of the analysis provided a load on the abutment of 141.5 kips due to the contribution of the distributed loads.

Load Distribution

Concentrated loads applied to the footing, P, from the bridge abutment were assumed to distribute evenly over a length of the footing, L, as shown in Figure B8. For the live loads, the length of one lane was assumed to be L = 10 ft. For the dead loads (DC and DW), the length of distribution was assumed to be the approximate length of the entire bridge (L = 35 ft). The resulting surcharge pressures, q, were:

Live load: $q_{U_{LL}} = \frac{127 \text{ k}}{6 \text{ ft}*10 \text{ ft}} = 2.1 \text{ ksf}$

Dead load: $q_{U_{DL}} = \frac{(142.1 \text{ k} + 141.5 \text{ k})}{6 \text{ ft}*35 \text{ ft}} = 1.4 \text{ ksf}$

Therefore the total factored surcharge load on the backfill from the bridge, $q_U = 3.5 \text{ ksf}$
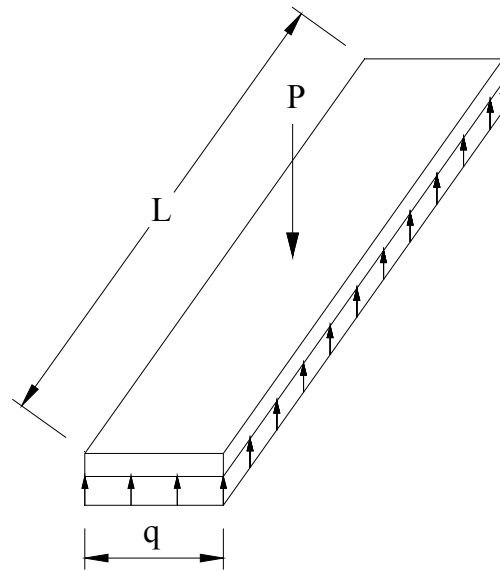
Figure B8. Diagram of load distribution from bridge abutment to footing.

Sheet Pile Retaining Wall Design

To determine the lateral earth pressure associated with this surcharge pressure, the load was assumed to act against a rigid wall (which is conservative due to the flexibility of sheet piling) and lateral earth pressure was calculated according to AASHTO (1998) Section 3.11.6.1. A diagram showing the analysis for the surcharge earth pressure is presented in Figure B9a. The resulting distribution of earth pressure was simplified for analysis as shown in Figure B9b; the peak lateral earth pressure was assumed to be 1.5 ksf at a depth of 6 ft from the top of the wall.

All of the loads applied to the sheet pile wall (from the loads associated with the abutment in profile in Figure B10a) are described with reference to the numbered loads in Figure B10b. For the design, the location of the anchor system was assumed to be 6 ft below the top of the wall; the location of the anchor was assumed to be a rigid support for translation (pinned). The modeling method for the analysis of the sheet pile wall is presented in Figure B10c. After selecting the location of the anchor, moments of all the loads on the wall are summed about the anchor location to determine the minimum depth of the wall for stability. For this design, the minimum required embedment depth was approximately 25 ft; the piling length ordered was 30 ft (additional factor of safety). To determine the most efficient location of the anchor (minimizing sheet pile length and tie rod force), several potential anchor locations should be analyzed.

a.) Surcharge on rigid wall   b.) Analysis results
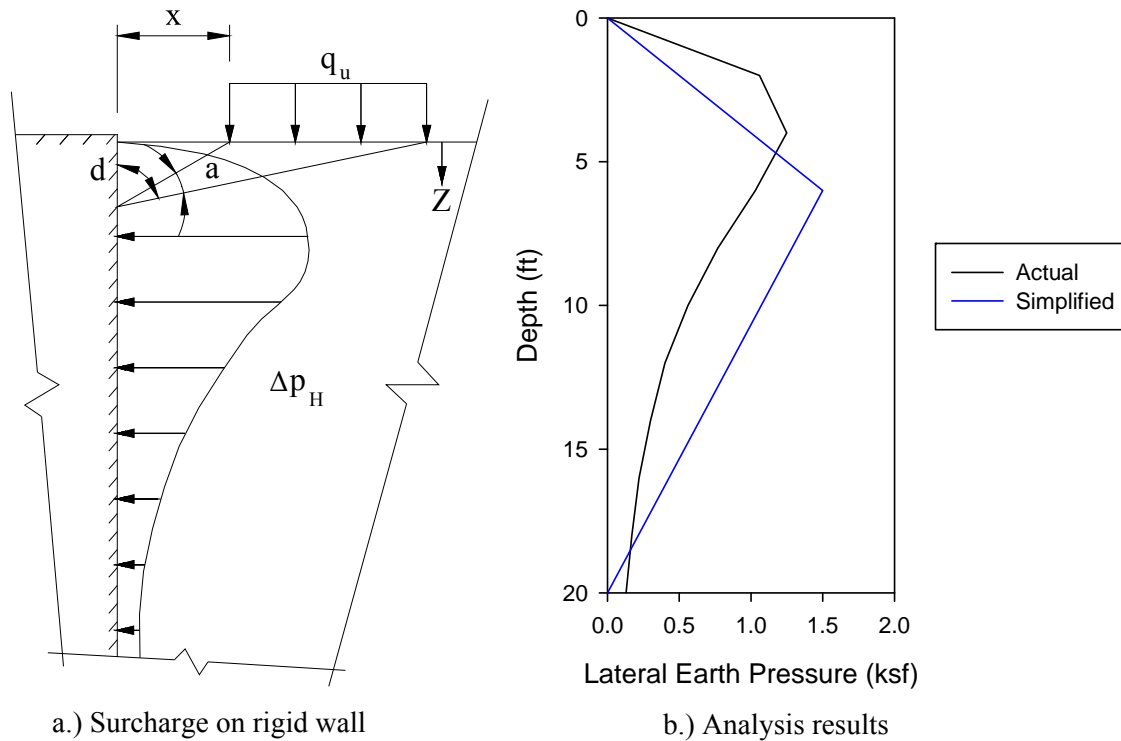
Figure B9. Determination of lateral earth pressure due to bridge surcharge loads.

Load 1 - Retained soil surcharge (behind abutment cap) and LL surcharge:

$$p_1 = 0.271(120 \text{ kcf})(6 \text{ ft soil depth})(1.50 \text{ ES load factor}) + (0.11 \text{ ksf}) = 0.40 \text{ ksf}$$

Load 2 - Retained soil active pressure:

$$p_2 = 0.271(0.120 \text{ kcf})(z)(1.50 \text{ EH load factor}) = 0.049(z) \text{ ksf} \text{ for } 0 < z \leq 13 \text{ ft}$$

$$p_2 = 0.271(0.120 \text{ kcf} - 0.0624 \text{ kcf})(z)(1.50 \text{ EH load factor}) + 0.64 \text{ ksf}$$

$$= 0.023(z - 13 \text{ ft}) \text{ ksf} \text{ for } 13 \text{ ft} \leq z$$

Load 3 - Bridge surcharge: $p_3 = 1.50$ ksf (previously calculated)

Load 4 – Passive soil pressure:

$$p_4 = 3.69(0.120 \text{ kcf} - 0.0624 \text{ kcf})(z) = 0.214(z - 13 \text{ ft}) \text{ ksf}$$

a.) Abutment overview   b.) Loading diagram   c.) Model for analysis
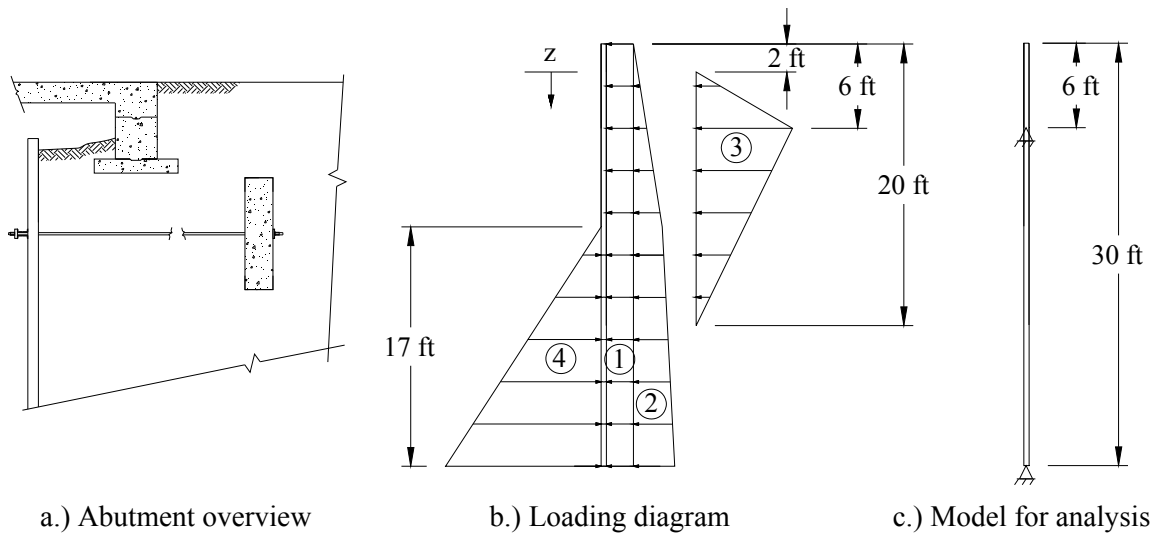
Figure B10. Design profile of sheet pile wall.

For analysis of the loading, the computer program STAAD (2008) was again used. The results of the analysis showed a bending moment of 38.6 ft-kip per ft width of wall and a tie rod force of 21.0 k per ft width of wall. The design shear force was the same as the tie rod force. The sheet pile section selected to resist the design shear and moment was the PZ 22 (moment capacity of 67.5 ft-kip).

Anchor System Design

For the design of the tie rods and anchor system, the skew of the abutment had to be taken into account as it required greater force in the rods as shown in Figure B11.

$$\sin 60° = \frac{21 \text{ k per ft}}{T} \qquad \qquad \therefore T = \frac{21 \text{ k per ft}}{\sin 60°} = 24.3 \text{ k per ft of wall}$$
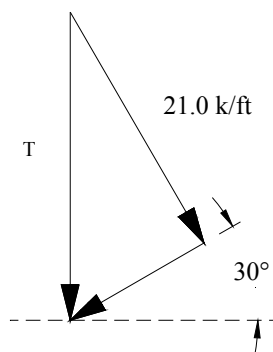
Figure B11. Tie rod force increase due to skew of abutment.

The anchor force was assumed to act over the width of the wall (42 ft) and thus a total force of 24.3 klf ∗ 42 ft = 1020.6 kips needed to be developed. The tie rods selected were #14, Grade 75 steel fully threaded rods. Each rod had a design strength φP$_n$ = 151 kips and thus 7 rods were required spaced 6 ft on center. For the design of the waler, an analysis was performed which modeled the waler as a beam with simple supports at each anchor location (6 ft on center) and applied a distribute tie rod force of 24.3 k per ft across the entire beam as shown in Figure B12. The analysis yielded a moment of 109.4 ft-kip (controlling factor in design). The sections selected to resist this load were two C9x20's (Grade 50 steel). The channels were spaced 3 in. apart as shown in Figure B13 and required two 0.25 in. thick stiffeners at the location of each tie rod to increase shear resistance and prevent flange-local buckling. The bearing plates were designed to develop the full strength of the tie rods and were required to be 6 in. x 6 in. x 2.25 in. The triangular legs of the bearing plates (shown in Figure B13b) needed to be 1 in. thick to prevent buckling under full tie rod loads. The design of the wingwall anchor system was performed similar to the primary wall using only one tie rod (#18 Grade 75 fully threaded rod) and bearing plates with legs to accommodate the different angles.

24.3 k/ft

2.5 ft   6 ft (Typ.)
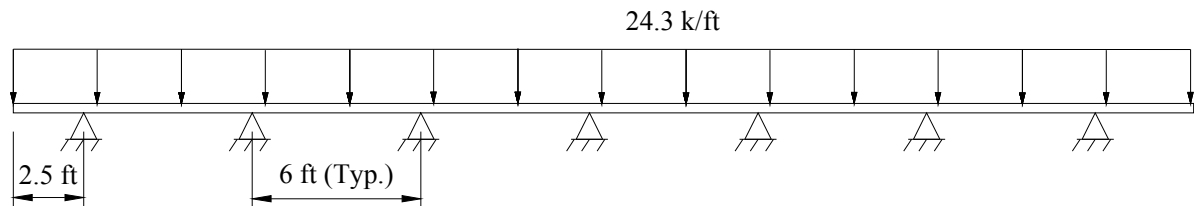
Figure B12. Waler analysis model.

a.) Cross-section of waler

b.) Isometric view of bearing plate
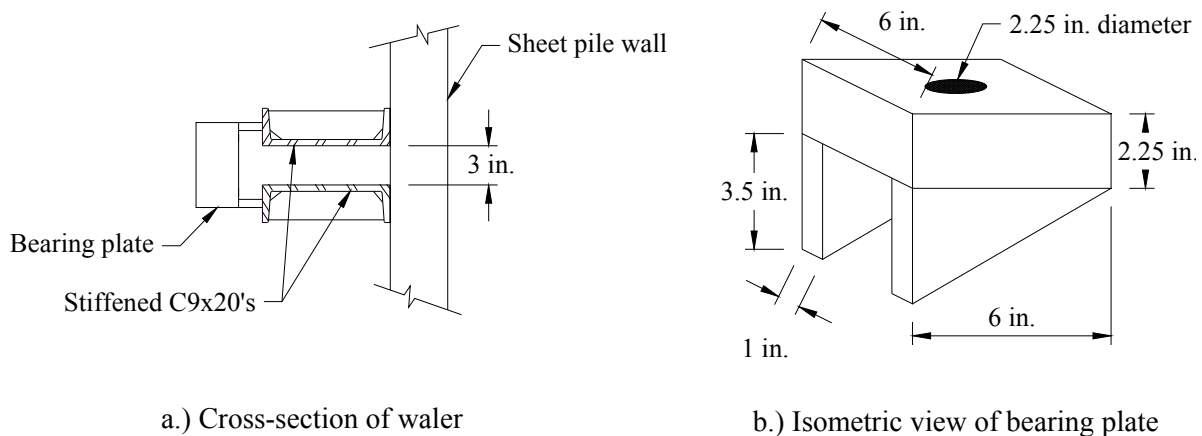
Figure B13. Cross-section of waler and tie rod bearing plate.

The reinforced concrete deadman needed to develop the full strength of the tie rods (24.3 k/ft). The anchor was located 6 ft below the top of the sheet pile wall which correlated to a depth of 10 ft below grade behind the bridge where the deadman was located. For the deadman to develop full resistance it had to be far enough from the sheet pile wall such that the passive soil zone of the deadman (which develops the resistance) does not intersect with the active soil zone of the wall (the failure plane of the backfill) as shown in Figure B14; this distance was approximately 45 ft.
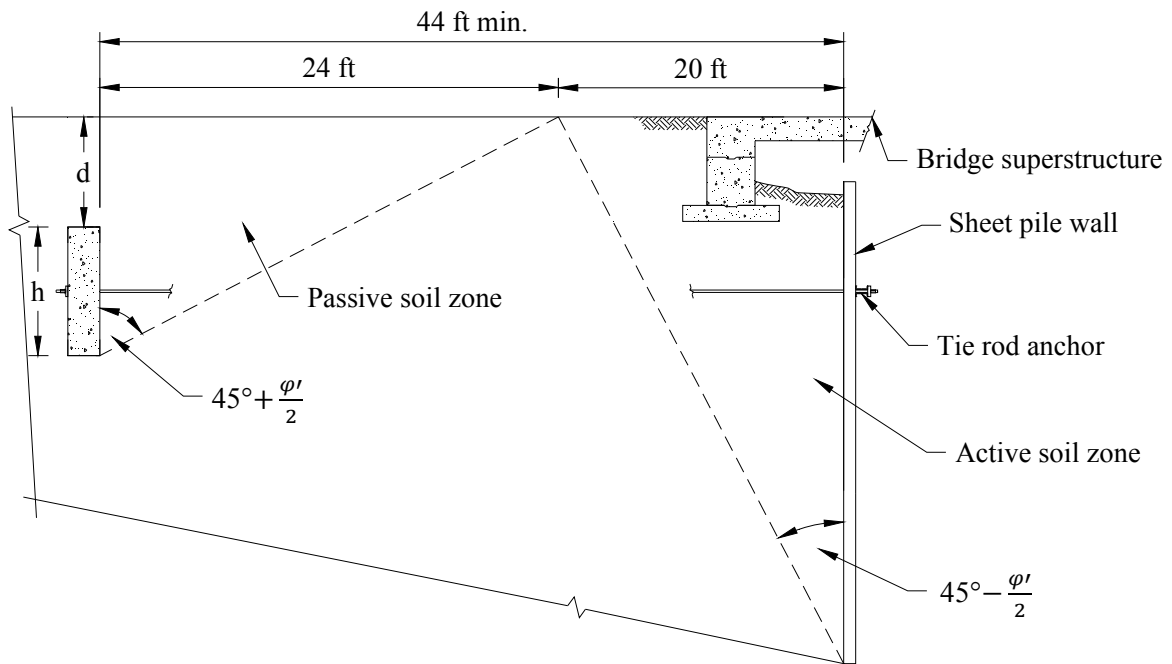
Figure B14. Required distance of deadman from sheet pile wall.

The resistance of the deadman was calculated as the net effect of the active and passive earth pressures. The selected deadman height to develop the strength of the tie rods was 8 ft. The net resistance, P_{net}, is calculated below assuming $\varphi' = 30°$ and $\gamma = 120$ pcf for the material around the deadman:

$$P_{passive} = k_p(\gamma)(d)h + 0.5(k_p)(\gamma)h^2 = 3.0(0.120 \text{ kcf})(6 \text{ ft})(8 \text{ ft}) + 0.5(3.0)(0.120 \text{ kcf})(8 \text{ ft})^2$$
$$= 28.8 \text{ k/ft}$$

$$P_{active} = k_p(\gamma)(d)h + 0.5(k_p)(\gamma)h^2] * EH$$
$$= [0.333(0.120 \text{ kcf})(6 \text{ ft})(8 \text{ ft}) + 0.5(0.333)(0.120 \text{ kcf})(8 \text{ ft})^2] * 1.50 = 4.8 \text{ k/ft}$$

$$P_{net} = P_{passive} - P_{active} = 24.0 \text{ k/ft}$$

Since base friction and the contribution of the flowable grout to resistance were neglected, P_{net} was considered sufficient for resisting the anchor force required for the wall. The dimensions of the deadman were 35 ft x 8 ft x 2 ft. For the design of reinforcement in the deadman, the tie rod force to be resisted was assumed to distribute evenly across the surface area of the deadman as shown in Figure B15:

$$w = \frac{24.3 \text{ k per ft}}{8 \text{ ft}} = 3.1 \text{ ksf}$$
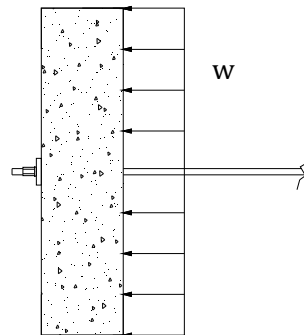
Figure B15. Load distribution for design of internal strength of deadman.

For transverse reinforcement, the design moment to be resisted was $M = \frac{3.1 \text{ ksf} * (4 \text{ ft})^2}{2} = 24.8 \text{ ft} -$ k per ft. The reinforcement selected to resist the transverse bending moment were #5's at 4 in. on center. The maximum shear force in the section ($V = 3.1 \text{ ksf} * 4 \text{ ft} = 12.4 \text{ k per ft}$) did not require the addition of shear reinforcement ($V_u \leq \frac{\emptyset V_c}{2}$). For the longitudinal direction, the deadman was designed for the same loads as the waler; a design moment of 109.4 ft-k and a shear of 72.9 k. The longitudinal reinforcement selected were #5's at 4 in. on center with no shear reinforcement required. The layout of reinforcement is presented in Figure B1 and Figure B2.

Spread Footing Design

As previously mentioned, the loads from the superstructure (transferred through the abutment cap) were assumed to distribute evenly over the spread footing; the design bearing pressure was 3500 psf.

The critical section for shear and flexure on the spread footing is shown in Figure B16. After adding the assumed weight of the footing to the bearing pressure, the design forces are calculated:

$$M_u = \frac{3.7 \text{ ksf} * (1.5 \text{ ft})^2}{2}(1\text{ft strip width}) = 4.1 \text{ ft} - k$$

$$V_u = 3.7 \text{ ksf}(1.5 \text{ ft})(1 \text{ ft strip width}) = 5.6 \text{ k}$$
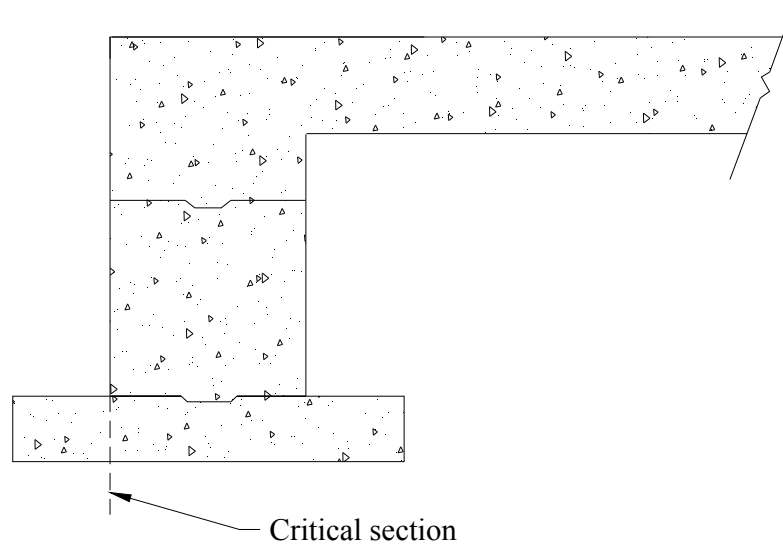
Figure B16. Critical section of spread footing for shear and flexure.

The reinforcement selected for the transverse direction were #4's at 7 in. on center with no shear reinforcement required. The longitudinal direction required reinforcement only for temperature and shrinkage induced stresses and were #4's at 8 in. on center. Details of reinforcement layouts are presented in Figure B1 and Figure B2.

Geogrid Reinforcement Design

As previously mentioned, the contribution of the geogrid reinforcement was not considered in the design of the sheet pile wall and anchor system thus an in depth design was not performed for this reinforcement. The design calculations are however included in this section for future designers.

Internal Strength of Geogrid Reinforcement

Each layer of geogrid must be designed to resist the total lateral earth pressure at the corresponding location in the GRS system. In the BC project, the maximum location of lateral earth pressure (due to bridge surcharge, live load surcharge, and retained soil) is approximately 6 ft below the top of the wall (see Figure B10b). The total earth pressure at this location:

$$\sigma_{max} = (1500 \text{ psf}) + (110 \text{ psf}) + 49 \text{ pcf} * (6 \text{ ft}) = 1904 \text{ psf}$$

The vertical spacing, S_v, of the geogrid layers was selected to be 1 ft. At the location of maximum lateral earth pressure, the geogrid must resist:

$$T = \sigma_{max} * S_v = 1904 \text{ psf}(1 \text{ ft}) = 1904 \text{ lb/ft}$$

A geogrid material should be selected with an ultimate strength of 1904 lb/lf. The ultimate strength of Tensar[®] BX1200 is 1310 lb/ft in the MD and 1970 lb/ft in the XMD with a 10% reduction in strength recommended to account for installation damage with gravel backfill. Although the BX1200 is sufficient in the XMD (the strong axis of the material), a material should have been selected with sufficient strength in both MD and XMD as earth pressure loads on the material will be the same in each direction. An alternative to selecting stronger material would be to reduce the vertical spacing of geogrid layers.

External Stability of Reinforcement

To develop the full strength of the geogrid material, sufficient embedment must be provided or another means of mechanically developing the strength (such as wrapping each layer into the layer above as shown in Figure B2). To provide sufficient embedment length, the geogrid layer must extend beyond the active zone of the backfill (shown in Figure B14) soil a minimum length that develops the ultimate strength of the material through friction against the surrounding soil (calculated by an accepted method).

Other Design Considerations

The factor of safety of the GRS mass must also be satisfied for sliding, overturning, slumping failure, and bearing capacity on the material at the base of the excavation.

Example Analysis Calculations for Live Load Test Data Comparison

This section of Appendix B provides the methods and assumptions used in calculating the values presented in Table 5-26 through Table 5-31; calculations for test Run D, Location 5 are presented to demonstrate the methods used.

It should be noted that the "estimated" values are calculated using the same approach that was used for the design of the bridge; this was done to provide a reference value (stress or deflection) for comparison of the data collected during the live load testing. Although the load distribution and analysis methods may not accurately predict the behavior of the structure, the comparison of the theoretical analysis to the live load test data will provide an indication of the adequacy (i.e., conservative or unconservative) of the design method utilized. In the following section of Appendix B, an alternative analysis of the superstructure and spread footing is presented to provide a more accurate estimate of the loads on the GRS backfill transmitted through the spread footing.

Locations of each of the truck wheels are determined from dimensions measured in the field and are labeled in Figure B17. The load applied to the bridge per wheel is:

- 10.12 kips for wheels 1, 2, 5, and 6.
- 8.71 kips for wheels 3, 4, 7, and 8.
- 7.71 kips for wheels 9 and 10.
- 7.70 kips for wheels 11 and 12.
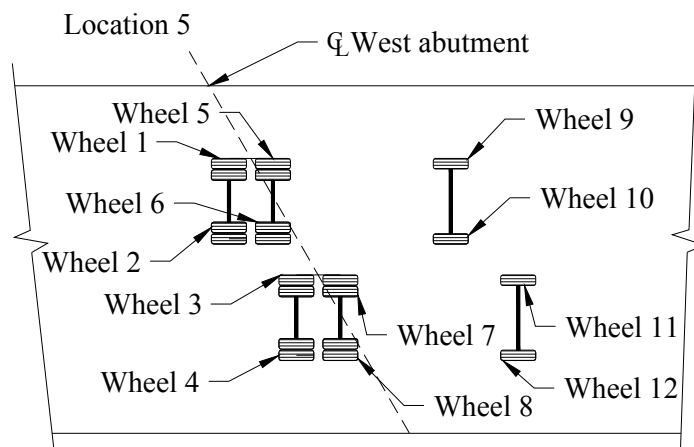
Figure B17. Wheel numbering system.

The longitudinal distance (x-direction) of each wheel from the centerline bearing of the west abutment is presented in Table B1; negative values are to the west of centerline (off the bridge) and positive values are to the east. A cross-section of the west bridge abutment showing the locations of each wheel load is presented in Figure B18; all wheels on the bridge or within the boundary of the spread footing (within 3 ft of bearing centerline) are assumed to be applied to the backfill through the spread footing (only wheels 2 and 4 are not through the footing).
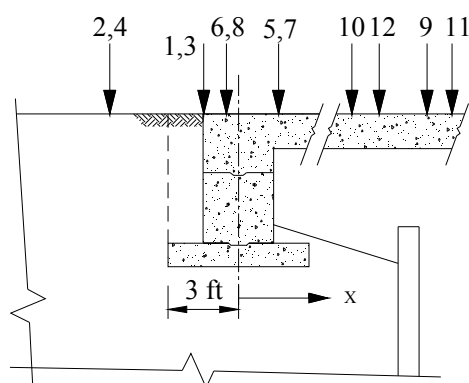
Figure B18. Profile of west bridge abutment wheel loads.

Table B1. Wheel distance from centerline bearing of the west abutment.

Wheel	Long. Distance from centerline of west abutment, x (ft)
1	-2.2
2	-5.8
3	-2.3
4	-5.9
5	+2.2
6	-1.4
7	+2.3
8	-1.3
9	+17.3
10	+13.8
11	+18.4
12	+14.8

To determine the dead load applied to the sheet pile bridge abutment system backfill, the superstructure was modeled with STAAD (2008) to determine the dead load distributed to the

abutment. The total dead load (including weight of the superstructure, the abutment cap, and the spread footing) was determined to be 206,500 lbs. The area of the spread footing was 229.43 ft^2, thus the dead load surcharge on the backfill applied through the spread footing is calculated to be 900 psf.

For application of wheel live loads on the bridge superstructure, the load distribution methods utilized are the same for which the bridge was designed (10 ft width per loaded lane) to investigate the accuracy of the design methods used. Since two trucks are present in Run D, the distribution width of the live loads is 20 ft (2 lanes). The adequacy of this assumed load distribution is investigated in the next section of Appendix B which presents an alternate analysis for test Run D, Location 5.

An analysis was performed considering the bridge deck to be a continuous beam with simple supports at each abutment and both piers. The moment of inertia of the bridge deck (for the full width of the bridge) was calculated by ISU, using an uncracked section including the contribution of the steel reinforcement, to be:

Between supports: $I_{span} = 216,632 \text{ in}^4$

Over the piers: $I_{pier} = 935,764 \text{ in}^4$

The analysis of the superstructure provided bending moments along the bridge as well as support reactions at the abutments.   The total live load reaction applied to the west abutment was 69,340 lbs. Assuming this is distributed over the 20 ft length of the 6 ft wide spread footing, the live load surcharge applied through the spread footing to the backfill is 578 psf.

For determination of the expected earth pressures at each pressure cell (both total and live load only), stresses below the footing were estimated using the stress influence factor method presented by Coduto (2001); for a continuous spread footing of 6 ft width, the strain influence factors determined for the three vertical earth pressure cells are given in Table B2. The vertical earth pressure, $\Delta\sigma_v$, at each cell was then determined by:

$$\Delta\sigma_v = I_\sigma(\Delta q)$$

where

$\Delta\sigma_v$ = Change in vertical earth pressure due to surcharge load (psf)
I_σ = Stress influence factor determined from Fig. 7.2 in Coduto (2001)
Δq = Surcharge load applied by spread footing on backfill (psf)

thus the vertical earth pressure at each cell is calculated by:

$$\Delta\sigma_{v_{LL}} = 0.97(578 \text{ psf}) = 560.7 \text{ psf}$$

$$\Delta\sigma_{v_{DL}} = 0.97(900 \text{ psf}) = 873.0 \text{ psf}$$

$$\Delta\sigma_{v_{Load\ 1}} = \Delta\sigma_{v_{DL}} + \Delta\sigma_{v_{LL}} = 560.7 \text{ psf} + 873.0 \text{ psf} = 1433.7 \text{ psf}$$

Table B2. Strain influence factors determined from Figure 7.2 in Coduto (2001).

Pressure Cell	Stress Influence Factor
D1	0.97
D2	0.78
D3	0.53

As previously mentioned, Load 1 refers to loads or deformations relative to zero readings taken after the construction of the west sheet pile bridge abutment system (including the abutment cap and spread footing) was completed; loads and deformations due to construction of the abutment (such as backfill material, compaction, etc.) are therefore not included.

For earth pressure Cells C1, C2, and C3, the horizontal earth pressure, σ_h, was approximated using an active earth pressure coefficient of 0.271 ($\varphi' = 30$ degrees) with the vertical earth pressure estimated at corresponding Cells D1, D2, and D3; the calculation is shown:

$$\sigma_h = \sigma_v * k_a$$

For Cell C1:

$$\sigma_{h_{LL}} = 560.7 \text{ psf} * 0.271 = 152.0 \text{ psf}$$

$$\sigma_{h_{DL}} = 900 \text{ psf} * 0.97 * 0.271 = 236.6 \text{ psf}$$

Live load surcharge effects from the wheel loads on the backfill (wheels 2 and 4) must also be included to estimate the horizontal earth pressures; these loads are calculated using AASHTO (1998) Equation 3.11.6.1-3. For Cell C1, the horizontal earth pressure due to wheels 2 and 4 were determined to be 18.8 psf and 10.9 psf, respectively; the estimated earth pressure in Cell C1 is calculated below:

$$\sigma_{h_{Load\ 1}} = 152.0\ \text{psf} + 256.8\ \text{psf} + 18.8\ \text{psf} + 10.9\ \text{psf} = 439\ \text{psf}$$

The method used to calculate the horizontal loads from the wheel loads applied to the backfill is intended for estimating the loads on a rigid wall. Since Cells C1, C2, and C3 are 4.5 ft back from the wall, use of this method overestimates the loads.

For horizontal loads near the sheet pile wall (acting on Cells B1 and B2 as well as the instrumented sheet pile) a different method of analysis was used. Loads acting through the footing were applied laterally to the sheet pile wall according to AASHTO (1998) Section 3.11.6.1 (described in the design calculations section of this Appendix); the load distribution was approximated for analysis (refer to Figure B9b). Partial results of the analysis for a live load surcharge of $q = 578\ psf$ are presented in Table B3:

Table B3. Horizontal earth pressure due to live load surcharge from the spread footing at the face of the sheet pile wall.

Depth below footing (ft)	$\sigma_{h_{LL_1}}$ (psf)
0.0	0.0
0.5	54.3
1.0	103.6
1.5	144.2
2.0	174.4
2.5	194.2
3.0	204.9
3.5	208.2

Cells B1 and B2 are 0.5 ft and 3.5 ft below the base of the spread footing and thus the horizontal earth pressures (due to superstructure live loads applied through the footing only) at these locations are 54.3 psf and 208.2 psf, respectively. The wheel loads not applied through the footing (wheels 2 and 4) are analyzed according to AASHTO (1998) Equation 3.11.6.1-3; the resulting horizontal earth pressures due to the wheel loads on the backfill are presented in Table B4.

Table B4. Horizontal earth pressure due to wheel loads on the backfill at the face of the sheet pile wall.

Depth below wheel (ft)	$\sigma_{h_{LL_2}}$ (psf)	
	Wheel 2	Wheel 4
7.5	15.6	6.3
8.0	15.3	6.3
8.5	14.9	6.3
9.0	14.4	6.2
9.5	13.9	6.2
10.0	13.3	6.0
10.5	12.8	5.9

The bottom of the footing is approximately 7.0 ft below the elevation of the road (where the wheel loads are applied) therefore Cells B1 and B2 are 7.5 ft and 10.5 ft below the road, respectively. The estimated earth pressures (due to live loads only) in Cells B1 and B2 are calculated below:

Cell B1: $\quad\quad \sigma_{h_{LL}} = \sigma_{h_{LL_1}} + \sigma_{h_{LL_2}} = 54.3 \text{ psf} + 15.6 \text{ psf} + 6.3 \text{ psf} = 76.2 \text{ psf}$

Cell B2: $\quad\quad \sigma_{h_{LL}} = \sigma_{h_{LL_1}} + \sigma_{h_{LL_2}} = 208.2 \text{ psf} + 12.8 \text{ psf} + 5.9 \text{ psf} = 226.9 \text{ psf}$

It should be noted that, for the previous equations, estimation of Load 1 values are performed by including the superstructure dead loads in the analyses.

The sheet pile wall was analyzed (for both live load and total load conditions) as a beam with simple supports at the base and the location of the tie rod anchor system (6 ft below the top of the wall). Figure B19 presents a loading and support diagram for the sheet pile wall; Surcharge Pressure 1 represents the horizontal earth pressure due to live loads on the superstructure and Surcharge Pressure 2 represents the horizontal earth pressure due to wheel live loads on the backfill (the upper portion of Surcharge Pressure 2 is resisted by the superstructure). The wall analysis, performed using STAAD (2008), provided bending moments and deflections along the length of the sheet pile wall as well as the tie rod anchor force; all values were calculated per 1 ft width of wall.
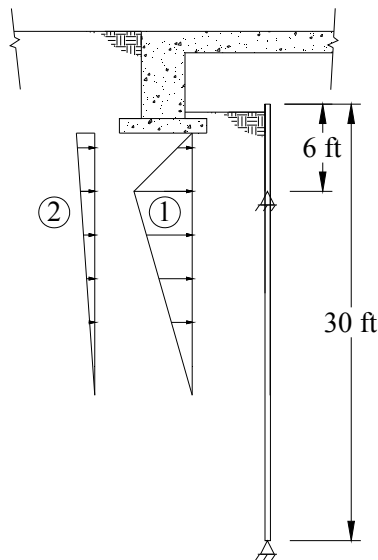
Figure B19. Loading and support diagram for analysis of sheet pile wall.

The tie rod force output from the analysis was 1.765 k/ft. The tie rod stress, σ_T, was calculated as shown:

$$\sigma_T = (\text{force per width}) * \frac{\text{tie rod spacing}}{\text{tie rod area}} = (1.765 \text{ k/ft}) * \frac{6 \text{ ft}}{2.25 \text{ in}^2} = 5.52 \text{ ksi}$$

At the location of wall strain Gages A1 and A2 (6 ft below the top of the wall), the bending moment in the wall was 0.551 k-ft. The section modulus of a PZ 22 sheet pile is 18.1 in³/ft. The flexural stress (at the extreme fibers) at location A1/A2 is calculated as shown:

$$\sigma_{f_{A1/A2}} = \frac{M}{S} = (0.551 \text{ k} - \text{ft}) * \frac{12}{18.1 \text{ in}^3} = 0.37 \text{ ksi}$$

The resulting bending moments from the bridge deck analysis (described previously) were used to determine the expected flexural stresses at the locations instrumented (the west span and over the west pier). The calculation for flexural stress over the west pier is shown:

$$\sigma_{f_{pier}} = \frac{M * c}{I_{pier}} = \frac{(77.36 \text{ k} - \text{ft}) * 12 \frac{\text{in}}{\text{ft}} * (29.5 \text{ in} - 15.33 \text{ in})}{935,764 \text{ in}^4} = 0.01 \text{ ksi}$$

For estimating the stress in the wingwall tie rod, the force per unit width for the analysis for the main wall was used; force was assumed to be applied over the 14 ft depth (the perpendicular distance back from the main wall) of the wingwall. The wingwall tie rod stress is calculated below:

$$\sigma_T = (1.765 \text{ k/ft}) * \frac{14 \text{ ft}}{4 \text{ in}^2} = 6.18 \text{ ksi}$$

Although the east abutment was instrumented with deflection transducers, analysis of the bridge deck provided a live load reaction on the east abutment of 0.006 psf; wall deflection was estimated to be 0.000 in.

For the estimation of pressures on Cells X1 (at the concrete deadman face) and X2 (the southwest wingwall face), loads in the tie rods were used to determine the corresponding distributed loads on the deadman and wingwall, respectively; estimation for Cell X1 is shown below:

Earth pressure at Cell X1 (deadman):

$$T = (\text{force per width}) * (\text{spacing}) * (7 \text{ rods}) = \left(1.765 \frac{\text{lb}}{\text{ft}}\right) * 6\text{ft} * 7 = 112{,}150 \text{ lb}$$

$$\sigma_{\text{deadman}} = \frac{\text{total tie rod force}}{\text{area of deadman}} = \frac{112{,}150 \text{ lb}}{8 \text{ ft} * 35 \text{ ft}} = 401 \text{ psf}$$

Earth pressure at Cell X2 (wingwall):

$$T = (\text{force per width}) * (\text{depth of wingwall}) = \left(1{,}765 \frac{\text{lb}}{\text{ft}}\right) * 14 \text{ ft} = 24{,}710 \text{ lb}$$

$$\sigma_{\text{wingwall}} = \frac{\text{total tie rod force}}{\text{area of wingwall}} = \frac{24{,}710 \text{ lb}}{14 \text{ ft} * 30 \text{ ft}} = 59 \text{ psf}$$

It should be noted that the tie rod force per unit width is a maximum estimate; the use of this tie rod force for estimating the earth pressure at the deadman will overestimate loads (not all tie rods are loaded to maximum at once); this method also is applied with the assumption that all loads applied to the deadman are distributed evenly across the area.

Analysis of Spread Footing Load Distribution

In the preceding analyses, live loads on the superstructure were assumed to distribute over a 10 ft width through the abutment cap and spread footing for calculation of loads and deflections to be compared with data recorded during the live load testing. As previously mentioned, this analysis assumption was the same as that which was used in the design of the sheet pile bridge abutment system; the live load test data was subsequently compared to the theoretical analysis results to determine the adequacy of the design approach utilized.

In this section of the Appendix, an analysis of the superstructure and spread footing, created in STAAD (2008) using beam elements, is analyzed for test Run D, Location 5 to provide a more accurate estimate of the loads on the GRS backfill transmitted through the spread footing. The backfill soil was modeled as a series of springs, spaced 1 ft on center, along the length of the spread footing. The resistance of each spring was determined using a modulus of subgrade reaction of 250 lb/in^3; this value was assumed using a correlation by Iowa Statewide Urban Design and Specifications (2009) for subgrade modulus based on crushed stone with a CBR of 50 (determined from the DCP test results presented previously in Figure 5-82a). The spring constant utilized for each support, representing a 1 ft long increment of the 6 ft wide footing, was determined to be 2592 k/ft.

The complete model analyzed is presented in Figure B20. The bridge deck was modeled as four lines of beam elements (positioned corresponding to each line of test truck wheels during Run D); the beam element properties were selected to represent tributary widths of the deck slab. The abutment cap and spread footing was modeled as a transverse beam supported by the spring supports previously described. The interior piers and the east abutment of the bridge were modeled as pinned supports along the beams.
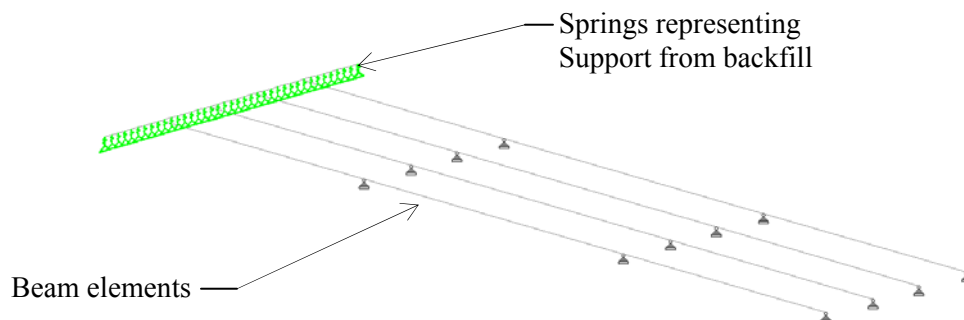
Figure B20. Model of superstructure and west abutment in BC, Iowa.

The analysis resulted in a reaction force of 2,612 lb in the spring support located over Pressure Cell D1; dividing this force over the represented footing area of 6 ft^2 resulted in a live load surcharge pressure of 435 psf. The live load surcharge pressure calculated using the 10 ft distribution method (described in the previous section of Appendix B) was 578 psf; the method of load distribution utilized in design was conservative (according to this analysis and live load test data).

The remaining loads and deflections were calculated using the same methods described in the previous section of Appendix B. Due to uncertainty in the degree of fixity at the base of the wall, two analyses were performed; the results for both a pinned and fixed support at the base of wall are presented in Table B5.

Table B5. Results of analysis for determining footing load distribution with both pinned and fixed support at base of wall.

Load or deflection	Live Loads Only	
	Pinned Base	Fixed Base
Vertical earth pressure		
D1	420 psf	420 psf
D2	340 psf	340 psf
D3	230 psf	230 psf
Horizontal earth pressure		
C1	115 psf	115 psf
C2	90 psf	90 psf
C3	60 psf	60 psf
B1	60 psf	60 psf
B2	175 psf	175 psf
X1 (deadman)	210 psf	195 psf
X2 (wingwall)	45 psf	45 psf
Wall flexural stress		
A1/A2	0.38 ksi	0.38 ksi
A3/A4	1.87 ksi	1.49 ksi
A5/A6	1.71 ksi	0.95 ksi
A7/A8	0.86 ksi	0.54 ksi
2 ft below top of wall	0.00 ksi	0.00 ksi
Tie rod axial stress		
main wall (max)	3.74 ksi	3.49 ksi
wingwall	4.91 ksi	4.58 ksi
Bridge deck stress		
over pier (max)	0.07 ksi	0.07 ksi
west span (max)	0.10 ksi	0.10 ksi
Wall displacements		
west (max)	0.066 in.	0.040 in.
east (max)	0.000 in.	0.000 in.

When comparing these results with the data presented in Table 5-26 (Run D, Location 5 analyzed using the original method of a 10 ft live load distribution through the footing), the method of analysis used in this section provides theoretical results that are, in general, more accurate. The earth pressure calculated for Cell D1 was within 3% of the actual test data although calculations for the other pressure cells were still significantly overestimated.

Analysis as a fixed base provided reductions in wall displacements and stresses but continued to overestimate the test data; the contribution of the geogrid in the backfill soil (which was not accounted for in analysis or design) significantly reduces the loading on the sheet pile wall. Stresses in the bridge deck (over the pier and in the west span of the bridge) were more accurately estimated with this model, suggesting that use of a 10 ft load distribution for wheel loads on the bridge deck was not an appropriate method (the load distribution is more concentrated).

APPENDIX C: TAMA COUNTY

EXPERIMENTAL BRIDGE 3

ESTIMATED QUANTITIES FOR SUBSTRUCTURE PER ONE ABUTMENT

ITEM	UNITS	Qty.	LENGTH	WEIGHT	UNITS
Main Wall PZC13	EA	10	40'	202	CWT
Wing Wall PZC13	EA	10	40'	202	CWT
Wing Wall PZC13	EA	8	30'	122	CWT
PilePro PZ-COLT	EA	2	40'	547	LB
Eng. Fabric (per 4196.01b)	SY	200			
Tensar BX1200 Geogrid	SY	1200			
1½" Roadstone	CY	240			
Porous Backfill	CY	40			
10"x10" Timbers	EA	14	20'		

ESTIMATED QUANTITIES FOR THREADROD ANCHOR SYSTEM (per abt.)

ITEM	UNITS	Qty.	LENGTH	Min.	UNITS
Structural Concrete	CY	2			
RRFC Strut	EA	4	2'-6"	$Z_x = 138$	IN³
Top Waler Strut	EA	5	2'-0"	W8	
Bottom Waler Strut	EA	5	2'-0"	W8	
Wingwall Waler	EA	2	19'-0"	$Z_x = 31$	IN³
Top Wall Waler	EA	1	20'-0"	$Z_x = 44$	IN³
Bottom Wall Waler	EA	1	20'-0"	$Z_x = 94$	IN³
RRFC Waler	EA	1	16'-0"	T = 18	IN
5c1 – Strut Reinforcement	EA	15	1'-4"	21	LB
PL 4x4x1½ (2¼" hole in center)	EA	8			
PL 4x4x1½ (1¾" hole in center)	EA	2			
Angled PL 4x4x2⅜" (Detail 1)	EA	8			
Angled PL 4x4x2⅜" (Detail 2)	EA	2			

BILL OF A722 THREADRODS PER ONE ABUTMENT

ITEM	SHAPE	BAR	No.	LENGTH*	WEIGHT	UNITS
1¾" dia. Threadrods		14b1	4	33'	1218	LB
1¾" dia. Threadrods		10b2	2	26'	228	LB
Wingwall Threadrod		10o2	1	35'	154	LB
Wingwall Threadrod		10o3	1	41'	180	LB
Wingwall Threadrod		10o4	1	47'	206	LB
Wingwall Threadrod		10o5	1	53'	233	LB
					Total: 2219	

*Note: Lengths given are desired total length.
Couplers may be used for splicing bars.

See Detail 1

#10 Threadrod (A722)

Hex nut/washer for #10 rod

Waler struts (top and bottom sections) use minimum W8 sections

3 spaces @ 3'

19'-7"
23'-3"
18'-11"

14b1
10b2
14b1
10b2
14b1

10o2
10o3
10o4
10o5

Logging rods

Geogrid zone

PL 4"x4"x1½" (2¼" hole, center)

Section A–A

W-Shape bent about weak-axis (min. $Z_x = 31.0$ in³)
1½" Threadrod
See Detail 1

Section B–B

10" x 10" timbers (1800 psi all. stress)
Logging rods

Alternative Footing

#6's @ 18" o.c.
#6's @ 5" o.c.
Drill 1¾" hole centered on plate
*min. A36 steel

Section E–E

Detail 1

Drill 1¾" hole centered on plate
*min. Gr. 50 steel

Reinforced concrete

Detail 1 (Alternate)

Notes: #5 reinforcement and struts must be welded to RRFC for development of strength.

RRFC Strut
5c1
18 spaces @ 10" o.c. (min. $Z_x = 138$ in³)

Section F–F

TAMA COUNTY
79' x 17'-2" RRFC BRIDGE
ABUTMENT PLAN
SHEET 1 OF 5

Figure C1. Plan view of abutment for demonstration project in TC, Iowa.

Notes:

Superstructure consists of two 89' Rail-Road Flat Cars (RRFCs). Bridge abutments designed for HL-93 loading.

Structural concrete to be normalweight with f'c = 4ksi.
Structural steel Grade 50.
Steel reinforcement Grade 60.
Threadrod steel Grade 150.
Bearing plate steel Grade 36 (unless otherwise noted).

Clear cover of 3' to be provided for all reinforced concrete structures. Minimum 1" clear spacing to be provided for all reinforcement.

Wingwall bearing plates require special fabrication (see Detail 1). All threadrods shall be obtained from Dywidag Systems International, Inc.

Sheet pile wall to be driven with existing abutment in place.

Excavation behind existing abutment to be performed down to level of tie rods. Geogrid reinforcement zone to consist of 7 layers of geogrid reinforcement with 12" of 1½' crushed roadstone between each layer. Roadstone must conform to gradation requirements, be placed in a maximum lift thickness of 6', and be compacted to min. 98% standard effort compaction test (ASTM D698) within 2% of optimum moisture content.

Geogrid to be Tensar BX1200 (available in 9.8' x 164' rolls). Each layer to be laid in strips, perpendicular to abutment wall, with a 12" min. overlap between strips. Edges of each layer to be folded over fill layer above (as shown in abutment cross-section) according to manufacturer's recommendations.

Excavated material may be used as fill outside of geogrid reinforcement zone provided it is moisture conditioned and free of deleterious material. Fill must be placed in maximum 8" lifts and compacted to min. 98% of ASTM D698 and placed within 2% of optimum moisture content.

After backfilling is completed, abutment to be flooded with water pumped from stream prior to placement of the bridge superstructure in coordination with Iowa State team.

The four bottom wall tie rods are to be positioned so they bear as near as possible to the RRFC struts attached to the superstructure. Top wall rods may be placed in between RRFC struts.

Wall waler to be a W-section bent about its weak axis (min plastic modulus for top and bottom are 44 in^3 and 94 in^3, respectively). To obtain correct angle for each waler, 5 struts (per waler) are to be fabricated from W-sections as shown in details 3 and 4. Struts must be welded to the sheet pile wall with a minimum length of weld as shown.

Guardrail to be provided by Tama County.

Geogrid zone to be wrapped on all sides with layer of engineering fabric.

Timbers for the bridge footing are to be lagged together and bolted to the RRFC units (each individual footing will be 10' by 10' in plan). Timbers used must have a minimum allowable flexural stress of 1800 psi. An alternative reinforced concrete footing is shown on Sheet 1.

TAMA COUNTY

79' x 17'-2" RRFC BRIDGE

ABUTMENT CROSS-SECTION

SHEET 2 OF 5

Scale   5'—0"

2 – 89' RRFC's

59' cl. to cl.

89'

79' cl brg. to cl. brg.

min. Z=43.2 in^3 about week axis
W-shape cut to 25' (see Detail 4)

PL 4x4x1½
(1¾" hole drilled through center)

min. Z=93.3 in^3 about week axis
W-shape cut to 45' (see Detail 3)

PL 4x4x1½
(2¼" hole drilled through center)

PZC 13

See Detail 3
See Detail 2

Cut through timbers for top tie rods

Engineering fabric layer (all sides of geogrid zone)

7 layers bioxial geogrid (1'-0" layer spacing)

10a5 10a4 10a3 10a2
14b1
10b2

Porous backfill

Subdrain (see Sheet 4)

Existing timber structure (trimmed to excavation level)

8'

18'

20'

10'

W—Section
Detail 4
25°
45°
Drill 1¾" hole centered on plate
*min. Gr. 50 steel
4"

W—Section
Detail 3

Detail 2
4"
5"
2-3/8"
4"

Detail 2 (alternate)
4"
2.5"
Drill 1¾" hole centered on plate
*min. A36 steel
4"

Please Note:
This project is part of a research study for Iowa State University (ISU) and will be equipped with instrumentation not shown on these plans. ISU researchers will be present for documentation purposes and will be pausing construction at various stages for installation of monitoring equipment. Please contact Ryan Evans @ (952) 215-4767 with any questions.

Figure C2. Cross-section of abutment for demonstration project in TC, Iowa.

Figure C3. Profile of abutment for demonstration project in TC, Iowa.

TAMA COUNTY

79' x 17'-2" RRFC BRIDGE

ABUTMENT PROFILE

SHEET 3 OF 5

Section C–C

Section D–D

Bolt together

17'-2"

2'-6"

2"

Bolt timbers to RRFC's
(Do not center RRFC on 10'x10' pad)

20'

10'

5'-8"

8"

4'

10"

Figure C4. Situation plan and drainage system details for demonstration project in TC, Iowa.

Figure C5. Profile of bridge for demonstration project in TC, Iowa.

ESTIMATED QUANTITIES FOR SUBSTRUCTURE PER ONE ABUTMENT

ITEM	UNITS	Qty.	LENGTH	WEIGHT	UNITS
Main Wall PZ27	EA	10	50'	203	CWT
Wing Wall PZ27	EA	14	40'	227	CWT
Wing Wall PZ27	EA	14	20'	114	CWT
W12x96	EA	5	50'	24000	LB
PilePro BBS (M)	EA	5	50'	2150	LB
PilePro BBS (F)	EA	5	50'	2275	LB
PilePro PZ-COLT	EA	2	40'	547	LB
Eng. Fabric (per 4196.01b)	SY	200			
Tensar BX1200 Geogrid	SY	900			
1½" Roadstone	CY	240			
Porous Backfill	CY	40			
10"x10" Timbers	EA	14	20'		

ESTIMATED QUANTITIES FOR DEADMAN ANCHOR SYSTEM

ITEM	UNITS	Qty.	LENGTH	WEIGHT	UNITS
Structural Concrete	CY	12			
HSS 12x10x⅜	EA	3	20'	2160	LB
Flowable Grout (non-shrink)	CY	3			
PL 4x4x1 (A36)	EA	8		37	LB
Angled PL 4x4x1 (see Detail 1)	EA	8		109	LB
Hex Nuts/Washers for #14	EA	16			

BILL OF REINFORCING STEEL PER ONE ABUTMENT

ITEM	SHAPE	BAR	No.	LENGTH*	WEIGHT	UNITS
Main Wall Threadrods		14a1	4	60'	1836	LB
Wingwall Threadrod		14a2	1	35'	268	LB
Wingwall Threadrod		14a3	1	41'	314	LB
Wingwall Threadrod		14a4	1	47'	360	LB
Wingwall Threadrod		14a5	1	53'	406	LB
Deadman Longitudinal		5b1	32	19'-6"	651	LB
Deadman Transverse		5b2	26	7'-6"	203	LB
Deadman Transverse Hoop		5b3	14	19'-0"	277	LB
				Total:	4315	

*Note: Lengths given are desired total length. Couplers may be used for splicing bars.

BAR BEND DETAIL

5b3 D=¾" 1'-6½" 7'-6"

Notes:

All quantity estimates are per abutment.

Footing timbers to be lagged together to form two 10' by 10' bearing pads. Each pad to then be bolted to a RRFC as shown in Section D-D (see Sheet 2).

See continued construction and design notes on Sheet 2.

TAMA COUNTY

79' x 17'-2" RRFC BRIDGE

ABUTMENT PLAN

SHEET 1 OF 5

5'-0"

Scale

PZ-Colt Connector
PZ-27
BBS Connector (Male)
BBS Connector (Female)
W12x96

Place rods through webs of sheet piling

Lagging rods

Geogrid zone

Section A-A

Section B-B

HSS 12x10x⅜
Flowable Grout
#14 Threadrod
See Detail 1

10' x 10" timbers (1800 psi all. stress)

Lagging rods

Alternative Footing

Reinforced concrete

Detail 1

Drill 2¼" hole centered on plate
(A36 steel)

See Detail 1
#14 Threadrod
Hex nut/washer for #14 rod (epoxy coated)

PL 4x4x1 (Drill 2¼" hole centered on plate)

#6's @ 18" o.c.
#6's @ 5" o.c.

Section F-E

39 spaces @ 6" ea.

Please Note:

This project is part of a research study for Iowa State University (ISU) and will be equipped with instrumentation not shown on these plans. ISU researchers will be present for documentation purposes and will be pausing construction at various stages for installation of monitoring equipment. Please contact Ryan Evans @ (992) 215-4767 with any questions.

Figure C6. Abutment plan (alternative system) for demonstration project in TC, Iowa.

Notes:

Superstructure consists of two 89' Rail-Road Flat Cars (RRFC's). Bridge abutments designed for HL-93 loading.

Structural concrete to be normalweight with f'c = 4ksi.
Structural steel Grade 50.
Steel reinforcement Grade 60.
Threadrod steel Grade 75.
Bearing plate steel Grade 36.

Clear cover of 3" to be provided for all reinforced concrete structures. Minimum 1" clear spacing to be provided for all reinforcement.

Threadrods (and corresponding hex nuts and washers) to be epoxy coated. Wingwall bearing plates require special fabrication (see Detail 1). All threadrods and bearing plates shall be obtained from Dywidag Systems International, Inc.

Sheet pile wall to be driven with existing abutment in place. For combination wall (PZ27 and W12x96 sections), it is recommended the modified W12x96 sections (with connectors attached) are placed first.

Excavation behind existing abutment to be performed down to level of tie rods. Geogrid reinforcement zone to consist of 7 layers of geogrid reinforcement with 12" of 1½" crushed roadstone between each layer. Roadstone must conform to gradation requirements, be placed in a maximum lift thickness of 6", and be compacted to min. 98% standard effort compaction test (ASTM D698) within 2% of optimum moisture content.

Geogrid to be Tensar BX1200 (available in 9.8' x 164' rolls). Each layer to be laid in strips, perpendicular to abutment wall, with a 12" min. overlap between strips. Edges of each layer to be folded over fill layer above (as shown in abutment cross-section) according to manufacturer's recommendations.

Excavated material may be used as fill outside of geogrid reinforcement zone provided it is moisture conditioned and free of deleterious material. Fill must be placed in maximum 8" lifts and compacted to min. 98% of ASTM D698 and placed within 2% of optimum moisture content.

After backfilling is completed, abutment to be flooded with water pumped from stream prior to placement of the bridge superstructure in coordination with Iowa State team.

HSS section to be completely filled with flowable non-shrink grout. Wingwall walers are to be welded (9" long ⅜" weld) at each contact point on sheet pile wall. Main waler need only be tack welded into position.

Guardrail to be provided by Tama County.

Geogrid zone to be wrapped on all sides with layer of engineering fabric.

Timbers for the bridge footing are to be lagged together and bolted to the RRFC units (each individual timber will be 10' by 10' in plan). Timbers used must have a minimum allowable flexural stress of 1800 psi. An alternative reinforced concrete footing is shown on Sheet 1.

Two (20' long) timbers to be bolted to ends of RRFC's to prevent backfill loss.

TAMA COUNTY

79' x 17'-2" RRFC BRIDGE

ABUTMENT CROSS-SECTION

SHEET 2 OF 5

5'-0"

Scale

2 - 89' RRFC's

59' cl. to cl.

8'

89'

79' cl brg. to cl. brg.

20'

10'

50'

PZ27's and W12x96's

55'

20' timbers placed bolted
along ends of RRFC's

Engineering fabric layer
(all sides of geogrid zone)

7 layers biaxial geogrid
(1'-0" layer spacing)

14a5 14a4 14a3 14a2

14a1

Porous backfill

Subdrain (see Sheet 4)

Existing timber structure
(trimmed to excavation level)

See Detail 2

Detail 2

2'

6"

8'

5b2

5b3

5b1

Figure C7. Abutment cross-section (alternative system) for demonstration project in TC, Iowa.
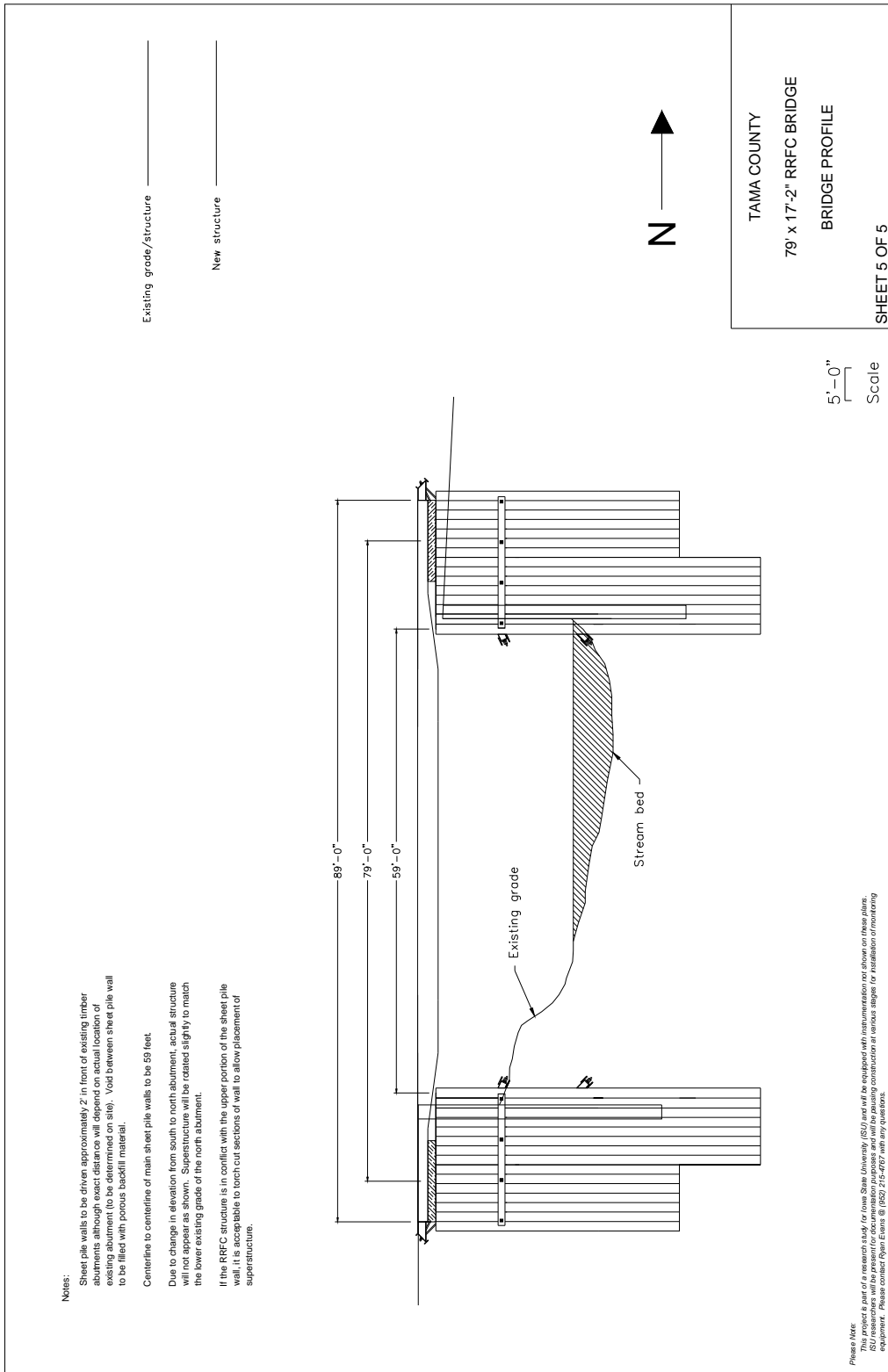
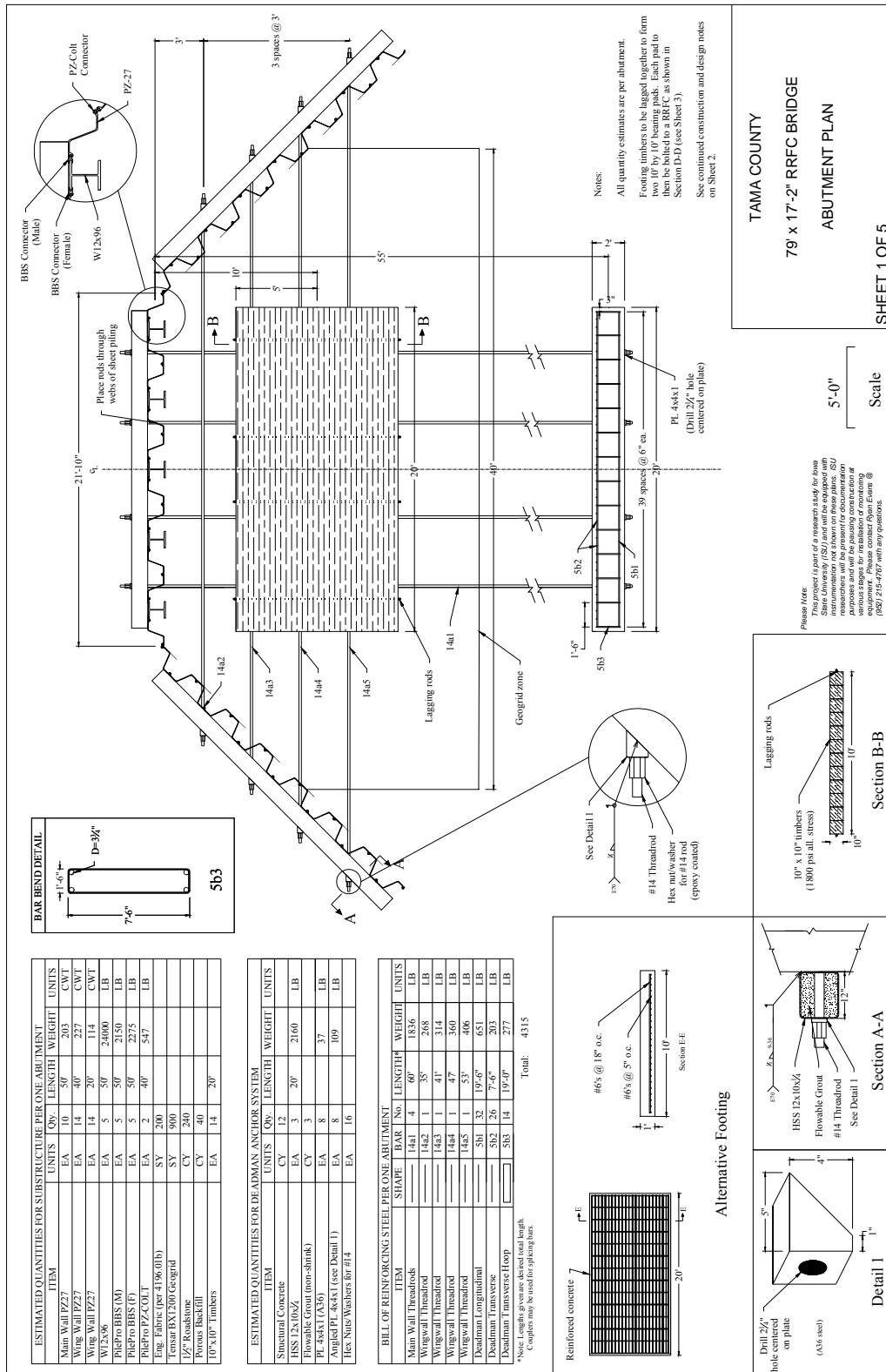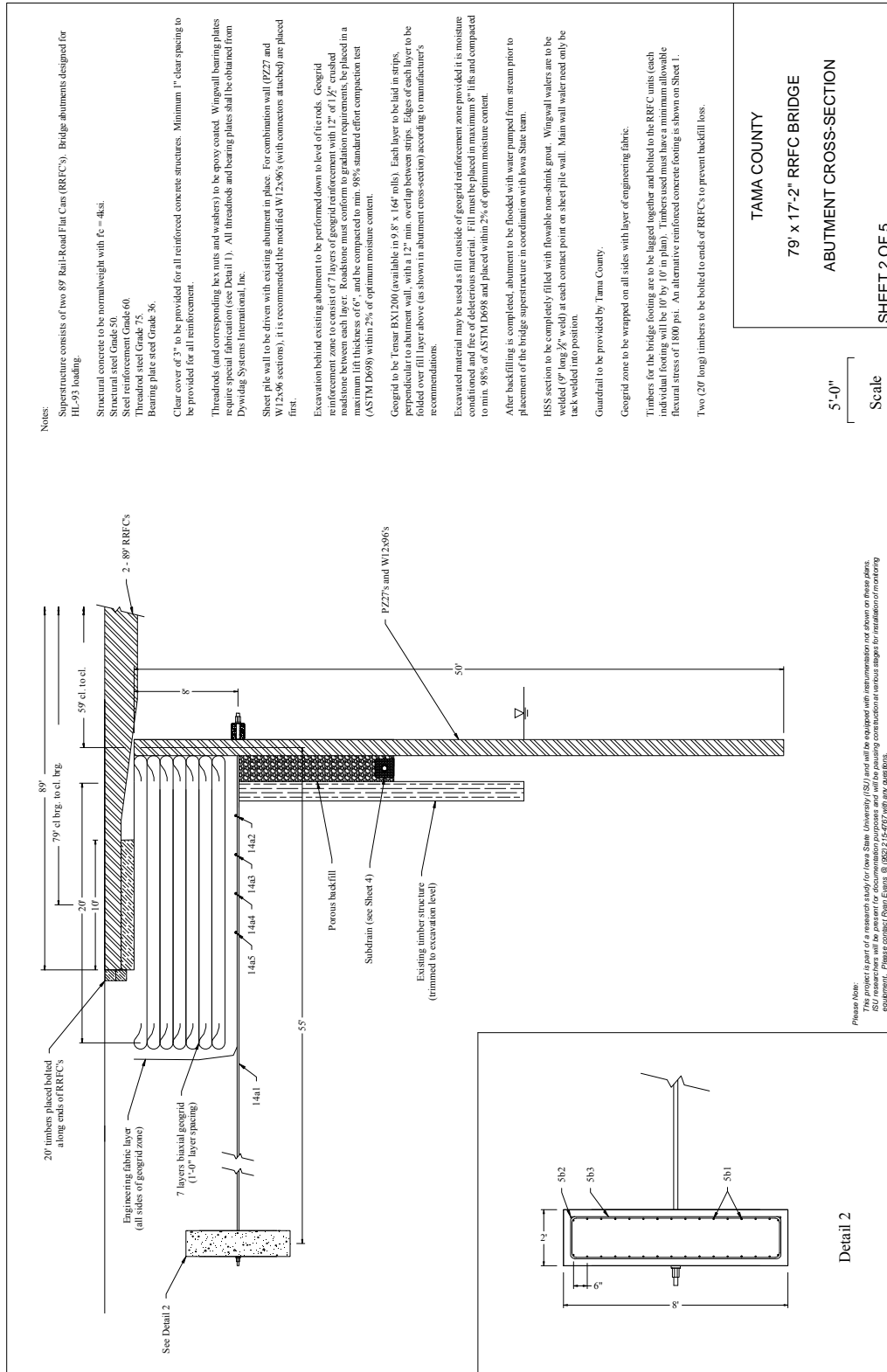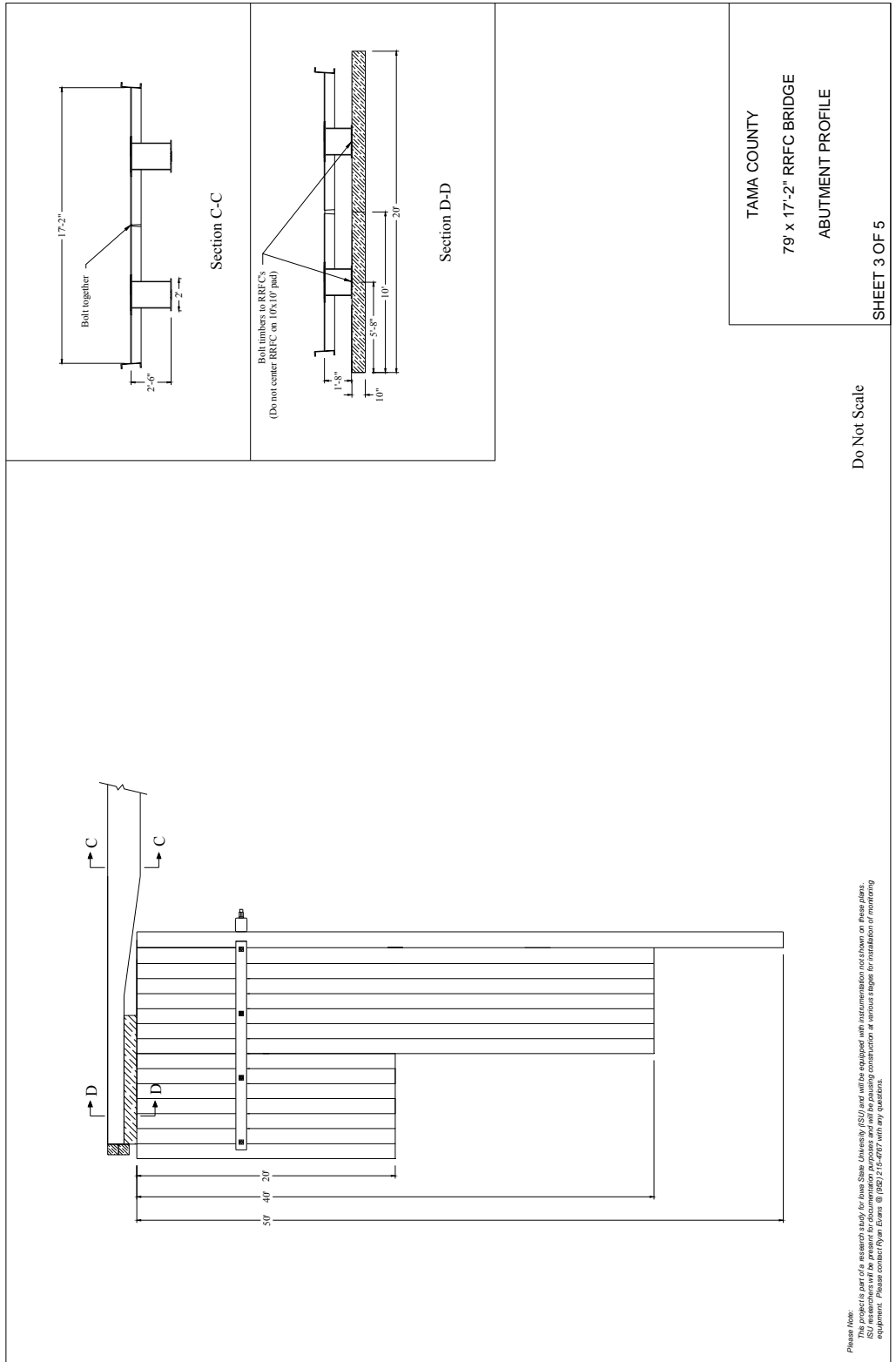**Figure C8. Abutment profile (alternative system) for demonstration project in TC, Iowa.**
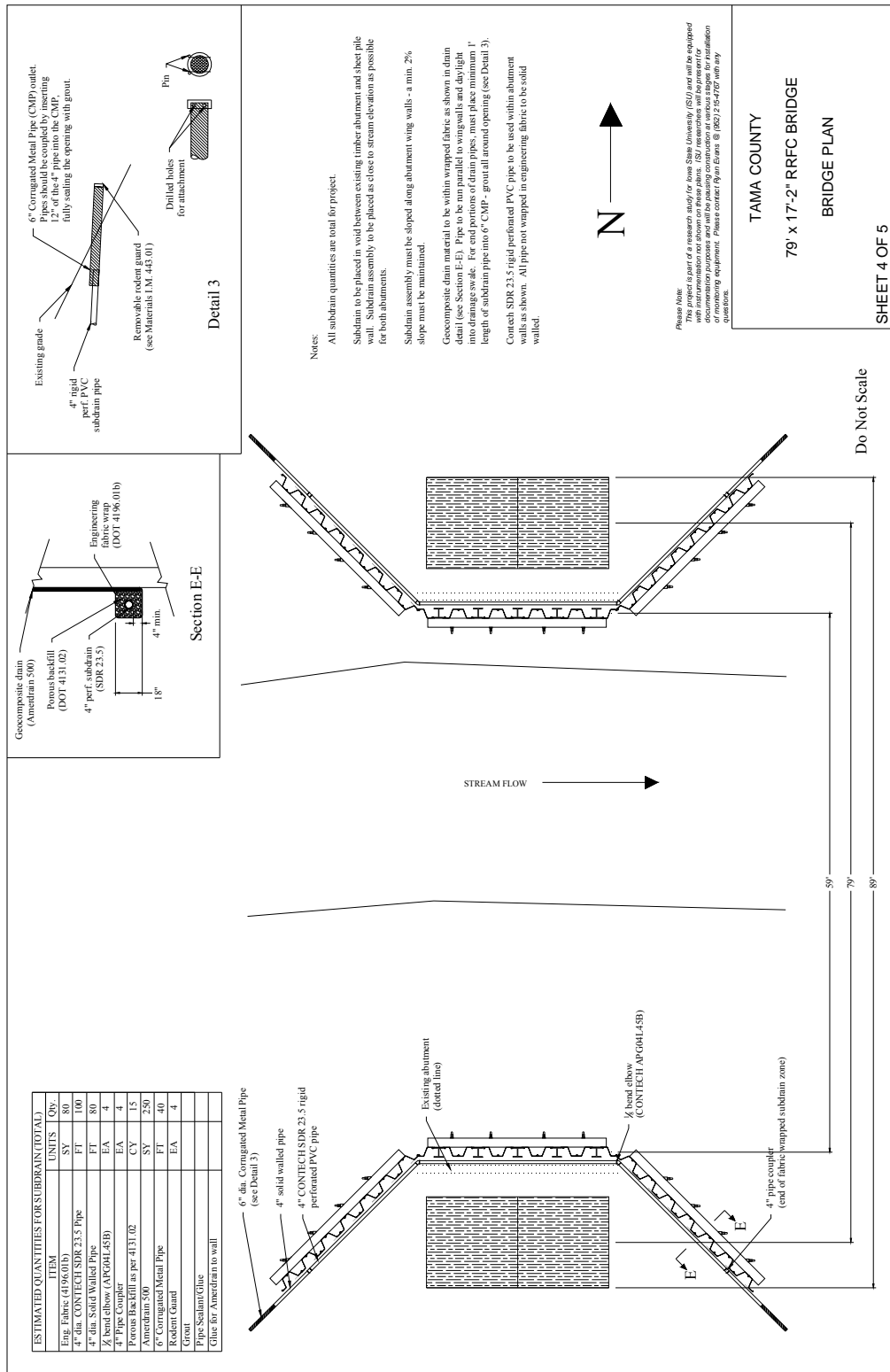
Figure C9. Bridge plan (alternative system) for demonstration project in TC, Iowa.
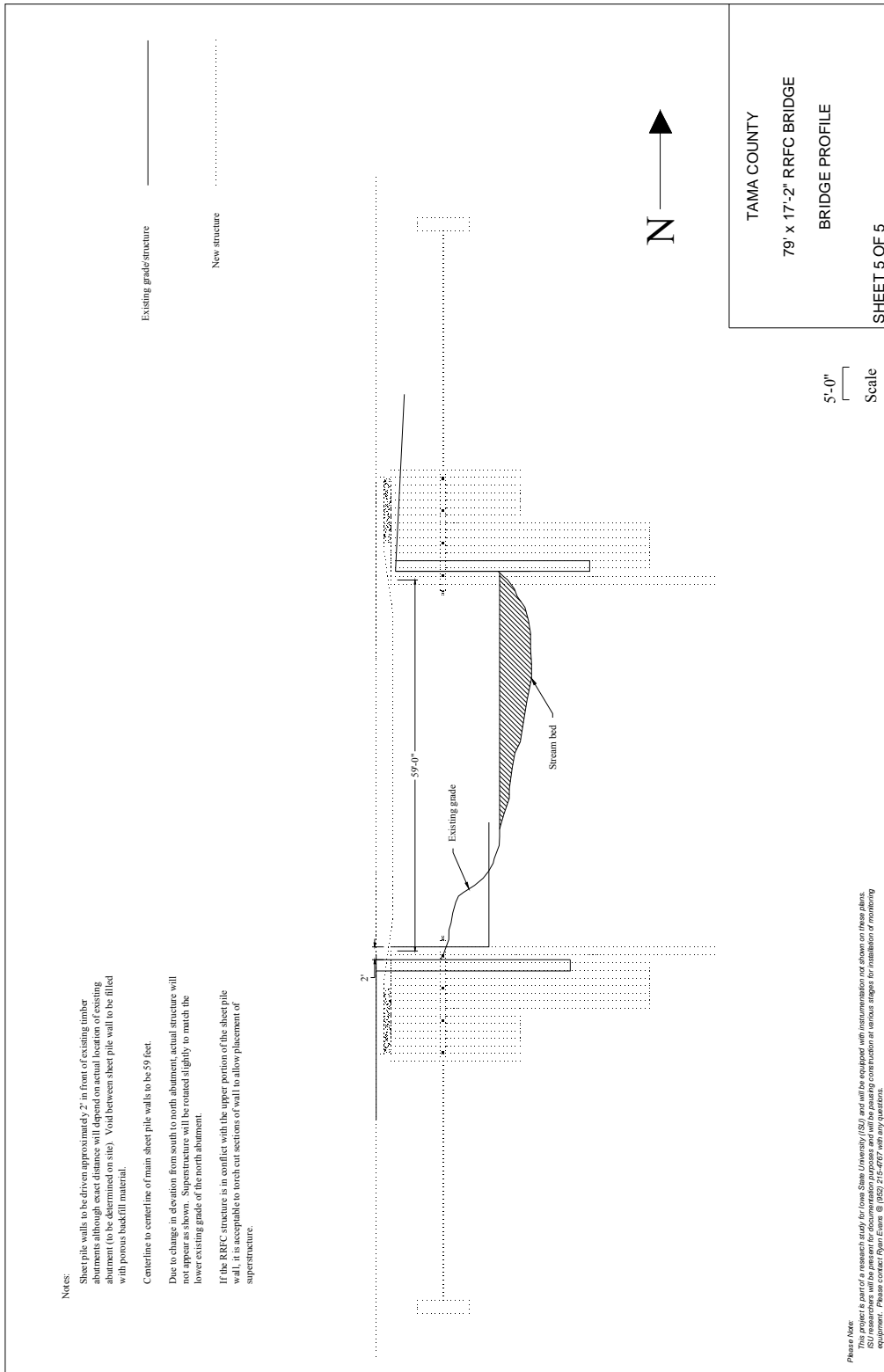
Notes:

Sheet pile walls to be driven approximately 2' in front of existing timber abutments although exact distance will depend on actual location of existing abutment (to be determined on site). Void between sheet pile wall to be filled with porous backfill material.

Centerline to centerline of main sheet pile walls to be 59 feet.

Due to change in elevation from south to north abutment, actual structure will not appear as shown. Superstructure will be rotated slightly to match the lower existing grade of the north abutment.

If the RRFC structure is in conflict with the upper portion of the sheet pile wall, it is acceptable to torch cut sections of wall to allow placement of superstructure.

Existing grade/structure

New structure

Existing grade

Stream bed

59'-0"

2'

N

5'-0"
Scale

TAMA COUNTY
79' x 17'-2" RRFC BRIDGE
BRIDGE PROFILE

SHEET 5 OF 5

Figure C10. Bridge profile (alternative system) for demonstration project in TC, Iowa.

GSI

June 19, 2008

Dr. David J. White, PhD
Associate Professor
Iowa State University
476 Town Engineering Building
Ames, IA 50011

RE: CONE PENETRATION TEST SOUNDING DATA AND INTERPRETATION
     EXISTING CREEK CROSSING BRIDGE
     MM AVENUE NORTH OF 380TH STREET, TAMA COUNTY, IOWA
     GSI PROJECT NO. 086114

Dear Dr. White:

Geotechnical Services, Inc. (GSI) is pleased to submit the results of our cone penetration testing performed at the above referenced site on June 9, 2008. The work was authorized by Iowa State University Purchase Order No. I8 63293 00 and performed in accordance with GSI proposal P086121 dated May 18, 2008.

The project site consisted of a single-span bridge over Richland Creek which is a tributary to the Iowa River. MM Avenue was surfaced with crushed limestone at the time of our field exploration and this road leads to a single farmstead where the road ends. Mr. Ryan Evans of Iowa State University stated that no subsurface soil information was available for this bridge site.

The electronic piezocone test (CPT_u) soundings were performed south and north of the bridge abutments. The test locations were approximately 15 feet south and north of the center of each abutment in order to avoid any rubble or ties between the wing walls.

This investigation utilized a 20-ton capacity, truck-mounted rig hydraulically advancing a Hogentogler Type 2, 10-ton subtraction cone. The electronic cone has a 60° tip angle, tip area of 10 cm^2, a net area ratio of 0.8, and a friction sleeve area of 150 cm^2, and was advanced at a rate of approximately one inch per second. The data collection system recorded data at five centimeter (2-inch) intervals. The CPT_u testing was performed in general accordance with ASTM D5778, "Performing Electric Friction Cone and Piezocone Penetration Testing of Soils." The uncorrected tip stress, sleeve friction, and pore pressure graphical results are provided with this report. The soil behavior type is also shown on the attached graphs and is reported for the average of three reading intervals. These classifications are based on the Simplified Soil Classification Chart for Electric Friction Cone by Robertson and Campanella (1986) and are a general indication of the soils encountered at this site. Uncorrected tip stress, sleeve friction, and pore pressure have been converted to text data and will be included with this report.

These CPT_u soundings were used to provide a nearly continuous subsurface soil profile that will be used to obtain soil shear strength parameters. These parameters will then be used to model the

Figure C11. CPT report for TC, Iowa demonstration project.

GSI

soil-structure interaction of the bridge structure and the new sheetpile abutment system. Both soundings were advanced to planned depths of 55.5 and 55.8 feet below existing grades.

Surface topography within the flood plain exhibits little local relief and is essentially horizontal. The natural soil profile within the flood plain is typified by alluvial silt and clay soils near the surface, which gradually alter to extensive deposits of sand and gravel associated with depositional events of the waterway. Alluvial deposits may be underlain by cohesive glacial till associated with the Pre-Illinoian glacial advances or by clay shale and limestone bedrock of the Devonian bedrock system. The surficial soil profile has been altered over time by manmade cut-and-fill construction associated with reclamation of the flood plain area.

The profiles encountered during CPT_u sounding generally consist of cohesive soils underlain by predominately granular soil based on Robertson and Campenella's soil behavior types. Both profiles indicate the presence of very soft material in the upper 6 to 20 feet. These very soft soils transition to granular deposits that extended to approximately 38 and 37 feet below existing grades in CPT 1 and 2, respectively. The lower 18 to 19 feet of each sounding generally consisted of fine grained soil which could be Pre-Illinoian glacial till common to the Tama County area.

GSI is proud to be part of Iowa State University's continued research in the field of geotechnical engineering and soil behavior. Please contact us at (515) 270-6542 if you have any questions on this job or if you would like our assistance on future projects.

Respectfully,
Geotechnical Services, Inc.

Zachary G. Thomas, P.E.
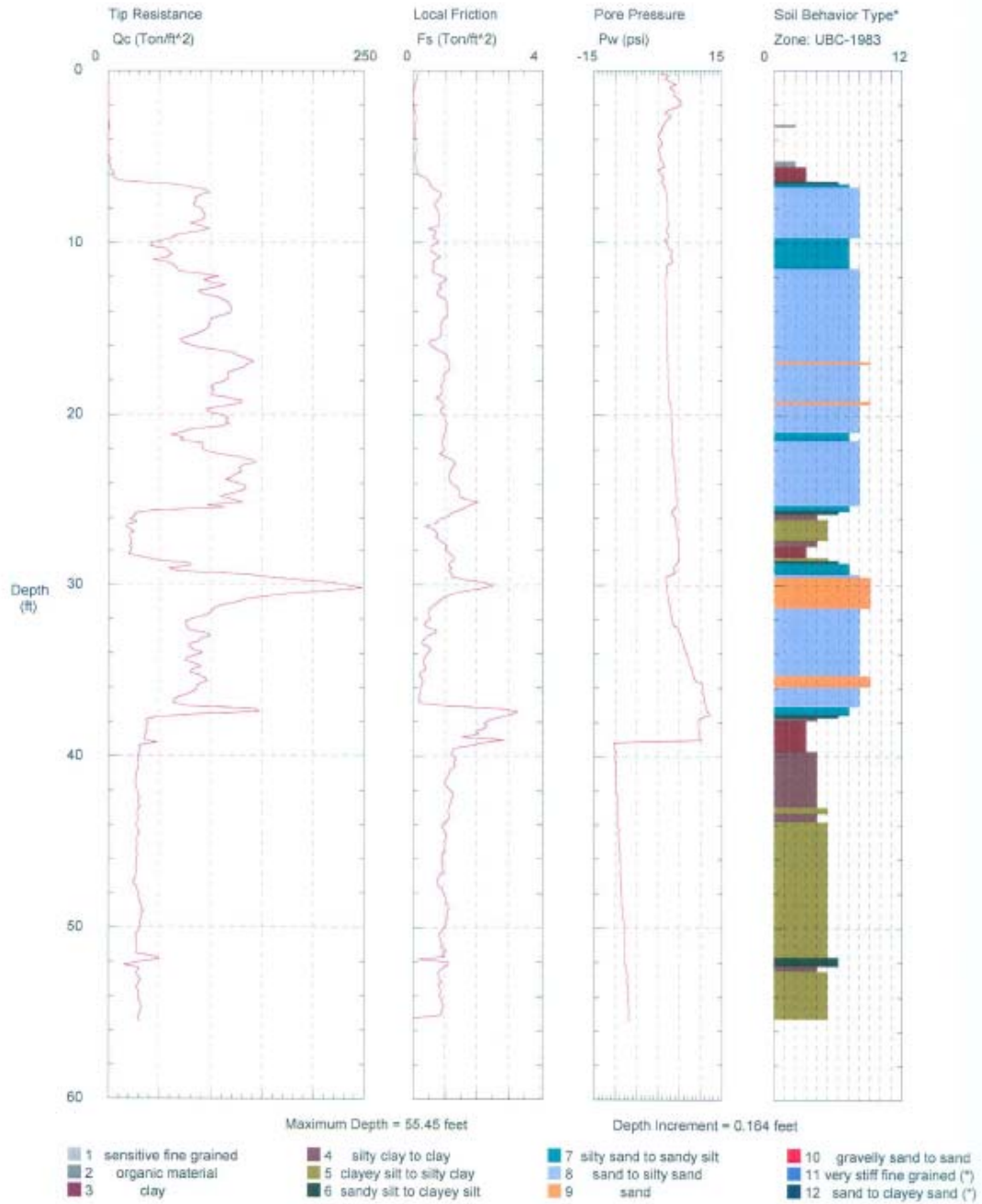Project Engineer

Michael T. Lustig, P.E.
Principal Engineer

Attachments: Graphical CPT_u Logs (3), Electronic Raw Data Disk

GSI No. 086114   2   June 19, 2008

Figure C11. (continued).

Figure C11. (continued).

Figure C11. (continued).

Figure C11. (continued).

Log of Soil Boring No. _SB 1_

Sheet	1 of 2

Project: *MM Ave. Bridge*
Location: *Tama County, IA*
Project No.: *Tama 0801*

Logged By: Ryan Evans
Driller: Brian
Drill Rig: Mobile
Date: **August 1, 2008**

Client: *Iowa DOT/Tama County*
Proj. Mgr.: *Ryan Evans*
GPS: Latitude N **Longitude:** W

Depth (feet)	Depth Range	Type	No.	Container	Recovery	(P) SPT OVA	Visual Classification	Depth	Stratigraphy	Depth	Assignment
	12" - 24"	A		B			Tan Sandy Gravel / Stiff, black and dark gray silty clay				
	24" - 48"	T		T	~18"	2.75 tsf	Firm tan and light gray silty clay		Silty Clay		
5	48" - 72"	T		T	~8"	1.50 tsf	Stiff tan and light gray silty clay				
	72"	A		B							
	72" - 96"	T		T	~20"	1.25 tsf	Stiff tan and light gray silty clay				
	96" - 108"	A		B			Tan silty sand				
10	108" - 132"	T		T		1.25 tsf	Tan silty sand		Silty Sand		
	132" - 156"	T		T		1.75 tsf	Tan silty sand				
15							Terminate boring @ 13 ft				
20											
25											

Boring Advancement

Depth Range	Method
0 - 13 ft	Cont. flight Ag

Boring Abandonment

Cuttings ☐
Grout ☒
Grout Mixture:

Groundwater Information

First Encountered: N/A feet
Rise: after
Static: after

Topsoil Depth / Surface Conditions: ~ 30 ft south of south abutment

Start Time: Finish Time:

Figure C12. Log of soil boring SB 1 for demonstration project in TC, Iowa.

Log of Soil Boring No. *SB 2*

Sheet 2 of 2

Project: *MM Ave. Bridge*	
Logged By: Ryan Evans	**Driller:** Brian
Client: *Iowa DOT/Tama County*	**Proj. Mgr.:** *Ryan Evans*

Location: *Tama County, IA*

Drill Rig: Mobile

GPS: Latitude N

Project No.: *Tama 0801*

Date: **August 1, 2008**

Longitude: W

Depth (feet)	Depth Range	Type	No.	Container	Recovery	(P) SPT OVA	Visual Classification	Depth	Stratigraphy	Depth	Assignment
	0" - 12"	A		B			Light gray sandy gravel				
	12" - 24"	A		B			Light gray sandy gravel				
	24" - 36"	A		B			Light gray sandy gravel				
	36" - 48"	A		B			Light gray silty sand		Silty Clay/		
5	48" - 60"	A		B			Tan silty sand with silty clay and organic		Clayey Silt		
	60" - 84"	T		T		1.50 tsf	Loose, light gray clayey silt				
	84" - 96"	A		B			Loose, light gray clayey silt				
10	96" - 120"	T		T		1.50 tsf	Loose, light gray clayey silt				
	132" - 156"	T		T		1.25 tsf	Loose, light gray clayey silt				
15	168" - 192"	T		T		1.25 tsf	Loose, light gray clayey silt				
	210"						Water encountered		water level		
20	216" - 240"	T		T		1.00 tsf	Loose, light gray clayey silt with water				
	276"						Tan silty sand - unable to sample (terminate boring)		Silty Sand		
25											

Sample / **Field Data** / **Visual Classification** / **Stratigraphy** / **Laboratory Assignments**

| Boring Advancement		Boring Abandonment	Groundwater Information	Topsoil Depth / Surface Conditions:
Depth Range	Method	Cuttings ☑	First Encountered: 17.5 feet	~ 10 ft north of north abutment
0 - 23 ft	Cont. flight Ag	Grout ☐	Rise: _____ after _____	
		Grout Mixture:	Static: _____ after _____	Start Time: _____ Finish Time: _____

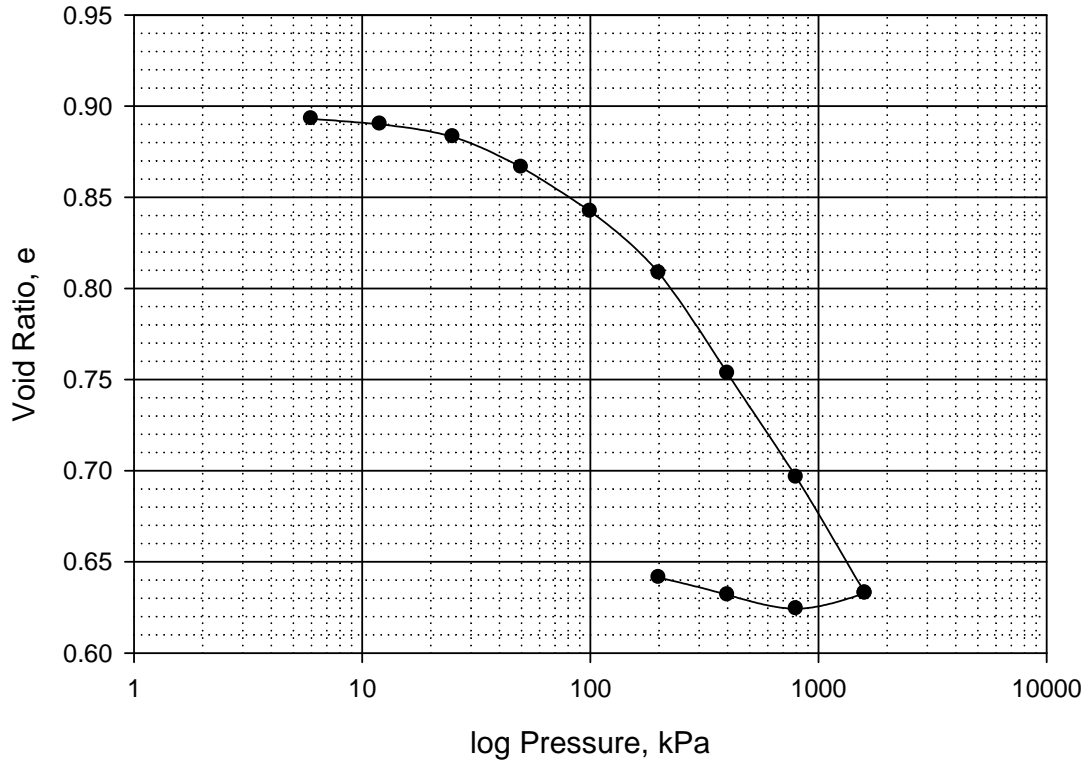**Figure C13. Log of soil boring SB 2 for demonstration project in TC, Iowa.**
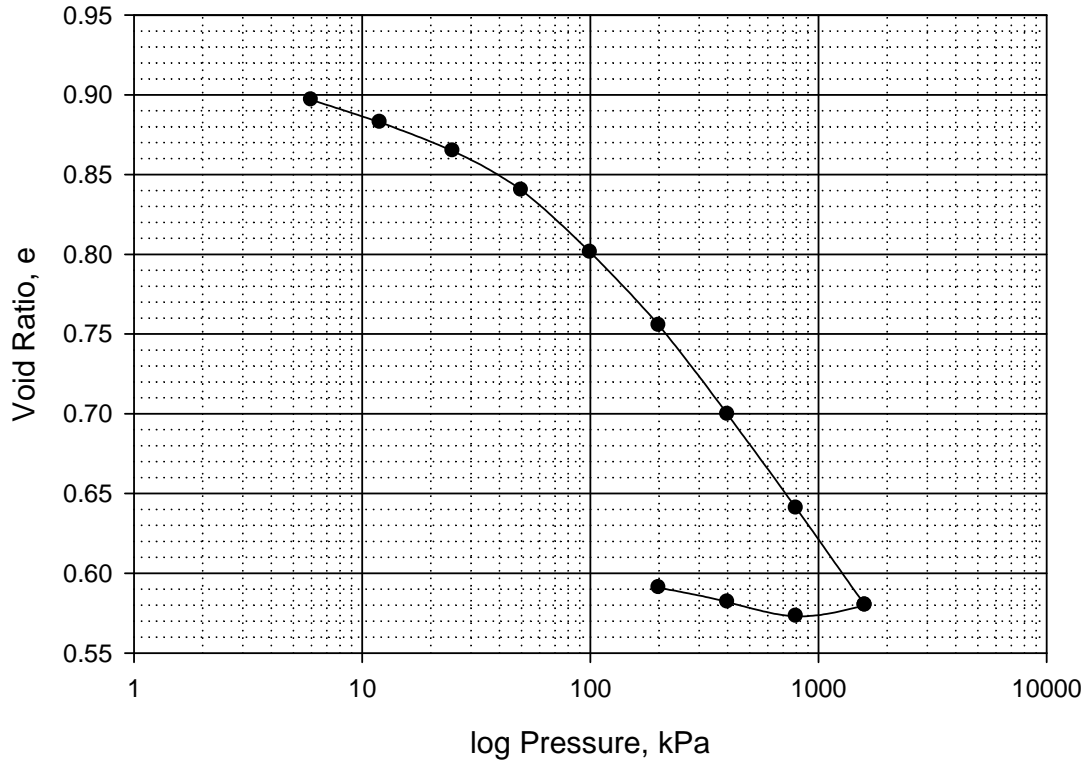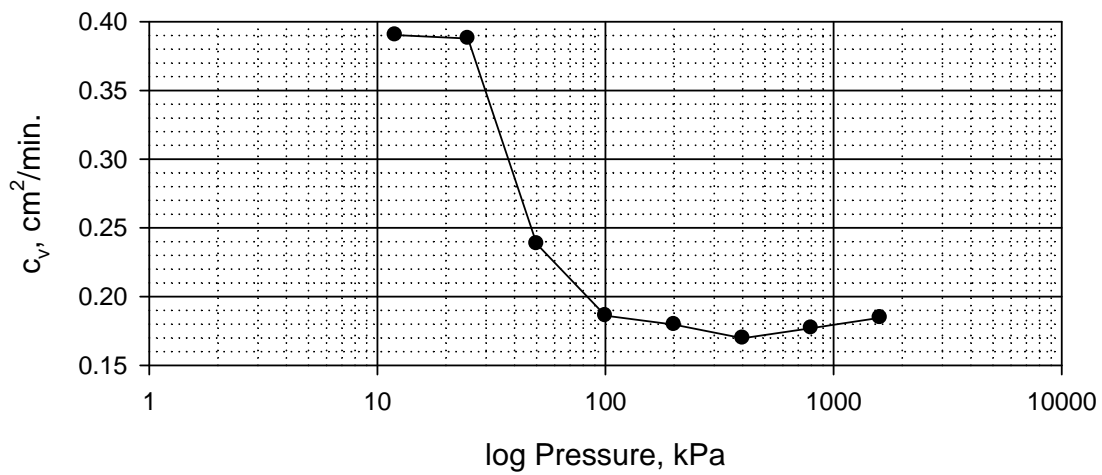
b.) Void ratio vs. log pressure
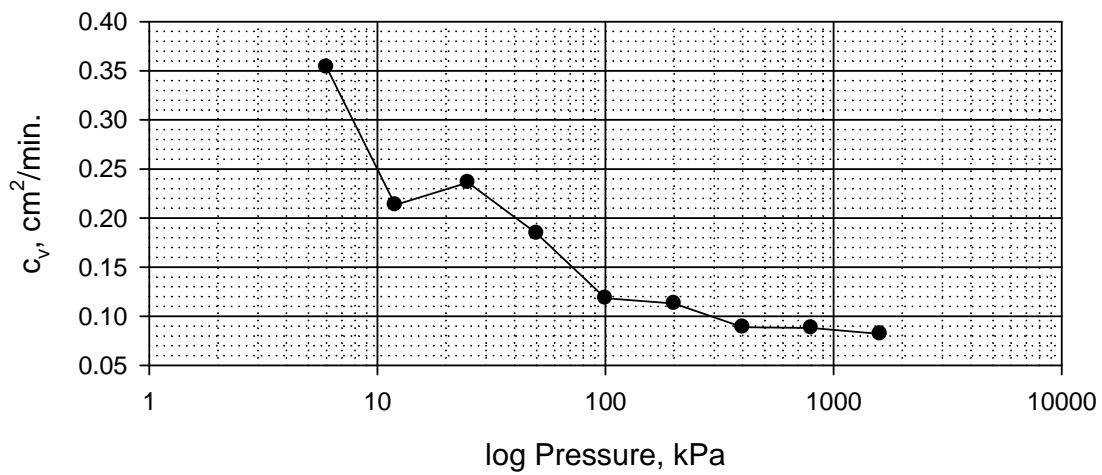
a.) Coefficient of consolidation, c_v vs. log pressure

Figure C14. Consolidation test results for SB 2 at a sample depth of 94 in. for demonstration project in TC, Iowa.
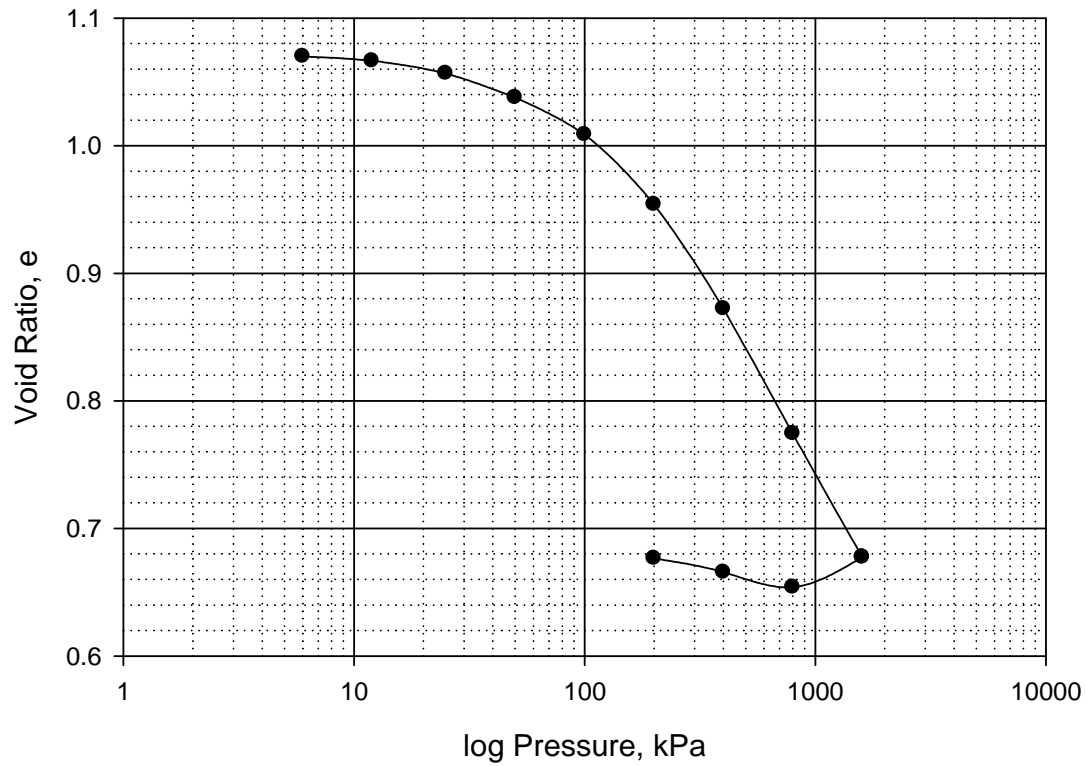
a.) Void ratio vs. log pressure

b.) Coefficient of consolidation, c_v vs. log pressure

Figure C15. Consolidation test results for SB 2 at a sample depth of 107 in. for demonstration project in TC, Iowa.
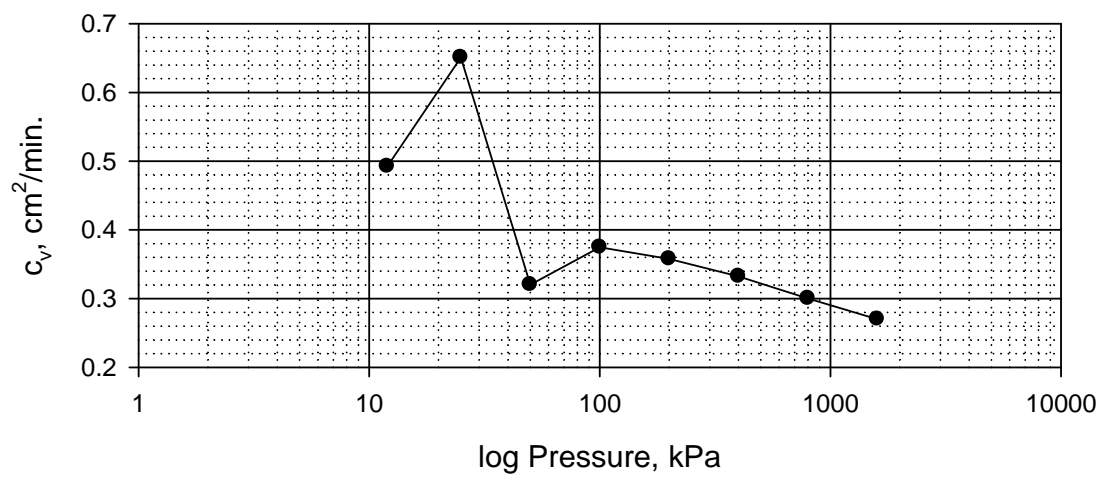
a.) Void ratio vs. log pressure

b.) Coefficient of consolidation, c_v vs. log pressure

Figure C16. Consolidation test results for SB 2 at a sample depth of 179 in. for demonstration project in TC, Iowa.

Design Calculations

Loading summary

Preliminary design assumptions for loading calculation (assumptions for flatcar loads taken from previous report TR-498):

- Weight of reinforced concrete = 150 pcf

- Two RRFC's for superstructure @ 472 lb/ft each

- Bridge width of 20 ft

- 100 lb/ft guardrail system

- 4.5 in. thick gravel surface for roadway @ 110 pcf

- retained soil: $\gamma_s = 120$ pcf;, $\varphi' = 25°$; $\delta = 22°$ from AASHTO (1998) Table 3.11.5.3-1

- stream-side soil: $\gamma_s = 120$ pcf;, $\varphi' = 20°$; $\delta = 11°$; c = 250 psf

AASHTO (1998) Section 3.4 specifies the following maximum load factors for Strength I limit state design (the critical limit state determined for this design):

- Dead loads of structural components (DC): 1.25

- Horizontal earth pressure (EH): 1.50 active and 1.35 at-rest

- Dynamic impact load (IM): 1.33

- Earth surcharge load (ES): 1.50

- Vertical pressure from earth dead load (EV): 1.35 for retaining structures (continued)

- Vehicular live load (LL): 1.75

- Live load surcharge (LS): 1.75

Coefficient of Lateral Earth Pressure Calculation

For the soil on the retained side of the sheet pile wall, the coefficient of lateral earth pressure (active) was calculated using AASHTO (1998) Section 3.11.5.3 (a less conservative method than used for the project in BC):

$$k_a = \frac{\sin^2(\theta+\varphi\prime)}{\Gamma \sin^2(\theta) \sin(\theta-\delta)} \text{ where } \Gamma = \left[1 + \sqrt{\frac{\sin(\varphi'+\delta)\sin(\varphi'-\beta)}{\sin(\theta-\delta)\sin(\theta+\beta)}}\right]^2$$

$$\therefore \Gamma = \left[1 + \sqrt{\frac{\sin(25°+22°)\sin(25°-0°)}{\sin(90°-22°)\sin(90°+0°)}}\right]^2 = 2.488 \text{ and } k_a = \frac{\sin^2(90°+25°)}{2.488\sin^2(90°)\sin(90°-22°)} = 0.356$$

On the stream side of the sheet pile wall, the coefficient of lateral earth pressure (passive) for the soil resistance to outward movement of the wall was calculated from AASHTO (1998) Figure 3.11.5.4-1 using the following values:

$$\frac{\delta}{\varphi\prime} = \frac{11}{20} = 0.55 \text{ therefore R} = 0.882 \text{ (interpolated)}$$

$$k_p = R * 3.0 = 2.645$$

The stream side soil also will resist movement due to cohesion and is calculated in AASHTO (1998) Section 3.11.5.4:

$$2 * c * \sqrt{k_p} = 2(250\text{psf})\sqrt{2.645} = 810 \text{ psf}$$

Thus passive resistance, p_p, is calculated as the following:

$$p_p = k_p\gamma_s z + 2c\sqrt{k_p}$$

DC Load Estimates

RRFC's: $(0.472 \text{ klf per RRFC})(2 \text{ RRFC's}) = 0.944 \text{ klf}$

Guardrail: 0.100 klf

Roadway gravel: $\left(\frac{4.5}{12} \text{ ft thick}\right)(0.120 \text{ kcf})(20 \text{ ft wide roadway}) = 0.900 \text{ klf}$

$$P_{DL} = \frac{(0.944 \text{ klf} + 0.100 \text{ klf} + 0.900 \text{ klf}) * 89 \text{ ft}}{(2 \text{ abutments})} = 86.5 \text{ k (per abutment)}$$

LL Estimates

The live loads applied to the abutment through the timber spread footing were estimated by analyzing the superstructure for HL-93 loading using QConBridge (2005); the maximum live load calculated at an abutment was 109.7 kips per lane. The critical condition was calculated as follows (loading shown in Figure C17):

$$\sum M_{END} = [(32 \text{ k})(14 \text{ ft}) + (8 \text{ k})(28 \text{ ft})] * 1.33 + (0.64 \text{ klf})\frac{(79 \text{ ft})^2}{2} - R_2(79 \text{ ft}) = 0$$

$$\therefore R_2 = 36.6 \text{ k}$$

$$\sum F = [32\text{k} + 32\text{k} + 8\text{k}] * 1.33 + (0.64\text{klf}) * 79 \text{ ft} - R_2 = R_1$$

$$\therefore R_1 = P_{LL} = 109.7 \text{ k}$$
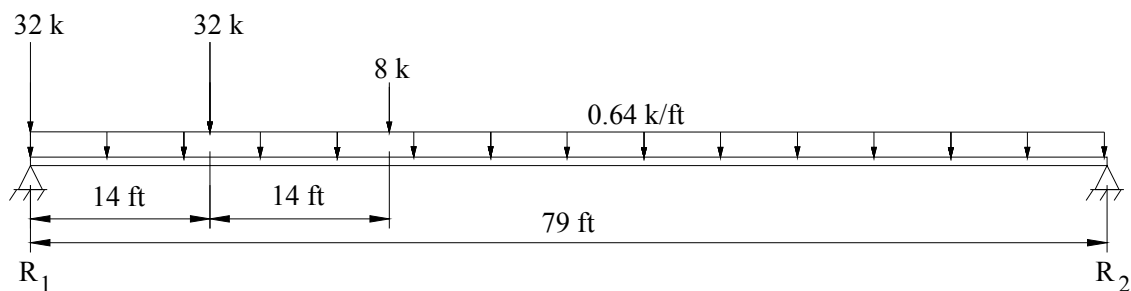
Figure C17. HL-93 critical loading diagram.

For live load surcharge on the retained backfill (due to vehicles approaching the superstructure), AASHTO (1998) Section 3.11.6.4 recommends the use of the following empirical formula:

LS: $p_{ll} = k_a * \gamma_s * h_{eq} = 0.356(0.120 \text{ kcf})(2.0 \text{ ft}) = 0.085$ ksf equivalent lateral earth pressure

where h_{eq} = equivalent height of backfill = 2.0 ft (for retaining walls higher than 20 ft)

Factored-level Loads

Dead load on abutment, $P_{U_{DL}} = 1.25(86.5 \text{ k}) = 108.1$ k (per abutment)

Live load on abutment, $P_{U_{LL}} = 1.75(109.7 \text{ k}) = 192.0$ k (per lane)

Live load surcharge, $p_{ll} = 1.75(0.085 \text{ ksf}) = 0.150$ ksf

Load Distribution

Concentrated loads applied to the timber footing from the superstructure were assumed to distribute evenly over a length of the footing, L. For the live loads, the length of one lane was assumed to be L = 10 ft. For the dead loads (DC), the length of distribution was assumed to be the approximate width of the bridge (L = 20 ft). The resulting surcharge pressures, q, were:

Live load: $q_{U_{LL}} = \frac{192.0 \text{ k}}{10 \text{ ft} * 10 \text{ ft}} = 1.9$ ksf

Dead load: $q_{U_{DL}} = \frac{108.1 \text{ k}}{20 \text{ ft} * 10 \text{ ft}} = 0.5$ ksf

Therefore the total factored surcharge load on the backfill from the bridge, $q_U = 2.4$ ksf

Sheet Pile Retaining Wall Design

To determine the lateral earth pressure associated with this surcharge pressure, the load was assumed to act against a rigid wall (which is conservative due to the flexibility of sheet piling) and lateral earth pressure was calculated according to AASHTO (1998) Section 3.11.6.1. A diagram showing the analysis for the surcharge earth pressure is presented in Figure C18a. The resulting distribution of

earth pressure was simplified for analysis as shown in Figure C18b; the peak lateral earth pressure was assumed to be 1.0 ksf at a depth of 6 ft from the top of the wall extending to a depth of 20 ft.
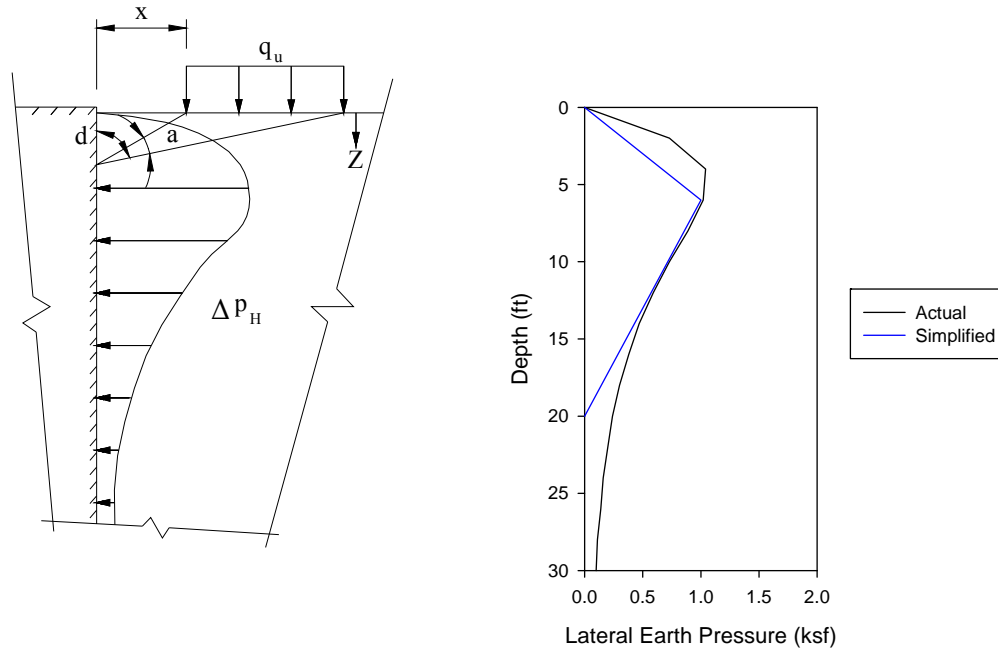
a.) Surcharge on rigid wall   b.) Analysis results

Figure C18. Determination of lateral earth pressure due to bridge surcharge loads.

All of the loads applied to the sheet pile wall (from the loads associated with the abutment in profile in Figure C19a) are described with reference to the numbered loads in Figure C19b. The contribution of the geogrid is modeled by considering no lateral earth pressures are transferred to the sheet pile wall in the GRS zone. For the design, the location of the anchors was assumed to be 8 ft and 18 ft below the top of the wall; the location of the anchors were assumed to be a rigid support for translation (pinned). The modeling method for the analysis of the sheet pile wall is presented in Figure C19c.

Load 1 - Retained soil surcharge (behind abutment cap) and LL surcharge:

$$p_1 = 150 \text{ psf} + 8 \text{ ft}(120 \text{ pcf})(0.356)(1.50) = 663 \text{ psf}$$

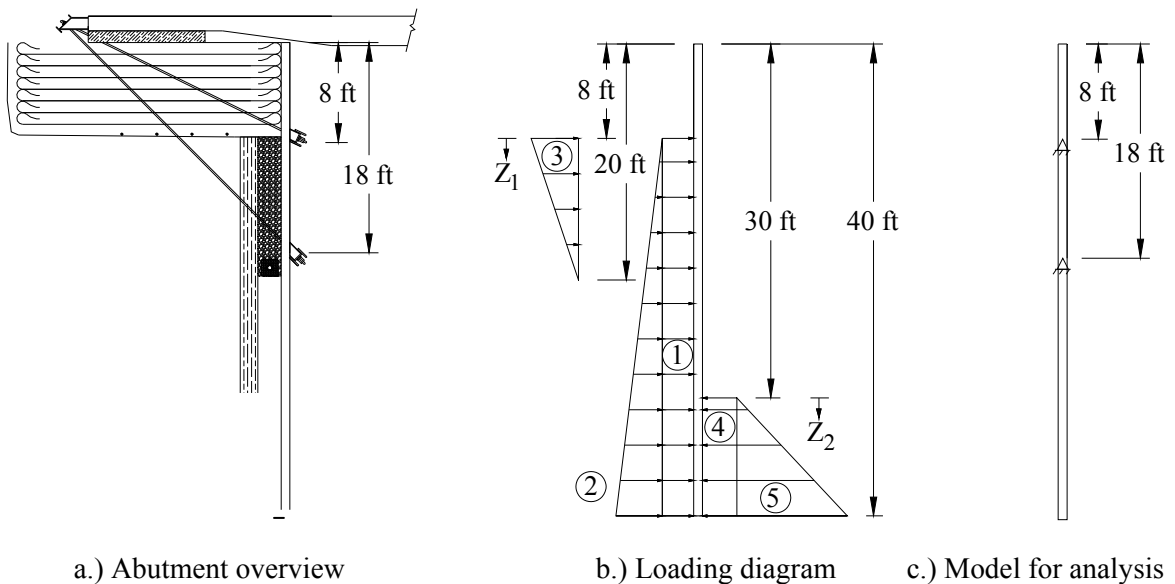Load 2 - Retained soil active pressure:

$$p_2 = 1.50(120 \text{ pcf})(.356)(z_1) = 64.1(z_1)$$

Load 3 - Bridge surcharge: $p_3 = 1000$ psf (previously calculated)

Load 4 – Soil cohesion resistance: $p_4 = 810$ psf (previously calculated)

Load 5 – Passive soil pressure:

$$p_5 = 2.645(120 \text{ pcf})(z_2) = 317.4 \text{ psf}$$

      a.) Abutment overview   b.) Loading diagram   c.) Model for analysis
Figure C19. Design profile of sheet pile wall.

For analysis of the loading, the computer program STAAD (2005) was used. A preliminary analysis was performed with tie rod anchors at 5 ft and 15 ft below the top of the sheet pile wall which resulted in a bending moment of 38.6 ft-kip per ft width of wall. The sheet pile section required to resist the design moment was the PZ 35 (moment capacity of 214.4 ft-kip). This section is approximately 60% heavier than a PZ 22 and was considered to be too expensive by the TC Engineer's Office. A subsequent analysis that was modeled with anchors at 8 ft and 20 ft below the top of the wall resulted in a design bending moment of 71.3 ft-kip per ft, making the PZ 22 a sufficient section (design moment capacity of 81.7 ft-kip per ft).

Additional analysis was performed on the wall to determine the influence of the factor of safety on the design loads. Each analysis involved removing the load factors (EH, ES, and LL) from the loads due to the retained soil; load factors on bridge surcharge loads (dead and live loads applied to the abutment from the superstructure) remained. An analysis with anchors at 5 ft and 15 ft below the top of the sheet pile wall resulted in a bending moment of 50.1 ft-kip/ft (a 72% reduction from an analysis with maximum load factors). An analysis with anchors at 8 ft and 20 ft below the top of the sheet pile wall resulted in a bending moment of 16.7 ft-kip/ft (a 77% reduction from an analysis with maximum load factors). These results showed a significant contribution from load factors on the retained soil loads to the design loads in the sheet pile wall.

As can be seen from the various analyses performed, location of the bottom tie rod has a significant influence on the size of the sheet pile section required. Although placement of the bottom anchor 20 ft below the top of the sheet pile wall would make the PZ 22 section sufficient, this may not be feasible to construct due to the level of the stream (see Figure C5 for a profile of the placement of the proposed structure). After consultation with the TC Engineer's Office, it was determined that considering the design life (20 to 40 years) and functional importance (service to one residence) of the bridge a reduction in load factors on the retained soil loads would be acceptable. As a result, construction of the bottom anchor 20 ft below the top of the wall will be attempted; a minimum distance of 18 ft however was specified.

Anchor System Design

To avoid the extensive excavation required for a reinforced concrete deadman, the tie rods were designed to be connected to the RRFC superstructure as shown in Figure C1 and Figure C2. The design tie rod anchor forces determined in the analyses were 4 k/ft and 18 k/ft for the top and bottom anchors, respectively. Since the width of the sheet pile wall was approximately 20 ft, forces of 80 k and 360 k needed to be resisted at the top and bottom anchor locations, respectively. To develop the required lateral force, P_h, a tie rod force, T, which is a function of the angle of the rod, θ, shown in Figure C20; a vertical force of P_v is also developed. The forces are given in terms of the required force P_h (the subscripts *t* and *b* correspond to top and bottom anchors, respectively):

$$T_t = \frac{P_{h_t}}{\cos\theta_t} \quad \text{and} \quad P_{v_t} = P_{h_t}\tan\theta_t$$

$$T_b = \frac{P_{h_b}}{\cos \theta_b} \quad \text{and} \quad P_{v_b} = P_{h_b} \tan \theta_b$$
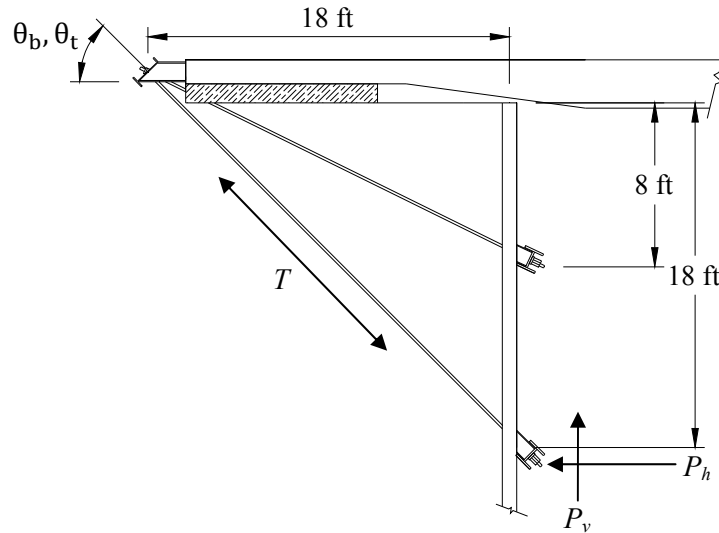
where:

$$\theta_t = \tan^{-1}\left(\frac{10 \text{ ft}}{18 \text{ ft}}\right) = 29°$$

$$\theta_b = \tan^{-1}\left(\frac{20 \text{ ft}}{18 \text{ ft}}\right) = 48°$$

thus:

$$T_t = \frac{80 \text{ k}}{\cos 29°} = 92 \text{ k} \quad \text{and} \quad P_{v_t} = 80 \text{ k}(\tan 29°) = 44 \text{ k (uplift)}$$

$$T_b = \frac{360 \text{ k}}{\cos 48°} = 538 \text{ k} \quad \text{and} \quad P_{v_b} = 360 \text{ k}(\tan 48°) = 400 \text{ k (uplift)}$$

Figure C20. Tie rod force increase due to angle of rod.

Additional stresses were assumed to be induced in the tie rods due to the expansion of the superstructure. Thermal expansion of the steel RRFC's were determined using a thermal expansion coefficient, $\alpha = 0.00000645$ in./in./°F and a temperature difference, $\Delta T = 150$°F. The change in length, ΔL, is calculated as follows:

$$\Delta L = (0.00000645 \text{ in./in./(°F)})(150°F)(89 \text{ ft})\left(12\frac{\text{in.}}{\text{ft}}\right) = 1 \text{ in.}$$

A thermal-induced expansion of 0.5 in. per abutment was assumed for design. The force induced in the tie rod from this expansion was estimated using the stiffness of a 1.375 in. diameter rod assumed to have modulus of elasticity of 30,000 ksi. The induced force, $T_{thermal}$, is calculated as follows:

$$T_{thermal} = \Delta\ell * \left(\frac{AE}{\ell}\right)$$

where $\Delta\ell$ is the elongation of the tie rod and is determined using the diagram in Figure C21. Under elongation the change in the angle φ is assumed to be negligible. It should be noted that:

$$\varphi_t = 90° - \theta_t$$

$$\varphi_b = 90° - \theta_b$$

For the top rod:

$$\Delta\ell = \ell' - \ell = \left[\frac{18 \text{ ft} + \frac{0.5}{12}\text{ft}}{\sin(\varphi_t)} - \frac{18 \text{ ft}}{\sin(\varphi_t)}\right] * \left(12\frac{\text{in.}}{\text{ft}}\right) = 0.57 \text{ in.}$$

$$(T_t)_{thermal} = (0.57 \text{ in.})\left(\frac{(1.58 \text{ in.}^2)(30,000 \text{ ksi})}{\frac{18 \text{ ft} * 12 \text{ in./ft}}{\sin(\varphi_t)}}\right) = 109 \text{ k}$$
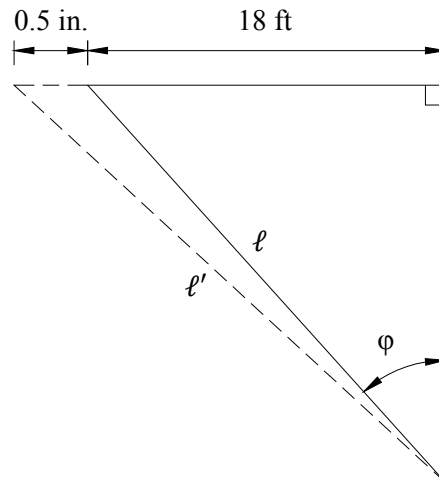
For the bottom rod:

$$\Delta\ell = \ell' - \ell = \left[\frac{18 \text{ ft} + \frac{0.5}{12}\text{ft}}{\sin(\varphi_b)} - \frac{18 \text{ ft}}{\sin(\varphi_b)}\right] * \left(12\frac{\text{in.}}{\text{ft}}\right) = 0.72 \text{ in.}$$

$$(T_b)_{thermal} = (0.72 \text{ in.})\left(\frac{(1.58 \text{ in.}^2)(30{,}000 \text{ ksi})}{\dfrac{18 \text{ ft}}{\sin(\varphi_b)}} \right) = 117 \text{ k}$$

Figure C21. Determination of tie rod elongation from thermal expansion.

Another superstructure-induced stress in the rods is the elongation due to the release of camber in the bridge. The compressive forces applied to the RRFC's from the tie rods is assumed to longitudinally shorten and camber, Δ, the bridge as shown in Figure C22. Over a period of time, there is potential for movement of the retained soil to lock in these deformations. When a vehicle travels over the bridge, the deflection of the superstructure will reduce the "locked in" camber and elongate the superstructure thus inducing additional forces in the tie rods. To account for this effect, the potential *additional* load is assumed to be 100% of the load determined in the initial analysis; since expected bridge camber was unknown, this very conservative assumption was made.
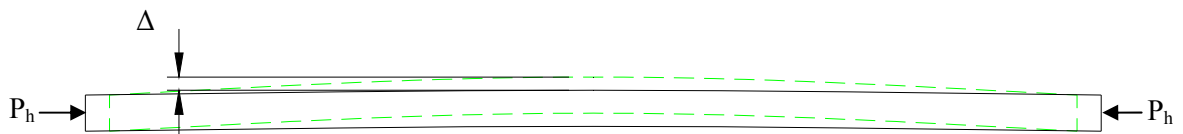
Figure C22. Camber of bridge superstructure due to compression from tie rods.

The total design load for each anchor location is calculated as follows:

$$(T_t)_{design} = 2 * (T_t) + (T_t)_{thermal} = 2(92 \text{ k}) + 109 \text{ k} = 293 \text{ k}$$

$$(T_b)_{design} = 2 * (T_b) + (T_b)_{thermal} = 2(538 \text{ k}) + 117 \text{ k} = 1194 \text{ k}$$

The tie rods selected for resisting the anchor loads were Dywidag Systems International® Threadrods (A722 Grade 150 steel). The top anchor utilized two 1.25 in. diameter rods (design capacity of 168 k each) and the bottom anchor utilized four 1.75 in. diameter rods (design capacity of 360 k each).

The system for connecting the tie rods to the RRFC superstructure was a series of four W-shape struts, welded to the RRFC's, with reinforced concrete cast between them (see Figure C1and Figure C2 for details). The struts extended 2 ft beyond the end of the RRFC's and thus needed to resist the sum of the vertical components of all of the tie rods (1030 k) which created a bending moment, M = (2 ft)(1030 k) = 2060 ft-kip. The shape sizes required to resist part of this load (with the additional resistance provided by the reinforced concrete) were specified to have a minimum plastic section modulus of 132 in.[3]; the reinforced concrete consisted of 15 #5 bars at 10 in. on center with a 28-day concrete strength of 3,000 psi.

For the transfer of tie rod forces to the sheet pile wall, the waler system consisted of a W-shape beam (bent about the weak axis) that set on 5 angled W-shape struts welded to the sheet pile wall. Analysis of the waler determined a maximum bending moment of 180 ft-kip for the bottom waler and thus required a W10x88 section (or equivalent weak-axis plastic section modulus). The W10x88 was also (conservatively) specified for the top waler. To prevent punching shear through the webs of the waler, 4 in. x 4 in. x 1.5 in. bearing plates were specified for each tie rod. Details of the waler systems are shown in Figure C1and Figure C2.

For transfer of the tie rod forces to the struts attached to the RRFC, bending moment in the waler was not a design consideration as the use of reinforced concrete between struts was assumed to provide a continuous bearing surface; the waler had to have a minimum clear distance between flanges of 18 in. to allow attachment to the RRFC strut. The bearing plates required 4 in. x 4 in. x 1.5 in. (A36 steel) for the four 1.75 in. rods. Since the two 1.25 in. rods were at a different angle than the 1.75 in. rods, skewed bearing plates were required; details are shown in Figure C2.

The wingwalls were assumed to be loaded with the same lateral forces as the main wall and thus the wingwall tie rods needed to resist a load of P_h = 80 k + 360 k = 440 k; three 1.25 in. A722 Threadrods were selected. The analysis for the waler (a W-shape to be bent about the weak axis) determined a minimum weak-axis plastic section modulus of 31.0 in³ was required. Due to the angle of the wingwalls, the wingwall waler needed to be welded to the sheet piling to provide resistance to the translational force required to develop the tie rod forces. Details of the wingwall waler are presented in Figure C1 and Figure C2.

Buckling of RRFC Superstructure

Connection of the tie rods to the RRFC superstructure resists lateral loads on the sheet pile wall by developing a compressive force in the RRFC's. A buckling analysis of the RRFC's was performed to ensure the compressive loads could be resisted. To verify sufficient buckling capacity, the Euler critical buckling load was calculated as follows:

$$P_{cr} = \frac{\pi^2 EI}{(kL)^2}$$

where:

k = 1.0 (ends of bridge assumed free to rotate)

I = 8670 in⁴ per RRFC

therefore:

$$P_{cr} = \frac{\pi^2 (29{,}000 \text{ ksi})(8670 \text{ in.}^4)}{[(1.0)(89 \text{ ft})(12 \text{ in./ft})]^2} = 2176 \text{ k (per RRFC)}$$

The moment of inertia, I, was conservatively calculated assuming only interior girders resisted buckling (neglecting deck and exterior elements) since actual section properties were unknown at the time of design. The total tie rod force to be resisted (calculated for the full strength of the rods) is:

$$P_{total} = \frac{4(400 \text{ k}) + 2(187.5 \text{ k})}{2 \text{ RRFC's}} = 989 \text{ k (per RRFC)}$$

Since $P_{total} < P_{cr}$ buckling of the RRFC's is not a concern and full tie rod force can be developed.

Geogrid Reinforcement Design

Internal Strength of Geogrid Reinforcement

Each layer of geogrid must be designed to resist the total lateral earth pressure at the corresponding location in the GRS system. In the TC project, the maximum location of lateral earth pressure (due to bridge surcharge, live load surcharge, and retained soil) is considered to be the base of the GRS system; as mentioned previously, load factors were not included on the retained soil after consultation with the TC Engineer's Office. The total earth pressure at this location is:

$$\sigma_{max} = (1000 \text{ psf}) + (427 \text{ psf}) = 1427 \text{ psf}$$

The vertical spacing, S_v, of the geogrid layers was selected to be 1 ft. At the location of maximum lateral earth pressure, the geogrid must resist:

$$T = \sigma_{max} * S_v = (1427 \text{ psf})(1 \text{ ft}) = 1427 \text{ lb/ft}$$

The allowable ultimate strength (after a 10% reduction for installation damage) of Tensar® BX1200 is 1773 lb/ft and is thus sufficient for design in the XMD.

The strength of the BX1200 in the MD, however, is insufficient (allowable ultimate tensile strength of 1179 lb/ft) for developing full resistance of the design loads in the direction perpendicular to the centerline of the roadway. As previously mentioned, a reduction of factor of safety on this bridge was considered acceptable to the TC Engineer's Office due to the low probability of design-level vehicular traffic loads occurring during the short design life of the structure. Neglecting the vehicular live load surcharge on the backfill (which has a low probability of occurrence at the same instant of full HL-93 loading on the superstructure), the lateral earth pressure in the MD of the geogrid would be 1342 psf. Assuming full ultimate strength of the geogrid material, the factor of safety for loads in the MD is 0.98; a failure of the geogrid would occur under full (factored) HL-93 loading of the superstructure.

<u>External Stability of Reinforcement</u>

To develop the full strength of the geogrid material, each layer was wrapped into the layer above as shown previously in Figure B2.

<u>Other Design Considerations</u>

Design checks for slumping, overturning, and sliding of the abutment system were not performed; the anchor system is integral with the superstructure and these failure modes are not considered.